CANADIAN THESES ON MICROFICHE

THÈSES CANADIENNES SUR MICROFICHE

National Library of Canada
Collections Development Branch

Canadian Theses on
Microfiche Service

Ottawa, Canada
K1A 0N4

Bibliothèque nationale du Canada
Direction du développement des collections

Service des thèses canadiennes
sur microfiche

NOTICE

The quality of this microfiche is heavily dependent upon the quality of the original thesis submitted for microfilming. Every effort has been made to ensure the highest quality of reproduction possible.

If pages are missing, contact the university which granted the degree.

Some pages may have indistinct print especially if the original pages were typed with a poor typewriter ribbon or if the university sent us an inferior photocopy.

Previously copyrighted materials (journal articles, published tests, etc.) are not filmed.

Reproduction in full or in part of this film is governed by the Canadian Copyright Act, R.S.C. 1970, c. C-30. Please read the authorization forms which accompany this thesis.

AVIS

La qualité de cette microfiche dépend grandement de la qualité de la thèse soumise au microfilmage. Nous avons tout fait pour assurer une qualité supérieure de reproduction.

S'il manque des pages, veuillez communiquer avec l'université qui a conféré le grade.

La qualité d'impression de certaines pages peut laisser à désirer, surtout si les pages originales ont été dactylographiées à l'aide d'un ruban usé ou si l'université nous a fait parvenir une photocopie de qualité inférieure.

Les documents qui font déjà l'objet d'un droit d'auteur (articles de revue, examens publiés, etc.) ne sont pas microfilmés.

La reproduction, même partielle, de ce microfilm est soumise à la Loi canadienne sur le droit d'auteur, SRC 1970, c. C-30. Veuillez prendre connaissance des formules d'autorisation qui accompagnent cette thèse.

THIS DISSERTATION
HAS BEEN MICROFILMED
EXACTLY AS RECEIVED

LA THÈSE A ÉTÉ
MICROFILMÉE TELLE QUE
NOUS L'AVONS REÇUE

Canada

NL-339 (r. 86/09)

National Library of Canada
Bibliothèque nationale du Canada

2b

0-315-19606-8

Canadian Theses Division
Division des thèses canadiennes

Ottawa, Canada
K1A 0N4

67514

PERMISSION TO MICROFILM — AUTORISATION DE MICROFILMER

- Please print or type — Écrire en lettres moulées ou dactylographier

Full Name of Author — Nom complet de l'auteur JEAN GARIÉPY	
Date of Birth — Date de naissance 28 october 1954	Country of Birth — Lieu de naissance CANADA
Permanent Address — Résidence fixe 8787 WAVERLY, MONTREAL, PROVINCE OF QUEBEC H2N 1T7	
Title of Thesis — Titre de la thèse MOLECULAR ANALYSIS OF A MODEL EF HAND DOMAIN REPRESENTING SITE III OF RABBIT SKELETAL TROPONIN C.	
University — Université UNIVERSITY OF ALBERTA	
Degree for which thesis was presented — Grade pour lequel cette thèse fut présentée Ph. D.	
Year this degree conferred — Année d'obtention de ce grade 1983	Name of Supervisor — Nom du directeur de thèse ROBERT S. HODGES

Permission is hereby granted to the NATIONAL LIBRARY OF CANADA to microfilm this thesis and to lend or sell copies of the film.

The author reserves other publication rights, and neither the thesis nor extensive extracts from it may be printed or otherwise reproduced without the author's written permission.

L'autorisation est, par la présente, accordée à la BIBLIOTHÈQUE NATIONALE DU CANADA de microfilmer cette thèse et de prêter ou de vendre des exemplaires du film.

L'auteur se réserve les autres droits de publication; ni la thèse ni de longs extraits de celle-ci ne doivent être imprimés ou autrement reproduits sans l'autorisation écrite de l'auteur.

Date MAY 9, 1983	Signature Jean Gariépy

NL-91 (4/77)

THE UNIVERSITY OF ALBERTA

Molecular analysis of a model EF hand domain representing site III of rabbit skeletal troponin C

by

© Jean Gariépy

A THESIS

SUBMITTED TO THE FACULTY OF GRADUATE STUDIES AND RESEARCH
IN PARTIAL FULFILMENT OF THE REQUIREMENTS FOR THE DEGREE
OF Doctor of Philosophy

DEPARTMENT OF BIOCHEMISTRY

EDMONTON, ALBERTA

FALL, 1983

1

MICRO

THE UNIVERSITY OF ALBERTA

RELEASE FORM

NAME OF AUTHOR Jean Gariépy

TITLE OF THESIS Molecular analysis of a model EF hand domain representing site III of rabbit skeletal troponin C

DEGREE FOR WHICH THESIS WAS PRESENTED Doctor of Philosophy

YEAR THIS DEGREE GRANTED FALL, 1983

Permission is hereby granted to THE UNIVERSITY OF ALBERTA LIBRARY to reproduce single copies of this thesis and to lend or sell such copies for private, scholarly or scientific research purposes only.

The author reserves other publication rights, and neither the thesis nor extensive extracts from it may be printed or otherwise reproduced without the author's written permission.

(SIGNED) Jean Gariépy

PERMANENT ADDRESS:

8787 WAVERLY
MONTREAL, QUEBEC
H2N 1T7

DATED May 9 1983

THE UNIVERSITY OF ALBERTA

FACULTY OF GRADUATE STUDIES AND RESEARCH

The undersigned certify that they have read, and recommend to the Faculty of Graduate Studies and Research, for acceptance, a thesis entitled Molecular analysis of a model EF hand domain representing site III of rabbit skeletal troponin C submitted by Jean Gariépy in partial fulfilment of the requirements for the degree of Doctor of Philosophy.

Robert A Hodges
Supervisor
Brian D. Sykes
Cyril M. Kay

External Examiner

Date April 20, 1983

To my parents, and Mr. Ping Chan.

ABSTRACT

An EF hand can be described as a linear sequence of 30 to 35 amino acids, where the N- and C-terminal α-helical regions are flanking a 12-residue long calcium binding loop. The calcium ion is near octahedrally coordinated by oxygen ligands from the peptide backbone and side chains, or by water molecules. A number of proteins such as calmodulin, troponin C and parvalbumin possess up to 4 of these EF hand sites. We have investigated some structural properties of a model EF hand in relation to its calcium binding affinity and the effect of calcium on the overall structure of the site. We have synthesized several analogs of site III of rabbit skeletal troponin C because this site has a high affinity for calcium in the native protein (K*ca* $\sim 10^{7}M^{-1}$) and still retains its ability to bind calcium when isolated as a cyanogen bromide fragment of troponin C (CB9 fragment; K*ca* $\sim 10^{5}M^{-1}$). A 12-residue long calcium binding loop (AcF^{112}STnC(103-114)) was initially synthesized but demonstrated only a weak affinity for calcium (K*ca* $\sim 10^{3}M^{-1}$; Reid *et al.*, 1980; Kanellis *et al.*, 1983). The presence of the C-terminal region (*loop-helix* analogs, AcSTnC(103-123) and AcF^{112}STnC(103-123)) did not increase the ability of this site to bind calcium in aqueous medium (K*ca* $2-3 \times 10^{3}M^{-1}$). However, the presence of trifluoroethanol induced the formation of an α-helix in the C-terminal part of the peptide (as monitored by circular dichroism) and resulted in

an enhancement of the affinity of the site for calcium (K*ca* 3-9 x $10^{3}M^{-1}$). The sequential lengthening of the N-terminal region (*helix-loop-helix* analogs; 26 residues, AcA^{98}-STnC(98-123)amide; and 34 residues, AcA^{90}STnC(90-123)amide) led to a proportional increase in the calcium affinity of the resulting sites (K*ca* (26-residue), 4 x $10^{4}M^{-1}$; K*ca* (34-residue), 3 x $10^{5}M^{-1}$) and of the peptide α-helical content in the presence of calcium. However, the affinity of all the synthetic analogs leveled off to ~ $10^{5}M^{-1}$, in the presence of trifluoroethanol. Proton magnetic resonance results have indicated that the environment of side chains in both the N- and C-terminal regions are affected by the presence of calcium and that the elongation of the N-terminal region correlates with slower off rates for the calcium:peptide complexes formed. In summary, both the N- and C-terminal regions and their folding into an α-helical configuration represent important factors in the ability of the EF site to bind calcium. Reciprocally, the induction of helix in the N-terminal region of the EF site is dependent on the presence of calcium.

The lanthanides because of their spectroscopic properties, were used as calcium analogs in order to answer questions relating to the geometry of a metal:peptide complex. The conformation adopted by a 13-residue long synthetic peptide (AcSTnC(103-115)amide) around the lanthanides lutetium and lanthanum, was studied by proton magnetic resonance techniques. These two metals were initially selected because of their diamagnetic properties (no unpaired electrons), their strong binding to this model peptide in comparison to calcium and their difference in ionic radius (Lu^{3+}, 0.86 Å; La^{3+}, 1.03 Å; Ca^{2+}, 1.00 Å). The ^{1}H NMR spectra observed for a lutetium titration of the peptide differed significantly from the spectra obtained for a lanthanum titration, indicating that the folding pattern adopted by the synthetic peptide around these metals is different. In addition, this synthetic analog has a weaker affinity for Lu^{3+} ($1.3 \times 10^{4} M^{-1}$) than for La^{3+} ($1.1 \times 10^{5} M^{-1}$), indicating that the primary sequence of the loop region may well code for the formation of metal:peptide complexes involving cations of specific charge (calcium versus lanthanides) and size (lanthanum versus lutetium). Attempts were also made to reconstruct the geometry of this 13-residue long analog as a lanthanide:peptide complex in solution. In the presence of lanthanum, addition of gadolinium results in the differential broadening of the proton resonances of this peptide. The magnitude of the broadening is inversely proportional to the sixth power of the distance separating the Gd^{3+} ion and the proton nucleus investigated. Measurements of relaxation times were made at various times during the gadolinium titration of a lanthanum-saturated peptide solution. The calculated relaxation times values for a 1:1 gadolinium to peptide complex were then used to determine several proton-metal distances in the complex. A series of possible conformations can then be generated for this metal:peptide complex, by using these distance restrictions as boundary conditions in a distance-geometry algorithm devised by Kuntz and his co-workers (Havel *et al.*, 1979; Kuntz *et al.*, 1979). We are presently pursuing this task.

By using synthetic analogs of the N-terminal region alone (AcA^{90}STnC(90-104)amide) and of the entire *helix-loop-helix* region (AcA^{90}STnC(90-123)amide) in addition to a cyanogen bromide fragment containing site III of rabbit skeletal troponin C (CB9, HSer^{135}STnC(84-135)), we have localized a phenothiazine specific binding site in the N-terminal region of site III of rabbit skeletal troponin C. This site is composed of hydrophobic and negatively charged domains that probably interact with complementary domains of phenothiazines. The primary sequence alignment of various EF hands has indicated that this phenothiazine binding site is a common feature to all EF hands. The binding site is generated by the proper positioning of side chains along the N-terminal region. This occurs when the N-terminal region adopts an α-helical arrangement. Such a folding pattern is partly induced by the presence of calcium. However, apo-troponin C and apo-calmodulin do possess preformed helical regions. Thus the action of calcium as a second messenger probably lies in its ability to induce and expose these hydrophobic sites upon binding to EF hand sites.

ACKNOWLEDGEMENTS

It is impossible to point out one particular individual who contributed the most toward my doctoral degree, although Dr. Bob Hodges, Pélé Chong and my parents are probably the first four persons that come to mind. The first two because of their moral support, guidance, friendship, and involvement in sports, and the two last ones, because they always wanted me to do well. Other honorable contributors to this milestone include fellow graduate students and postdocs such as Judith Shelling, Heather Dettman, Lana Lee, Jim Lees-Miller, Graham Coté, John Silvius, John Robinson, Brian McDonough, Jim Talbot, Joe Ng, Masao Fuginaga, Randy Read, Clive Sanders and Ruthven Lewis. These individuals have provided the much needed spiritual support, to go through such an endeavour. I would also like to acknowledge the help and friendship of members of my lab; Morris Aarbo, Ashok Taneja, Paul Cachia, Jenny Van Eyk, Pieter Asselbergs, Donna Clare, Amrit Saund, and Ron Reid. One should add to this list, the newcomers, Colin Mant, Bob Parker and Constant Addo and other friends from neighboring labs in particular Krystyna Golosinska , Mike Nattriss, Mike Carpenter, Bill McCubbin, Joyce Pearlstone, Steven Lau, Don Stewart, Alan Mak and Rajam Mani. Special thanks should be given to Dr. Brian Sykes and Dr. Cyril Kay for helping me gain confidence in myself as a scientist, and to the rest of the professorial staff for their friendly advice and the use of their facilities.

Finally, I am grateful to Ms. Tania Watts for her kindness and friendship in the last two years of my doctoral degree and to the Medical Research Council of Canada and the Alberta Heritage Foundation for Medical Research for their financial assistance in the form of studentships and research allowances.

TABLE OF CONTENTS

Page

DEDICATION iv

ABSTRACT v

ACKNOWLEDGEMENTS ix

LIST OF TABLES xviii

LIST OF FIGURES xix

LIST OF ABBREVIATIONS xxiii

CHAPTER I: INTRODUCTION 1

A. CALCIUM DISTRIBUTION 1

B. CALCIUM INVOLVEMENT IN CELL PHYSIOLOGY 3

- 1. Control of cytosolic calcium levels 3
- 2. Spacial and temporal considerations 7

C. ROLES OF CALCIUM IN LIVING SYSTEMS 10

D. CHEMISTRY OF CALCIUM 14

- 1. Metals and ligands 15
- 2. Radius ratio 16
- 3. Charge effect 18
- 4. Mechanism of complex formation 21
- 5. Dehydration and complexation properties of calcium 22

E. STRUCTURE AND FUNCTION OF CALCIUM BINDING PROTEINS 28

- 1. Criteria for calcium regulation 30
- 2. Concept of the EF hand domain 32
- 3. Structure and function of EF hand containing proteins 36
  - a. Calmodulin 36

b. Troponin C 39

c. Parvalbumin 42

d. Intestinal calcium binding proteins . . . 47

e. S-100 proteins 50

f. Myosin light chains 52

4. Design of an EF hand domain 57

F. AIMS OF THE PROJECT 59

CHAPTER II: EXPERIMENTAL PROCEDURES 63

A. SOURCES OF CHEMICALS AND SOLVENTS 63

B. AMINO ACID ANALYSIS AND PEPTIDE QUANTITATION . . . 64

C. MELTING POINT MEASUREMENTS AND ELEMENTAL ANALYSIS . 65

D. THIN LAYER CHROMATOGRAPHY 65

E. SDS GEL ELECTROPHORESIS 66

F. PAPER ELECTROPHORESIS 67

1. Experimental procedures 67

2. Ninhydrin:cadmium acetate solution 67

G. PEPTIDE SYNTHESIS 68

1. Solution synthesis 68

a. Synthesis of fragment A, Boc-Lys(Z) Ser(Bzl)-Glu(OBzl)-Glu(OBzl)-OH 68

b. Synthesis of fragment B, Boc-Glu(OBzl) Leu-Ala-Glu(OBzl)-OH 71

c. Synthesis of fragment C, Boc-Ala-Phe Arg(Tos)-OH 73

d. Synthesis of fragment D, Boc-Ile-Phe Asp(OBzl)-OH 75

e. Purification of protected peptide fragments 76

2. Solid phase peptide synthesis 77

a. Synthesis of AcSTnC(103-123) 80

b. Synthesis of AcA''STnC(98-123)amide and AcA''STnC(90-123)amide 83

c. Purification of peptides AcSTnC(103-123), AcA''STnC(98-123)amide and AcA''STnC(90-123)amide 86

d. Synthesis and purification of AcA''STnC(90-104)amide 87

e. Synthesis and purification of AcSTnC(103-115)amide 91

f. Cleavage of peptides from the resin . . . 92

3. Synthesis assessment and troubleshooting . . 94

H. CHEMICAL CLEAVAGE OF TROPONIN C 98

1. Modification and cyanogen bromide cleavage of rabbit skeletal troponin C . . . 98

2. Purification of a cyanogen bromide fragment containing the region 84 to 135 of rabbit skeletal troponin C 100

I. PREPARATION OF IODINATED PEPTIDES 100

J. ULTRAVIOLET SPECTROSCOPY 101

1. Experimental procedure 101

2. Peptide samples 101

3. Calcium solutions 102

K. CIRCULAR DICHROISM 102

1. Circular dichroism measurements 102

2. Precautions against metal contamination . . . 103

3. Calcium solutions 103

4. Calcium titrations of AcSTnC(103-123), AcA''STnC(98-123)amide and AcA''STnC(90-123)amide 103

a. Peptide samples 104

b. Determination of calcium binding constants 104

c. Determination of α-helical content 105

5. Calcium and trifluoperazine titrations of CB9 108

a. CB9 and TnC samples 109

b. Trifluoperazine titrations 109

c. Determination of TFP and calcium binding constants 110

6. Calcium titration of AcA''STnC(90-123)amide in the presence of neuroleptic drugs 111

a. Peptide:drug samples 111

L. NUCLEAR MAGNETIC RESONANCE 112

1. ^{1}H NMR measurements 112

2. Metal contamination 112

3. Metal solutions 113

4. Calcium titrations of AcSTnC(103-123), AcA''STnC(98-123)amide and AcA''STnC(90-123)amide 114

a. Peptide samples 114

b. Spectral parameters 114

c. Laser Photo-CIDNP experiments 114

5. Calcium and trifluoperazine titrations of CB9 and AcA''STnC(90-104)amide 117

a. Peptide samples 117

b. Trifluoperazine solutions 117

c. Spectral parameters 118

6. Lanthanide titrations of AcSTnC(103-115)amide 118

a. Peptide samples 118

b. Spectral parameters 119

c. Determination of La^{3+} and Lu^{3+} binding constants 119

d. Gadolinium titration 120

e. T_1 and T_2 measurements 122

CHAPTER III: CALCIUM-INDUCED PEPTIDE FOLDING 124

A. SPECTROSCOPIC STUDIES OF ANALOGS OF SITE III OF RABBIT SKELETAL TROPONIN C 124

B. SECONDARY STRUCTURE ANALYSIS 128

1. Circular dichroism results 128

a. Effect of calcium and trifluoroethanol on the peptide secondary structure 128

b. Analysis of the peptides α-helical content 135

c. Effect of elongating the N-terminal region on the calcium binding affinity of the site 140

2. Ultraviolet difference spectroscopy 141

3. Proposed model for the Ca^{2+}-induced protein folding of troponin C 143

C. ANALYSIS OF SIDE CHAIN PERTURBATIONS 153

1. Assignment of resonances in the apopeptides . 154

2. Effect of calcium addition 156

3. Titration of iodinated peptides 161

4. Laser Photo-CIDNP of Ca^{2+}-saturated peptides 163

5. Kinetic and thermodynamic aspects 165

D. SUMMARY 170

CHAPTER IV: LANTHANIDE-INDUCED FOLDING OF A SYNTHETIC CALCIUM BINDING LOOP 174

A. THE USE OF LANTHANIDES AS CALCIUM ANALOGS 174

B. VARIATIONS IN LANTHANIDE AFFINITY AND INDUCED PEPTIDE CONFORMATION 178

1. Assignment of apo AcSTnC(103-115)amide resonances 178

2. Lanthanide titrations 183

a. Lanthanum and lutetium titrations 183

b. Lanthanide binding constants 187

3. Peptide folding pattern 190

C. DETERMINATION OF METAL-PROTON DISTANCES IN A GADOLINIUM:PEPTIDE COMPLEX 195

1. Distance measurements 195

a. Gadolinium titration 195

b. Determination of relaxation times 199

c. Calculation of metal-proton distances . . 202

2. Key assumptions 203

3. Distance restrictions 206

D. SUMMARY 208

CHAPTER V: PHENOTHIAZINE BINDING SITE IN THE N-TERMINAL REGION OF SITE III OF RABBIT SKELETAL TROPONIN C 210

A. CALCIUM-INDUCED EXPOSURE OF HYDROPHOBIC REGIONS ON TROPONIN C AND CALMODULIN 210

B. LOCALIZATION OF A PHENOTHIAZINE BINDING SITE ON TROPONIN C. 214

1. Trifluoperazine behavior in solution 218

2. Effect of Ca^{2+} and TFP on the secondary structure of CB9 and troponin C 221

3. Investigation of peptide side chains involved in the TFP:peptide complex using proton magnetic resonance 223

a. Addition of calcium to CB9 in the presence and absence of trifluoperazine 224

b. Addition of trifluoperazine to CB9 in the presence and absence of calcium 226

c. Interaction of trifluoperazine with a synthetic analog of site III of rabbit skeletal troponin C 229

d. Proposed model of a phenothiazine binding site on rabbit skeletal troponin C 230

e. Possible location of other TFP-binding sites on troponin C and calmodulin 235

C. INTERACTION OF NEUROLEPTIC DRUGS WITH A SYNTHETIC CALCIUM BINDING ANALOG OF RABBIT SKELETAL TROPONIN C 238

1. Controversy surrounding the interaction of antipsychotic drugs with calmodulin 238

2. Circular dichroism results 240

D. SUMMARY 246

CHAPTER VI: COMMENTS ON THE STRUCTURE AND FUNCTION OF EF HANDS AND EXPERIMENTAL APPROACHES TO ACHIEVE A BETTER UNDERSTANDING OF THEIR DESIGN 249

A. PRIMARY SEQUENCE ANALYSIS AND FOLDING BEHAVIOR OF EF HANDS IN RELATION TO THE MECHANISM OF ACTION OF TROPONIN C AND CALMODULIN 249

1. Generation of an average EF hand sequence . . 250

2. Composition of a calcium binding loop 254

3. Composition of the C- and N-terminal regions 257

4. Importance of the EF hand structure in the function of calcium binding proteins 259

5. Conclusions on the mode of action of EF hand containing proteins 261

6. Origins of the ancestral EF hand gene ? . . . 262

B. FUTURE DIRECTION OF THE PROJECT 263

1. Technical problems 263

2. Key questions to answer 266

BIBLIOGRAPHY 271

APPENDIX 295

LIST OF TABLES

Page

I-1 Distribution of Group IA and IIA cations and some key anions 4

I-2 Some chemical and physical properties of Group IA and IIA cations 26

I-3 Calcium and magnesium binding constants for skeletal and cardiac troponin C 41

II-1 Amino acid composition of purified synthetic and cyanogen bromide peptides 89

II-2 Progress of the synthesis of peptide AcA^{110}STnC(90-123) amide 96

III-1 Calcium binding constants of the synthetic peptides and various fragments of the natural proteins containing a single Ca^{2+}-binding site 129

III-2 Circular dichroism studies on synthetic peptides and isolated fragments from calcium binding proteins 133

III-3 Structural changes induced by calcium and trifluoroethanol in the synthetic 21-, 26-, or 34-residue peptides 136

III-4 Correspondence between the number of residues in α-helical regions and molar ellipticity values in TnC and its fragments 148

IV-1 Ionic radius of several alkali, alkali earth and lanthanide cations as a function of coordination number 175

IV-2 Assignment of proton magnetic resonances of Apo-AcSTnC(103-115) amide 182

IV-3 Relaxation times and calculated proton-metal distances 200

VI-1 Tabulation of amino acid frequencies at each position of the EF hand 253

LIST OF FIGURES

Page

I.1 Distribution of elements 2

I.2 Mechanisms regulating the calcium concentration in the cytosol 5

I.3 Variations in the intracellular calcium concentration as a function of time following a stimulus and distance from the site of calcium entry 9

I.4 A. Reaction catalysed by phospholipase A_2. . . . 12

B. Proposed mechanism of action of phospholipase A_2 12

I.5 The Irving-Williams effect 17

I.6 A. Octahedral arrangement of hydroxide ligands around calcium in $Ca(OH)_2$ 19

B. Determination of the minimal r^+/r^- value for an octahedral arrangement 19

C. Minimal values of radius ratio as a function of packing geometry 19

I.7 Metal:protein complex formation 23

I.8 Characteristic rate constants for the substitution of water molecules from the inner-sphere of metal ions 24

I.9 Stereoprojections of various calcium binding sites in proteins 29

I.10 Representations of a model EF hand site . . . 33

I.11 Evolutionary trees of EF hand containing proteins

A. Barker's tree 35

B. Goodman's tree 35

I.12 Calcium-calmodulin regulated enzymes 38

I.13 A. The steric blocking model 43

B. Evolution in the positioning and

interaction of components involved in the mechanism of contraction in striated muscle. 43

I.14 Crystal structure of carp parvalbumin
A. Tridimensional representation 46

B. Stereoprojection along the α-carbon chain 46

I.15 Crystal structure of bovine intestinal calcium binding protein 49

I.16 Structure of myosin 53

II.1 Flow chart depicting the sequence of operations performed during the solid phase peptide synthesis of our analogs 79

II.2 Strategy used for the synthesis of the 26- (peptide II) and 34-residue (peptide III) peptides 84

II.3 Purification scheme of AcA''STnC(90-123) amide
A. DEAE-Sephacel purification 88

B. Hydroxyapatite purification 88

II.4 Purification scheme of AcSTnC(103-115) amide
A. HPLC purification on a preparative ion-exchange column 93

B. HPLC purification on a preparative reverse phase column 93

III.1 Amino acid sequences of rabbit skeletal TnC cyanogen bromide fragment 9 (CB9) and of the synthetic analogs 127

III.2 Circular dichroism spectra of the peptides . . 131

III.3 A model of conformational changes induced in the three synthetic peptides by Ca^{2+} and hydrophobic medium 137

III.4 Calcium-induced ultraviolet difference spectra of the peptides 142

III.5 Amino acid sequences of carp parvalbumin (MCBP 4.25) site II and of rabbit skeletal TnC site III 144

III.6 A model depicting calcium-induced protein folding in rabbit skeletal TnC during calcium binding to the four Ca^{2+}-binding units 147

III.7 ^1H NMR spectra of the synthetic peptides at various stages of calcium addition 155

III.8 ^1H NMR spectra of the iodinated peptides . . . 159

III.9 ^1H NMR laser photo-CIDNP difference spectra of the aromatic region of each analog in the presence of calcium 164

IV.1 Primary sequence of the synthetic fragment AcSTnC(103-115) amide 179

IV.2 ^1H NMR spectrum of apo-AcSTnC(103-115) amide . 180

IV.3 Lanthanum titration of AcSTnC(103-115) amide . 184

IV.4 Lutetium titration of AcSTnC(103-115) amide . 186

IV.5 Lanthanide titration plots of AcSTnC(103-115) amide 188

IV.6 Stereoprojection of rabbit skeletal TnC region 103-115 192

IV.7 Assignment of AcSTnC(103-115) amide ^1H NMR resonances 197

IV.8 Gadolinium titration of AcSTnC(103-115) amide in the presence of excess lanthanum 198

V.1 Structure and nitrogen p*Ka*'s of some representative phenothiazines 213

V.2 A. Tryptic fragments of bovine brain calmodulin 216

B. Interaction of tryptic fragments with target proteins 216

V.3 Primary sequence alignment of peptides shown to bind phenothiazines 217

V.4 Effect of trifluoperazine and divalent anion concentration on the ^1H NMR spectrum of trifluoperazine 220

V.5 Effect of calcium and trifluoperazine on the circular dichroism spectrum of CB9 222

V.6 Calcium titration of CB9 in the presence and absence of trifluoperazine 225

V.7 Trifluoperazine titration of CB9 in the presence and absence of calcium 227

V.8 Trifluoperazine titration of the synthetic fragment AcA''STnC(90-104) amide 231

V.9 Stereoprojection of rabbit skeletal TnC, region 90-104 234

V.10 Homologous sequence regions of rabbit skeletal TnC and bovine brain calmodulin containing short helical regions involving two aromatic side chains separated by one turn of helix . . 236

V.11 Amino acid sequence of bovine brain calmodulin, rabbit skeletal troponin C and the 34-residue peptide 242

V.12 Effect of various classes of drugs on the circular dichroism spectrum of a synthetic peptide 243

VI.1 Primary sequence of thirty EF hands that bind calcium 251

VI.2 Primary sequence and folding pattern of EF hands
  A. Average sequence of an EF hand 255
  B. Representation of a model EF hand along its α-carbon backbone 255
  C. Location of hydrophobic and charged domains in the helical regions of EF hands 255

VI.3 Possible pathways leading to the biosynthesis of an ancestral EF hand gene 264

ABBREVIATIONS

A	Alanine
Å	Angstrom
Actomyosin ATPase	The actin-activated Mg^{2+}-dependent hydrolysis of ATP by myosin
Ala	Alanine
Arg	Arginine
Asn	Asparagine
Asp	Aspartic acid
ATP	Adenosine-5'-triphosphate
Boc	*Tert*-butyloxycarbonyl
Bzl	Benzyl ether
C	Cysteine
CaM	Calmodulin
c-AMP	Cyclic adenosine 3',5'-monophosphate
CB9	Cyanogen bromide fragment 9 of rabbit skeletal troponin C (84-135)
CD	Circular dichroism
CHELEX 100	Styrene lattice resin with imido diacetic acid exchange groups
CIDNP	Chemically induced dynamic nuclear polarization
CNBr	Cyanogen bromide
C-terminal	Carboxyl terminal of a polypeptide chain
Cys	Cysteine
D	Aspartic acid
DCC	N,N'-dicyclohexylcarbodiimide
DEA	Diisopropylethylamine
DEAE	Diethylaminoethyl

DMF	N,N'-dimethylformamide
D_2O	Deuterium water
DSS	Sodium 4,4-dimethyl-4-silapentane 1-sulfonic acid
DTNB	5,5'-dithiobis-(2-nitrobenzoic acid)
DTT	Dithiothreitol
E	Glutamic acid
EDTA	Ethylenediamino-tetra-acetic disodium salt
EF hand	Kretsinger's abbreviation of the second calcium binding domain of carp parvalbumin, this site is thought to represent a typical calcium binding domain
EGTA	Ethylene glycol-bis-(β-aminoethylether) -N,N,N',N'-tetraacetic acid
F	Phenylalanine
FID	Free induction decay
FMN	Flavin mononucleotide
G	Glycine
Gly	Glycine
Gln	Glutamine
Glu	Glutamic acid
H	Histidine
His	Histidine
^1H NMR	Proton magnetic resonance
HOBt	1-hydroxybenztriazole
HPLC	High pressure liquid chromatography
Hser	Homoserine
I	Isoleucine
ICBP	Intestinal calcium binding protein

ID	Internal diameter
Ile	Isoleucine
K	Lysine
L	Leucine
Leu	Leucine
Lys	Lysine
M	Methionine
Mbh	4,4'-dimethoxybenzhydryl
MCBP 4.25	Muscle calcium binding protein (parvalbumin) having an isoelectric point of 4.25
MES	2-(N-Morpholino)-ethane sulfonic acid
Met	Methionine
MOPS	3-(N-morpholino)-propane sulfonic acid
MW	Molecular weight
N	Asparagine
NHS	N-hydroxysuccinimide
nm	Nanometers
NMR	Nuclear magnetic resonance
N-terminal	Amino terminal of a polypeptide chain
OBzl	Benzyl ester
P	Proline
PAGE	Polyacrylamide gel electrophoresis
Phe	Phenylalanine
Pi	Inorganic orthophosphate group
PIPES	Piperazine-N,N'-bis(2-ethane sulfonic acid)
Pro	Proline
Q	Glutamine
QAE	Quaternary anion exchanger

R	Arginine
Rf	Relative mobility of a compound on TLC plates relative to the solvent front
S	Serine
S-1	Soluble single headed fragment of myosin
S-100	Brain-specific calcium binding protein soluble in 100%-saturated ammonium sulfate at neutral pH
SDS	Sodium dodecyl sulfate
Ser	Serine
T	Threonine
TFA	Trifluoroacetic acid
TFE	Trifluoroethanol
TFP	Trifluoperazine
Thr	Threonine
TLC	Thin layer chromatography
TM	Tropomyosin
Tn	Rabbit skeletal troponin complex
TnC	Calcium binding subunit of troponin
TnI	Inhibitory subunit of troponin
TnT	Tropomyosin binding subunit of troponin
Tos	*p*-toluenesulfonyl
Tris	Tris-(hydroxymethyl)aminomethane
Trp	Tryptophan
Tyr	Tyrosine
UV	Ultraviolet
V	Valine
Val	Valine

Y	Tyrosine
W	Tryptophan
W-7	N-(6-aminohexyl)-5-chloro-1-naphtalene sulfonamide

CHAPTER I

INTRODUCTION

A. CALCIUM DISTRIBUTION

One of the most striking features of our universe is the unequal distribution and occurrence of its elements in nature. For example, a careful study of the composition of rocks making up the earth's crust reveals that oxygen accounts for about 47% of the crust by weight, while silicon comprises about 28% and aluminum, 8%. These elements plus iron, calcium, sodium , potassium and magnesium represent about 99% of the crust's composition.

Figure I.1 indicates that the elemental distribution fluctuates dramatically from one source to another. In man, for example, silicon has been replaced by carbon as a structural component of organic molecules. It is thus clear that the physical and chemical properties of each element are partly responsible for their selected concentration and role(s) in living systems. One further notices that besides the 4 essential elements involved in the organic chemistry of our body, the most abundant element is calcium . The bulk of this calcium however is present as an insoluble phosphate form and acts as a structural component in bones and teeth (1 kg for a 70 kg man) (Ochiai, 1977).

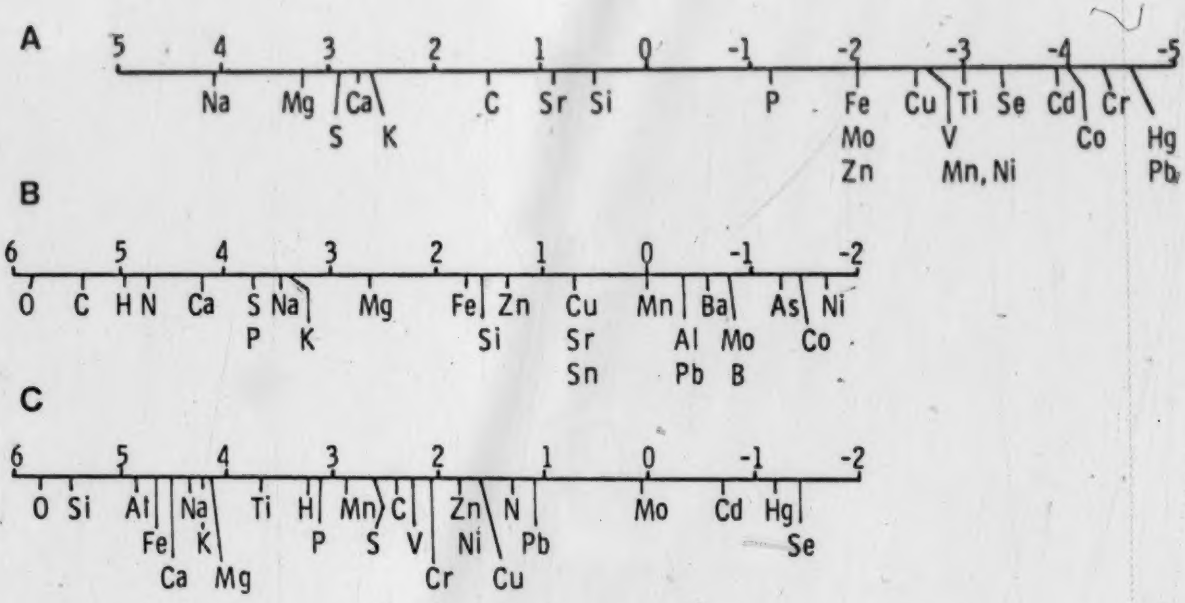

Fig. I.1 The distribution of elements in (A) sea water, (B) man, and (C) the earth's crust. The scales represent the logarithm of the concentration of each element in ppm [Adapted from Ochiai, 1977].

B. CALCIUM INVOLVEMENT IN CELL PHYSIOLOGY

1. Control of cytosolic calcium levels

One hundred years ago, Ringer (1882) showed that extracellular calcium was required for the normal contraction of frog heart. Experiments performed in the decades following the discovery confirmed that the level of extracellular calcium had a profound effect on the ability of cells to respond to stimuli.

Table I-1 illustrates that several cations including calcium are present in the 10^{-1}M to 10^{-3}M range in blood plasma and other extracellular fluids (Guyton, 1971; Ochiai, 1977; Kretsinger, 1979). The $[Ca^{2+}]$*out*/$[Ca^{2+}]$*in* ratio is about 2.5×10^4 and suggests that cells possess one or several ways of translocating (transporting or relocating) this cation. Figure I.2 depicts the various regulatory mechanisms a cell may use to control the level of intracellular calcium. Calcium can be eliminated by a Mg^{2+}-dependent, ATP-driven transmembrane Ca^{2+} pump (Schatzmann and Vincenzi, 1969; see review by Schatzmann and Roelofsen, 1977). Alternatively, the mitochondrium can regulate the cytosolic level of calcium by taking up calcium using the electrical component of its membrane proton gradient. This gradient is generated by ATP hydrolysis or

TABLE I-1

Distribution of Group IA and IIA cations and some key anions[a]

Fluids	Na^+ (mM)	K^+ (mM)	Mg^{2+} (mM)	Ca^{2+} (mM)	Cl^- (mM)	PO_4^{3-} (mM)	HCO_3^- (mM)
Blood plasma	152	5	1.5	2.3[b]	113	2.4[b]	27
Interstitial fluid	143	4	1.5	2.3[b]	117	2.4[b]	27
Cytosol	14	157	1-5	$\leq 10^{-4}$		38	10
E. coli (wet)	80	250	20	5			
Aerobacter aerogenes		410	124	5			

[a] Taken from Ochiai, 1977.

[b] Taken from Guyton, 1971.

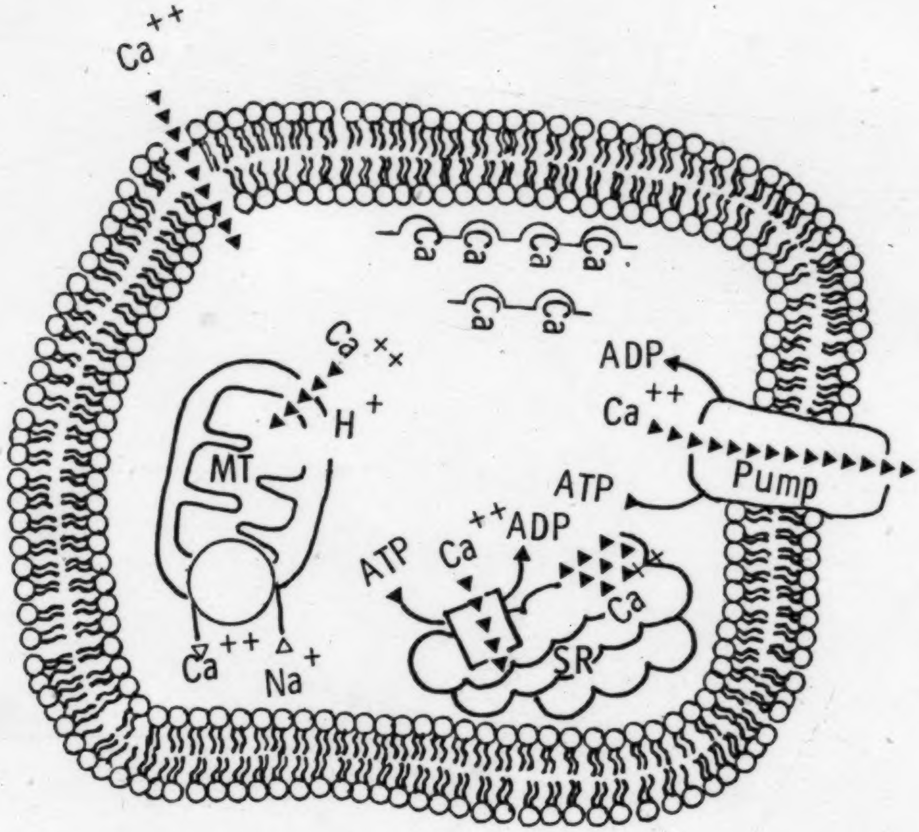
Ca++
Ca
Ca
Ca
Ca
Ca
Ca
Ca ++
H+
ADP
Ca++
ATP
Pump
MT
ATP
Ca++
ADP
Ca++
SR
Ca++
Na+

Fig. I.2 Mechanisms regulating the calcium concentration in the cytosol. MT, mitocondrium; Pump, membrane calcium ATPase pump; SR, sarcoplasmic reticulum (muscle cells only); ⌒⌒, ⌒⌒⌒⌒ , calcium binding proteins.

respiration (Rottenberg and Scarpa, 1974, Carafoli, 1980). The divalent cation release occurs via a Na^+-induced Ca^{2+} efflux mechanism (Crompton *et al.*, 1976, 1978; Carafoli, 1980). In the case of muscle cells, a specialized organelle called the sarcoplasmic reticulum offers an additional way for these cells to retain a finely tuned level of intracellular calcium. This organelle is composed of a network of vesicles arranged like a sleeve and covers each contractile unit. Calcium is sequestered in this network by means of an ATP-activated Ca^{2+} pump located in the vesicle membrane (Hasselbach and Makinose, 1963; Weber *et al.*, 1966; MacLennan and Wong, 1971; MacLennan and Holland, 1975; Green *et al.*, 1977). Electrical stimulation of the muscle fiber will depolarize the reticulum membrane and release calcium into the cytosol. This event triggers muscle contraction. Finally, several intracellular calcium binding proteins are present (i.e. calmodulin, troponin C, parvalbumin, calregulin) and bind calcium tightly (K_{ca} $\sim 10^{-6}$M to 10^{-7}M) but their concentration and distribution is tissue specific in most cases. Calmodulin however has been shown to affect calcium translocation by modulating the cytoplasmic membrane bound (Mg^{2+}-Ca^{2+}) ATPase pump (Gopinpath and Vincenzi, 1977; Jarret and Penniston, 1977; Pershadsingh *et al.*, 1980) and the ATP-dependent Ca^{2+} uptake by the sarcoplasmic reticulum (Katz and Remtulla, 1978; Horl *et al.*, 1978). It is doubtful that membrane phospholipids will play a role in controlling the cytosolic level of calcium since their interaction with this cation requires the presence of millimolar amounts of calcium (pK*ca* of 3 to 4) (Kretsinger, 1979).

2. Spacial and temporal considerations

The *resting state* of a cell is achieved when the cytosolic level of calcium is around 10^{-7}M. This calcium level can still vary since chemical, electrical and mechanical stimulations will trigger the depolarization of the cell membrane and provoke a calcium increase to 10^{-5}M in the cytosol. This represents the *excited state* of a cell.

The excited state of a cell may persist for long periods of time if a cascade of Ca^{2+}-modulated events occurs. A situation such as cell division exemplifies a chronic case of calcium stimulation. In view of the frequent occurrence of such prolonged excited states, Kretsinger (1979) commented that the concept of resting and excited states of a cell had been oversimplified. A commonly cited example is that of muscle contraction where a rapid transition in cellular states exists. However, one fails to realize that muscle cells, by virtue of their sarcoplasmic reticulum and the optimized geometry of their structural components, are the exception rather than the rule.

A cell possesses a finite volume. Upon excitation, a competition between the calcium influx rate and the opposing rates from calcium translocating mechanisms means that the calcium concentration at various points in the cell will differ and calcium regulated events will be influenced by temporal and spacial factors. This point is illustrated by the surface diagram shown in Fig. I.3. This diagram assumes the case of a spherical cell. The application of a stimulus will result in a rapid increase in cytoplasmic calcium level near the cell membrane but this calcium increase will be felt only later in time and to a lesser extent at the center of the cell depending on the length and pattern of stimulation. Similarly, calcium sequestration will be slower in the center of the cell than near the membrane where the Mg^{2+}-dependent, ATP-driven Ca^{2+} pumps are present. If one considers proteins such as parvalbumins and intestinal calcium binding proteins as specialized calcium buffering agents, then their concentration and location in the cell will certainly influence the duration and the extent of the calcium signal.

Furthermore, little is known about the amplification of the calcium signal. Since cells can be chronically stimulated by calcium, Ca^{2+} must act by positive feedback to stimulate directly or indirectly, its passage through the cell membrane. Positive feedback mechanisms yield states far

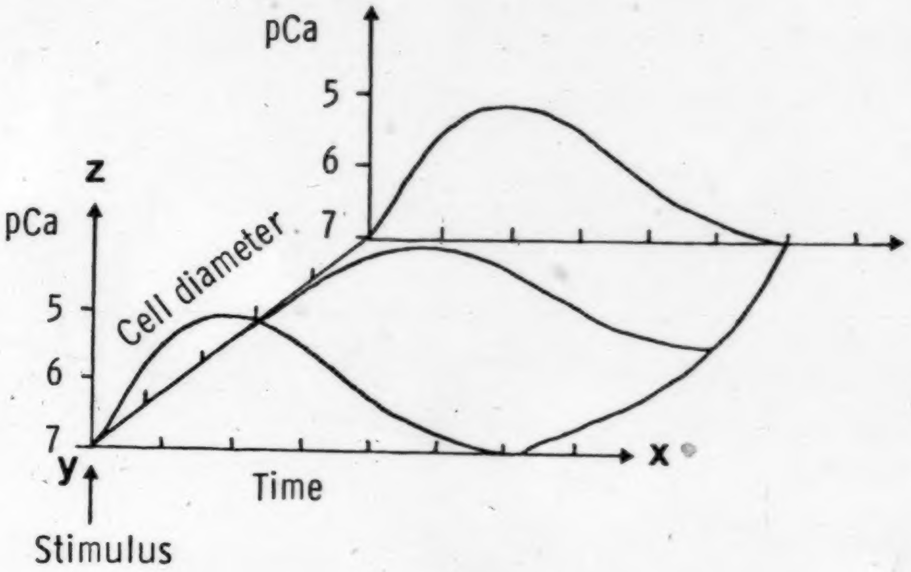

Fig. I.3 Variations in the intracellular calcium concentration as a function of time following a stimulus (X axis) and the distance from the site of calcium entry (Y axis). The cell was considered spherical and the movement of calcium in the cytosol was assumed diffusional [Adapted from Kretsinger, 1979].

removed from equilibrium (resting state of the cell in our case). This may explain how irreversible events such as DNA transcription and cell division could occur. A negative feedback mechanism is present in the excited state of a cell and is represented by the sum of all the calcium translocation mechanisms mentioned earlier (Fig. I.2). One can reason that a competition between both feedback mechanisms will modulate the cellular level of calcium. In summary, the cytosolic level of calcium adopts a cyclic pattern as a function of time which induces either the *resting* state (10^{-7}M Ca^{2+}) or the *excited* state (10^{-5}M Ca^{2+}) of the cell.

C. ROLES OF CALCIUM IN LIVING SYSTEMS

One can assign at least 3 major roles to calcium.

1) Structural role: The high levels of cellular anions (Table I-1) and the chemical properties of Ca(II) favoring the formation of insoluble compounds with PO_4^{3-}, CO_3^{2-}, $C_2O_4^{2-}$, represent the basic factors behind the formation of bones and shells. Calcium can also play a structural role at the protein level. For example, osteocalcin (Hauschka and Carr, 1982) is a 47- to 51-amino acid long protein containing 3 γ-carboxyglutamic acid residues. It possesses a modest affinity for ionic calcium

(*Kd* of 8 x 10^{-4} M; Hauschka and Gallop, 1977) but exhibits a strong binding to calcium phosphate surfaces . Its α-helical content increases from 8 to 38% in the presence of calcium (Hauschka and Carr, 1982). Similarly, calcium binding to thermolysin affects the thermal stability of this proteolytic enzyme (Feder *et al.*, 1971; Matthews *et al.*, 1974). Finally, calcium is known to interact with negatively charged phospholipids such as phosphatidyl serine and phosphatidic acid and influence membrane fusion properties.

2) Calcium as a protein cofactor: The role of Ca^{2+} as a cofactor appears limited to extracellular enzymes. Such a requirement is best exemplified by the esterolytic enzyme phospholipase A_2 (Verheij *et al.*, 1980) which cleaves the ester bond at the 2-acyl position of phosphoglycerides (Fig. I.4a). The calcium binding site lies close to the active site and the proposed catalytic mechanism involves a ternary complex (Ca^{2+}, protein, phosphoglyceride) where calcium interacts with the phosphate moiety of the phosphoglyceride (Verheij *et al.*, 1980, Dijkstra *et al.*, 1981)(Fig. I.4b). Such a cofactor role for calcium was also observed in the case of the enzyme staphylococcus nuclease (Cotton *et al.*, 1971) where again the cation is in proximity to the active site. The catalytic mechanism however remains to be elucidated.

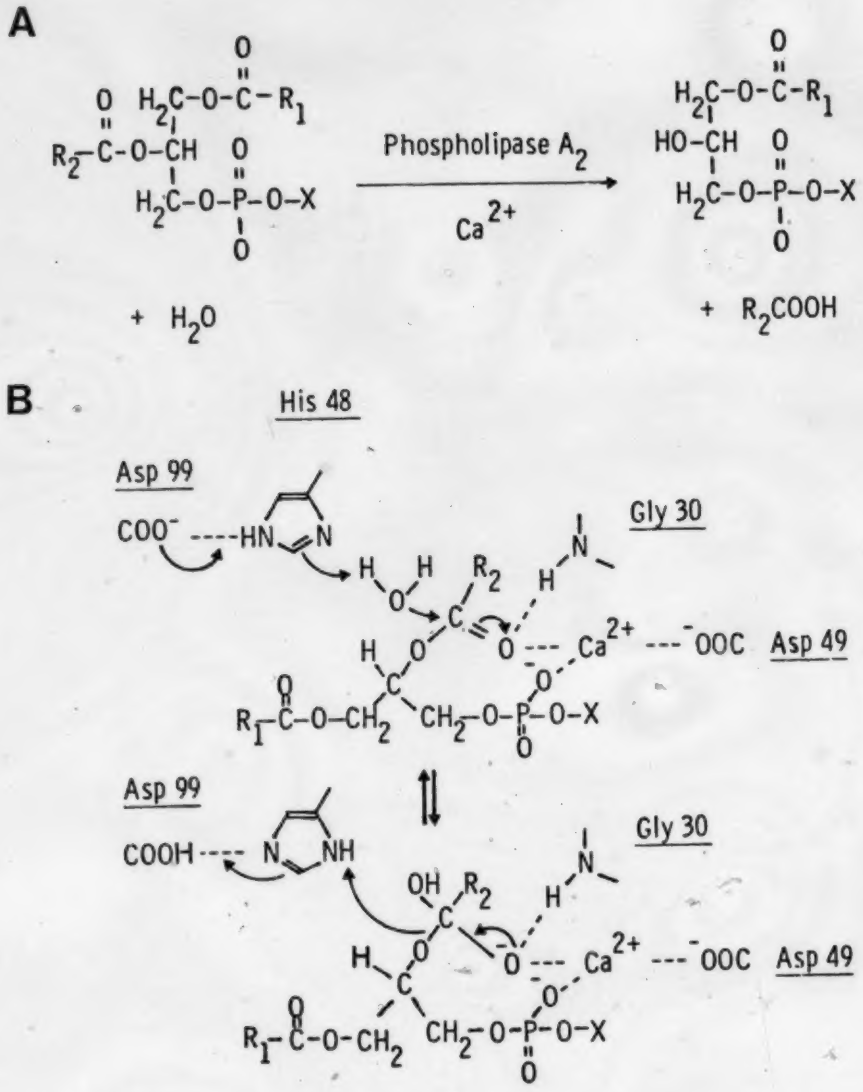
A
Phospholipase A2
Ca2+
+ H2O
+ R2COOH
B
His 48
Asp 99
Gly 30
Asp 49
COO-
HN
N
Ca2+
-OOC
COOH
NH
X

Fig. I.4 Example of calcium acting as a cofactor in the catalytic mechanism of pancreatic phospholipase A_2.
(A) Reaction catalysed by phospholipase A_2.
(B) Catalytic mechanism proposed by Verheij *et al.*, 1980.

3) Calcium as an intracellular regulator: This role concerns a network of regulatory proteins which have become synchronized to the cytosolic level of calcium. Calmodulin (Cheung, 1970) and its specialized version, troponin C (thin filament regulation of muscle contraction; Ebashi *et al.*, 1968) both possess several calcium binding sites sensitive to calcium concentrations of the order of 10^{-6}M. When a cell undergoes a transition from resting (10^{-7}M) to excited state (10^{-5}M), the secondary and tertiary structure of these proteins is altered to permit their interaction with regulatory proteins and enzymes and modulate their activity.

Calcium represents an essential element of the cellular second messenger system (Wang and Waisman, 1979). In the last decade, investigators have characterized some of the biochemical pathways modulated by calcium. However, the triggering mechanism which occurs during the initial interaction of calcium with calmodulin or other homologous proteins remains poorly understood. In the last few years, our group has focused its attention on this particular aspect of the calcium modulation scheme. Two major questions relevant to this mechanism can be formulated as follows:

1.) Why was calcium selected for this messenger role ?

This question remains largely unanswered although part of the solution lies in the chemistry of calcium. This aspect will be discussed in the next section.

2.) What structural features of calmodulin and other homologous proteins make them suitable to translate this chemical signal (i.e. calcium) into a biochemical one ?

Calcium binding to these proteins results in an increase in their α-helical content (van Eerd and Kawasaki, 1972; Kawasaki and van Eerd, 1972; Burtnick and Kay, 1976, 1977; Klee, 1977; Wolff *et al*., 1977; Leavis and Kraft, 1978; Nagy and Gergely, 1979) and the exposure of hydrophobic regions (Johnson *et al*., 1978, 1983; LaPorte *et al*., 1980; Tanaka and Hidaka, 1980, 1981) thought to interact with target proteins. This question will be discussed later in light of structural information gathered on these proteins.

D. CHEMISTRY OF CALCIUM

It is reasonable to assume that the appearance of calcium preceeded by orders of magnitude in time, the occurence of proteins and other complex organic molecules. The structural features adopted by calcium binding proteins have thus evolved to match the physical and chemical properties of the calcium ion. Several cations that have analogous properties to calcium are either present in trace quantities or form insoluble complexes in an aqueous environment (i.e. lanthanides). In the case of sea water

(Fig. I.1a), one realizes that besides Ca^{2+}, sodium, potassium and magnesium are all present in elevated concentrations. Since the composition of this medium has probably remained unchanged through history and represents the environment of choice for the evolution of biological organisms, one may assume that the cations Na^{+}, K^{+}, and Mg^{2+} represented natural constraints in terms of ionic radius, cation charge and choice of possible coordinating ligands imposed on the evolutionary development of calcium binding proteins.

1. Metals and ligands

Ahrland *et al.* (1958) have classified ligands and metal ions according to their preferential bonding properties. Class A metal ions include alkali and alkali earth metals such as Li^{+}, Na^{+}, K^{+}, Mg^{2+}, Ca^{2+} and a variety of higher oxidation state metals such as trivalent lanthanide ions. Class B are represented by heavy transition metals in lower oxidation states (i.e. Cu^{+}, Ag^{+}, Hg^{+} and Hg^{2+}). Ligands were classified according to their preference for class A or B. Pearson (1963,1968) suggested the term *hard* and *soft* to characterize the members of class A and B. The author proposed the rule of thumb that a hard acid like Ca^{2+} prefers to bind to hard bases like nitrogen, oxygen and small electronegative halide ligands. The theoretical basis for hard-hard interactions is that they are primarily the result of electrostatic or ionic effects as opposed to the covalent character (softness) arising from the presence of unpaired *d* electrons.

Another important factor in the calcium chemistry is illustrated by the Irving-Williams series (Fig. I.5) where alkali earths (i.e. Mg^{2+} and Ca^{2+}) preferably bind to ligands in the order O>N>S. Williams (1970) summarized in general terms, the selectivity of Na^+, K^+, Mg^{2+} and Ca^{2+} for simple binding sites in order to highlight features relevant to their biochemical roles. Firstly, Mg^{2+} is bound preferentially by nitrogen bases so that for multiligand sites containing nitrogen ligands, the order of complex stability will be $Mg^{2+} > Ca^{2+} > Na^+ > K^+$ and thus sites showing a preference for Mg^{2+} often include at least one nitrogen. Secondly, calcium interacts preferentially with multidentate anions and strong acid anions (order of complex stability; $Ca^{2+} > Mg^{2+} > Na^+ > K^+$) and in contrast to preferred Mg^{2+} sites, the ligands are predominantly phosphate, carboxylate and sulphonate ones with no nitrogen ligands present. Finally, magnesium and calcium demonstrate a tighter binding to multiligand sites as compared to sodium and potassium.

2. Radius ratio, r^+/r^-

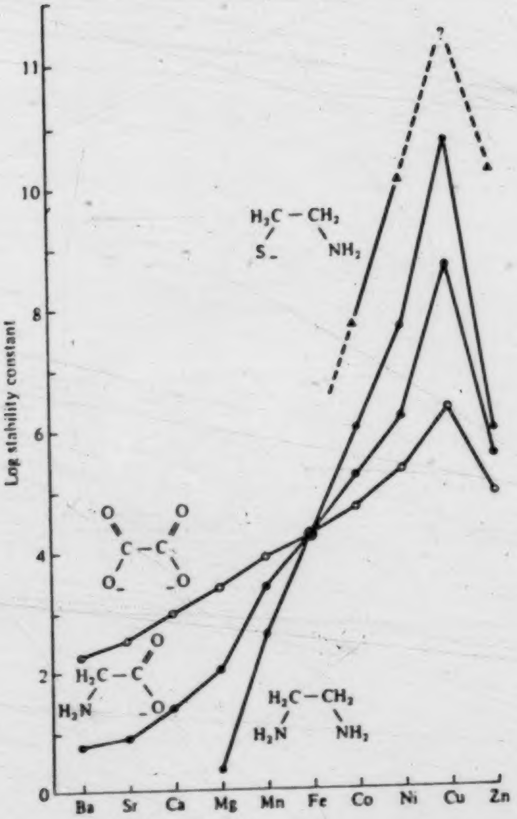

Fig. I.5 The Irwing-Williams effect. The stability of the complexes formed increases through the series Ba-Cu. In the case of magnesium and calcium, the stability constant of the complexes formed also increases as one goes from nitrogen ligands to oxygen ones [Adapted from Sigel and McCormick, 1970 and Huheey, 1972].

Since alkali and alkali earth metals are involved in electrostatic interactions with ligands, their charge and ionic radius represent important factors in bonding. The radius ratio (r^+/r^-) of a metal ligand complex is simply the ratio of the ionic radius of the metal ion over the radius of the ligand involved. This quantity is useful in estimating the preferred geometry or coordination number of hard acids, since it indicates packing requirements for ligands around the cation (Huheey, 1972). For example, Fig. I.6a illustrates an octahedral arrangement of hydroxide ligands around a Ca^{2+} ion (Busing and Levy, 1957). The calculated r^+/r^- value is of 0.71. Figure I.6b points out that the minimal r^+/r^- value for an octahedral arrangement is equal to 0.414. From packing considerations, one can thus calculated the limiting radius ratio for various geometries (Fig. I.6c). In conclusion, one realizes that a r^+/r^- value of 0.71 suggests that the hydroxide ligands are octahedrally arranged around the calcium ion.

3. Charge effect

One can appreciate the effect of cation charge on the stability of the resulting complex by estimating the energy involved in bringing six hydroxide ligands and a calcium ion into the geometry diagrammed in Fig. I.6a. In the case of a crystal structure, this quantity is known as the lattice

A

B

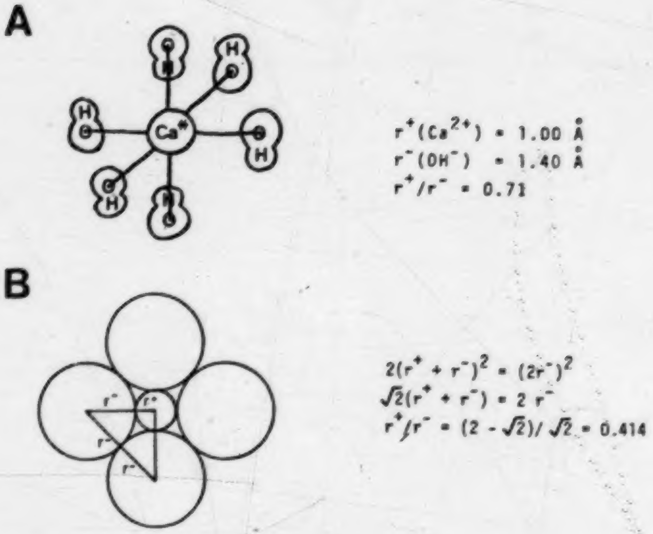

$r^+(Ca^{2+}) = 1.00$ Å
$r^-(OH^-) = 1.40$ Å
$r^+/r^- = 0.71$

$$2(r^+ + r^-)^2 = (2r^-)^2$$
$$\sqrt{2}(r^+ + r^-) = 2r^-$$
$$r^+/r^- = (2 - \sqrt{2})/\sqrt{2} = 0.414$$

C

Coordination number	Geometry	Limiting radius ratio (r^+/r^-)
2	Linear	
		0.155
3	Trigonal	
		0.225
4	Tetrahedral	
		0.414
4	Square planar	
6	Octahedral	
		0.732
8	Cubic	
		1.000
12	Dodecahedral	

Fig. I.6 (A) Octahedral arrangement of hydroxide ligands around calcium in $Ca(OH)_2$ [Adapted from Busing and Levy, 1957]. (B) Determination of the minimal r^+/r^- value for an octahedral arrangement of ligands around a cation. (C) Minimal values of radius ratio as a function of packing geometry.

energy U and can be approximated as follows:
The electrostatic energy involved between cation and ligands can be calculated from the relation

$$E_e = Ne^2/4\pi\varepsilon_0 \quad (6Z^+Z^-/r_o + 3Z^-Z^-/r_o + 12Z^-Z^-/\sqrt{2}\, r_o)$$

where $Ne^2/4\pi\varepsilon_0$ is equal to 1389 $kJmol^{-1}$Å, Z^- and Z^+ represents the charge of the ligand and metal respectively while r_o is the sum of the cation and ligand radii (1.00 Å + 1.40 Å). Repulsive forces arising from the ligand proximity to the electron cloud of the cation will contribute positively to the lattice energy by a factor equal to

$$E_r = NB/r^n$$

where N and B are constants and r represents the distance between both ions.

At an equilibrium distance (where $r = r_o$), the net lattice energy U will reach a minimum represented by the difference between attractive and repulsive energies

$$U = \{-2.0147\ Ne^2/4\pi\varepsilon_0 r_0\} + NB/r_o^{\,n}$$

The value B can be solved by differentiating this expression with respect to r and yields the value

$$B = \{2.0147\ e^2/4\pi\varepsilon_0 n\}\ r_o^{\,n-1}$$

and the term U can be simplified to

$$U = \left\{ -2.0147\ Ne^2/4\pi\varepsilon_0 r_0 \right\} \quad (1 - [1/n])$$

where n has a value between 9 and 10 and signifies that the repulsion term only contributes about a 10% decrease in this case to the minimal U value of the complex. Since we know the ionic radius of calcium (1.00 Å) and of the hydroxide ligand (1.40 Å; Waddington, 1959), the quantity r_0 can be calculated and U can be estimated to be about -1050 $KJmol^{-1}$. Assuming a hypothetical increase in the cation charge to +3 with no appreciable change in the metal ionic radius, then the factor $6Z^-Z^+/r_0$ becomes equal to $-18/r_0$ instead of $-12/r_0$ (as in the case of +2) and results in a final value for U of -2,400 $KJmol^{-1}$.

One can thus appreciate that for the octahedral arrangement presented in Fig. I.6a, an increase in the metal charge of 1 produces a 1.5 fold increase in the minimal energy of the complex. One should however keep in mind that the charge of the anions or changes in ionic radius of either ligands or cation will affect the coordination number of the complex and alter correspondingly its potential energy.

4. Mechanism of complex formation

The formation of a calcium complex involves several steps. Figure I.7 indicates that in the initial event (step A), an incoming ligand will form an ion pair with the hydrated cation. This association is termed an *outer-sphere* complex and is strictly a diffusion-controlled event. Following step A, the cation loses a water molecule from its *inner-sphere* complex. This dehydration step (step B) represents the main energy barrier to the formation of a calcium:protein complex and is rate limiting. The overall mechanism is often described as a S*n*1 mechanism in view of the dehydration step (unimolecular nucleophilic substitution; Taube and Posey, 1953; Eigen and Wilkins, 1965). Finally, the incoming ligand integrates the *inner-sphere* complex of the metal (step C). Since proteins can be considered as multidentate ligands, the calcium:protein complex will probably require a further dehydration of the cation which then may be promoted by the microenvironment of the protein (Reid and Hodges, 1980).

5. Dehydration and complexation properties of Ca^{2+}

Since the rate limiting step in the formation of a calcium:protein complex is the substitution of a water molecule from the calcium *inner-sphere* complex, one should investigate some of the dehydration properties of alkali earths. Figure I.8 lists the characteristic rate constants (sec^{-1}) observed for the substitution of water molecules from the *inner-sphere* of metal ions (Eigen, 1963; Winkler, 1972). One notices that water substitution rates generally

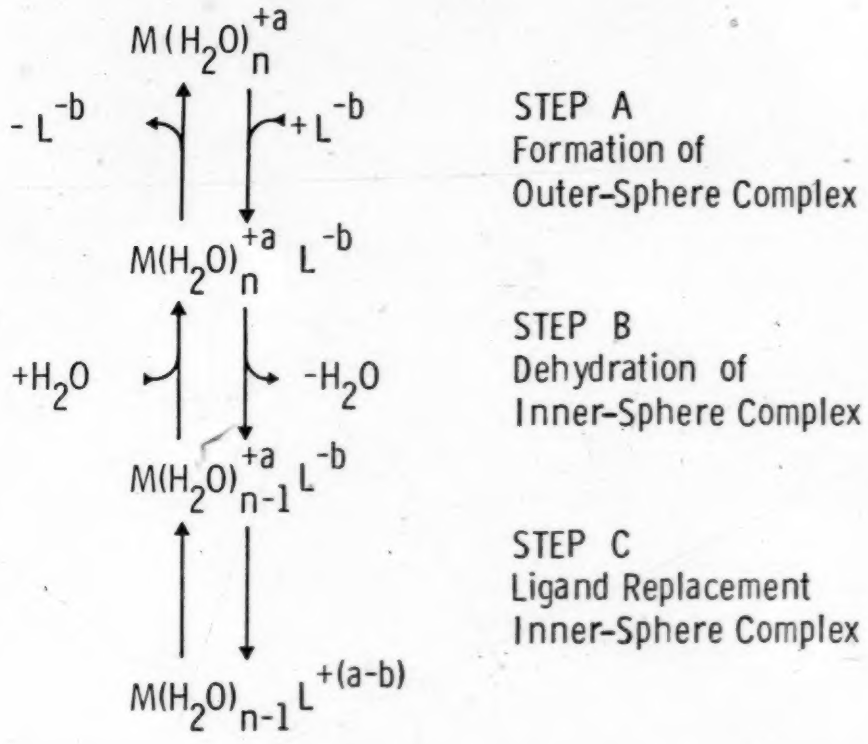
M(H2O)n +a
- L -b
+ L -b
STEP A
Formation of
Outer-Sphere Complex
M(H2O)n +a L -b
+H2O
-H2O
STEP B
Dehydration of
Inner-Sphere Complex
M(H2O)n-1 +a L -b
STEP C
Ligand Replacement
Inner-Sphere Complex
M(H2O)n-1 L +(a-b)

Fig. I.7 Metal:protein complex formation. Description of an S_N1 mechanism for the replacement of a cation (M) hydration sphere with protein or peptide ligands (L) [Eigen and Wilkins, 1965]. $M(H_2O)_n^{+a}\ L^{-b}$ is designated as the outer-sphere complex or the ion pair and $M(H_2O)_{n-1}L^{+(a-b)}$ is the inner-sphere complex. The reaction proceeds via an outer-sphere complex [Adapted from Reid and Hodges, 1980].

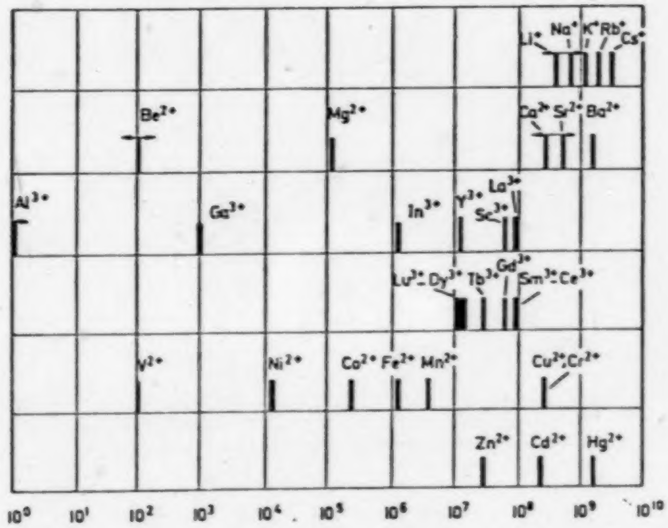

Fig. I.8 Characteristic rate constants (sec^{-1})for the substitution of water molecules from the inner sphere of metal ions [Taken from Winkler, 1972].

decrease with increasing charge and decreasing size of the metal ion. This observation is further emphasized in Table I-2, where an increase in the charge density of alkali and alkali earths correlates with a rapid decrease in their metal:water substitution rates. For example, Mg^{2+} displays a substitution rate for water molecules that is three orders of magnitude slower than in the case of Ca^{2+}, thus water molecules are tightly bound to Mg^{2+} as compared to calcium (a cation of equivalent charge). The difference in dehydration properties between these two metals becomes a crucial factor in the thin filament regulation of striated muscle tissue where parvalbumin and troponin C compete for the available calcium in the cytosol.

Key factors that contribute to the stability of a calcium:protein complex in solution are a) the type of ligands coordinating the calcium ion and b) the free energy of hydration of this cation (ΔGa; Table I-2). We will discuss in the next section that the Ca^{2+}-binding sites on proteins are composed of multidentate oxygen ligands and as described earlier will preferentially bind Ca^{2+} and Mg^{2+} over K^{+} and Na^{+} ions (Williams, 1970). However, even if a calcium ion is dehydrated faster than a magnesium ion, the resulting calcium:protein complex may be thermodynamically less favorable than the magnesium one. One should thus analyse the free energy involved in generating these

TABLE I-2

Some chemical and physical properties of Group IA and IIA cations

Cation	Ionic radius[a] (Å)	Charge density[b] (Å^{-3})	$-\Delta G_a$[c] (KJ/mole)	Metal:water[d] substitution rate (sec^{-1})
Li^+	0.76	0.54	511	∿ 5×10^8
Na^+	1.02	0.23	412	∿ 8×10^8
K^+	1.38	0.09	337	∿ 1×10^9
Be^{2+}	0.45	5.24	2436	∿ 1×10^2
Mg^{2+}	0.72	1.28	1900	∿ 1×10^5
Ca^{2+}	1.00	0.48	1587	∿ 1×10^8

[a] The values given correspond to cation complexes having a coordination number of 6. Taken from Shannon, 1976.

[b] Represent the charge to volume ratio where the volume of each cation was calculated from the given ionic radius.

[c] Taken from Lehn, 1973.

[d] Values are estimates taken from Fig. I.8 [from Winkler, 1972].

complexes.

The formation of a metal:protein complex in aqueous solution is described by the following equilibrium

$$M^{n+}(H_2O)x \; + \; P \rightleftarrows M^{n+}P(H_2O)y \; + \; (x-y)H_2O$$

The free energy term (ΔG) for this equilibrium can be approximated by $\Delta G = \Delta G b - \Delta G a$ where $\Delta G a$ is the free energy of hydration of the cation (Table I-2) and $\Delta G b$, the free energy for the protein:metal complex formation. The term ΔG is related to the equilibrium constant (*Keq*) for the complex formation by the relation

$$\Delta G = -RT \ln(Keq)$$

and can also be described as a function of the effective radius ra of a complex by the relation

$$\Delta G = -[B/(ra + \alpha)] + [A/ra]$$

where ra is the sum of the cation ionic radius and the effective radius of coordinated water molecules (0.85 Å); A and B are constants associated with the charges involved in the water:cation and the protein:cation complexes; and α represents the difference between the effective radius of coordinated water molecules and the radius of the incoming ligand (Williams, 1970; Ochiai, 1977). In the case of ligands such as CO$_3^{2-}$, PO$_4^{3-}$ and EDTA , the quantity B is larger than A and the resulting ΔG value is negative and becomes increasingly negative as ra becomes larger. Thus Ca^{2+} complexes involving these types of ligands possess an higher stability constant than the corresponding Mg^{2+} complexes.

In conclusion, a Ca^{2+} ion loses its coordinating water molecules more easily than a Mg^{2+} ion does. In addition, calcium complexes involving polydentate ligands composed of carboxyl type ligands, exibit a greater stability constant than similar Mg^{2+} complexes do.

E. STRUCTURE AND FUNCTION OF CALCIUM BINDING PROTEINS

Several proteins have one or several calcium binding sites. Thermolysin has four such sites (Matthews *et al.*, 1974), while trypsin (Bode and Schwager, 1975) and phospholipase A$_2$ (Verheij *et al.*, 1980) are enzymes possessing a single cation binding domain. Stereoprojections of their calcium binding regions (Fig. I.9) illustrate the following common features:

a) only oxygen ligands coordinate the metal, in agreement with the preferred order of calcium ligands mentioned previously,

b) oxygen ligands are contributed either by carboxylic

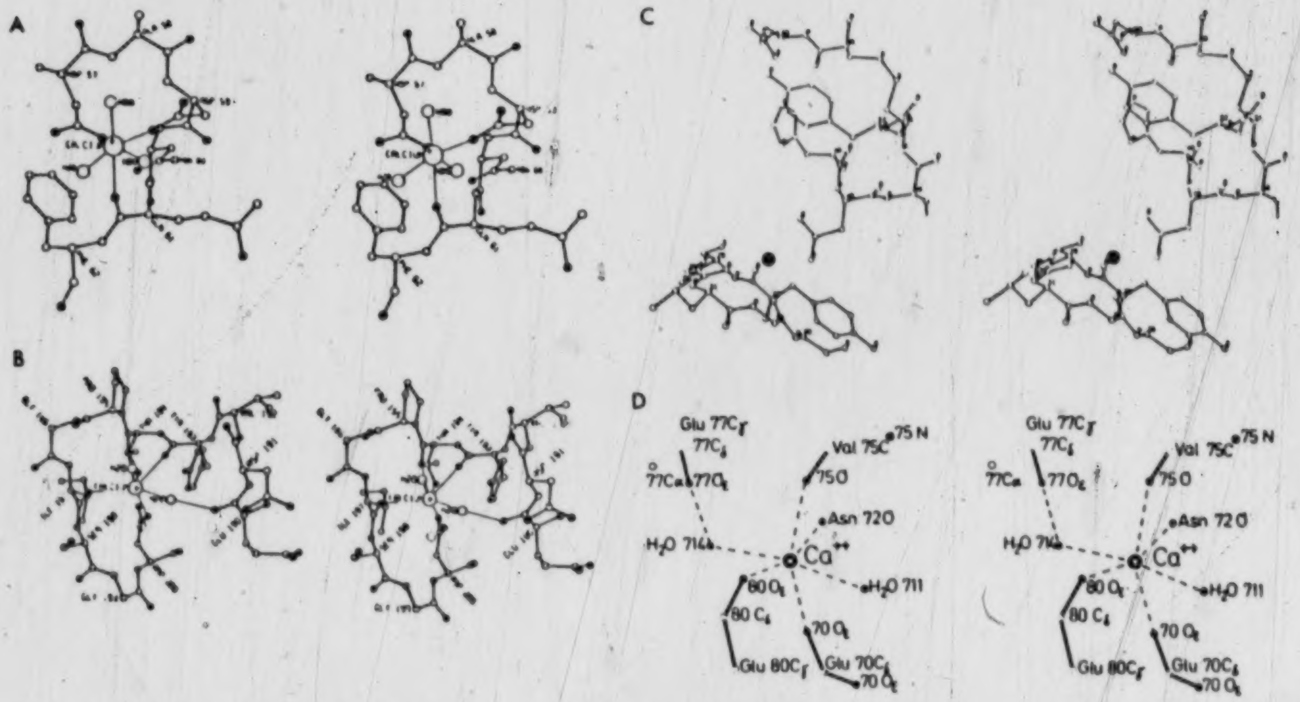
A
B
C
D
Glu 77Cγ
77Cδ
77Cα
77Oε
Val 75C
75N
75O
Asn 72O
H₂O 714
Ca++
H₂O 711
80Oε
80Cδ
Glu 80Cγ
70Oε
Glu 70Cδ
70Oε

Fig. I.9 Stereoprojections of various calcium binding sites in proteins. (A) and (B) are stereoprojections of the third and fourth calcium binding sites of the proteolytic enzyme thermolysin [Taken from Matthews *et al.*, 1974]. (C) Stereoprojection of the calcium binding site of bovine pancreatic phospholipase A_2 [Taken from Verheij *et al.*, 1980]. The calcium ion is bound to the side chain of Asp-49, to the carbonyl oxygen atoms of Tyr-28, Gly-30 and Gly-32 and to two or three water molecules. ●, calcium ion. (D) Stereoprojection of the calcium binding site of bovine β-trypsin [Taken from Bode and Schwager, 1975].

side chains of aspartic and glutamic acid residues, non ionic side chains from asparagine and glutamine residues, hydroxyl groups of serine and threonine, peptide backbone carbonyl groups or simply from bound water molecules,

c) the preferred calcium coordination number is 6 and the calcium binding site adopts a distorted octahedral geometry around the cation.

The calcium association constants determined for these various calcium binding sites differ significantly however. In the case of the four sites of thermolysin, the pK*ca* values range from 4.7 to >6 (Matthews *et al*., 1974; Voordouw and Roche, 1975). A tabulation of the binding affinities of several sites and the composition of ligands making up the coordination sphere suggests that no correlation exists between the number of carboxyl ligands (-COOH) and the calcium binding affinity of a site (Kretsinger, 1976).

1. Criteria for calcium regulation

Calcium regulation exists at the cytosolic level where the calcium concentration fluctuates from 10^{-7}M (resting state) to 10^{-5}M (excited state). The enzymes described previously are extracellular and function only in their calcium bound state since the large content of calcium in the extracellular environment ($\sim 10^{-3}$M) will saturate their calcium binding sites.

The following equilibrium,

$$Ca^{2+} + P \rightleftarrows PCa^{2+}$$

where P and PCa^{2+} represent the apopeptide and the calcium bound peptide states, possesses an association constant K_{Ca} defined by,

$$K_{Ca} = \frac{[PCa^{2+}]}{[Ca^{2+}][P]}$$

Developing this expression in a form similar to the Henderson-Hasselbach relation yields,

$$pCa = pK_{Ca} + \log [PCa^{2+}]/[P]$$

If one uses the boundary conditions that pCa varies from 7 to 5 and that a calcium binding protein adopts either a metal-bound or a metal-free conformation at these two extremes in pCa values (5 and 7), then the optimal pK_{Ca} value for a calcium binding site should be equal to 6. The pCa values of 5 and 7 represent only estimates, and may well fluctuate between 4 to 5 and 7 to 8 respectively. Several calcium binding proteins present in the cytosol offer sites having a pK_{Ca} value around 6. However, many of them can be regrouped under the same protein family since they possess homologous calcium binding domains known as EF hand regions (Kretsinger and Nockolds, 1973).

2. Concept of the EF hand domain

Parvalbumin is a small acidic protein (~11,000-12,000 daltons) isolated from lower vertebrate muscles (Hamoir and Konosu, 1965; Pechère and Focant, 1965; Pechère *et al*., 1971) that binds two moles of calcium per mole of protein (Pechère *et al*., 1971; Benzonana *et al*., 1972; Nockolds *et al*., 1972). The determination of the primary sequence (Coffee and Bradshaw, 1973) and the crystal structure (Kretsinger and Nockolds, 1973) of carp parvalbumin has permitted the analysis of its two calcium binding sites. Both sites are homologous in their sequence and their tridimensional structure. Each calcium binding site is composed of a linear sequence of 30 to 35 amino acids where the N- and C-terminal α-helical regions are approximatively perpendicular to each other and are flanking a 12-residue calcium binding loop. Kretsinger and Nockolds (1973) suggested the term *EF hand* to depict these sites following their original crystallographic work on carp parvalbumin where the second calcium binding site was composed of E- and F- terminal helical regions represented by the index and the thumb of a right hand. Figure I.10 illustrates a two- (A) and a three-dimensional (B) representation of an EF hand.

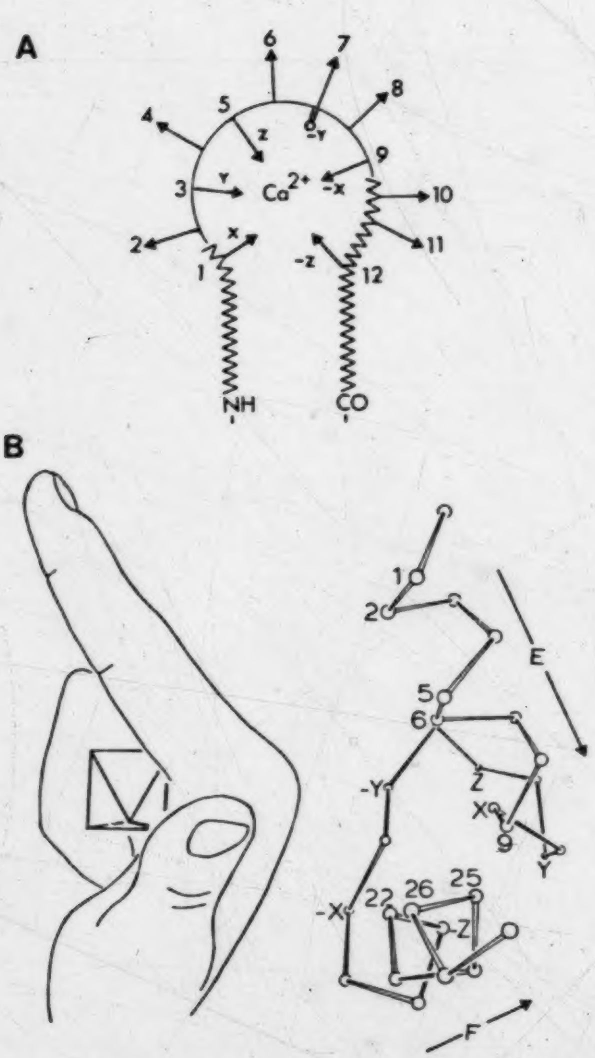

Fig. I.10 Representation of a model EF hand.
(A) A two-dimensional representation of a *helix-loop-helix* site. The jagged lines indicate the N- and C-terminal helical regions. These regions are flanking a 12-residue long calcium binding loop (labelled from 1 through 12). The calcium coordinating residues in the sequence occupy positions 1 (X),3 (Y),5 (Z),7 (-Y),9 (-X) and 12 (-Z). The side chain of the residue in position 7 (-Y) does not chelate calcium and is replaced by the peptide carbonyl oxygen from this residue [Adapted from Reid and Hodges, 1980].
(B) A tridimensional representation of the EF hand of carp parvalbumin along its α-carbon backbone [Taken from Kretsinger, 1977]. The E- and F-helical regions are approximatively perpendicular to each other as illustrated by the index and thumb of a right hand.

Note that the α-helical regions are partly initiated in the calcium binding loop.

The primary sequence of rabbit skeletal troponin C (Collins *et al.*, 1973; Collins *et al.*, 1977) and of some myosin light chains (Frank and Weeds, 1974; Collins, 1976; Jakes and Kendrick-Jones, 1976) were solved soon after the initial work on parvalbumins.. It was established from sequence homologies to parvalbumins that all these proteins possess EF hand sites.

To date, at least six families of EF hand containing proteins have been established: parvalbumins, troponin C's, calmodulins, myosin light chains, intestinal calcium binding proteins and the brain specific S-100 proteins. Other proteins such as the tumour calcium binding protein, oncolmodulin (MacManus, 1981), the human and rat brain calcium binding proteins (Baimbridge *et al.*, 1980, 1982) and the smooth muscle protein, leiotonin C (Mikawa *et al.*, 1978) may soon prove to be part of the superfamily of EF hand containing proteins. Two evolutionary trees have been constructed from the available sequences of EF hand containing proteins (Barker *et al.*, 1977, 1978; Goodman *et al.*, 1979; Goodman, 1980; Fig. I.11). The branching of these trees differs significantly due to the methods adopted to construct them (Dayhoff, 1976). However, both approaches

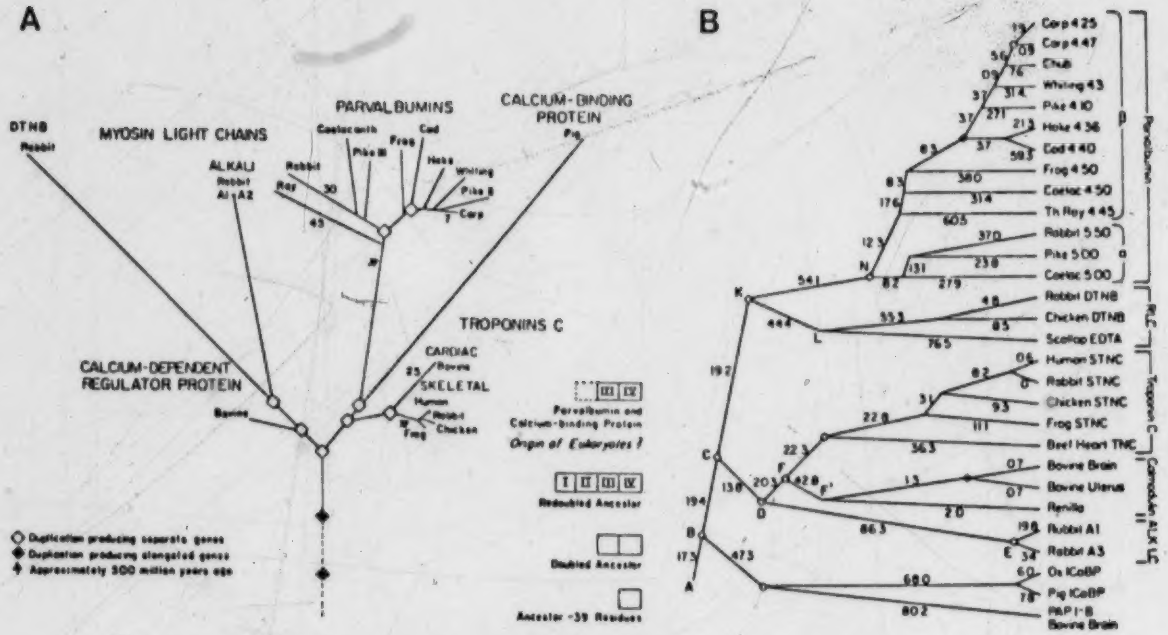
A
DTNB
Rabbit
MYOSIN LIGHT CHAINS
ALKALI
Rabbit
A1+A2
PARVALBUMINS
Coelacanth
Pike III
Frog
Cod
Hake
Whiting
Pike II
Carp
Rabbit
Ray
30
45
CALCIUM-BINDING
PROTEIN
Pig
TROPONINS C
CARDIAC
Bovine
25
SKELETAL
Human
Rabbit
Chicken
Frog
CALCIUM-DEPENDENT
REGULATOR PROTEIN
Bovine
Duplication producing separate genes
Duplication producing elongated genes
Approximately 500 million years ago
Parvalbumin and
Calcium-binding Protein
Origin of Eukaryotes ?
Redoubled Ancestor
Doubled Ancestor
Ancestor ~35 Residues
B
Carp 4.25
Carp 4.47
Chub
Whiting 4.3
Pike 4.10
Hake 4.36
Cod 4.40
Frog 4.50
Coelac 4.50
Th Ray 4.45
Rabbit 5.50
Pike 5.00
Coelac 5.00
Rabbit DTNB
Chicken DTNB
Scallop EDTA
Human STNC
Rabbit STNC
Chicken STNC
Frog STNC
Beef Heart TNC
Bovine Brain
Bovine Uterus
Renilla
Rabbit A1
Rabbit A3
Ox ICaBP
Pig ICaBP
PAP I-B
Bovine Brain
Parvalbumin
β
α
RLC
Troponin C
Calmodulin
ALK LC
A
B
C
D
E
F
F'
K
L
N

Fig. I.11 Evolutionary trees of EF hand containing proteins.
(A) Evolutionary tree proposed by Barker *et al.*, 1978. The numbers listed in the tree represent the number of accepted point mutations per 100 residues.
(B) Genealogical tree proposed by Goodman, 1980. The numbers on the links are nucleotide replacements per 100 codons. ◇, obvious gene duplication; ◆, circumstantial evidence for gene duplication.

suggest that an ancestral gene coding for a primordial 40-amino acid long calcium binding domain underwent 2 successive gene duplications to produce a four-domain protein with domain I genetically closer to III, and II to IV. Gene deletions and mutations are thought to have led to proteins with altered EF domains such as;

a) defunct and deleted sites in cardiac troponin C and parvalbumin, or

b) distorted sites through insertion or deletion of residues as in the case of myosin light chains, S-100 proteins and intestinal calcium binding proteins, or

c) substitutions generating high-affinity calcium binding sites as exemplified by site III and IV of troponin C and by the parvalbumin CD and EF sites.

In view of the diversity of proteins containing such sites, it is instructive to briefly highlight structural and functional aspects surrounding each of the six major protein families involved.

3. Structure and function of EF hand containing proteins

a. Calmodulin

Calmodulin (CaM) is a small acidic protein distributed in a broad variety of tissues and species and appears to regulate a constantly increasing number of cellular processes (see reviews by Wang and Waisman, 1979; Scharff, 1981; Means *et al.*, 1982). Figure I.12 points out that calmodulin action lies in its ability to modulate the activity of a wide range of enzymes. This protein was first described by Cheung (1970) and Kakiuchi *et al.* (1970) as a required factor for the activation of a calcium-dependent phosphodiesterase, while Teo and Wang (1973) demonstrated that this activator was a calcium binding protein. Calmodulin action can be described by the following general scheme

$$\mathrm{Ca^{2+}} + \mathrm{CaM} \rightleftarrows \mathrm{CaM{\sim}Ca^{2+}} \qquad (1)$$

$$\mathrm{CaM{\sim}Ca^{2+}} + \mathrm{Enzyme(inactive)} \rightleftarrows \mathrm{CaM{\sim}Ca^{2+}{\sim}Enzyme(active)} \qquad (2)$$

Calmodulin is a 148 amino acid long protein (MW ~16,700 daltons) and possesses four calcium binding sites. The calculated calcium association constants for these sites on calmodulin are usually near $10^{6}\mathrm{M}^{-1}$ (Teo and Wang, 1973; Lin *et al.*, 1974; Watterson *et al.*, 1976; Klee, 1977), however values as high as $10^{7}\mathrm{M}^{-1}$ have been reported at low ionic strength (Wolff *et al.*, 1977). Wolff *et al.* also commented that in the presence of physiological levels of magnesium (~ mM range) and low ionic strength, calmodulin only binds 3 moles of calcium. Calmodulin may represent a subunit of a particular enzyme as in the case of myosin light chain

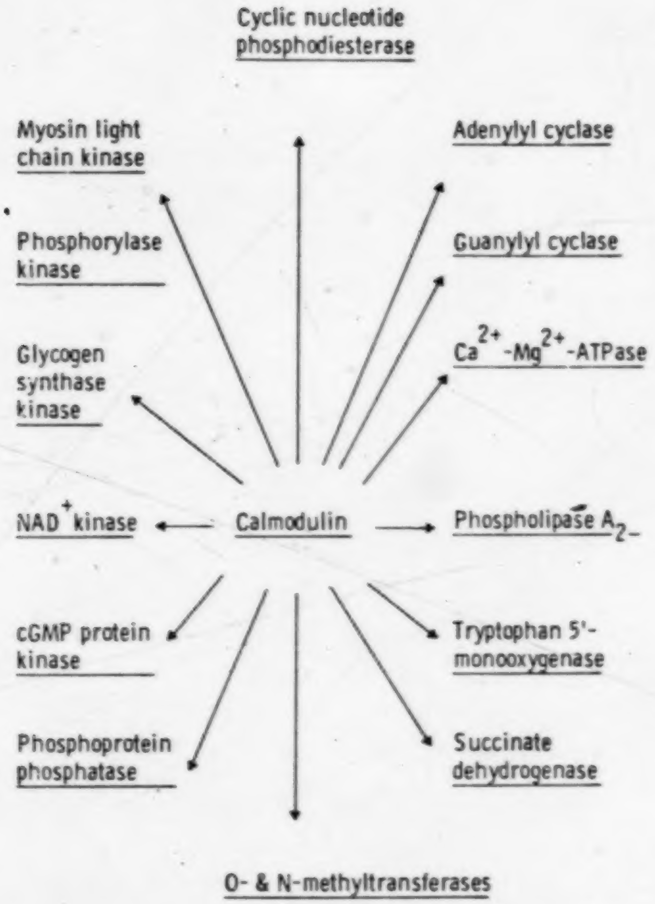
Cyclic nucleotide phosphodiesterase
Adenylyl cyclase
Guanylyl cyclase
Ca^{2+}-Mg^{2+}-ATPase
Phospholipase A_2
Tryptophan 5'-monooxygenase
Succinate dehydrogenase
O- & N-methyltransferases
Phosphoprotein phosphatase
cGMP protein kinase
NAD^+ kinase
Glycogen synthase kinase
Phosphorylase kinase
Myosin light chain kinase
Calmodulin

Fig. I.12 Calcium-calmodulin regulated enzymes [Adapted from Means *et al.*, 1982].

kinase (Dabrowska *et al.*, 1978) and glycogen phosphorylase kinase (Cohen *et al.*, 1978; Grand *et al.*, 1980) or it may interact with target proteins only in the presence of calcium. The amino acid sequences of bovine brain (Watterson *et al.*, 1980) and rat testis (Dedman *et al.*, 1978) calmodulins have been found to be virtually identical including the presence of the rare amino acid ε-N-trimethyllysine at position 115 (Jackson *et al.*, 1977). Only eleven amino acid substitutions and one deletion (position 146) have been observed in comparing the CaM primary sequence of the unicellular ciliated eukaryote *Tetrahymena Pyriformis* (Yazawa *et al.*, 1981) to the one obtained from bovine brain source, indicating that the primary sequence of calmodulin has withstood remarkably well evolutionary pressures (Iida, 1982).

b. Troponin C

The calcium binding protein troponin C is found in striated muscle cells (Ebashi and Endo, 1968) and is analogous in size (MW $\sim$18,000 daltons) and sequence to calmodulin (Collins *et al.*, 1977; Barker *et al.*, 1978). rabbit skeletal troponin C possesses two high-affinity (Ca^{2+},Mg^{2+}) binding sites ($\sim 10^{7} M^{-1}$) and two calcium-specific sites ($\sim 10^{5} M^{-1}$) (Potter and Gergely, 1975) while bovine cardiac troponin C possesses two high- and one low-affinity calcium binding sites (Burtnick and Kay, 1977; Hincke *et al.*, 1978; Leavis and Kraft, 1978; Holroyde *et al.*, 1980). Table I-3 lists the reported association constants for these two types of troponin C. Note that the presence of magnesium ions reduces the ability of the high-affinity sites to bind calcium.

Troponin C is part of an assembly of 3 subunit proteins forming the regulatory unit called the troponin complex (Tn). This complex is also composed of an inhibitory subunit called troponin I (TnI; MW ~21,000 daltons) which interacts with actin and inhibits the actomyosin ATPase activation. Troponin T (TnT; MW ~30,500 daltons), the third component of this complex exists in association with tropomyosin (TM), an α-helical rod-like protein occuring as a coiled-coil dimer. All three members of the troponin complex bind to each other. These four proteins (Tn + TM) through a network of interactions are responsible for the calcium regulation of striated muscle.

In summary, it is following the depolarization of the muscle fiber sarcolemma (muscle cell membrane) that the calcium concentration in the muscle cell rises above 10^{-6}M. Calcium binding to the calcium-specific sites of troponin C induces a change in its secondary structure and this structural change is communicated through the Tn/TM contacts

TABLE I-3

Calcium and magnesium binding constants for skeletal and cardiac Troponin C

	$[Mg^{2+}]$ (mM)	# of sites	K_{Ca} (M^{-1})	K_{Mg} (M^{-1})
Skeletal TnC[a]				
Troponin complex	-	2	5×10^{8}	
	-	2	5×10^{6}	
	2	4	5×10^{6}	5×10^{4}
Purified subunit	-	2	2×10^{7}	
	-	2	2×10^{5}	
	2	2	2×10^{6}	5×10^{3}
	2	2	2×10^{5}	
Cardiac TnC[b]				
Troponin complex	-	2	3×10^{8}	
	-	1	2×10^{6}	
	4	2	2×10^{7}	3×10^{3}
	4	1	2×10^{6}	
Purified subunit	-	2	1×10^{7}	
	-	1	2×10^{5}	
	4	2	4×10^{6}	0.7×10^{3}
	4	1	3×10^{5}	

[a] Taken from Potter and Gergely, 1975.

[b] Taken from Holroyde *et al.*, 1980.

to tropomyosin yielding its displacement toward the center of the F-actin groove (Fig. I.13a). Haselgrove (1972), Huxley (1972), Parry and Squire (1973) originally postulated the steric blocking hypothesis where the myosin head was prevented from interacting with the actin filament in the absence of calcium, by the presence of the Tn/TM unit. The actin-myosin interaction was made possible by the movement of the tropomyosin molecule in the presence of calcium (Fig. I.13a). Controversy still exists about the position of TM on the actin filament in relation to myosin (Moore *et al.*, 1970; Seymour and O'Brien, 1980). The recent analysis of image reconstruction patterns from electron micrographs of myofibrils, has indicated a two site contact of myosin with actin (Taylor and Amos, 1981; Amos *et al.*, 1982). Figure I.13b depicts some recent modifications made to the original concept proposed by Haselgrove, Huxley, Parry and Squire. Although reconstitution experiments have proven the importance of troponin and tropomyosin in the regulation of striated muscle contraction, the details of the regulatory mechanism remain unclear.

c. Parvalbumin

Parvalbumins represent a class of small acidic proteins (MW ~12,000 daltons) present at high concentrations (~ mM range; Baron *et al.*, 1975) in a variety of fish and

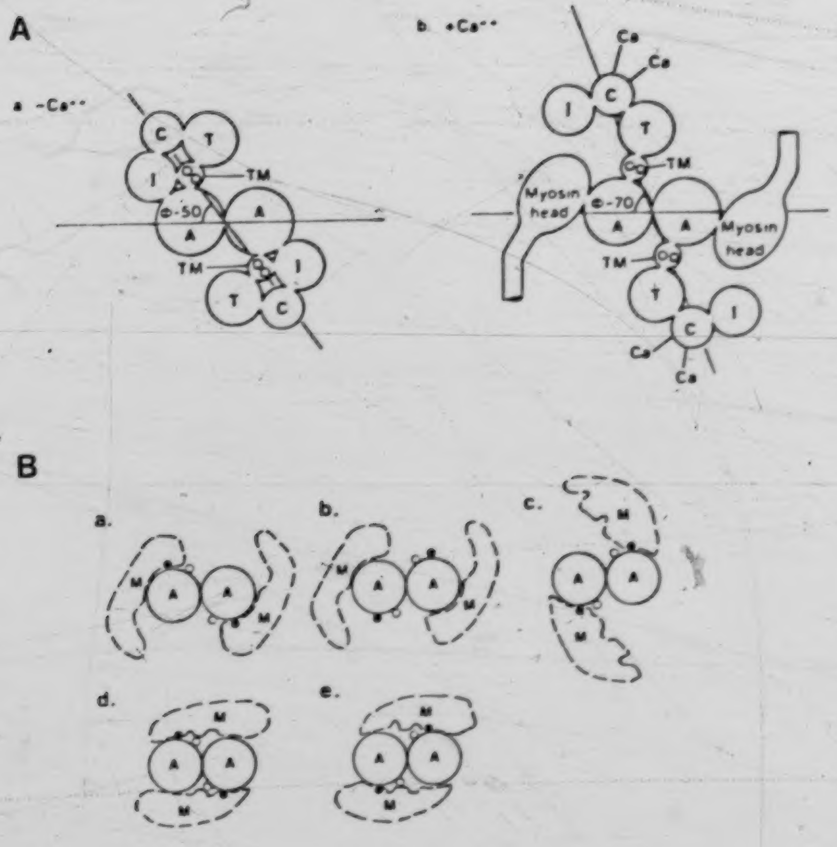

Fig. I.13 (A) The steric blocking model. This model has been suggested for the thin filament regulation of muscle contraction in striated muscle cells. A, actin; TM, tropomyosin; I, troponin I; C, troponin C; T, troponin T. In the absence of calcium (a), troponin I interacts with actin and prevents the interaction of the myosin head with actin. The binding of calcium to the regulatory sites of troponin C leads to the movement of tropomyosin toward the center of the actin groove (b) and permits the interaction of myosin with actin [Taken from McCubbin and Kay, 1980; adapted from Potter and Gergely, 1974].

(B) Evolution in the positioning and interaction of components involved in the mechanism of contraction in striated muscle. A, actin; M, myosin head; ●, tropomyosin position in the absence of calcium; ○, tropomyosin position in the presence of calcium. (a) adapted from Moore *et al.*, 1970, (b) adapted from Seymour and O'Brien, 1980, (c) adapted from Taylor and Amos, 1981, (d) and (e) adapted from Amos *et al.*, 1982.

amphibian fast muscle tissues (Deuticke, 1934; Hamoir *et al.*, 1965, 1968; Pechère *et al.*, 1965, 1969, 1971). In the case of higher vertebrates, this protein has been isolated from 3 sources; rabbit and rat fast muscles as well as from rat brain tissue (Baron *et al.*, 1975; Enfield *et al.*, 1975; Capony *et al.*, 1976; Berchtold *et al.*, 1982a,b). One should note that the parvalbumin content in rat brain is about 100 fold lower than in rat muscle and appears to be restricted to a distinct subpopulation of neurons (Celio and Heizmann, 1981; Berthold *et al.*, 1982b).

Parvalbumins were shown to bind two moles of calcium per mole of protein (Pechère *et al.*, 1971; Benzonana *et al.*, 1972; Nockolds *et al.*, 1972). The calcium binding affinity of these two sites ranges in values from 10^6 to $10^7 M^{-1}$ (Benzonana *et al.*, 1972; Pechère, 1977; Haiech *et al.*, 1979). Although the physiological role of these proteins remains unclear, Pechère (1977) suggested that parvalbumin participates in the contraction-relaxation cycle in fast muscle tissues, in light of 3 major points:

i) Parvalbumins appear to be tissue-specific, being primarily found in fast skeletal muscle cells and probably do not serve a ubiquitous role as in the case of calmodulin.

ii) This family of proteins does not interact with other proteins present in muscle tissue, in the presence or absence of calcium and does not represent a substrate for phosphorylation (Demaille *et al.*, 1975).

iii) Their strong affinity for calcium (K*d* ~ 3-20 *n*M) and magnesium (K*d* ~20-30 *u*M) means that parvalbumin binds two moles of magnesium ions in resting muscle (Haiech *et al.*, 1979; 1-5 mM Mg^{2+} in resting muscle).

The dissociation of magnesium ions occurs with a $t_{\frac{1}{2}}$ = 23-230 ms (Haiech *et al.*, 1979). This time delay allows the preferential binding of calcium to the calcium-specific sites of troponin C or calmodulin (Potter *et al.*, 1977). Parvalbumin can thus be viewed as a relaxing factor, as its high concentration in muscle tissue permits the removal of all calcium bound to the calcium-specific sites on troponin C and calmodulin. The final step in the calcium cycle is expected to take place in the sarcoplasmic reticulum (SR) where parvalbumin loses its calcium and binds two moles of magnesium (Pechère, 1977; Haiech *et al.*, 1979; Gillis, 1980).

It is from the crystal structure of carp parvalbumin (Kretsinger and Nockolds, 1973; Fig. I.14), that the concept of the EF hand has originated. The three-dimensional structure of troponin C (Kretsinger and Barry, 1975) and calmodulin (Kretsinger, 1980a) have since been approximated using the parvalbumin model. This site can be described as a linear sequence of 30 to 35 amino acids where a 12-residue

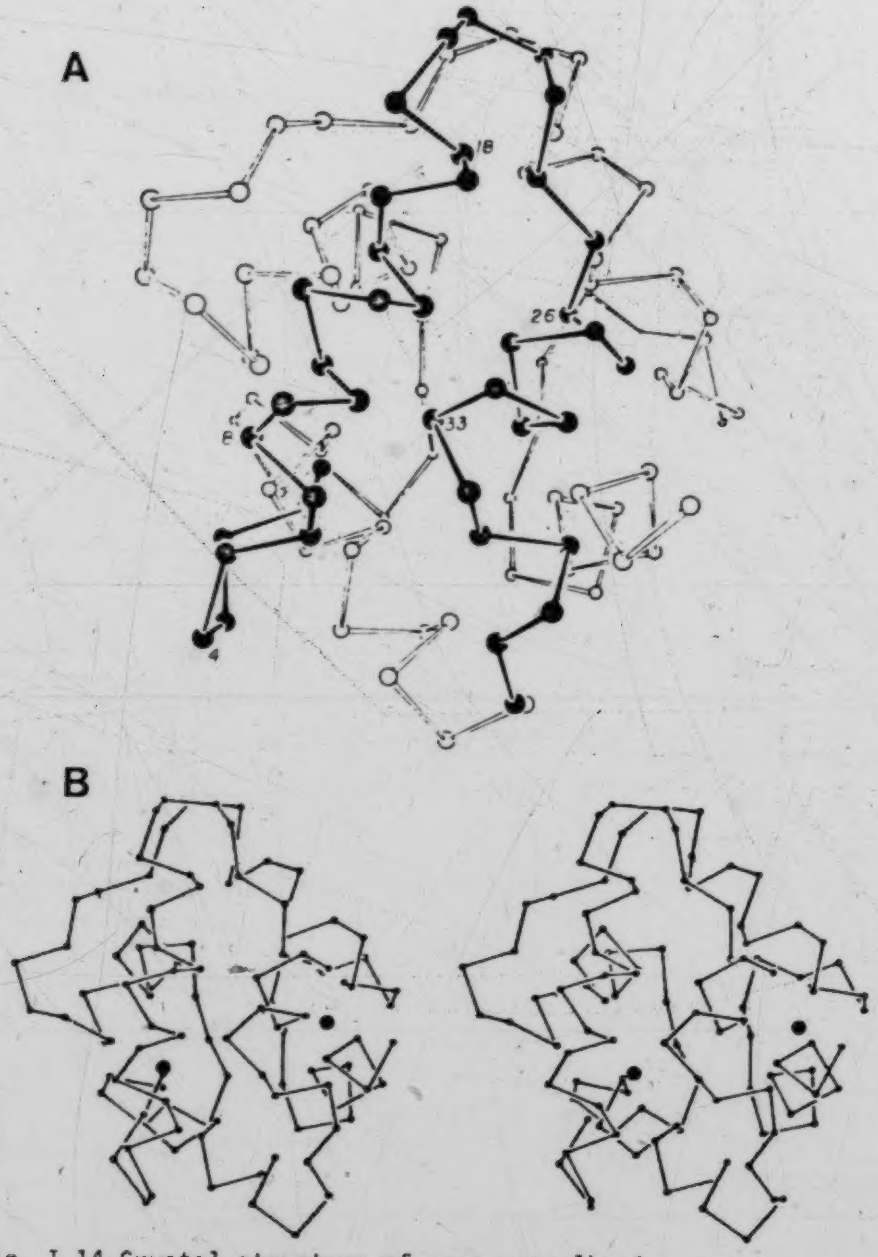

Fig. I.14 Crystal structure of carp parvalbumin.
(A) Tridimensional representation of the α-carbon backbone of carp parvalbumin. The first 40 residues are highlighted by solid lines between α-carbons. Although this region of parvalbumin possesses two helical domains flanking a turn region (AB bend), it does not bind calcium [Taken from Kretsinger and Nockolds, 1973].
(B) Stereoprojection of carp parvalbumin. ○, α-carbon; ●, calcium ion.

calcium binding region loops around the calcium ion. Alpha-helices are flanking this loop region from both sides (Fig. I.10) and in view of such a geometry, the EF site is also referred to as a *helix-loop-helix* domain.

d. Intestinal calcium binding proteins

Taylor and Wasserman (1965) first reported the presence of a vitamin D-induced calcium binding protein in chicken intestinal mucosa. This type of EF hand containing protein, abbreviated ICBP (*I*ntestinal *C*alcium *B*inding *P*rotein), was subsequently purified from other animal sources (Kallfelz *et al.*, 1967; Drescher and DeLuca, 1971; Harmeyer and DeLuca, 1969; Hitchman and Harrison, 1972) and has been shown to be located in the cytoplasm of intestinal absorptive cells (Morrissey *et al.*, 1978b; Taylor *et al.*, 1981). These proteins can be regrouped into two classes on the basis of their molecular weight and the number of high-affinity calcium binding sites (Wasserman, 1980). Mammalian ICBP's (MW ~9,000 daltons) possess two calcium binding sites ($K_{ca} \sim 10^{6} M^{-1}$) (Fullmer and Wasserman, 1973; Dorrington *et al.*, 1974, 1978; Shelling *et al.*, 1983). Avian ICBP's (MW ~28,000 daltons) bind 4 moles of calcium per mole of protein ($K_{ca} \sim 10^{6} M^{-1}$; Wasserman, 1980).

The sequence alignment of porcine and bovine ICBP (Hofmann *et al.*, 1979; Fullmer and Wasserman, 1981) reveals the presence of two EF hand domains. The recently published crystal structure of bovine intestinal calcium binding protein (Szebenyi *et al.*, 1981; Fig. I.15) points out that the first calcium binding site is distorted by the presence of amino acid insertions in the loop region, in comparison to other typical EF hands. A similar situation appears to occur in site I of bovine brain S-100 protein (Calissano *et al.*, 1974; Isobe and Okuyama, 1978,1981). Intestinal calcium binding proteins have been implicated in several functions but do not appear to serve any obvious biological role. Their synthesis requires the presence of 1α,25-dihydroxyvitamin D_3. Because the presence of this metabolite in calcium-deficient rats immediately induces the intestinal absorption of calcium and that the appearance of ICBP clearly occurs in the hours following the absorption step, it was proposed that the protein is not involved in the initiation of intestinal calcium absorption activity (Spencer *et al.*, 1976; Morrissey *et al.*, 1978; Thomasset *et al.*, 1979). Since a correlation exists between duodenal ICBP levels and the Ca^{2+} absorption activity, this protein may act as a buffering protein in diminishing increased intracellular concentrations of ionic calcium during the stimulated absorption processes (Spencer *et al.*, 1978;

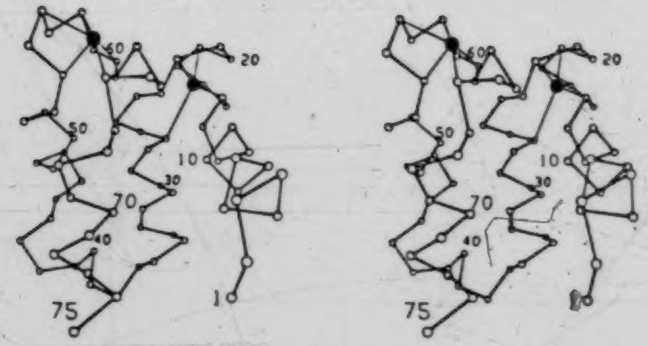
60
20
50
10
30
70
40
75
1
60
20
50
10
30
70
40
75

Fig. I.15 Crystal structure of bovine intestinal calcium binding protein. Stereoprojection of the α-carbon backbone. ○, α-carbon; ●, calcium ion [Taken from Szebenyi *et al.*, 1981].

Morrissey *et al.*, 1978; Skinki *et al.*, 1982).

e. S-100 proteins

S-100 represents a mixture of protein dimers (MW ~20,000 daltons) isolated from the central nervous system of mammals (Moore, 1965; Calissano *et al.*, 1969). These protein dimers are composed of highly homologous α- and β-subunits giving rise to S-100a (αβ) and S-100b (ββ) proteins (Vincendon *et al.*, 1970; Isobe *et al.*, 1977, 1981). Both subunit chains have been purified and sequenced (Isobe and Okuyama, 1978, 1981). S-100 exists both in soluble and membrane bound forms (Rusca *et al.*, 1973; Haglid and Stavrov, 1973; Donato and Michetti, 1974; Calissano *et al.*, 1974). Although it is a protein primarily associated with the nervous system (glial cells), S-100 has been detected in several non-nervous tissues; for example, in the reticulum cells of lymph nodes (Takahashi *et al.*, 1981), in human T lymphocytes (Kanamori *et al.*, 1982), in chondrocytes (Stefansson *et al.*, 1980). However, brain tissue contains 10^4 times more S-100 than any other organ (Moore, 1965).

The biological role of S-100 proteins remains unknown, however these proteins have been shown to facilitate the transport of γ-aminobutyric acid (GABA) through nerve cell membranes (Hyden *et al.*, 1980), to stimulate the activity of nuclear RNA polymerase in nuclei isolated from immature chicken brain (Miani *et al*., 1973), to induce the *in vitro* assembly of brain microtubules (Baudier *et al*., 1982), and to be involved in the functional maturation of the nervous system (Labourdette and Mandel, 1978; Bock, 1980).

S-100b protein has been shown to bind two moles of calcium per monomer (β-chain) at pH 8.5 (K*d* of 6 x 10^{-5}M and 2 x 10^{-4}M respectively) whereas only one mole of calcium was bound per protein monomer at pH 7.5 (K*d* of 2 x 10^{-4}M) (Calissano *et al*., 1974; Mani *et al*., 1983). The pH-dependent conformational changes observed by ^{1}H NMR when the protein was titrated from pH 6.0 to 8.6 gave support to the concept that a crucial histidine residue (His-25) located in one of the calcium binding sites is deprotonated at pH 8.5 leading to the exposure of the site. It was also demonstrated that in the presence of physiological amounts of potassium ions (50-100 mM), the protein affinity for calcium at the pH 7.5 site was lowered to 8 x 10^{-4}M. Examination of the primary sequence of S-100b (β-chain) reveals that two potential EF hand domains are present (Isobe and Okuyama, 1981). However, the first *helix-loop-helix* region (residues 1-40) is located in a cluster of positively charged residues. The sequence alignment of this particular site with other EF domains suggests that this site would adopt a distorted geometry as in the case of site I of bovine intestinal calcium binding protein (Szebenyi *et al.*, 1981; Fig. I.15).

f. Myosin light chains

The contractile response in both muscle and non-muscle cells results from the interaction of the globular portion of myosin filaments (myosin head) with the filament of actin polymers. It was mentioned in the discussion of the protein troponin C, that in the case of skeletal and cardiac muscle cells, the troponin complex in association with tropomyosin formed the key unit in the thin filament regulation of muscle contraction. In smooth muscle and non-muscle cells, the dominant regulatory system is at the level of the myosin molecule. As depicted in Fig. I.16, myosin is composed of six polypeptide chains. Two of the chains are called the heavy chains based on their molecular weight of ~200,000 daltons while the four remaining chains are referred to as the light chains. These light chains are non-covalently associated with the *head* of the myosin molecule. It was demonstrated by chemical means (Weeds, 1969; Weeds and Lowey, 1971) that myosin possesses two distinct classes of light chains. Treatment of rabbit skeletal myosin at alkaline pH results in the total loss of myosin ATPase activity (represents an *in vitro* assay for the *in vivo* contractile response) and the concomitant release of two

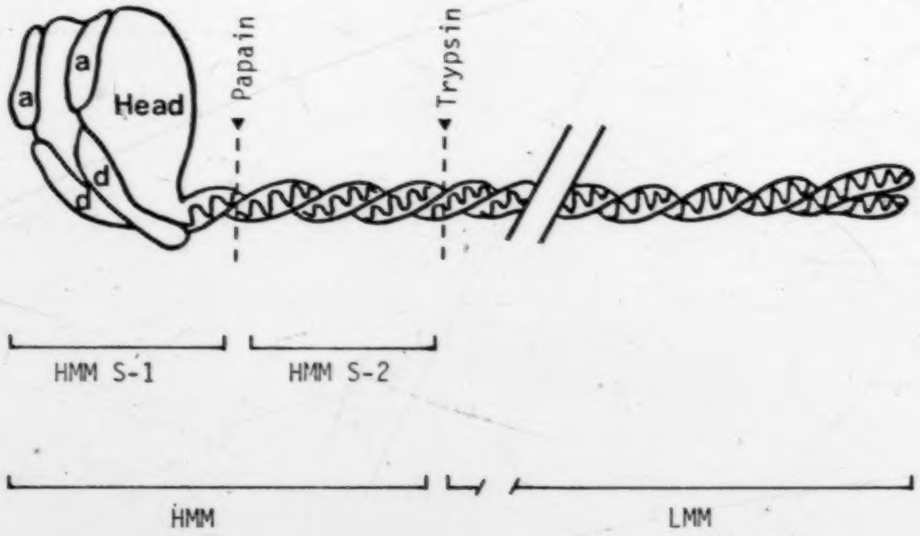
a
a
Head
d
d
Papain
Trypsin
HMM S-1
HMM S-2
HMM
LMM

Fig. I.16 Structure of myosin. A single myosin molecule can be viewed as being composed of a rod-like domain which serves a structural role and a globular head-like domain to which is associated both the ATPase activity of myosin and its binding site(s) to actin. Abbreviations: HMM, heavy meromyosin; LMM, light meromyosin; HMM S-1 and S-2, papain fragments of HMM; a, alkali light chain; d, DTNB light chain.

chains (MW of 21,000 and 17,000 daltons respectively) referred to as the *alkali* or *essential* light chains (Kominz *et al.*, 1959; Dreizen *et al.*, 1967; Frederiksen and Holtzer, 1968). These alkali light chains of rabbit skeletal myosin have been sequenced (Frank and Weeds, 1974) and although they do not bind calcium ions, their sequence alignment indicates the presence of structural homologies with troponin C and parvalbumin (Weeds and McLachlan, 1974; Tufty and Kretsinger, 1975). Treatment of rabbit skeletal myosin with 5,5'-dithiobis-(2-nitrobenzoic acid) (DTNB) leads to the selective release of two light chains referred to as *DTNB* or *regulatory* light chains (MW, ~20,000 daltons; Weeds, 1969). The loss of the DTNB chains has little effect on the ATPase activity or on the ability of myosin to interact with actin. This type of light chain, either isolated or as part of the whole myosin molecule, binds one mole of calcium per mole of light chain (Gaffin and Oplatka, 1974; Werber and Oplatka, 1974; Potter, 1975), but magnesium competes strongly for the site in intact myosin (K_{ca} of $5 \times 10^{6} M^{-1}$, absence of Mg^{2+}; K_{ca} of $5 \times 10^{5} M^{-1}$, K_{mg} of $3 \times 10^{4} M^{-1}$, 0.3 mM Mg^{2+}) so that no significant amounts of calcium are bound under physiological conditions (~2 mM Mg^{2+}; ~10^{-5}M Ca^{2+}). In the case of the isolated DTNB chain, a calcium binding constant of $1.2 \times 10^{5} M^{-1}$ has been calculated from ellipticity measurements at 222 nm (Chantler and

Szent-Gyorgyi, 1978). Analysis of its primary sequence indicates that it is related to other EF hand containing proteins (Collins, 1976) and that site I out of the four possible domains probably represents the metal binding domain. In the case of smooth muscle and non-muscle cells, it is the phosphorylation of myosin regulatory light chains, that regulates the interaction of myosin with actin (Chacko *et al.*, 1977; Sobieszek, 1977). One should note that no troponin complex has been identified in these types of cells. The phosphorylation is catalysed by a Ca^{2+}/calmodulin regulated myosin light chain kinase (Dabrowska and Hartshorne, 1978; Dabrowska *et al.*, 1978; Hathaway and Adelstein, 1979). Dephosphorylation of the chain occurs via a myosin light chain phosphatase (Morgan *et al.*, 1976; Pato and Adelstein, 1980). The DTNB light chain of rabbit skeletal myosin was also shown to be phosphorylated (Perrie and Perry, 1970; Perrie *et al.*, 1973) although the regulation of contraction in skeletal muscle cells remains under the thin filament control.

Ebashi and his co-workers (1982) have indicated the presence of the proteins leiotonin A and C in smooth muscle cells, and have suggested their role as the calcium-dependent regulatory complex involved in the actin linked regulation of smooth muscle contraction. However problems in purifying leiotonin A , coupled with the demonstration that Ca^{2+} regulation is effective at a leiotonin to actin molar ratio of less than 1:50 and the absence of interaction between this regulatory complex and tropomyosin, are major factors explaining why this mechanism has failed to gain general acceptance.

A final regulatory mechanism, which exists in invertebrate muscle cells such as scallops has been described by Szent-Gyorgyi and his co-workers (see Szent-Gyorgyi, 1975, 1980). In this system, the actin binding site of myosin is regulated by calcium. In the presence of regulatory light chains (analogous to the *DTNB* light chains of rabbit skeletal muscle), the actin-activated Mg^{2+}-ATPase of myosin is depressed and the inhibition is reversed by calcium or by the removal of these light chains (Kendrick-Jones *et al*., 1970; Szent-Gyorgyi *et al*., 1973).

One or both regulatory light chains of scallop myosin can be removed from the myofibrils by a short EDTA treatment (Szent-Gyorgyi *et al*., 1973; Chantler and Szent-Gyorgyi, 1980). These isolated regulatory light chains do not bind calcium strongly (K_{ca}, 5 x $10^3 M^{-1}$; K_{mg}, 1 x 10^3 M^{-1}) (Chantler and Szent-Gyorgyi, 1978), but their primary sequence indicates as in the case of other light chains, their relation to the superfamily of EF hand containing proteins (Jakes *et al*., 1976; Kendrick-Jones and Jakes, 1977). These light chains bind calcium with a high affinity only upon recombination with myosin (K_{ca} ~10^7-$10^8 M^{-1}$) (Kendrick-Jones *et al.*, 1976; Bagshaw and Kendrick-Jones, 1979). Finally, one should note that scallop myosin does not possess a phosphorylatable light chain (Frearson *et al.*, 1976; Jakes *et al.*, 1976) and no evidence has been found as yet that molluscan myosins require phosphorylation for their calcium sensitivity.

4. Design of an EF hand domain

Our understanding of how an EF hand domain binds Ca^{2+} and communicates this chemical signal to the rest of the protein was largely based on primary sequence alignments and on the crystal structures of carp parvalbumin and bovine ICBP. Although major structural changes occuring in the presence of calcium could be assessed by fluorescence spectroscopy, circular dichroism and nuclear magnetic resonance, it was only upon the isolation of chemical and proteolytic fragments of parvalbumin and troponin C that some insight was gained on the basic structural requirements necessary for an EF hand to bind calcium. For example, Derancourt *et al.* (1978) demonstrated that the tryptic fragments of carp parvalbumin representing the isolated CD (site I) and EF (site II) domains bound calcium weakly (K_{ca} for CD site, 1.1 x $10^4 M^{-1}$; K_{ca} for EF site, 3.3 x $10^3 M^{-1}$) in comparison to their Ca^{2+}-binding affinity in the intact protein (K*ca* ~10^7M^{-1}). It was thus apparent that although each calcium binding region was intact, the overall tertiary structure of the protein contributed in part to the calcium binding ability of the sites. This was evident also in the case of cyanogen bromide fragments representing site II (K*ca*, 8 x 10^3M^{-1}) and site III (K*ca*, 5 x 10^5M^{-1}) of rabbit skeletal troponin C where a nearly hundred fold decrease in Ca^{2+} affinity was noticed as compared to the same sites in the purified protein (Potter and Gergely, 1975; Leavis *et al.*, 1978).

However, the calcium binding constants calculated for these isolated single sites fluctuate in value by three orders of magnitude. Reid and Hodges (1980) proposed that the difference in affinity between these fragments could be rationalized at least in part by the amino acid composition of the twelve residue sequence involved in the chelation of the calcium ion. Their hypothesis suggested that a single site containing four acidic side chains (two acid pairs) arranged on the ± axes coordinates (±X, ±Z) would minimize ligand repulsions and would thus offer a higher complex stability. Another key factor was a possible mechanism of dehydration involving the presence of hydrophobic residues at position 7 (-Y) and position 10, of the calcium binding loop. These residues aided in the removal of the first molecules of water from the hydrated calcium ion *inner-sphere* complex leading to a destabilization of the remaining water molecules and the initiation of a protein:metal complex formation. Both these aspects were discussed in part earlier in the introduction. Since the hypothesis relied heavily on the information gathered from fragments of different size and amino acid composition, a major criticism to this hypothesis was that the loss of local elements of secondary structure (α-helical regions for example) could account for the large discrepancy observed in their respective calcium binding affinities. The validity of the hypothesis could however be assessed by synthesizing a model EF hand domain and by varying both its size and amino acid composition.

F. AIMS OF THE PROJECT

A research project always starts with a clear, simple idea. Hovewer when clear results are finally obtained, their interpretation often yields possibilities that were not covered by the original simple concept. This statement depicts well how my project has evolved.

Initially, a hypothesis postulated by Reid and Hodges (1980) suggested that the primary sequence of a 12-residue calcium binding loop encoded for 1) metal specificity and

2) stability of the metal:peptide complex. My initial goal was to prove this concept by synthesizing various analogs of a 12-residue calcium binding site. We had decided that site III of rabbit skeletal troponin C was a region of choice since the study of Potter and Gergely (1975) had indicated its high-affinity for calcium in the native protein. This region also appeared to retain its calcium binding ability when isolated from a cyanogen bromide digest of rabbit skeletal troponin C (Leavis *et al.*, 1978; Nagy *et al.*, 1978). One should note that the information gathered on this particular site had previously influenced the formulation of our single site model (Reid and Hodges, 1980).

It was realized early in the project, that the calcium affinity demonstrated by a 12-residue segment of this site (residues 103 to 114) was too low (K_{ca} in the order of $10^2 M^{-1}$) to permit an evaluation of our model (Reid *et al.*, 1980). My project was then reoriented towards the analysis of 2 major issues.

The first issue dealt with the importance of the C- and N- terminal regions flanking the metal binding loop as stabilizing factors for the metal:peptide complex. This question was partly answered by synthesizing analogs having both helical regions and by monitoring individual side chain movements (by ^1H NMR) and perturbations of the secondary structure (by circular dichroism) occuring upon calcium addition.

The second issue was primarily a technical one. We essentially wanted to study the sequence requirement at the metal binding site and especially the ligand arrangement involved in the coordination sphere. We wanted to reduce the peptide size to a minimum to simplify its analysis by 'H NMR. In order to regain the metal specificity of small synthetic peptides representing only the calcium binding domain, we decided to make use of lanthanides as substitutes to calcium. This part of my project proved to be quite informative in pointing out the importance of metal charge and radius, in the ability of these sites to bind metals. Since most lanthanides have unpaired 4f electrons, they possess spectroscopic properties that can be advantageously used in NMR spectroscopy to yield distance measurements. We thus made use of the relaxation probe gadolinium to measure some metal to proton distances in an attempt to reconstruct the geometry of the metal binding site.

Finally a third aspect to my project came about as a consequence of calcium-induced folding. By making use of synthetic and natural fragments of site III in conjunction with the antipsychotic drug trifluoperazine, we have located a phenothiazine binding site in the calcium-sensitive portion of the N-terminal region. Since this region of rabbit skeletal troponin C is homologous to a fluphenazine binding region of calmodulin and represents a known site of interaction with troponin I, it was expected to adopt a particular conformation suited for specific protein-protein interactions. We decided to analyse the relevant features of this site.

CHAPTER II

EXPERIMENTAL PROCEDURES

A. SOURCES OF CHEMICALS AND SOLVENTS

All chemicals and solvents are reagent grade unless otherwise stated. Methylene chloride from Fisher Scientific was distilled over $CaCO_3$ prior to use. Diisopropylethylamine was distilled first over NaH and then over ninhydrin prior to use. Picric acid from Eastman Organic Chemicals, Rochester, New York, was dissolved in methylene chloride and dried over $MgSO_4$ before use. Trifluoroethanol, 99%, Gold Label, and N,N-dimethylformamide, spectrophotometric grade, Gold Label, were purchased from Aldrich Chemical Company, Inc., Milwaukee, Wisconsin. Boc amino acids purchased from Spinco Division of Beckman Instruments Inc., Palo Alto, California, Protein Research Foundation, Japan, Vega-Fox Biochemicals, Tucson, Arizona, and Bachem Fine Chemicals, Inc., Marina Del Rey, California, were used without further purification. Copoly(styrene, 1% divinylbenzene) chloromethyl resin (0.9 mmol of chlorine/g of resin) was purchased from Pierce Chemical Co., Rockford, Illinois. Copoly(styrene, 1% divinylbenzene)benzhydrylamine hydrochloride resin (0.51 mg of nitrogen/g of resin) was purchased from Beckman. DEAE Sephacel was purchased from Pharmacia Fine Chemicals and hydroxyapatite DNA Grade Bio-Gel HTP was purchased from Bio-Rad Laboratories. Lanthanum chloride, gadolinium chloride and lutetium oxide were obtained from Alfa Inorganics-Ventron, Beverly, Massachusetts while calcium chloride was purchased from Fisher Scientific. Deuterated water was obtained from Bio-Rad, Richmond, California. The sulphydryl reagent 5,5'-dithio-bis(2'-nitrobenzoic acid) (DTNB) was purchased from Pierce Chemical Co., Rockford, Illinois. The drugs used in this study were generous gifts from the following companies: Trifluoperazine, Smith Kline and French Ltd., Montreal, Quebec; *cis*- and *trans*-thiothixene, Pfizer Inc., Groton, Connecticut; Benperidol, Janssen Pharmaceutica, Beerse, Belgium; Haloperidol, McNeil Laboratories, Stouffville, Ontario; Molindone, Endo Laboratories, Garden City, New York; Chlorpromazine and Promethazine, Poulenc Ltd., Montreal, Quebec; Fluphenazine, E.R. Squibb and Sons Ltd., Montreal, Quebec.

B. AMINO ACID ANALYSIS AND PEPTIDE QUANTITATION

Routine amino acid analyses were performed on a Durrum D-500 amino acid analyzer. Quantities of peptides were determined from either amino acid analysis after hydrolysis in 6 N HCl in evacuated sealed tubes at 110°C for 24 h using the mean of the molar ratios of all accurately measurable amino acids in the acid hydrolysate to calculate concentration. In the case of the peptide AcA''STnC-(90-123)amide, the concentration could be alternatively estimated by measuring the optical density of the peptide dissolved in 100 mM MOPS, 50 mM KCl and 1 mM EGTA at pH 7.2 using an ε_{275} of 1.708×10^{3} M^{-1} cm^{-1} determined using quantitative amino acid analysis. One can also determine the concentration of a solution of peptide AcSTnC(103-115)amide by measuring its absorbance at 280 nm and using an ε_{280} value of 2100 $M^{-1}cm^{-1}$.

C. MELTING POINT MEASUREMENTS AND ELEMENTAL ANALYSIS

Melting points were determined on an electrothermal melting point apparatus and are uncorrected. Elemental analyses were performed at the Microanalytical Laboratory, Department of Chemistry, University of Alberta.

D. THIN LAYER CHROMATOGRAPHY

Thin layer chromatography was carried out on Silica Gel 60 F_{254} plates (0.25 mm) purchased from E. Merck, Darmstadt, Germany, using the following solvent systems: chloroform:methanol:acetic acid in ratios 85:10:5 v/v (system A);

acetone-acetic acid in a ratio 98:2 (v/v) (system B); and 1-butanol-acetic acid-water in ratios 4:1:1 v/v (system C). Peptides were detected directly under ultraviolet light or by treatment with ninhydrin spray (0.2% in acetone) after removal of the Boc-group by exposure of the dry thin layer plate to HCl fumes for 15 min. The peptides were declared homogeneous by thin layer chromatography when no impurities could be detected in the solvent systems described after application of 300 μg of peptide to the plates.

E. SDS GEL ELECTROPHORESIS

Gel electrophoresis was typically performed on 12% acrylamide 6 M urea gels (Weber and Osborne, 1969). Samples were dissolved in a buffer containing 6 M urea, 0.03 M Na_2HPO_4, 0.02 M NaH_2PO_4, 1% SDS, 1% β-mercaptoethanol, pH 7.0 and heated at 60°C for 1 hour. Bromophenol blue was used as the tracking dye (0.0005% w/v in the sample buffer mentioned above). The running buffer composition was of 0.06 M Na_2HPO_4, 0.04 M NaH_2PO_4, 0.1% SDS, pH 7.0. After electrophoresis, gels were first washed in methanol/acetic acid/water (1:1:8, v/v/v) for 1 hour in order to remove the excess detergent. They were then stained for 30 minutes with Coomasie Brilliant Blue R-250 (0.25% solution in methanol/acetic acid/water, 5:1:4, v/v/v) followed by a 12 to 48 hours destaining period in methanol/acetic acid/water

(1:1:8, v/v/v) to insure the removal of unbound dye.

F. PAPER ELECTROPHORESIS

1. Experimental procedure

Paper electrophoresis was performed at pH 6.5 and pH 1.8 on Whatman #1 electrophoresis paper. The buffer systems were pyridine/acetic acid/water (100:3:900 , v/v), pH 6.5 and formic acid/acetic acid/ water (1:4:45 , v/v), pH 1.8. Samples were lyophilized and dissolved in a minimal volume of the buffer system used or any volatile solvent in order to facilitate sample application. Standards representing mixtures of amino acids were also prepared in the above buffer. Following the spotting of samples and standards, the paper was folded along the sample line and was wetted on both sides of the line with the running buffer. After the buffer front has reached the line simultaneously from both sides, the paper was blotted carefully, placed in a tank containing the running buffer. Electrophoresis was carried out at 60 volts/cm for 45 minutes. The peptides were visualized by spraying the paper electrophoregram with the ninhydrin:cadmium acetate reagent of Heilmann *et al*. (1957). Color development was achieved by drying the paper in a 60°C chamber for 15 minutes.

2. Ninhydrin:cadmium acetate solution

This solution was freshly prepared and was composed of a ninhydrin acetone solution (1 g ninhydrin in 100 ml of acetone) mixed with a cadmium acetate solution (1 g cadmium acetate/50 ml acetic acid/100 ml water) in a 7 to 1 ratio (v/v).

G. PEPTIDE SYNTHESIS

1. Solution synthesis

Because of synthetic problems associated with the stepwise solid phase synthesis of Boc-amino acids to prepare analogs of site III of rabbit skeletal troponin C, solid phase fragment couplings were carried out in the later stages of the synthesis in order to secure a proper yield of the final peptides. This section discusses the use of solution phase methods where N-hydroxysuccinimidyl esters (Anderson *et al.*, 1964) were employed for the stepwise synthesis of four protected peptides.

a. Synthesis of Fragment A, Boc-Lys(Z)-Ser(Bzl)-Glu-(OBzl)-Glu(OBzl)-OH

Boc-Glu(OBzl)-OSu (I) was prepared by a previously described method (St-Pierre and Hodges, 1977). A solution of α-benzyl glutamate (2.5 g; 10.5 mmol) dissolved in warm water (100 ml) was added to Compound I (4.35 g; 10 mmol) in dioxane (50 ml). Sodium bicarbonate (882 mg; 10.5 mmol) in water was added with vigorous stirring and the pH maintained between 7 - 8 while stirring the reaction mixture at room temperature for 24 hours. The dioxane was removed in vacuo at 30 °C, then the aqueous residue was diluted with 100 ml of water and cooled to 0 °C. The pH was ajusted to 3 with ice cold 0.1 N HCl and the solution extracted with ethyl acetate (3 x 150 ml). The organic extract was washed with water (3 x 150 ml) and saturated sodium chloride (200 ml), then dried over anhydrous sodium sulfate. The dry solution was filtered and the solvent evaporated in vacuo to give 5.45 g (yield 98%) of the oily product Boc-Glu(OBzl)-Glu-(OBzl)-OH (II) which did not crystallize but was homogeneous by TLC: Rf(system A) 0.55, (system B) 0.57.

Compound II (5.45 g; 9.8 mmol) was dissolved in 2 N HCl/ dioxane (9 ml) and left to stand at room temperature for 2 hours taking adequate precautions against moisture. The solution was evaporated to dryness and the oily residue triturated with anhydrous ether to give 3.28 g of the hydrochloride salt (III), a white hygroscopic solid (yield 67%): Rf (system C) 0.60.

Boc-Ser(Bzl)-OSu (IV) was prepared as described for Compound I and obtained in 83% yield: m.p. 108-110 °C, Rf (system A) 0.74, (system B) 0.79. Anal. calcd. for $C_{19}H_{24}N_2$

O_7 (M.W. 392.43): C, 58.15; H, 6.18; N, 7.14. Found: C, 57.85; H, 6.01; N, 6.84.

Compound III (3.28 g; 7.77 mmol) was dissolved in water (25 ml) and sodium bicarbonate (1.3 g; 15.5 mmol) was added with vigorous stirring followed by Compound IV (2.9 g; 7.4 mmol) in dioxane (30 ml). The pH was maintained between 7 - 8 while stirring at room temperature for 24 hours, then the reaction mixture was worked up as described for Compound II yielding 3.8 g (yield 70%) of Boc-Ser(Bzl)-Glu(OBzl)-Glu-(OBzl)-OH (V) as a white hygroscopic solid: Rf (system A) 0.57, (system B) 0.65 . Amino acid analysis : Ser (1.04), Glu (1.95).

Compound V (3.8 g; 5.2 mmol) was dissolved in 2N HCl/dioxane (5 ml) and left to stand at room temperature for 2 hours. The hydrochloride salt (VI) was isolated as previously described to give 3.4 g of a white solid (yield 97.5%) which crystallized from ether: pet. ether (1:4 v/v): m.p. 68-70 °C; Rf (system C) 0.61.

Anal. calcd. for $C_{34}H_{40}N_3O_9Cl$ (M.W. 670.19): C, 60.93; H, 6.03; N, 6.27; Cl, 5.29. Found: C, 60.57; H, 5.96; N, 5.91; Cl, 5.16.

Boc-Lys(Z)-OSu (VII) was prepared as described for Compound I and obtained in 81% yield: m.p. 70-71 °C; Rf (system A) 0.77 , (system B) 0.84. Anal. calcd. for $C_{23}H_{31}N_3O_8$ (M.W. 477.54): C, 57.84; H, 6.56; N, 8.80. Found: C, 57.73; H, 6.48; N, 8.64.

Compound VI (3.4 g; 5.07 mmol) was dissolved in water (20 ml) and sodium bicarbonate (852 mg; 10.14 mmol) was added with vigorous stirring followed by Compound VII (2.3 g; 4.82 mmol) in dioxane (25 ml). The pH was maintained between 7 - 8 and the mixture was stirred at room temperature for 24 hours, then worked up as previously described for Compound II to yield 3.99 g of Boc-Lys(Z)Ser-(Bzl)-Glu(OBzl)-Glu(OBzl)-OH (VIII) (yield 83%) crystallized from ether:pet. ether (1:4 v/v). After purification by Sephadex LH-20 chromatography, the peptide was crystallized with ether to give a 55% yield (this represent a 20.5% yield when compared to the original compound I): m.p. 88-90 °C; Rf (system A) 0.70, (system B) 0.71. Amino acid analysis: Lys (1.07), Ser (0.92), Glu (2.00).

Anal calcd. for $C_{53}H_{65}N_5O_{14}$ (M.W. 996.18): C, 63.90; H, 6.59; N, 7.03. Found: C, 63.60; H, 6.71; N, 7.05.

b. Synthesis of Fragment B, Boc-Glu(OBzl)-Leu-Ala-Glu-(OBzl)-OH

Boc-Ala-Glu(OBzl)-OH (IX) was prepared in a manner similar to the preparation of Compound II using Glu(OBzl)

(2.5 g; 10.5 mmol) , sodium bicarbonate (882 mg; 10.5 mmol) and Boc-Ala-OSu (2.86 g; 10 mmol). The product was obtained as 3.45 g of a white solid (yield 84.5%) : m.p. 84-85 °C; Rf (system A) 0.53, (system B) 0.58. Amino acid analysis: Ala (0.97), Glu (1.03).

Anal. calcd. for $C_{20}H_{28}N_2O_7$ (M.W. 408.48): C, 58.80; H, 6.92; N, 6.85. Found: C, 58.57; H, 6.69; N, 6.82.

Compound IX was deprotected with 2 N HCl/dioxane as previously described. The hydrochloride salt (X) was obtained as a white hygroscopic solid in 70.7% yield: Rf (system C) 0.48.

Boc-Leu-Ala-Glu(OBzl)-OH (XI) was prepared in a similar way to Compound V using the hydrochloride salt (X) (1.86 g; 5.4 mmol), sodium bicarbonate (907 mg; 10.8 mmol) and Boc-Leu-OSu (1.68 g; 5.13 mmol). The product was obtained as 2.46 g of a white solid (yield 91.8%): m.p. 73-74 °C; Rf (system A) 0.44, (system B) 0.48. Amino acid analysis: Leu (1.04), Ala (0.99), Glu (0.96).

Anal. calcd. for $C_{26}H_{39}N_3O_8$ (M.W. 521.65): C, 59.86; H, 7.55; N, 8.05. Found: C, 59.49; H, 7.44; N, 7.79.

Compound XI was deprotected with 2 N HCl/dioxane as previously described. The hydrochloride salt (XII) was obtained in 93.7% yield: m.p. 112-114 °C; Rf (system C)

0.46.

Anal. calcd. for $C_{21}H_{32}N_3O_6Cl$ (M.W. 457.98): C, 55.07; H, 7.06; N, 9.17; Cl, 7.74. Found: C, 55.38; H, 7.24; N, 8.92; Cl, 7.56.

Boc-Glu(OBzl)-Leu-Ala-Glu(OBzl)-OH (XIII) was prepared in a similar way to Compound V using the hydrochloride salt XII (1.83 g; 4 mmol), sodium bicarbonate (672 mg; 8 mmol) and Boc-Glu(OBzl)-OSu (1.65 g; 3.8 mmol). The product was obtained as 2.5 g of a white solid (90% yield) which was purified by LH -20 column chromatography and crystallized from ether:pet. ether (1:4 v/v) (21.3% yield based on the original compound Boc-Ala-OSu): m.p. 84-86 °C; Rf (system A) 0.50, (system B) 0.57. Amino acid analysis: Glu (1.98), Leu (0.99), Ala (1.02).

Anal. calcd. for $C_{38}H_{52}N_4O_{11}$ (M.W. 740.9): C, 61.60; H, 7.09; N, 7.56. Found: C, 61.13; H, 7.15; N, 7.62.

c. Synthesis of Fragment C, Boc-Ala-Phe-Arg(Tos)-OH

Boc-Phe-Arg(Tos)-OH (XIV) was prepared in a manner similar to the preparation of compound V using the hydrochloride salt of Arg(Tos)-OH (5.74 g; 15.75 mmol), sodium bicarbonate (2.65 g; 31.5 mmol) and Boc-Phe-OSu (5.43 g; 15.0 mmol). The product was obtained as 7.16 g of a crystalline white solid (yield 80.4%): m.p.117-119 °C; Rf (system A) 0.41, (system B) 0.61. Amino acid analysis: Phe (1.03), Arg (0.97).

Anal. calcd. for $C_{27}H_{37}N_5O_7S$ (M.W. 575.7): C, 56.32; H, 6.49; N, 12.16; S, 5.57. Found: C, 56.75; H, 6.52; N, 11.46; S, 4.96.

Compound XIV was deprotected with 2 N HCl/dioxane as previously described. The hydrochloride salt (XV) was obtained in quantitative yield; m.p. 115-117 °C; Rf (system C) 0.56.

Anal. calcd. for $C_{22}H_{30}N_5O_5SCl$ (M.W. 512.03): C, 51.60; H, 5.92; N, 13.67; S, 6.26; Cl, 6.92. Found: C, 50.06; H, 6.21; N, 12.00; S, 5.47; Cl, 8.69.

Boc-Ala-Phe-Arg(Tos)-OH (XVI) was prepared in a similar fashion to Compound V using the hydrochloride salt XV (2.15 g; 4.2 mmol), sodium bicarbonate (706 mg; 8.4 mmol) and Boc-Ala-OSu (1.14 g; 4 mmol). The product was obtained as a crystalline white solid (2.0 g; 78% yield) which was purified on Sephadex LH-20 followed by crystallization from water (45.7% yield based on the original compound Boc-Phe-OSu): m.p. 124-125 °C; Rf (system A) 0.38, (system B) 0.51. Amino acid analysis: Ala (1.07), Phe (0.97), Arg (0.95).

Anal. calcd. for $C_{30}H_{42}N_6O_8S$ (M.W. 646.78); C, 55.70; H, 6.56; N, 12.99; S, 4.96. Found: C, 54.88, H, 6.73; N, 12.46; S, 4.61.

d. Synthesis of Fragment D, Boc-Ile-Phe-Asp(OBzl)-OH

Boc-Phe-Asp(OBzl)-OH (XVIII) was prepared in a similar way to Compound V using Asp(OBzl)-OH (2.23 g; 10 mmol), sodium bicarbonate (1.68 g; 20 mmol) and Boc-Phe-OSu (3.6 g; 10 mmol). The product was obtained as a white crystalline solid (3.38 g; 71% yield): m.p. 61-63 °C; Rf (system A) 0.62, (system B) 0.56. Amino acid analysis: Phe (0.98), Asp (1.02). Anal. calcd. for $C_{25}H_{30}N_2O_7$ (M.W. 470.55): C, 63.81; H, 6.44; N, 5.95. Found: C, 63.72; H, 6.49; N, 5.87.

/ Compound XVII was deprotected with 2 N HCl/dioxane as previously described. The hydrochloride salt XVIII was obtained in quantitative yield: m.p. 100 °C; Rf (system C) 0.40.

Anal. calcd. for $C_{20}H_{23}N_2O_5Cl$ (M.W. 406.88): C, 59.04; H, 5.71; N, 6.88; Cl, 8.71. Found: C, 58.36; H, 5.72; N, 6.56; Cl, 8.92.

Boc-Ile-Phe-Asp(OBzl)-OH (XIX) was prepared in a similar manner to Compound V using the hydrochloride salt XVIII (1.92 g; 4.73 mmol), sodium bicarbonate (795 mg; 9.46

mmol) and Boc-Ile-OSu (1.48 g; 4.5 mmol). The product was obtained as a crystalline white solid (1.99 g; 76% yield; 53% yield based on the original compound Boc-Phe-OSu): m.p. 146-147 °C ; Rf (system A) 0.63, (system B) 0.54. Amino acid analysis: Ile (1.02), Phe (0.92), Asp (1.05).

Anal. calcd. for $C_{31}H_{41}N_3O_8$ (M.W. 583.72): C, 63.78; H, 7.09; N, 7.20. Found: C, 64.75; H, 7.03; N, 7.16.

e. Purification of protected peptide fragments

Analytical samples of the completed protected tripeptides and tetrapeptides (5 mg) were deprotected with hydrofluoric acid (10 ml) at 0 °C for 30 min with anisole (10% v/v) as a cation scavenger. The hydrofluoric acid and the bulk of the anisole were removed under vacuum at 0 °C. Purity of the deprotected peptides was assessed by paper electrophoresis.

If the hydrofluoric acid deprotected peptides were not homogeneous, purification of the protected peptides was carried out on Sephadex LH-20 in a 2.6 cm x 100 cm column equilibrated with dichloromethane-methanol (3:7, v/v). Samples of 500 mg dissolved in 2 ml of column solvent were applied to the column and eluted at a flow rate of 15 ml/hr collecting 2.5 ml fractions while monitoring the column effluent at 232 nm or 255 nm. An aliquot (50 ul) of each fraction in the detected peak areas was spotted on Silica Gel 60 F_{254} plates (0.25 mm) and the plates developed in chloroform-methanol-acetic acid (85:10:5, v/v). The peptides were detected by spraying the plates with a ninhydrin solution. Fractions from the LH-20 chromatography were pooled based upon the thin layer chromatography results, evaporated in vacuo and the residue crystallized from ether or water. Homogeneity of the protected peptides was re-examined by repeating the hydrofluoric acid cleavage and the high voltage paper electrophoresis.

2. Solid phase peptide synthesis

Most of the peptides used in this study were synthesized by solid phase peptide synthesis. The experimental background surrounding the use of solid phase peptide synthesis and its applications to biochemistry have been adequately described in several reviews (Stewart and Young, 1969; Erickson and Merrifield, 1976; Birr, 1978). The technique was devised by Merrifield (1962) and involves the use of an insoluble resin support to which amino acids or small peptides having their side chains blocked by protecting groups are coupled sequentially. The preferred direction of coupling is to activate the α-carboxyl group of an amino acid and to couple it to the amino terminal of a peptide chain being synthesized on the resin. Some of the advantages of such an approach over other synthetic methods lie in the ease it offers in removing soluble reaction contaminants after each amino acid coupling, the ability to use an excess of reactants (i.e. protected amino acids, coupling agent) to force the coupling reaction to completion and, the possibility of automation. Speed and reproducibility at each step of the synthesis can thus be achieved. One major drawback has been the difficulty in purifying the peptide having the proper sequence from ones having one or more amino acid deletions. This problem has now been partly overcome by the advent of high pressure liquid chromatography.

Figure II.1 represents a flow chart of steps performed during a typical synthesis. The salient points can be described as follows: 1) The first protected amino acid is covalently coupled to a resin support by the cesium salt attachment method (Gisin, 1973) in the case of a chloromethyl type resin. Alternatively, the initial residue can be linked to a benzhydrylamine support in the presence of a coupling agent such as dicyclohexylcarbodiimide (DCC) . Both resin matrices were used in this study.

2) Protected amino acids are then coupled following a cyclic sequence of operations where the Boc group of the peptide chain is first removed by treating the peptide resin with trifluoroacetic acid (TFA). The deprotected peptide is

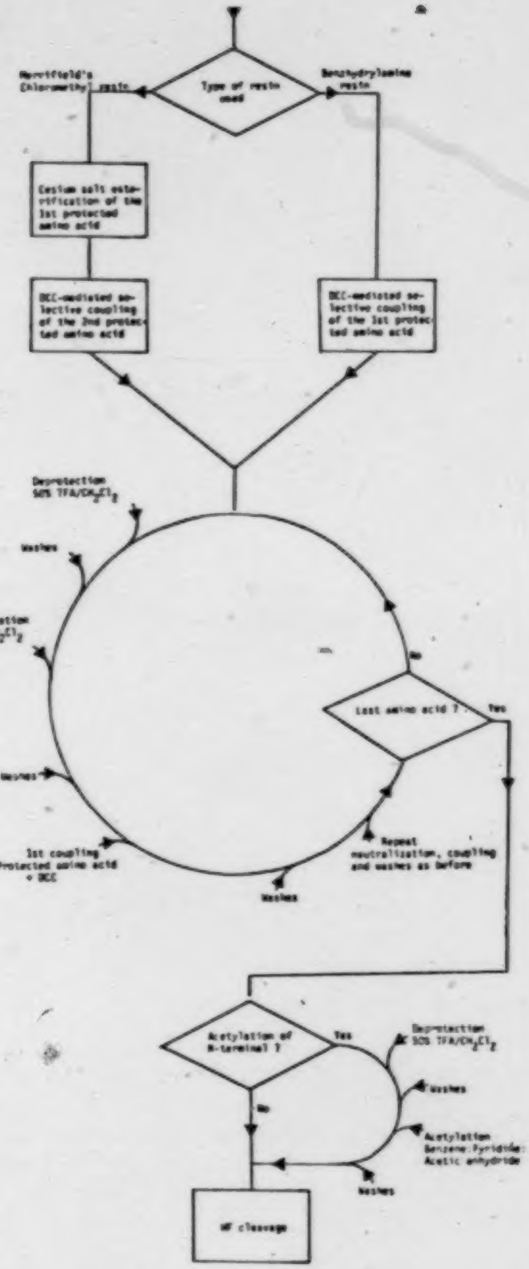
Merrifield's Chloromethyl resin
Type of resin used
Benzhydrylamine resin
Cesium salt esterification of the 1st protected amino acid
DCC-mediated selective coupling of the 2nd protected amino acid
DCC-mediated selective coupling of the 1st protected amino acid
Deprotection 50% TFA/CH_2Cl_2
Washes
Neutralization 5% DIEA/CH_2Cl_2
Washes
1st coupling Protected amino acid + DCC
Washes
Repeat neutralization, coupling and washes as before
No
Last amino acid ?
Yes
Acetylation of N-terminal ?
Yes
Deprotection 50% TFA/CH_2Cl_2
Washes
Acetylation Benzene:Pyridine:Acetic anhydride
Washes
No
HF cleavage

Fig. II.1 Flow chart depicting the sequence of operations performed during the solid phase peptide synthesis of our analogs.

then washed and neutralized with diisopropylethylamine. The Boc-amino acid and a carboxyl group activating agent such as dicyclohexylcarbodiimide (DCC) are then added. After the peptide bond formation, the resin is washed and the coupling cycle is repeated if necessary. 3) The synthetic peptide is then detached from the resin and all the side chain blocking groups are removed by treating the peptide resin with anhydrous hydrofluoric acid.

Experimental parameters surrounding the synthesis and purification of each peptide used in this study will now be discussed individually.

a. Synthesis of AcSTnC(103-123) (peptide I)

The acetylated 21-residue analog was synthesized on a Beckman 990 peptide synthesizer. Boc-Gly (13.5 mmol, 5 equivalents) was esterified to chloromethyl resin (3 g; 0.90 mmol of chlorine/g of resin) using the cesium salt method (Gisin, 1973). Boc-glycine resin (0.78 mmol of glycine/g of Boc-Gly resin) was deprotected and selectively coupled with Boc-Ser(Bzl) (0.25 mmol of Boc-Ser/g of Boc-Gly resin) and the remaining free amino groups were acetylated with a mixture of pyridine-acetic anhydride-benzene (3:1:3, v/v) for 90 minutes. The third amino acid, Boc-Ala, was coupled to the dipeptide resin using the reverse coupling procedure to reduce loss of peptide from the resin due to diketopiperazine formation (Gisin and Merrifield, 1972). The initial coupling of Boc-Gly, the selective coupling of Boc-Ser(Bzl) and the reverse coupling of Boc-Ala were all monitored using the picric acid procedure of Hodges and Merrifield (1975). The remainder of the peptide was synthesized using two 60 minutes dicyclohexylcarbodiimide mediated couplings with 3 equivalents of Boc-amino acid based on the amount of tripeptide on the resin determined by picric acid monitoring.

Deprotection was carried out in 50% trifluoroacetic acid/ CH_2Cl_2 (v/v) for 30 minutes and neutralization was carried out using 5% diisopropylethylamine/CH_2Cl_2 (v/v). The α-amino group of all amino acids was protected by the Boc group and the following side chain blocking groups were used: Glu(OBzl), Asp(OBzl), Arg(Tos), Asn(Mbh), Tyr-(2,6-dichlorobenzyl) and Ser(Bzl). All amino acids were 60 mM in CH_2Cl_2 during coupling with the exception of Boc-Arg(Tos) and Boc-Asn(Mbh), which were 60 mM in 3% dimethylformamide/CH_2Cl_2 (v/v).

The program used for the consecutive attachment of each amino acid to the tripeptide resin consisted of the following steps: Deprotection cycle: 50% TFA/CH_2Cl_2, 1 minute; 50% TFA/CH_2Cl_2, 30 minutes; CH_2Cl_2, four times, 1

minute; 80% isopropanol/CH_2Cl_2, two times, 1 minute; CH_2Cl_2, eight times, 1 minute. Coupling cycle: 5% DEA/CH_2Cl_2, three times, 2 minutes; CH_2Cl_2, seven times, 1 minute; Boc-amino acid, 5 minutes; DCC, 60 minutes; CH_2Cl_2, three times, 1 minute; 80% isopropanol/CH_2Cl_2, two times, 1 minute; CH_2Cl_2, two times, 1 minute; 80% isopropanol/CH_2Cl_2, two times, 1 minute; CH_2Cl_2, eight times, 1 minute. The coupling cycle was repeated. The CH_2Cl_2 and isopropanol washes were 75 and 30 ml, respectively. The 50% TFA/CH_2Cl_2 and the 5% DEA/CH_2Cl_2 volumes were both 30 ml.

The program used for the picric acid monitoring of free amino groups consisted of the following steps: 5% DEA/CH_2Cl_2, three times, 2 minutes; CH_2Cl_2, five times, 1 minute; 0.1 M picric acid/CH_2Cl_2, two times, 5 minutes; CH_2Cl_2, seven times, 1 minute; 5% DEA/CH_2Cl_2, three times, 2 minutes; CH_2Cl_2, seven times, 1 minute. The volume of the picric acid treatments was 30 ml. When monitoring was performed after deprotection, the above program was introduced after the deprotection cycle and was followed by an additional deprotection cycle with a 5-minute treatment of 50% TFA/CH_2Cl_2 instead of 30 minutes in order to remove any nonspecifically bound picric acid before continuing with the synthesis.

The completed peptide was acetylated by treatment with the previous acetylation mixture after removal of the N-terminal Boc group.

b. Synthesis of AcA''STnC(98-123)amide (peptide II) and AcA''STnC(90-123)amide (peptide III)

Peptides II and III and the remaining peptides were synthesized using a benzhydrylamine resin (Pietta and Marshall, 1970) to minimize the loss of growing peptide chains during the deprotection steps of the synthesis. A second advantage in using a benzhydrylamine support is that the C-terminal carboxyl group linked to the resin is converted to an amide group when cleaved from the resin by HF (Southard, 1971). An amide group is more appropriate in this C-terminal position since the sequence of the synthetic fragment is in the interior of the protein and the C-terminal carboxyl group would be involved in a peptide bond.

The peptides AcA''STnC(98-123)amide (peptide II) and AcA''STnC(90-123)amide (peptide III) were prepared by a combination of stepwise and fragment coupling solid phase procedures (Fig. II.2). Boc-Gly (0.5 mmol) was coupled to benzhydrylamine resin (2 g; 0.51 mmol NH_2/g resin) using one dicyclohexylcarbodiimide mediated coupling in CH_2Cl_2.

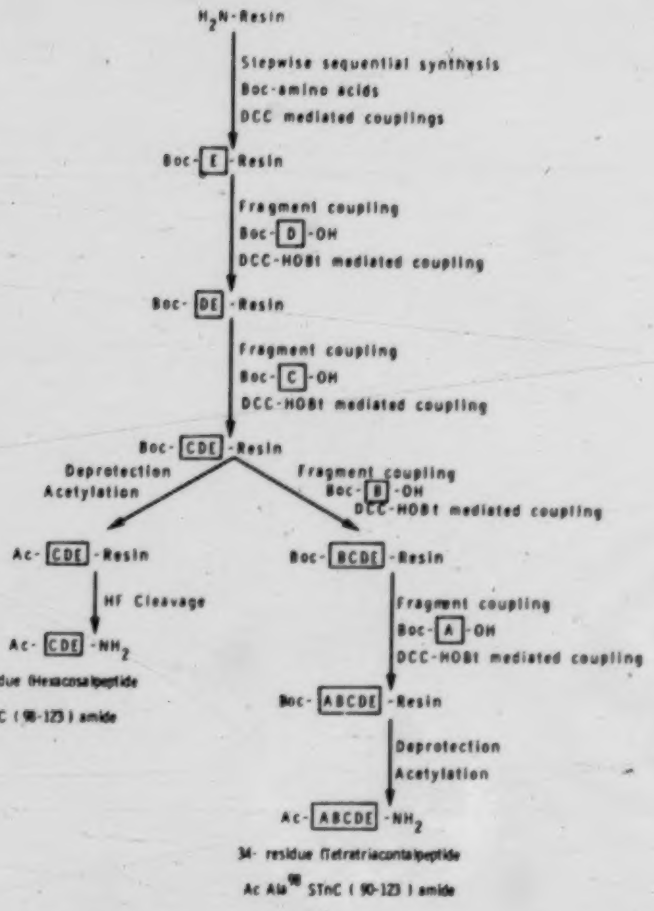
H2N-Resin
Stepwise sequential synthesis
Boc-amino acids
DCC mediated couplings
Boc-E-Resin
Fragment coupling
Boc-D-OH
DCC-HOBt mediated coupling
Boc-DE-Resin
Fragment coupling
Boc-C-OH
DCC-HOBt mediated coupling
Boc-CDE-Resin
Deprotection
Acetylation
Fragment coupling
Boc-B-OH
DCC-HOBt mediated coupling
Ac-CDE-Resin
HF Cleavage
Ac-CDE-NH2
26-residue (Hexacosa)peptide
Ac Ala98 STnC (98-123) amide
Boc-BCDE-Resin
Fragment coupling
Boc-A-OH
DCC-HOBt mediated coupling
Boc-ABCDE-Resin
Deprotection
Acetylation
Ac-ABCDE-NH2
34- residue (Tetratriaconta)peptide
Ac Ala98 STnC (90-123) amide

Fragment	Amino Acid Sequence
A	90 93 KSEE
B	94 97 ELAE
C	98 100 AFR
D	101 103 IFD
E	104 123 RNADGYIDAEELAEIFRASG

Fig. II.2 Strategy used for the synthesis of the 26- (peptide II) and 34-residue (peptide III) peptides. Fragment E denotes the 20-residue protected fragment prepared by solid phase peptide synthesis on the resin. Fragments A, B, C and D denote those protected fragments prepared by the solution method and then coupled to the 20-residue fragment on the resin.

Boc-Gly resin (237 μmol glycine/g Boc-Gly resin) was acetylated with pyridine-acetic anhydride-benzene (3:1:3 v/v) to terminate free amino acid groups on the benzhydrylamine resin which did not couple Boc-glycine. The next 19 residues were coupled by the standard stepwise automated coupling procedure described earlier for peptide I.

The protected fragments were coupled using the hydroxybenztriazole active ester procedure (Konig and Geiger, 1970; Gisin et al., 1977). The appropriate fragment (2.5 equivalents to free amino groups on the eicosapeptide resin) was dissolved in CH_2Cl_2 (8 ml). Hydroxybenztriazole in a 1:1 molar ratio with the fragment was dissolved in dimethylformamide (4 ml). The fragment and hydroxybenztriazole solutions were added to the deprotected and neutralized eicosapeptide resin in CH_2Cl_2 (~ 6 ml) and the mixture was stirred for five minutes. Dicyclohexylcarbodiimide (1.05 equivalents to hydroxybenztriazole and fragment) in dimethylformamide (4 ml) was added to the mixture and the coupling proceeded for 48 hours at room temperature. With the exception of the above coupling procedure and the fact that one coupling of each fragment was carried out , the programs used for the deprotection and coupling cycles were identical to the ones described for peptide I.

After coupling fragments C and D, the resin was divided in half by weight. One half of the hexacosapeptide resin was deprotected, acetylated with pyridine-acetic anhydride-benzene (3:1:3, v/v) and cleaved with HF as described below to produce crude AcA''STnC(98-123)amide. The synthesis was continued using the other half of the hexacosapeptide resin and coupling fragments A and B in the same manner described for C and D using half the volumes. The protected 34 residue peptide resin was deprotected, acetylated and cleaved with HF to produce crude AcA''STnC(90-123)amide.

c. Purification of peptides AcSTnC(103-123), AcA''STnC-(98-123)amide and AcA''STnC(90-123)amide (peptides I, II and III)

The residue obtained from HF cleavage (section G.2.f) was dissolved in a small volume (3-5 ml) of 50 mM NH_4HCO_3 and desalted on a Bio-Gel P-2 column (1.5 cm x 120 cm) eluting with 50 mM NH_4HCO_3 at a flow rate of 10 ml/hour and monitoring the column effluent at 230 nm. The desalted and lyophilized product was dissolved in 10-15 ml of 50 mM Tris-HCl, 50 mM KCl, 1 mM EGTA at pH 7.5 and applied to a DEAE-Sephacel column (2 cm x 36 cm) equilibrated with the same buffer and eluted with 200 ml of the starting buffer followed by a linear ionic gradient of 1000 ml of starting buffer and 1000 ml of 50 mM Tris-HCl, 500 mM KCl, 1 mM EGTA at pH 7.5 with a flow rate of 60 ml/hour. The effluent was monitored at 230 nm and fractions of 10 ml were collected. The fractions containing the major peak (Peak I in Fig. II.3a) were combined, lyophilized, desalted as described above and the residue thus obtained was dissolved in a small volume (2-3 ml) of 1.0 mM KH_2PO_4, 200 mM KCl at pH 7.0. The solution was applied to a hydroxyapatite column (1 cm x 25 cm) and eluted with 40 ml of 1.0 mM KH_2PO_4, 200 mM KCl, pH 7.0 followed by a linear phosphate gradient of 250 ml of starting buffer and 250 ml of 50 mM KH_2PO_4, 200 mM KCl, pH 7.0 with a flow rate of 10 ml/hour. The column was monitored at 280 nm and fractions of 3.3 ml were collected. The fractions containing the major peak eluting from the column (Peak II in Fig. II.3b) were combined and lyophilized, then desalted as described above. The purity of the 26 and 34 residue peptides was estimated from the amino acid analysis (Table II-1) while the purity of the 21 residue fragment was estimated from amino acid analysis (Table II-1) and high voltage paper electrophoresis at pH 6.5. Percentage yields of the 21, 26 and 34 residue peptides based on original amino acid esterified to the resin were 11, 13 and 16%, respectively, after all purification steps.

d. Synthesis and purification of AcA''STnC(90-104)amide (peptide IV)

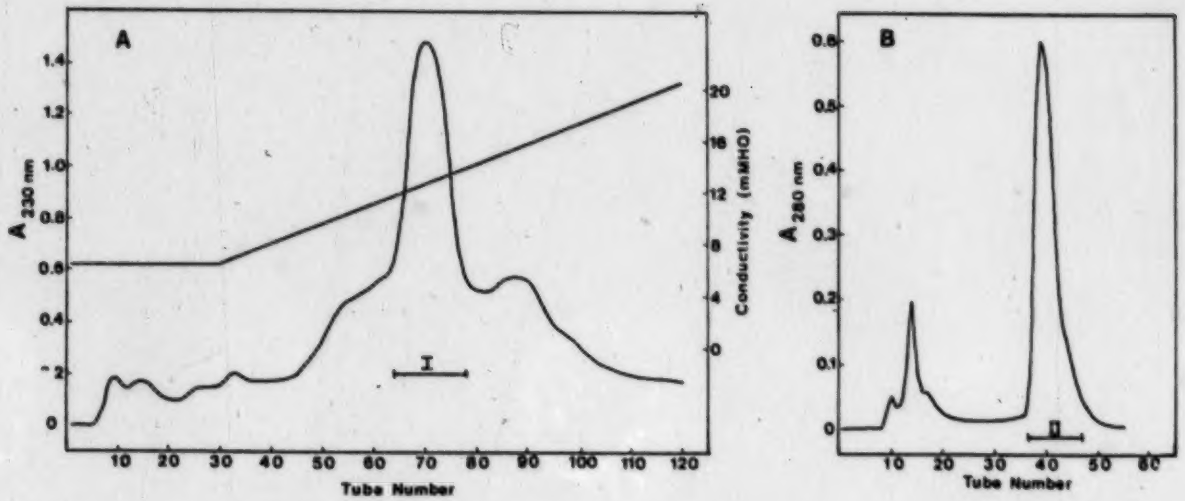

Fig. II.3 Purification scheme of AcA^{98}STnC(90-123) amide. The crude sample from HF cleavage was applied to a DEAE-Sephacel column (A), then peak I from this column was applied to an hydroxyapatite column (B). Experimental details are described in the text. The conductivity measurements in (A) were blanked against double distilled deionized water.

TABLE II-1

AMINO ACID COMPOSITION OF PURIFIED SYNTHETIC AND CYANOGEN BROMIDE PEPTIDES

Amino Acid Residue	AcSTnC(103-115) amide		AcSTnC(103-123)		AcA^{98}STnC (98-123)amide		AcA^{98}STnC (90-123)amide		AcA^{98}STnC (90-104)amide		HSer^{135}STnC (84-135)	
	Theoretical	Experimental	Theoretical	Experimental	Theoretical	Experimental	Theoretical	Experimental	Theoretical	Experimental	Theoretical	Experimental
Asx	4	3.97	4	4.00	4	4.03	4	4.12	1	0.98	6	6.29
Thr	-	-	-	-	-	-	-	-	-	-	1	1.03
Ser[a]	-	-	1	1.05	1	0.93	2	1.86	1	0.78	3	2.54
Glu	2	2.01	3	2.95	3	2.99	7	7.31	4	3.94	12	11.80
Gly	1	1.02	2	2.17	2	1.99	2	2.02	-	-	3	3.20
Ala	2	2.01	4	4.29	5	5.15	6	5.81	2	1.99	6	5.80
Val	-	-	-	-	-	-	-	-	-	-	1	1.16
Ile	1	0.95	2	1.60	3	2.84	3	2.64	1	1.00	4	3.77
Leu	1	1.02	1	1.02	1	1.19	2	2.16	1	1.02	3	3.07
Tyr	1	0.99	1	1.01	1	1.02	1	0.93	-	-	1	0.96
Phe	-	-	1	0.84	3	2.86	3	2.95	2	2.03	3	3.03
Lys	-	-	-	-	-	-	1	0.96	1	1.05	3	3.17
His	-	-	-	-	-	-	-	-	-	-	1	0.92
Arg	1	1.04	2	2.07	3	3.00	3	3.24	2	2.19	3	3.35
HSer	-	-	-	-	-	-	-	-	-	-	1	1.40
Cys	-	-	-	-	-	-	-	-	-	-	1	n.d.[b]

[a] Partly destroyed during acid hydrolysis

[b] n.d. stands for not determined

Boc-Arg(Tos) (0.275 mmol) was selectively coupled to a benzhydrylamine support (1.03 g; 0.56 meq/g resin) using a 1.1:1 equivalent of dicyclohexylcarbodiimide (0.3 mmol).

Boc-Arg(Tos) resin (167 μmol Arg(Tos)/g Arg(Tos) resin) was acetylated with pyridine-acetic anhydride-benzene (3:1:3, v/v) to terminate free amino groups on the resin which did not couple Boc-Arg(Tos). The remaining 14 residues were coupled using the stepwise solid phase procedure described for peptide I. Each Boc-amino acid were coupled twice using 6 and 3 equivalents for the first and second coupling respectively. The coupling time was increased to 90 minutes.

The final peptide was acetylated with pyridine- acetic anhydride-benzene (3:1:3, v/v) in a manner similar to the one described for peptide I. After HF cleavage from the resin, the crude peptide was initially purified on a QAE A25 column (30 cm x 1 cm) using a 100 mM KH_2PO_4, 10 mM KCl, pH 6.50 buffer as the eluent. The major peak from this purification was lyophilized and desalted on either a Biogel P2 column equilibrated in 50 mM NH_4HCO_3 or by reverse phase high pressure liquid chromatography on a SynChropak RP-P C18 preparative column (1 cm x 25 cm) (Linden, Indiana) using a 0.1% TFA/water, 0.1% TFA/acetonitrile gradient. For this later purification method, a 0% to 60% gradient of 0.1%

TFA/acetonitrile (60 min gradient with a flow rate of 2 ml/min) was sufficient to elute the peptide as a single peak. The composition and concentration of the pure peptide was verified by amino acid analysis (Table II-1).

e. Synthesis and purification of AcSTnC(103-115)amide (peptide V)

Boc-Leu (0.55 mmol) was selectively coupled to a benzhydrylamine support (2.0 g; 0.56 meq/g. resin) using 1 equivalent of dicyclohexylcarbodiimide (0.55 mmol).

Boc-Leu resin (240 μmol Leu/g of Leu resin) was acetylated as described earlier in order to terminate free amino acid groups on the benzhydrylamine resin which did not couple Boc-leucine. The remaining 12 residues were coupled by stepwise solid phase peptide synthesis as described for peptide IV. The peptide N-terminal was acetylated using a previously described procedure.

The crude peptide was initially purified by high pressure liquid chromatography (HPLC) on a SynChropak AX300 ion exchange column (Linden, Indiana; 250 x 10.0 mm ID). The crude peptide was dissolved in 5 mM KH_2PO_4, pH 7.5 buffer and the sample pH reajusted to 7.5 with 1 M KOH. The undissolved material was centrifuged. Aliquots of the supernatant were then injected on the column. A gradient was constructed using 5 mM (buffer A) and 300 mM (buffer B) KH_2PO_4 buffers ajusted to pH 7.5. The program used to isolate the pure peptide was as follows: 100% A, 5 minutes; linear gradient from 100% A to 85% A:15% B, 40 minutes; 85% A:15% B, 5 minutes; linear gradient from 85% A:15% B to 75% A:25% B, 5 minutes; linear gradient from 75% A:25% B to 100% A, 5 minutes; 100% A, 10 minutes. The flow rate was 2 ml/min and the absorbance was recorded at 220 nm using a 3 mm path cell. Figure II.4a illustrates a typical purification pattern observed using our HPLC approach. The major peak was desalted on a HPLC preparative C-18 SynChropak RP-P column (Linden, Indiana; 250 x 10.0 mm ID). The peptide was dissolved in 0.1% TFA/water and the pH was ajusted to pH 2.5 with concentrated hydrochloric acid. The peptide was eluted off as a single peak using a 0% to 30% gradient of 0.1% TFA/acetonitrile (45 minute gradient; 2 ml/min flow rate) (Fig. II.4b). The composition and concentration of the pure peptide were verified by amino acid analysis (Table II-1).

f. Cleavage of peptides from the resin

Cleavage of peptides from their support and the removal of blocking groups were carried out in hydrofluoric acid at 0 °C for 30 minutes (in the case of peptide I) or 45 minutes (in the case of peptide II, III, IV and V) in a type 1 hydrofluoric acid apparatus from Protein Research Foundation

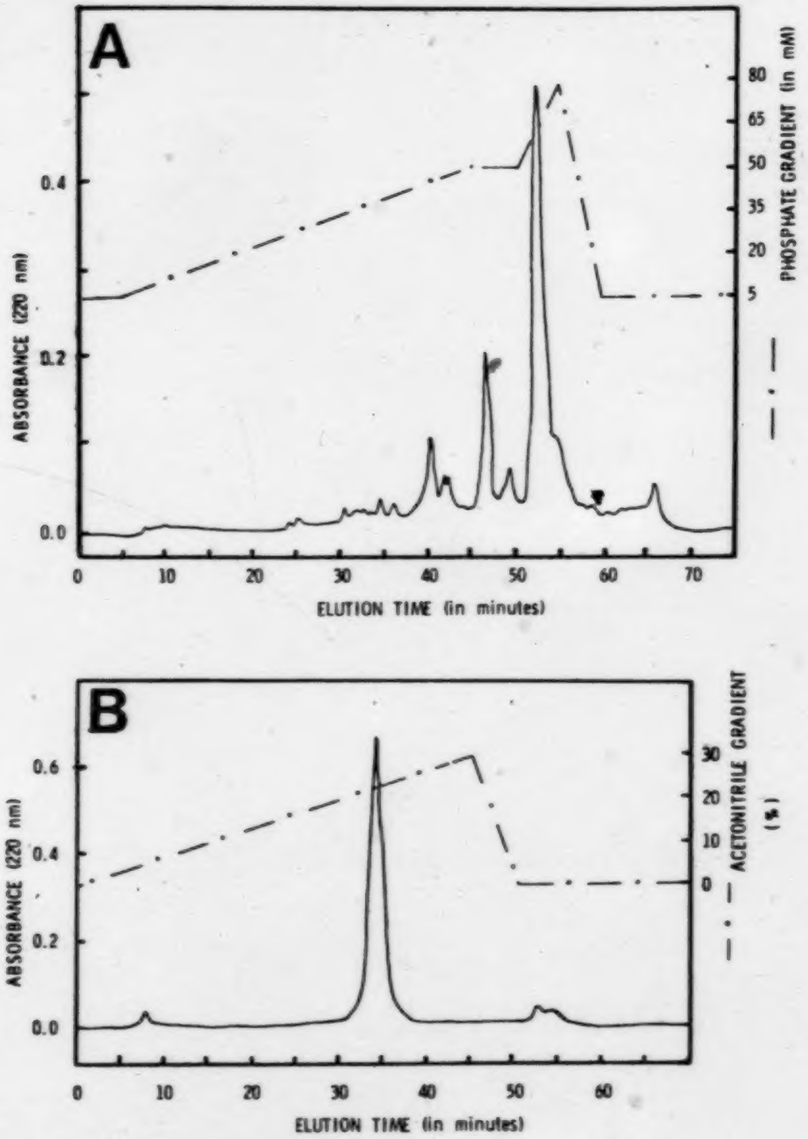

Fig. II.4 Purification scheme of AcSTnC(103-115) amide.
(A) HPLC purification of the crude peptide on a preparative ion-exchange column. The flow rate was 2 ml/min, and 500 µl of a 16 mg/ml solution of the crude peptide was typically injected on the column. The phosphate gradient used to elute the fragment is described in the text.
(B) HPLC purification of the major peak eluted from the ion-exchange column on a preparative reverse phase column. The flow rate was 2 ml/min. The 0.1% TFA/water:0.1% TFA/acetonitrile gradient is described in the text.

with 10% distilled anisole (v/v) as a cation scavenger. The HF and the bulk of the anisole were removed under vacuum below 0 °C. The residue was washed with ether (3 x 5 ml) to remove the remaining anisole and other by-products, then extracted with 50% acetic acid (4 x 10 ml). The acetic acid extracts were evaporated to dryness and the residue dissolved in 50 mM ammonium bicarbonate by adjusting to pH 8.0 with 1 M sodium hydroxide, then the solution was lyophilised.

3. Synthesis assessment and troubleshooting

The primary sequence of rabbit skeletal troponin C (residues 90 to 123) is composed of several aspartic and glutamic acid residues. Some are involved in metal chelation while others are clustered together and offer a site of interaction for target proteins. However, most of the problems surrounding the chemical synthesis of such analogs revolve around these essential residues.

Attempts to synthesize the sequence 89 to 123, by stepwise solid phase synthesis on a chloromethyl resin support was unsuccessful. Weak couplings were observed for Ile-110, Asp-103, Arg-100 and in the Glu-94 to Glu-92 region. Amino acid analysis of peptide-resin samples collected during the synthesis also revealed that the ratio of Arg-100 to Leu-114 was only 0.20. Thus the amount of growing peptide chains having the correct sequence was already down to less than 20% after only 24 amino acid couplings. Purification of the HF crude peptide on a DEAE-Sephacel column gave a complex mixture of peaks. Efforts to purify the proper sequence failed, as the further purification of selected peaks yielded further mixtures of peptides. Poor amino acid analysis results were consistently observed.

The synthesis was repeated on a benzhydrylamine support to minimize peptide chain loss during the deprotection steps (Pietta and Marshall, 1970). The first 20 amino acids were coupled by stepwise solid phase peptide synthesis. To cope with the weak coupling steps previously mentioned, we decided to synthesize small tri- and tetrapeptides and coupled them in solution to the eicosapeptide (i.e. 20-amino acid) resin using the hydroxybenztriazole active ester method (Konig and Geiger, 1970; Gisin *et al.*,1977). This scheme was presented earlier in Fig. II.2. The synthesis performance is illustrated in Table II-2. The synthesis appeared to have proceeded correctly for the initial 20 amino acids. The first fragment reacted with an 82% coupling yield. The second and third fragments coupled well (>90% coupling) while the last fragment showed a poor coupling performance (only 64% coupling observed). Only one major

TABLE II-2

PROGRESS OF THE SYNTHESIS OF PEPTIDE AcA^{98}STnC(90-123)amide

SYNTHESIS ORDER	SEQUENCE NUMBER	AMINO ACID	HYDROLYSIS								
			1	2	3	4	5	6	7	8	9
1	123	Gly	1.10	1.10	1.10	1.10	1.10	1.10	1.10	1.10	1.10
2	122	Ser[a]	0.62	0.62	0.62	0.62	0.62	0.62	0.62	0.62	0.62
3	121	Ala	1.04	1.04	1.04	1.04	1.04	1.04	1.04	1.04	1.04
4	120	Arg	0.99	0.99	0.99	0.99	0.99	0.99	0.99	0.99	0.99
5	119	Phe	0.96	0.96	0.96	0.96	0.96	0.96	0.96	0.96	0.96
6	118	Ile	0.96	0.96	0.96	0.96	0.96	0.96	0.96	0.96	0.96
7	117	Glu	0.94	0.94	0.94	0.94	0.94	0.94	0.94	0.94	0.94
8	116	Ala		1.06	1.06	1.06	1.06	1.06	1.06	1.06	1.06
9	115	Leu		0.96	0.96	0.96	0.96	0.96	0.96	0.96	0.96
10	114	Glu		0.93	0.93	0.93	0.93	0.93	0.93	0.93	0.93
11	113	Glu			0.95	0.95	0.95	0.95	0.95	0.95	0.95
12	112	Ala			0.94	0.94	0.94	0.94	0.94	0.94	0.94
13	111	Asp			0.96	0.96	0.96	0.96	0.96	0.96	0.96
14	110	Ile			0.89	0.89	0.89	0.89	0.89	0.89	0.89
15	109	Tyr			0.84	0.84	0.84	0.84	0.84	0.84	0.84
16	108	Gly			0.88	0.88	0.88	0.88	0.88	0.88	0.88
17	107	Asp				0.92	0.92	0.92	0.92	0.92	0.92
18	106	Ala				0.93	0.93	0.93	0.93	0.93	0.93
19	105	Asn					0.92	0.92	0.92	0.92	0.92
20	104	Arg					0.80	0.80	0.80	0.80	0.80
21	103	Asp						0.73	0.73	0.73	0.73
22	102	Phe						0.82	0.82	0.82	0.82
23	101	Ile						0.90	0.90	0.90	0.90
24	100	Arg							0.99	0.99	0.99
25	99	Phe							0.73	0.73	0.73
26	98	Ala							1.08	1.08	1.08
27	97	Glu								0.90[b]	0.90
28	96	Ala								0.85	0.85
29	95	Leu								0.93	0.93
30	94	Glu								0.90[b]	0.90
31	93	Glu									0.64[b]
32	92	Glu									0.64[b]
33	91	Ser[a]									0.28
34	90	Lys									0.65

[a] Serine was partly destroyed during acid hydrolysis

[b] Average value

SAMPLING POINTS

```
  90                 100               110                   120   123
Ac-K-S-E-E-E-L-A-E-A-F-R-I-F-D-R-N-A-D-G-Y-I-D-A-E-E-L-A-E-I-F-R-A-S-G-OH
 9       8       7     6     5   4   3           2     1
```

product was observed in the purification step. Similarly, the major peptide impurity from the synthesis of AcA''STnC-(90-104)amide was purified by HPLC on a C18 column and was shown to lack a single glutamic acid residue. Finally, the sequential synthesis of the fragment AcA''STnC(90-115)amide was attempted (Clare, D.M., personal communication) with little success, as Asp-103 coupled poorly (less than 25% coupling yield). In summary, synthesis problems associated with the N-terminal region are centered around the coupling of Asp-103 and of one or more of the glutamic acid residues (Glu-92, -93, -94 and -97), particularly Glu-94.

Synthesis difficulties arose also in synthesizing the calcium binding loop region. For example, Reid (personal communication) noticed in his attempt to synthesize the peptide region 90 to 115, the poor coupling of Glu-113, Asp-111 and -107, Ile-110, Gly-108 and Asn-105. It was also discovered during the purification of a crude preparation of AcSTnC(103-115)amide, that the major peptide impurity represented a fragment lacking one of the glutamic acid residues (either Glu-113 or -114).

The C-terminal region (115 to 123) of our fragments was relatively free of synthesis problems.

In summary, the residues suspected to be involved in weak couplings are underlined in the sequence listed below

Table II-2. Although this section has depicted the synthesis of these analogs as an almost impossible task, one should realize that the adequate solid phase synthesis of the first 20 amino acids is not difficult to achieve. The major problem associated with the synthesis of longer peptides is rather related to the tendency of our tri- and tetrapeptides to degrade even upon storage at 4 °C in a crystalline state. This experimental parameter can however be improved by recrystallizing these fragments prior to their use and by assessing their purity by thin layer chromatography. Alternatively, liquid chromatography might prove to be necessary to achieve a proper level of purification of these tri- and tetrapeptides.

H. CHEMICAL CLEAVAGE OF TROPONIN C

1. Modification and cyanogen bromide cleavage of rabbit skeletal troponin C

Rabbit skeletal troponin C was prepared as described elsewhere (Chong and Hodges, 1981). This protein was then modified with 5,5'-dithiobis(2-nitrobenzoic acid) (DTNB) in order to protect cysteine 98 from modification during the cyanogen bromide cleavage (Nagy *et al.*, 1978). The modification step was performed as follows, troponin C was first dissolved in a buffer containing 8 M urea, 0.2 M Tris acetate, 0.1 M EGTA, 50 mM DTT, pH 8.0 (200 mg TnC/12 ml buffer) and dialysed against the above buffer for 4 hours to insure the denaturation of the protein and the reduction of the sulphydryl group. DTNB (100 mg, DTNB/-SH ratio of 16:1) was then added to the dialysis bag and dialysis was continued for 30 minutes at room temperature. The protein solution was then dialysed against 50 mM NH_4HCO_3 (3 x 8 liters, 6 hours per change at 4 °C) to insure the removal of unbound DTNB (change in color from orange to light yellow) and of the components of the original buffer used. This step was followed by a further dialysis against 5% formic acid (2 x 8 liters, 6 hours per change at 4 °C). The protein solution showed traces of precipitate at this stage probably due to the transition from pH 8 to pH 2 (the isoelectric point of TnC is around 4). The entire contents of the bag was lyophilized in a flask of adequate dimension (1200 ml) to allow the direct cyanogen bromide cleavage of the modified troponin C. The protein was then dissolved in 70% formic acid to a final concentration of 10 mg/ml. Protein cleavage was initiated by treating the modified protein with a 200 fold excess of cyanogen bromide. The reaction was left to proceed for 24 hours at room temperature. Digestion was complete as demonstrated by the absence of a troponin C band on SDS urea polyacrylamide gel electrophoresis of the digest.

2. Purification of a cyanogen bromide fragment containing the region 84 to 135 of rabbit skeletal troponin C

The digest was fractionated on a Sephadex G-50 superfine column (190 cm x 1.5 cm) equilibrated in 50 mM NH_4HCO_3. The CB9 containing peak was further purified on the same column. This material showed a single band on SDS urea polyacrylamide gel electrophoresis and a single peak by reverse phase high pressure liquid chromatography. The HPLC column used in this case was a preparative C18 SynChropak RP-P column mentioned above. The peptide CB9 was eluted from the column using a 0% to 60% gradient of 0.1% TFA/acetonitrile (60 min gradient with a flow rate of 2 ml/min). The peptide sequence and concentration were determined by amino acid analysis (Table II-1).

I. PREPARATION OF IODINATED PEPTIDES

Lactoperoxidase was used to catalyse the iodination of the single tyrosine present in AcA''STnC(98-123)amide and AcA''STnC(90-123)amide using a methodology previously described (Seamon *et al.*, 1977; Morrison and Bayse, 1970). The 10 ml reaction mixture consisted of 0.1 mM of the peptide, 0.1 mM KI, 50 mM sodium phosphate buffer, pH 7.0, 0.1 mM H_2O_2, 0.30 IU of lactoperoxidase (Sigma) and 5 mM EGTA. The iodination was initiated by the addition of the enzyme and monitored by the decrease in tyrosine fluorescence at 305 nm (excitation at 280 nm). Successive additions of KI and H_2O_2 were made to insure total iodination of the tyrosine. When the residual fluorescence was reduced to 5% of the original intensity, the reaction was stopped by the addition of 100 μl of a 50 mM DTT solution.

J. ULTRAVIOLET SPECTROSCOPY

1. Experimental procedure

The absorption and difference spectra were measured on a Cary 118 C recording spectrophotometer at 25 °C over a wavelength range from 250 to 350 nm. Spectra were recorded using two quartz cells having a 1 cm path length and a 1 ml volume. Constant dry N_2 flushing was used to purge the optical track and cell component as it enhanced the stability of the instrument. Typically an absorption spectrum was obtained after calibrating both cells (sample and reference) in the presence of starting buffer while a difference spectrum required the calibration of both cells with the peptide solution investigated. In the latter case, equal volumes of calcium solution or buffer were added to the sample cell (+ Ca^{2+}) and the reference cell (+ buffer) before the spectrum was recorded.

2. Peptide samples

Solutions of AcSTnC(103-123), AcA''STnC(98-123)amide and AcA''STnC(90-123)amide (0.4 mM) were prepared in either 100 mM MOPS, 50 mM KCl, 1 mM EGTA, pH 7.5 (aqueous medium) or 50 mM MOPS, 25 mM KCl, 0.5 mM EGTA, 50% trifluoroethanol (TFE), pH 7.5 (hydrophobic medium). Note that all buffers were prepared with double distilled water previously treated with chelex resin and filtered through a 0.45 μm millipore filter prior to their use. The peptide concentration was determined by amino acid analysis.

3. Calcium solutions

Calcium solutions (10 to 100 mM) were prepared from reagent grade $CaCl_2$ dihydrate in either the aqueous or the hydrophobic buffers mentioned above. Their calcium content was accurately measured by titration with a standard EDTA solution using murexide as the end point indicator (Blaedel and Knight, 1954).

K. CIRCULAR DICHROISM

1. Circular dichroism measurements

Circular dichroism measurements were performed using a Cary 60 recording spectropolarimeter equipped with a Cary 6001 CD attachment (Oikawa *et al.*, 1968) or on a Jasco J-500C spectropolarimeter.

The mean residue ellipticity, $[\theta]_\lambda$, at a wavelength λ, was calculated from the expression:

$$[\theta]_\lambda = \theta_\lambda \times MRW/(100 \times l \times c)$$

where MRW represents the mean residue weight (taken as 113 in these studies), θ_λ is the observed ellipticity value at a selected wavelength, l represents the cell path length and was equal to 0.005 dm and c is the peptide concentration in gcm^{-3}. The units of $[\theta]_\lambda$ are $degree.cm^2.dmole^{-1}$.

2. Precautions against metal contamination

Nalgene beakers, plastic pipettes and vials were used throughout the study to avoid the calcium contamination of peptide and drug solutions. In addition, Ca^{2+}-free buffers were prepared from deionized distilled water which had been treated with Chelex resin.

3. Calcium solutions

Calcium solutions (10 to 100 mM) were prepared from reagent grade $CaCl_2$ dihydrate and their concentration was determined by titration with a standard EDTA solution using murexide as the end point indicator (Blaedel and Knight, 1954).

4. Calcium titrations of AcSTnC(103-123), AcA''STnC(98-123)amide and AcA''STnC(90-123)amide

a. Peptide samples

The lyophilized peptides AcSTnC(103-123), AcA''•STnC-(98-123)amide and AcA''•STnC(90-123)amide were initially dissolved and diluted to a concentration of 0.4 mM in either 8 M urea, 100 mM Tris, 50 mM KCl, 5 mM EGTA, pH 7.2 (denaturing medium) or 100 mM MOPS, 50 mM KCl, 1 mM EGTA, pH 7.5 (aqueous medium) or 50 mM MOPS, 25 mM KCl, 0.5 mM EGTA, 50% trifluoroethanol (v/v), pH 7.1-7.5 (hydrophobic medium).

b. Determination of calcium binding constants

The concentration of free Ca^{2+} in solution was controlled by an EGTA-containing buffer and calculated using the computer program of Perrin and Sayce (1967) with the $\log_{10}$ of the association constants for the complexing. species of EGTA (Sillin and Martell, 1964) set at: H^+ to $EGTA^{4-}$, 9.46; H^+ to H_1EGTA^{3-}, 8.85; H^+ to H_2EGTA^{2-}, 2.68; H^+ to H_3EGTA^{1-}, 2; CaL, 11.00; and CaHL, 5.33. Free metal ion concentrations were corrected for peptide-bound Ca^{2+} assuming 1 mole of Ca^{2+} is bound/mol of peptide using the Perrin and Sayce computer program for two ligands. An estimate of the $\log_{10}$ of the association constant for the calcium peptide complex (CaP) was inserted into the program, and the free Ca^{2+} values determined were used to calculate an association constant as described below. The calculated value of the association constant was used to revise the estimate of the association constant (CaP) in the Perrin and Sayce program for two ligands. This procedure was repeated until the calculated association constant equalled that inserted in the Perrin and Sayce program. The $4H^+$ to peptide association constant was set at 4.00 to correspond roughly to the pK*a* of the side chains of the acid residues involved in chelation. These calculations also assume that the cumulative association constants for EGTA complexing species remain the same in both hydrophobic and aqueous solvents.

A second computer program (Hincke *et al.*, 1978) is used to perform a nonlinear curve-fitting iterative procedure which fit the data to an equation of the form:

$$\Delta[\Theta]_{220} = \sum_{i} \frac{n_i \; K_i \; [Ca^{2+}]}{1 + K_i \; [Ca^{2+}]}$$

where *i* = 1, and extracted the values of n*i* and K*i*. Here, n*i* is the maximum value of $[\theta]_{220}$ which can be elicited from the *i*th class of Ca^{2+}-dependent transitions, K*i* is the apparent association constant of the *i*th class of binding sites, and $[Ca^{2+}]$ is the concentration of free Ca^{2+} calculated as described.

c. Determination of α-helical content

The effect of Ca^{2+} and trifluoroethanol on the CD spectra of the 21-, 26- and 34-residue peptides have been analyzed in terms of helix content based on the Chen, Yang and Chau equation (Chen *et al.*, 1974) for chain length dependence of helices:

$$[\Theta]_{\lambda} = (f_{H} - ik/N) [\Theta]^{\infty}_{H\lambda} + f_{R} [\Theta]_{R\lambda} \qquad 1.$$

where $[\theta]_{\lambda}$ is the observed mean residue ellipticity at wavelength λ, $[\theta]^{\infty}_{H}$ is the maximum mean residue ellipticity of a helix (H) of infinite length, $[\theta]_{R}$ is the mean residue ellipticity for the pure unordered form (R), the f values are the fractions of the two forms in the molecule, i is the number of helical segments, N is the total number of residues and k is a wavelength-dependent constant. The $f\beta[\theta]\beta$ term is ignored for these calculations since we assume no β-sheet formation in any of our peptides under any of the conditions studied. The $[\theta]_{R}$ values for 1-nm intervals between 215-240 nm were empirically determined as the average CD spectra for the 26- and 34-residue apopeptides in 8 M urea. The $[\theta]^{\infty}_{H}$ values at 1-nm intervals were obtained from Chang *et al.* (1978). The CD spectra in the presence of Ca^{2+} were analyzed in terms of helix content by first subtracting the contribution to the mean residue ellipticity due to loop formation $[\theta]_{L\lambda}$:

$$[\Theta]_{\lambda} - [\Theta]_{L\lambda} = (f_H - ik/N) [\Theta]^{\infty}_{H\lambda} + f_R [\Theta]_{R\lambda} \qquad 2.$$

$[\theta]_L$ values at 1-nm intervals between 215-240 nm were obtained by subtracting the $[\theta]$ values obtained from the spectra of the peptide in trifluoroethanol in the presence of Ca^{2+} from that obtained in trifluoroethanol in the absence of Ca^{2+}. Using empirically determined $[\theta]$ values between 215-240 nm, the values of f in equation 1 were varied to give the best fit to the experimental CD curve using a least-squares computer curve fitting procedure.

The values of i used to calculate f were as follows: apopeptides in aqueous medium, $i = 0$; apopeptides in the presence of trifluoroethanol for the 21-, 26- and 34-residue peptides, $i = 1$, 2 and 2, respectively; apopeptides in the presence of Ca^{2+}, $i = 0$, 1 and 1 or $i = 1$, 2 and 2 for the 21-, 26- and 34-residue peptides, respectively. The basic assumption used in the choice of an i value is that on proceeding from the 21-residue peptide (*loop-helix*) to the 26- or 34-residue peptides (*helix-loop-helix*) we are inducing the formation of the N-terminal helix with Ca^{2+} or trifluoroethanol, thus the *l* value increases by one. Though the α-helix content will vary with the value of *l* used in the calculation the relative changes in f_H between the 26- or 34-residue peptide and the 21-residue peptide remained unchanged, using the above assumption.

Nagy *et al*. (1978) showed that the α-helix content from $[\theta]_{222}$ for a pure α-helix with the added refinement of allowing for lengths of the helical segments (Chen *et al*., 1974) can be used to arrive at an α-helix content for CB9 with and without Ca^{2+} and the difference between these two values was in good agreement with the value derived from the difference CD spectrum by the curve fitting procedure. We have used this method to calculate the number of α-helical residues in TnC and its fragments with and without Ca^{2+} as shown in Table III-4:

$$[\Theta]_{222} = f_H \, [\Theta]_H^{\infty} \left(1 - k/\bar{n} \right)$$

where $\bar{n}$ is the average number of residues per helical segment of the protein molecule. As reported by Nagy *et al*. (1978), the helical segments in TnC and its fragments are unlikely to contain more than 8 to 10 residues.

5. Calcium and trifluoperazine titrations of CB9

a. CB9 and TnC samples

The CB9 sample was dissolved in 100 mM MES, 50 mM KCl, 1 mM DTT, 1 mM EGTA, pH 6.0 buffer to a concentration of 0.4 mM. The rabbit skeletal troponin C was dialysed against a 50 mM NH_4HCO_3, 1 mM EGTA, 1 mM DTT solution followed by water in the presence of chelex resin. The lyophilised sample was dissolved in 100 mM MES, 50 mM KCl, 1 mM DTT, pH 6.0 buffer to a concentration of 1mg/ml. The concentration of these samples was verified by amino acid analysis.

b. Trifluoperazine solutions

Trifluoperazine was obtained as a hydrochloride powder. The purity of this material was assessed by thin layer chromatography on silica gel plates (Merck). The first solvent system used was composed of 3 grams of ammonium acetate in 20 mls of water and 100 mls of methanol. The Rf value of the only spot observed under both U.V. light and phenothiazine staining conditions was 0.40. The second system used was composed of ammonium hydroxide, benzene and dioxane at a ratio of 5:60:35 respectively. The Rf value for the drug was 0.32. The positive identification of trifluoperazine was obtained using the sulphuric acid/formaldehyde test described by Clarke (1969). The concentration of a typical TFP solution prepared was determined both by weight and by optical density measurement at 256 nm, using an extinction coefficient value of 30,110 $M^{-1}cm^{-1}$ (Clarke,1969). Both approaches yielded similar values. Because of the light sensitivity of phenothiazines, only fresh solutions of the drug were prepared and kept in the dark for the remainder of the experiment. Typically, 5 to 30 mM stock solutions were made up for the C.D. experiments. Note that the pH of these stocks solutions was low (2.8 to 3.3) depending on the trifluoperazine hydrochloride concentration. We avoided going above a drug concentration of 1 mM during the titrations since at these concentrations, the drug outbuffered the buffering capacity of our samples. The pH of the sample at the end of the titration was reduced by only 0.05 of a pH unit under these conditions.

c. Determination of TFP and calcium binding constants

The ellipticity values obtained at 222 nm for the calcium titrations were used to evaluate the calcium binding constant of CB9. The non-linear fitting procedure used was described elsewhere (section 4.b). In the case of the TFP titration of CB9 in the absence of calcium, the binding constant of the drug was evaluated using the following Hill plot equation:

$$\log Y/(1-Y) = \log K_{ass.} + m \log [TFP]_{free}$$

where Y is the ratio of observed ellipticity at 222 nm over the maximum ellipticity recorded. $K_{ass.}$ represents the association constant of TFP with the peptide CB9 and $[TFP]_{free}$ represent the calculated concentration of the free drug during each step of the titration. A linear least-squares fitting of the data gave a correlation coefficient of 0.99 while the observed slope was of 1.4.

6. Calcium titration of AcA''STnC(90-123)amide in the presence of neuroleptic drugs

a. Peptide:drug samples

The following drugs were used without further purification; *cis*- and *trans*-thiothixene, benperidol, haloperidol, molindone, promethazine, chlorpromazine and fluphenazine. Their purity can be assessed by thin layer chromatography on silica gel plates, using a solvent system composed of a ammonia-methanol solution at a ratio of 1.5 to 100 (Clarke, 1969). Plates are then examined under ultraviolet light at 254 nm or by spraying them with an acidified iodoplatinate reagent (Clarke, 1969).

The buffer system chosen for the CD spectrophotometric studies was 100 mM MOPS pH 6.0, 50 mM KCl, 5 mM EGTA. The use of MES buffer is however preferable in future experiments since its p*Ka* (6.15) insures a better buffering capacity at pH 6.0 than MOPS (p*Ka* of 7.2). The peptide was dissolved in the above buffer and dialysed overnight against the same buffer in order to remove traces of calcium. The appropriate drug was dissolved in the above buffer, then the peptide and drug solutions were mixed to produce a drug/peptide ratio of 2.3/1 (1.0 mM drug/0.43 mM peptide) and the CD spectra were determined. All peptide:drug solutions were freshly prepared and maintained in the dark throughout the circular dichroism experiments. Ellipticity measurements and the determination of the calcium binding constant of the peptide in the presence of these drugs were described in previous sections.

L. NUCLEAR MAGNETIC RESONANCE

1. ^{1}H NMR measurements

^{1}H NMR experiments were performed with a Bruker HXS 270 MHz spectrometer operating in the Fourier transform mode and equipped for quadrature detection.

2. Metal contamination

Peptide and TFP solutions were prepared in plastic vails and beakers to minimize calcium and lanthanides contamination arising from their presence in glass matrices. All buffers were prepared from deuterated water and treated with Chelex resin (previously equilibrated in D_2O).

Calcium and lanthanides will interact with the glass surface of the NMR tubes. One should thus insure the removal of all traces of metal prior to the use of these tubes. The following sequence of soaks and washes was adopted:

i) Chromic acid soak, 30 minutes
ii) Double distilled water wash
iii) 3 N HCl/25% ethanol soak, 30 minutes
iv) Double distilled water wash
v) Deuterated water rinse
vi) Lyophilization of NMR tubes

The tubes were cleaned and lyophilized one day prior to their use.

3. Metal solutions

All calcium stock solutions were prepared from reagent grade $CaCl_2 \cdot 2H_2O$ dissolved in D_2O. The Ca^{2+} content was determined by EDTA titration using murexide as the end point indicator (Blaedel and Knight, 1954).

The lanthanum, lutetium and gadolinium solutions used in this study were prepared from reagent grade $LaCl_3.5\ H_2O$, Lu_2O_3 and $GdCl_3.6\ H_2O$. The lutetium oxide was converted to its chloride form by addition of an equimolar quantity of hydrochloric acid. The solutions were made up in 100 mM KCl, 0.1 mM DSS and adjusted to pH 6.0 with NaOD or DCl. Their lanthanide content was determined by EDTA titration using xylenol orange as the end point indicator (Lee and Sykes, 1980).

4. Calcium titrations of AcSTnC(103-123), AcA''STnC-(98-123)amide and AcA''STnC(90-123)amide

a. Peptide samples

The peptides were dissolved in 10 mM PIPES, 0.1 M KCl, 0.5 mM DSS in D_2O, pH 6.8.

b. Spectral parameters

A typical spectrum was obtained from 1000 acquisitions, using a 1 second acquisition time, a 9 μs pulse width (~90°), a ± 2000 Hz sweep width and a line broadening value of 1 Hz.

c. Laser Photo-CIDNP experiments

Kaptein (1978) has developed a NMR technique which allows the selective detection and assignment of resonances from exposed histidine, tyrosine and tryptophan residues.

The technique abbreviated laser photo-CIDNP is based on the use of a laser to produce a photochemically induced dynamic nuclear polarization effect on the protons of these aromatic side chains. Essentially, the method involves the use of a flavin dye which is photochemically excited to a triplet state during a brief laser irradiation of the NMR sample (step (1)).

$$F \xrightarrow{h\nu \text{ light}} {}^1F \rightarrow {}^3F \qquad (1)$$ *Photo excitation of the dye*

Any peptide or protein tyrosine, tryptophan or histidine side chains (Tyr(109) of rabbit skeletal troponin C in our case) accessible to the excited flavin will reversibly react with the dye to yield a transient radical pair. This step is depicted in the case of tyrosine 109 where the triplet state species ^3F abstracts its phenolic hydrogen atom (step (2)).

$$\text{Tyr(109)-OH} + {}^3F \rightarrow \text{Tyr(109)-O}\bullet + \text{FH}\bullet \qquad (2)$$ *Radical formation*

Nuclear polarization will occur upon recombination of the radical pair created (step (3)).

$$\text{Tyr(109)-O}\bullet + \text{FH}\bullet \rightarrow \text{Tyr(109)-OH} + F \qquad (3)$$ *Radical pairing*

Photobleaching of the dye may also occur as flavin molecules can recombine to generate a non-excitable form of the dye (step (4)).

$$2\ FH\bullet \rightarrow FH_2 + F \qquad (4)\ \textit{Photobleaching}$$

Similarly, an overexposure of the sample to laser light will increase the chances of protein or peptide modification through the presence of reactive side chain species.

The effect of nuclear polarization can be readily monitored by ^1H NMR as the spectral lines belonging to these particular side chain protons will be selectively enhanced. The enhancement pattern (emission or absorption) can be predicted by a series of CIDNP sign rules described by Kaptein (1971). In the case of tyrosine aromatic protons, a strong emission pattern (a negative enhancement of 28 times the size of the doublet) is observed for the 3,5 proton doublet while the 2,6 proton doublet is only slighty enhanced (1.7 fold increase in absorption).

A Spectra Physics Model 164 argon ion laser was utilized to illuminate the flavin containing sample. The 10 mm flat bottomed NMR tubes used contained typically 1.2 ml of a 0.5 mM peptide solution (10 mM PIPES, 0.1 M KCl, 0.5 mM DSS in D_2O, 5 mM $CaCl_2$, pH 6.8). A 5 μl aliquot of a 50 mM FMN stock solution was added to the NMR tube. The data was acquired in an alternating pattern, i.e., one spectrum of the non-irradiated sample followed by one of the irradiated sample, with a 10-second delay between the light and dark spectra. The light spectra were irradiated with 3.5 watts of power for 1 second prior to accumulation of the FID. Blocks of 8 spectra were collected using the spectral parameters mentioned before (section G.4.b).

5. Calcium and trifluoperazine titrations of CB9 and AcA''STnC(90-104)amide

a. Peptide samples

The peptide CB9 was dissolved in 15 mM PIPES, 0.1 M KCl, 0.2 mM DSS, pH 6.80. A 2 μl aliquot of β-mercaptoethanol was added to the 400 μl NMR samples before the experiment. As observed in a preliminary NMR spectrum, the addition of a reducing agent is essential for the proper folding of the fragment (spectrum not shown). As for the peptide AcA''STnC(90-104)amide, it was taken up in 25 mM KH_2PO_4, 50 mM KCl, pH 6.0.

b. Trifluoperazine solutions

The purity of the drug was assessed earlier (section J.5.b) and proven adequate for ^1H NMR studies. Solutions of trifluoperazine (30 mM) were freshly prepared in either 15 mM PIPES, 0.1 M KCl, 0.2 mM DSS, pH 6.80 or 25 mM KH_2PO_4, 50 mM KCl, pH 6.0 and were maintained in a dark environment throughout the ^{1}H NMR experiments.

c. Spectral parameters

For the peptide AcA''STnC(90-104)amide, a typical spectrum was obtained from 1000 acquisitions using a 1 s acquisition time, a 9 μs pulse width and a line broadening of 1 Hz. For the CB9 fragment, spectra were obtained from 4000 acquisitions using a 0.5 s acquisition time. All other parameters were as described above.

6. Lanthanide titrations of AcSTnC(103-115)amide

a. Peptide samples

The metal-free spectrum was obtained from a 8.3 mM peptide sample (400 μl) dissolved in 15 mM deuterated Imidazole, 100 mM KCl, 0.2 mM DSS, pH 7.0. The lanthanide titrations were performed on 0.8 mM samples of AcSTnC-(103-115)amide taken up in 100 mM KCl, 0.1 mM DSS and reajusted to pH 6.0 with a 0.5 N NaOD solution. In the case of the gadolinium titration, the 0.8 mM sample also contained 1.3 mM $LaCl_3$. The pH of the samples were monitored before and after the metal titration and were shown to remain at their initial value of 6.0. The exact peptide concentrations were determined by amino acid analysis.

Alternatively, absorbance measurements at 280 nm (extinction coefficient value of 2100 $M^{-1}cm^{-1}$) can be used to estimate the peptide concentration.

b. Spectral parameters

For the apopeptide (metal-free), the spectrum was obtained from 4000 acquisitions with a sweep width of ±2000 Hz and a 2 s acquisition time. The resolution in the spectrum was enhanced by zerofilling the 16 K FID to 32 K. The decoupling experiments were performed by irradiating selected resonances in the apopeptide spectrum and observing their connectivities with other resonances. Typically, 256 acquisitions were taken for each spectrum with a sweep width of ±2000 Hz, a 1 s acquisition time, a 8 μs pulse width (~80°) and a line broadening of 1 Hz. Spectrum parameters for the lanthanide titrations where as follows; 4000 acquisitions with a sweep width of ±2000 Hz, a 0.5 s acquisition time , a pulse width of 8 μs and a spectral line broadening value of 1 Hz.

c. Determination of La^{3+} and Lu^{3+} binding constants

The following equation was used to determine the quantity Y:

$$Y = (\delta_0 - \delta_f)/(\delta_s - \delta_f)$$

where δ_s represents the chemical shift of a peptide resonance in the metal-saturated spectrum, δ_o is the observed chemical shift value for this resonance at a particular point of the titration, while δ_f represents the resonance position in the absence of metal. This quantity was calculated for a variety of resonances during the course of a lanthanide titration. The averaged Y value for each titration point was plotted against the metal:peptide ratio and the binding constant was determined by a least-squares fitting of the data set to the equation;

$$Y = [(M_0+P_0+Kd)-((M_0+P_0+Kd)^2 - 4M_0P_0)^{1/2}]/2P_0$$

where M_0 and P_0 represent the total concentration of metal and peptide in the sample and Kd is the metal dissociation constant to be determined . Note that metal precipitation problems occured when the peptide solutions were titrated rapidly (addition of large aliquots of metal ion) or when the pH of the peptide solution was close to 7.0 (slow formation of hydroxides). Binding constants were determined from titrations where no precipitation was observed.

d. Gadolinium titration

The gadolinium titration was performed on a 0.8 mM sample of AcSTnC(103-115)amide dissolved in 100 mM KCl, 0.1 mM DSS, 1.3 mM $LaCl_3$ and reajusted to pH 6.0 with a

0.5 N NaOD solution. The sample was titrated by adding aliquots of a 1 mM Gd^{3+} solution to the NMR tube. Note that since most protons are within 10 Å of the metal, only trace amounts of gadolinium (≤ 5% of the peptide concentration) are required to excessively broaden the observed resonances. It was thus necessary to add an excess amount of lanthanum to the NMR tube to insure that the small concentrations of Gd^{3+} present in the sample did not fluctuate due to the known interaction of such metals with glass matrices (Jones *et al.*, 1974; Marinetti *et al.*, 1976). The exact peptide concentration was determined by amino acid analysis.

At the initial lanthanum and AcSTnC(103-115)amide concentrations of 1.27 mM and 0.77 mM, respectively; 98 % of the peptide can be calculated to exist in the bound state using a La^{3+} binding constant of $1.1 \times 10^5 M^{-1}$ (chapter IV). The percent peptide bound to gadolinium was calculated using the following relationship

$$\%Gd^{3+} \text{ bound} = \frac{98 \times [Gd^{3+}]_o}{[Gd^{3+}]_o + [La^{3+}]_o}$$

The terms $[Gd^{3+}]_o$ and $[La^{3+}]_o$ indicate the total concentration of gadolinium and lanthanum in the NMR tube. This expression assumes that Gd^{3+} and La^{3+} have the same affinity for the peptide and that the amount of Gd^{3+} added is small so that the fractional saturation of peptide by metal is unchanged.

e. T_1 and T_2 measurements

The spin-lattice relaxation times (T_1) of well defined proton resonances were determined from progressive saturation experiments. Typically the total delay time between spectral acquisitions was varied from 0.21 s to 4 s and 300 free induction decays (FID) were collected for each delay time, using a 9.5 μs (90°) pulse width, a 0.2 s acquisition time, a ± 2500 Hz sweep width and a line broadening value of 1 Hz. Peak heights of the resonances were measured and plotted as a function of total delay time between pulses following the equation

$$M_0 = M_\infty \, (1 - e^{-t/T_1})$$

where t is the total delay time, M_∞ and M_0 are the maximum and observed resonance peak heights and T_1 the spin-lattice relaxation time for the proton nucleus investigated.

The spin-spin relaxation times (T_2) of six well defined resonance patterns (Gly-108, 3.5 ppm doublet; Tyr-109, 7.00 ppm and 6.80 ppm doublets; Ala-106,-112), 1.45 ppm and 1.30 ppm doublets; Acetyl-Asp-103, 2.00 ppm singlet) were determined using a lineshape analysis program to determine $\pi\Delta\nu$ and the relationship

$$\pi \Delta\nu = 1/T_2$$

where $\Delta\nu$ represents the line width (in Hz) of a particular resonance line at half height. Spectra used for the line width measurements were obtained from 4000 acquisitions using a 0.5 s acquisition time, a 8 μs pulse width, a ± 2000 Hz sweep width and a line broadening value of 1 Hz.

CHAPTER III

CALCIUM-INDUCED PEPTIDE FOLDING: IMPORTANCE OF N- AND C-TERMINAL HELICAL REGIONS OF THE EF HAND

A. SPECTROSCOPIC STUDIES OF ANALOGS OF SITE III OF RABBIT SKELETAL TROPONIN C

Our group has been involved in developing a dynamic model to describe calcium-induced protein folding in troponin C, calmodulin and related proteins. Upon Ca^{2+} addition to these Ca^{2+}-modulated proteins, large increases in the α-helical content and a general increase in compactness of these molecules have been observed by intrinsic fluorescence (Leavis and Kraft, 1978; Dedman *et al.*, 1977; Dabrowska *et al.*, 1978; Cox *et al.*, 1979) and circular dichroism (Leavis and Kraft, 1978a; Liu and Cheung, 1976; Wolff *et al.*, 1977; Hincke *et al.*, 1978; Walsh *et al.*, 1978). ^1H NMR spectroscopy has also been used to study the conformational changes in these proteins (Seamon *et al.*, 1977; Levine *et al.*, 1977; Levine *et al.*, 1978; Seamon, 1980; Hincke *et al.*, 1981b). However, it is extremely difficult to probe local molecular events in a single calcium binding site in these multi-calcium binding site proteins. To overcome this problem several groups have isolated fragments containing one or several calcium binding sites from parvalbumin (Derancourt *et al.*,1978), troponin C (Leavis *et al.*, 1977, 1978; Grabarek *et al.*, 1981) and calmodulin (Drabikowski *et al.*, 1977); Walsh *et al.*, 1977). Biochemical and spectroscopic studies on these peptides have generated a wealth of information about regions of interaction of these calcium binding proteins with target proteins such as troponin I, phosphodiesterase and phosphorylase kinase (Leavis *et al.*, 1978; Grabarek *et al.*, 1981; Kuznicki *et al.*, 1981). Similarly, the calcium affinity of these isolated sites and the amount of secondary and tertiary structure perturbations observed as a result of calcium addition (Leavis *et al.*,1978; Nagy *et al.*, 1978; Birnbaum and Sykes, 1978; Evans *et al.*, 1980; Leavis *et al.*, 1982) have permitted a partial description of the folding pattern of such peptides in the apo- and metal-bound states and have enabled investigators to propose as in the case of troponin C, the location and extent of structural changes due to the presence of calcium. However, the size and choice of chemical and enzymatic fragments obtained often limit their usefulness in generating information about calcium-induced folding and the location of α-helical regions.

The unique approach adopted by our group was to study folding events by chemically synthesizing a single calcium binding site and analogs thereof, and to compare their calcium binding characteristics and observed folding pattern. Site III of rabbit skeletal troponin C was chosen as the model for our synthetic analogs on the basis of the following two criteria:

1) This site has previously been shown to retain its calcium binding ability ($K_{Ca} \sim 10^{5}M^{-1}$) when isolated as a cyanogen bromide fragment of rabbit skeletal troponin C (Fig. III.1, first sequence) and,

2) Its calcium binding loop possesses key features predicted to affect the stability of the calcium:peptide complex (Reid and Hodges, 1980).

The sequences of three synthetic analogs are presented in Fig. III.1. Their synthesis and purification have been discussed in chapter II. The first sequence represents the cyanogen bromide fragment containing the Ca^{2+} high-affinity site III of rabbit skeletal troponin C (CB9) (Collins *et al.*, 1973). The synthetic peptides have an identical sequence to the native fragment CB9, except for the replacement of cysteine 98 by alanine, in order to avoid problems associated with sulfhydryl groups. Their lengths vary from 21- (Ac STnC(103-123)) to 26- (AcA^{98}STnC-(98-123)amide) and finally 34-amino acid residues (AcA^{98}-STnC(90-123)amide), through the extension of the N-terminal region of the molecule. The peptides were acetylated at the

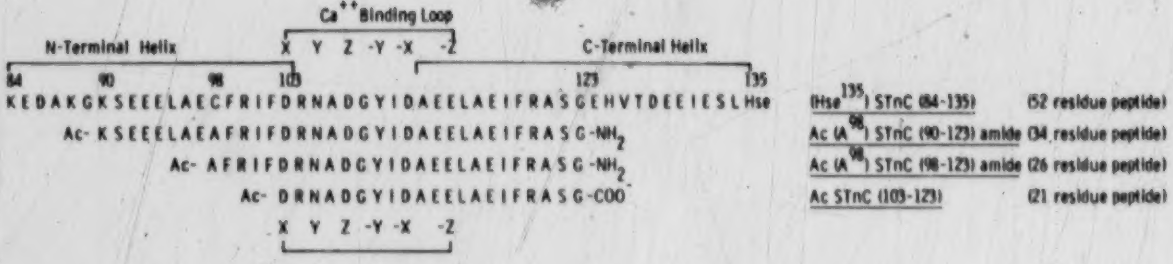
Ca⁺⁺Binding Loop
N-Terminal Helix
X Y Z -Y -X -Z
C-Terminal Helix
84
90
98
103
123
135
K E D A K G K S E E E L A E C F R I F D R N A D G Y I D A E E L A E I F R A S G E H V T D E E I E S L Hse
Ac- K S E E E L A E A F R I F D R N A D G Y I D A E E L A E I F R A S G -NH2
Ac- A F R I F D R N A D G Y I D A E E L A E I F R A S G -NH2
Ac- D R N A D G Y I D A E E L A E I F R A S G -COO⁻
X Y Z -Y -X -Z
(Hse135) STnC (84-135) (52 residue peptide)
Ac (A98) STnC (90-123) amide (34 residue peptide)
Ac (A98) STnC (98-123) amide (26 residue peptide)
Ac STnC (103-123) (21 residue peptide)

Fig. III.1 Amino acid sequences of rabbit skeletal troponin C cyanogen bromide fragment 9 (CB9) and of the synthetic analogs. Symbols X,Y,Z,-X,-Y, and -Z represent the proposed calcium coordinating ligands. Regions corresponding to the N- and C-terminal helices as well as the calcium binding loop are indicated. Hse, homoserine; Ac, Nα-acetyl; NH_2, Cα-amide.

N-terminus and the C-terminus blocked as an amide, except for the 21-residue analog which contains an unblocked α-carboxyl group. By protecting the ends of these fragments we do not generate extra charges which are absent in the natural protein.

B. SECONDARY STRUCTURE ANALYSIS

1. Circular dichroism results

a. Effect of calcium and trifluoroethanol on the peptide secondary structure

The preparation of a 21-residue synthetic analog of the *helix-loop-helix* unit (Reid *et al*., 1980) provided a model with which to study Ca^{2+}-protein interactions. However, the Ca^{2+}-binding constant of the model peptide studied was too low in aqueous medium (Table III-1) to be of any value in structure affinity studies. Another 21-residue analog reported here has similar Ca^{2+}-binding properties in both aqueous and hydrophobic media. As found previously, acetylation of the 21-residue analog resulted in changing an inactive Ca^{2+}-binding unit to a low-affinity Ca^{2+}-binding unit which could be explained on the basis of removing the repulsion between the positively charged N-terminal amino group and the cation (Reid *et al*., 1980). Therefore, elongation of the peptide by addition of residues to the

TABLE III-1

Ca^{2+} binding constants of the synthetic peptides and various fragments of the natural proteins containing a single calcium binding site

	K_{Ca} (M^{-1})	
Analog	Aqueous buffer[a]	Hydrophobic buffer[a]
AcF^{112}STnC(103-123)[b]	2.3×10^2	9.2×10^5
AcSTnC(103-123)	3.1×10^2	3.5×10^5
AcA^{98}STnC(98-123) amide	3.8×10^4	4.9×10^5
AcA^{98}STnC(90-123) amide	2.6×10^5	9.2×10^5
Carp MCBP 4.25 (1-75)[c]	1.1×10^4	
Carp MCBP 4.25 (76-108)[c]	3.3×10^2	
HSer^{135}STnC(84-135) (CB9)[d]	5×10^5	
STnC(121-159) (TH2)[e]	2.5×10^4	

[a] Aqueous and hydrophobic buffers are described under experimental procedures, chapter II.

[b] Taken from Reid *et al.*, 1980.

[c] Taken from Derancourt *et al.*, 1978.

[d] Taken from Nagy *et al.*, 1978.

[e] Taken from Leavis *et al.*, 1978.

N-terminal should be expected to produce the same effect as acetylation. Preparation of 26- and 34-residue peptides (AcA''STnC(98-123)amide and AcA''STnC(90-123)amide) not only resulted in peptides which bound calcium in aqueous medium but the K*ca* values were orders of magnitude higher (Table III-1) than the 21-residue acetylated peptide (AcSTnC-(103-123)). This result suggested that the extra residues added to the N-terminal region did more than just eliminate the detrimental affect of the N-terminal amino group on calcium chelation. Lenkinski and his co-workers (1983) recently noted that 12-amino acid long analogs (residues 64 to 75) of site II of rabbit skeletal troponin C did not require blocking of the N-terminal amino group to achieve an apparent calcium binding affinity of 1-2 x 10^2M^{-1}.

Before considering the CD spectra of the peptides shown in Fig. III.2, it is important to understand the basic assumptions involved in their interpretation. The 21-, 26- and 34-residue apopeptides in aqueous medium show increases in negative ellipticity when compared with the *random coil* spectra observed for the peptides in 8 M urea (Fig. III.2). We interpret these changes as the development of *nascent helix* representing a structural change which is not large enough to account for the formation of a minimum helix of one turn. Addition of calcium or trifluoroethanol to the apopeptides in aqueous medium produces large increases in

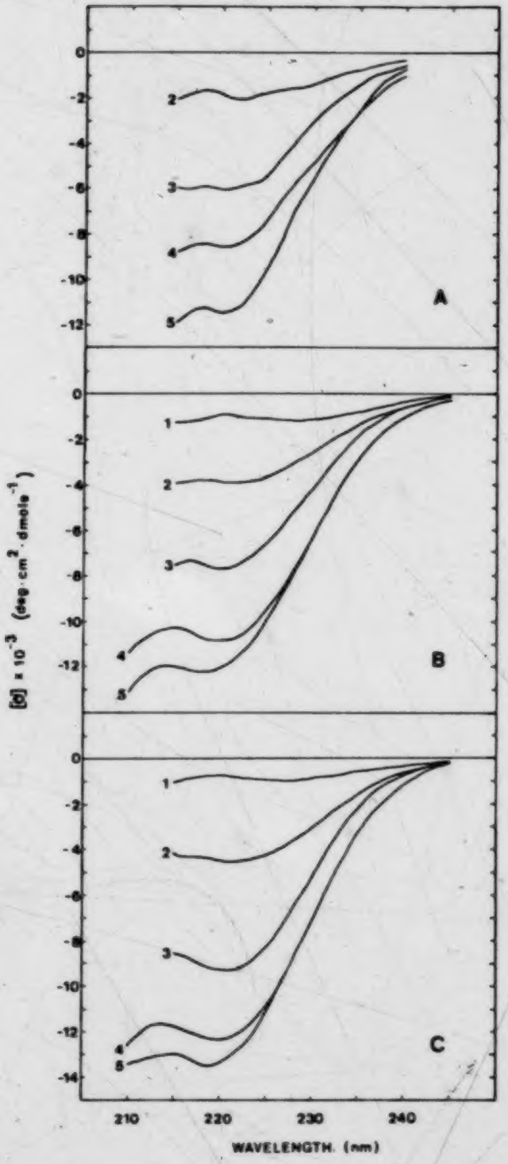

Fig. III.2 Circular dichroism spectra of the peptides. Calcium, trifluoroethanol, and 8 M urea-induced CD spectra of (A) the 21-residue, (B) the 26-residue, and (C) the 34-residue peptide. 1, apopeptide in 8 M urea, 100 mM Tris, 50 mM KCl, 5 mM EGTA, pH 7.2; 2, apopeptide in aqueous medium; 3, calcium-saturated peptide in aqueous medium; 4, apopeptide in hydrophobic medium; 5, calcium-saturated peptide in hydrophobic medium.

negative ellipticity, indicative of secondary structural changes involving α-helix formation (Fig. III.2; Table III-2). Maximum $[\theta]_{222}$ values were elicited from all peptides in the presence of 50% trifluoroethanol and we conclude that this indicates the formation of the maximum amount of α-helix possible with these peptides. The 21-residue peptide is the common segment in all three peptides and this segment consists of the loop region and C-terminal helix of the *helix-loop-helix* Ca^{2+}-binding unit; therefore, all helix changes determined by CD which are greater than those determined for the 21-residue peptide under corresponding conditions are assigned to the N-terminal helix region of the 26- or 34-residue peptides. Lastly, since the maximum amount of helix possible is formed in 50% trifluoroethanol, any CD changes elicited by addition of Ca^{2+} to the peptide in 50% trifluoroethanol must be attributed to loop formation and will not be considered as part of the $[\theta]_{222}$ values involved in the helix formation. As a result, all Ca^{2+}-saturated peptide spectra are corrected for loop formation by subtracting the loop spectra determined as the difference spectra between the appropriate peptide in 50% trifluoroethanol with and without calcium. The difference spectra so obtained are similar for the 26- and 34-residue peptides ($[\theta]_{222}$ for the 26-residue peptide loop formation, -772°; $[\theta]_{222}$ for the 34-residue peptide

TABLE III-2

Circular dichroism studies on synthetic peptides and isolated fragments from calcium binding proteins

	$[\theta]_{220}$			
Analog[a]	Aqueous medium		Hydrophobic medium	
	$-Ca^{2+}$	$+Ca^{2+}$	$-Ca^{2+}$	$+Ca^{2+}$
$AcF^{112}STnC(103-123)$	-1,900	-6,600	-9,100	-12,000
AcSTnC(103-123)	-1,900	-6,100	-8,600	-11,400
AcA STnC(98-123) amide	-3,900	-7,700	-10,800	-12,100
AcA STnC(90-123) amide	-4,500	-9,200	-12,300	-13,400
Carp MCBP 4.25 (1-75)				
Carp MCBP 4.25 (76-108)				
HSer STnC(84-135)(CB9)[b]	-5,730	-10,800		
STnC (121-159)(TH2)[b]	-5,000	-9,800		

[a] All synthetic peptides and fragments of the calcium binding proteins contain a single calcium binding site.

[b] CB9 and TH2 [θ] values are at 222 nm from Nagy *et al.*, 1978 and Leavis *et al.*, 1978.

loop formation, -724°); however the 21-residue peptide gives a larger difference than obtained with the former two peptides ($[\theta]_{222}$, -2800°). The reason for this discrepancy is not known but likely involves structural change in addition to loop formation upon addition of calcium in trifluoroethanol. Therefore, the 21-residue spectra in the presence of calcium were corrected for loop formation using $[\theta]_{222}$ values obtained for the 34-residue peptide. The significance of this alteration in calculations for the 21-residue peptide became obvious during the curve fitting procedure when the fit went from poor (<70% variance accounted for) to good (>96% variance account for) when the 21-residue $[\theta]_{222}$ values for loop formation were replaced by the 34-residue $[\theta]_{222}$ values.

To examine the structural changes occurring in the peptides in response to the presence of trifluoroethanol or Ca^{2+} we subjected our CD data to a nonlinear least-squares computer program for curve fitting based on the equations of Chen *et al*. (1974), as described in chapter II. Contrary to the inability of Nagy *et al*. (1978) and Leavis *et al*. (1978) to obtain reasonable computer generated fits with the CD data for their fragments, we were able to generate reasonable fits (>95% variance accounted for in all generated fits). This ability may have arisen from our use of the 26- and 34-residue spectra in 8M urea as the CD data at $[\theta]_{222}$ for random structure, since if we used the data of Chen *et al*. (1974) for random structure we did not get reasonable fits to our data.

Table III-3 shows the number of residues involved in structural changes induced by calcium and trifluoroethanol in the 21-, 26- and 34-residue peptides over and above the structure of the 21-residue peptide in the absence of calcium, presence of calcium and presence of trifluoroethanol.

b. Analysis of the peptides α-helical content

The addition of calcium to the 21-residue peptide in aqueous medium induces the formation of 2 to 4 residues of *nascent helix* most likely involving residues 112-114 of the peptide (Fig. III.3) The calcium ion can be seen as a stabilizing factor involved in the *nascent helix* formation. As seen in the crystal structure of parvalbumin (Kretsinger and Nockolds, 1973) and discussed previously (Reid *et al*., 1980; Reid and Hodges, 1980), the glutamic acid residue in position 12 of the loop region (Glu-114) must be in a position to chelate the cation in the -Z coordinate of the octahedral coordination sphere. This orientation of Glu-114 can best be made if this residue is part of an α-helix involving residues 112 to 114.

TABLE III-3

Structural changes induced by Ca^{2+} and trifluoroethanol in the synthetic 21-,26-, or 34-residue peptides

Reagent	Ca^{2+}	Trifluoroethanol
$\Delta 21_R\text{-}21_{Apo}$[a]	2-4[b]	6
$\Delta 26_R\text{-}21_R$	4	5
$\Delta 34_R\text{-}21_R$	7	9

[a] $\Delta 21_R$, the number of residues of α-helix induced by reagent where R is either Ca^{2+} or trifluoroethanol; 21_{Apo}, the 21-residue apopeptide; 21_R, the 21-residue peptide in aqueous medium containing Ca^{2+} or trifluoroethanol.

[b] Less than 4 residues of α-helix will be referred to as nascent helix.

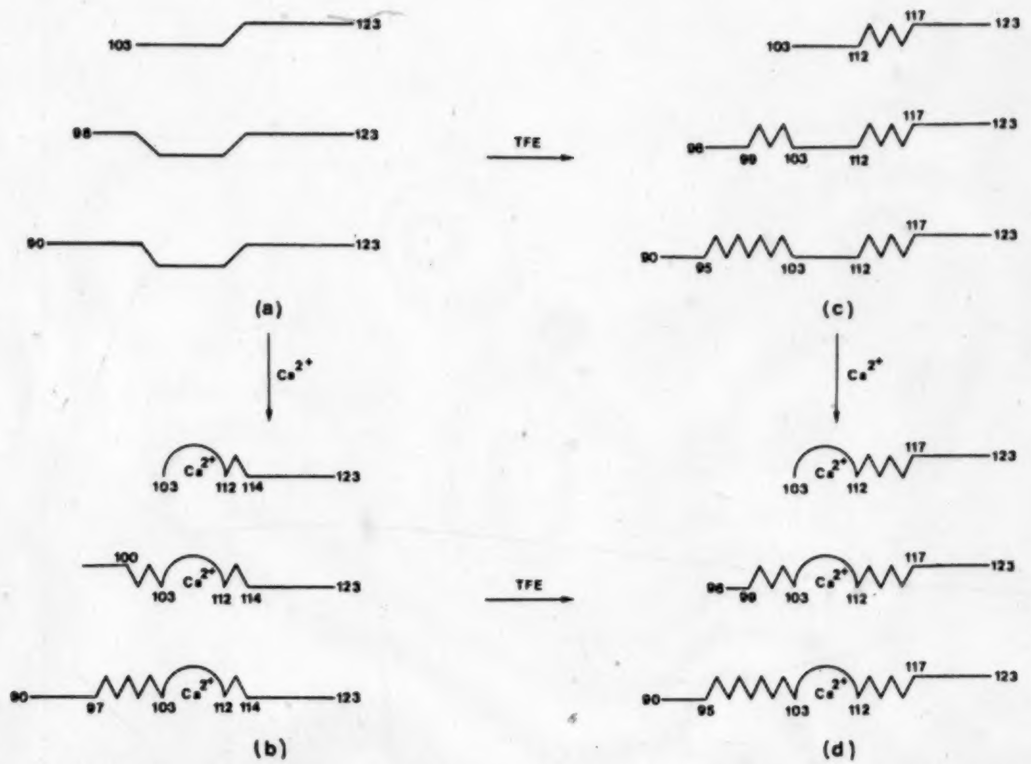
103
123
98
123
90
123
(a)
Ca2+
103
112
114
123
100
103
112
114
123
90
97
103
112
114
123
(b)
TFE
TFE
103
112
117
123
98
99
103
112
117
123
90
95
103
112
117
123
(c)
Ca2+
103
112
117
123
98
99
103
112
117
123
90
95
103
112
117
123
(d)

Fig. III.3 A model of conformational changes induced in the three synthetic peptides by calcium and hydrophobic medium. The top line in each group denotes AcSTnC(103-123) (21-residue peptide); the second line denotes AcA^{98}STnC(98-123) amide (the 26-residue peptide); and the third line denotes AcA^{98}STnC(90-123) amide (the 34-residue peptide). α-helical and nascent α-helical regions are denoted by jagged lines. (a), apopeptides in aqueous medium; (b), calcium-saturated peptides in aqueous medium; (c), apopeptides in hydrophobic medium; (d), calcium-saturated peptides in hydrophobic medium. TFE, trifluoroethanol.

The addition of trifluoroethanol to the 21-residue apopeptide results in the induction of a single helix since the peptide contains only the C-terminal helix region of the *helix-loop-helix* unit. These 6 residues of α-helix induced by trifluoroethanol (Table III-3) can be assigned to the region covering residues 112 to 117.

The 26- and 34-residue apopeptides can be seen to contain more structure in aqueous medium than the 21-residue apopeptide (Table III-2, Fig. III.2) with the 34-residue apopeptide having the largest amount of structure of the three peptides in aqueous medium. The 26- and 34-residue peptides are therefore assumed to have two areas of *nascent helix* as shown in Fig. III.3.

The addition of calcium to the 26-residue peptide results in the addition of four residues of α-helix over and above that obtained for the Ca^{2+}-saturated 21-residue peptide in aqueous medium (Table III-3). These structural changes are assigned to the N-terminal side of the loop (Fig. III.3). Just as Glu-114 chelating Ca^{2+} stabilizes the C-terminal *nascent helix*, Asp-103 chelating Ca^{2+} in the +X coordinate of an octahedral coordination shell could be responsible for stabilizing the N-terminal α-helix. For this reason we attribute the four residues of α-helix to the region 100-103. Thus we can see the beginning of a

Ca^{2+}-initiated helix on the N-terminal side of the loop region. The addition of trifluoroethanol to the 26-residue peptide results in the addition of 5 residues of α-helix over and above that obtained for the 21-residue peptide in aqueous medium (Table III-3). The close agreement between the helix induced by calcium and trifluoroethanol suggests that calcium has induced essentially all the potential helix on the N-terminal of the peptide.

Finally, addition of calcium to the 34-residue peptide in aqueous medium results in the addition of seven residues of α-helix over that obtained in the Ca^{2+}-saturated 21-residue peptide (Table III-3). These seven residues are assigned to the N-terminal side of the loop region around residues 97-103 (Fig. III.3), thus extending the N-terminal helix formed by addition of calcium to the 26-residue peptide. Similarly, trifluoroethanol shows an increase of 9 residues of α-helix. Again, calcium has induced almost all of the inducible α-helix (7 vs. 9 residues) on the N-terminal end. Thus, the interpretation of the CD data outlined in Table III-3 and Fig. III.3 places the majority of the α-helical structure induced by Ca^{2+} in the N-terminal of the *helix-loop-helix* unit. This interpretation seems reasonable if we assume that the extension of the peptide on the N-terminal beyond that of the acetylated 21-residue peptide does not increase the amount of structure in the C-terminal helix beyond that found in the 21-residue analog. This suggests that the majority of Ca^{2+}-inducible structure resides in the N-terminal helix of the *helix-loop-helix* unit and is in agreement with previous studies using the CB9 fragment (Nagy *et al.*, 1978) in which Nagy *et al.* assumed that one helical segment is formed upon calcium binding and that the segment is located in the N-terminal region of the Ca^{2+}-binding site.

c. Effect of elongating the N-terminal region on the calcium binding affinity of the site

The extension of the N-terminal region in the Ca^{2+}-binding peptides results in an increase in the K_{Ca} value of the 34-residue peptide by 800 fold (Table III-1) indicating that this region provides some form of thermodynamic stability to the metal:peptide complex. It is also interesting to note that the work of Leavis *et al.* (1978) has suggested one of the TnI binding sites to TnC is located in the N-terminal region of the calcium binding site III. Thus it would appear that region 90-103 in skeletal TnC and the homologous region, residues 80-93 of calmodulin (Watterson *et al.*, 1980) may be directly involved in the biochemical function of these proteins.

The Ca^{2+}-binding constants (Table III-1) of the 21-, 26- and 34-residue peptides in hydrophobic medium are similar to one another and are 3, 1 and 0.4 orders of magnitude higher, respectively, than the corresponding peptide in aqueous medium. As previously discussed for the $AcF^{112}STnC$ (103-123) peptide (Reid *et al.*, 1980), these increases could be due to a prepositioning of the Glu-114 in a position ideal for chelation as well as by creating an environment unfavorable to ionized acidic residues. Whatever the reason, the effect becomes less pronounced as the N-terminal helix is lengthened.

2. Ultraviolet difference spectroscopy

The Ca^{2+}-induced uv difference spectra of all three acetylated peptides in aqueous and hydrophobic medium is presented in Fig. III.4. The experimental approach used is described in chapter II (section J). All our analogs possess only one tyrosine located at the -Y position in the calcium binding loop. In the ultraviolet spectrum of the apopeptides, one observes a broad tyrosine absorption band peaking at 275 nm but the difference spectra (Fig. III.4) resulting from the addition of calcium to each peptide solutions yielded a minimum in the 276-278 nm region in all 3 cases. This represents a slight red-shift in agreement with similar observations made in the case of troponin C and

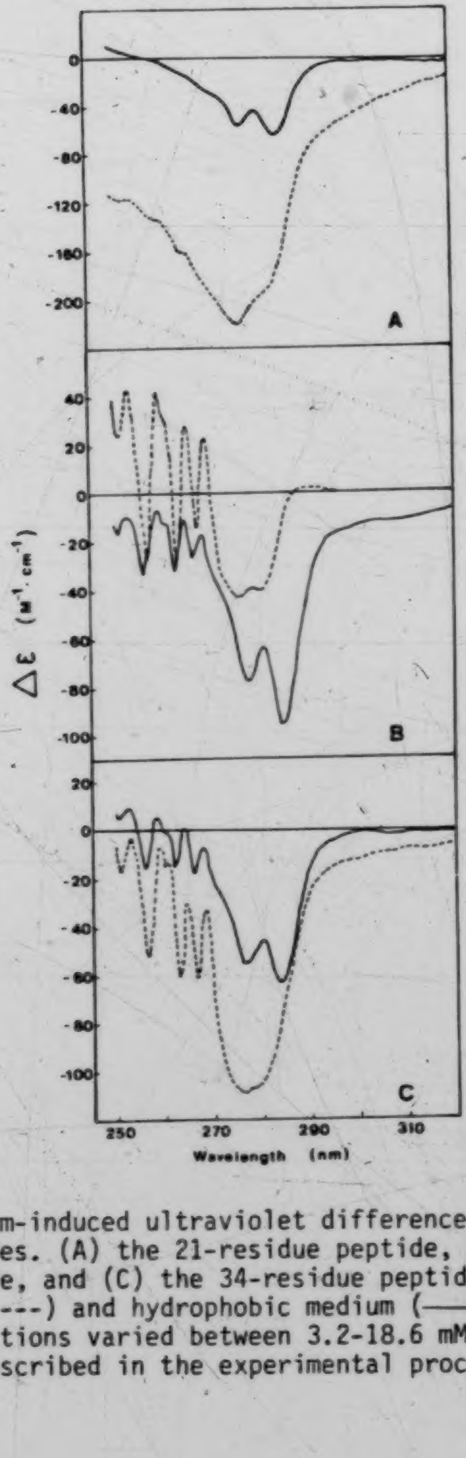

Fig. III.4 Calcium-induced ultraviolet difference spectra of the peptides. (A) the 21-residue peptide, (B) the 26-residue peptide, and (C) the 34-residue peptide in aqueous medium (---) and hydrophobic medium (——). Calcium concentrations varied between 3.2-18.6 mM. Conditions used are described in the experimental procedures section.

its cyanogen bromide fragment CB9 (Nagy *et al.*, 1978). The red-shift is accentuated in the presence of trifluoroethanol were 2 minima are now observed (276-277 nm and 284-285 nm).

It is doubtful that the single tyrosine side chain has moved to a more hydrophobic environment upon addition of the metal since iodination and laser CIDNP experiments have proven its exposure to solvent at all times. The slight red-shift is more in line with a charge neutralization process arising from the binding of calcium in the vicinity of the side chain.

3. Proposed model for the Ca^{2+}-induced protein folding of troponin C

The maximum amount of helix attainable by the 34-residue analog in hydrophobic medium (Fig. III.3) is less than that found in the crystal structure of site II in carp MCBP 4.25 (Kretsinger and Nockolds, 1973) and less than that predicted by the Chou and Fasman method (1974a) (Fig. III.5). However, the maximum amount of C-terminal α-helix determined in the synthetic peptides (Fig. III.3) agrees reasonably well with that predicted by the Chou and Fasman method (i.e., residues 112-119) while the maximum amount of N-terminal α-helix determined in the synthetic analog (Fig. III.3, residues 95-103) is less than the length of

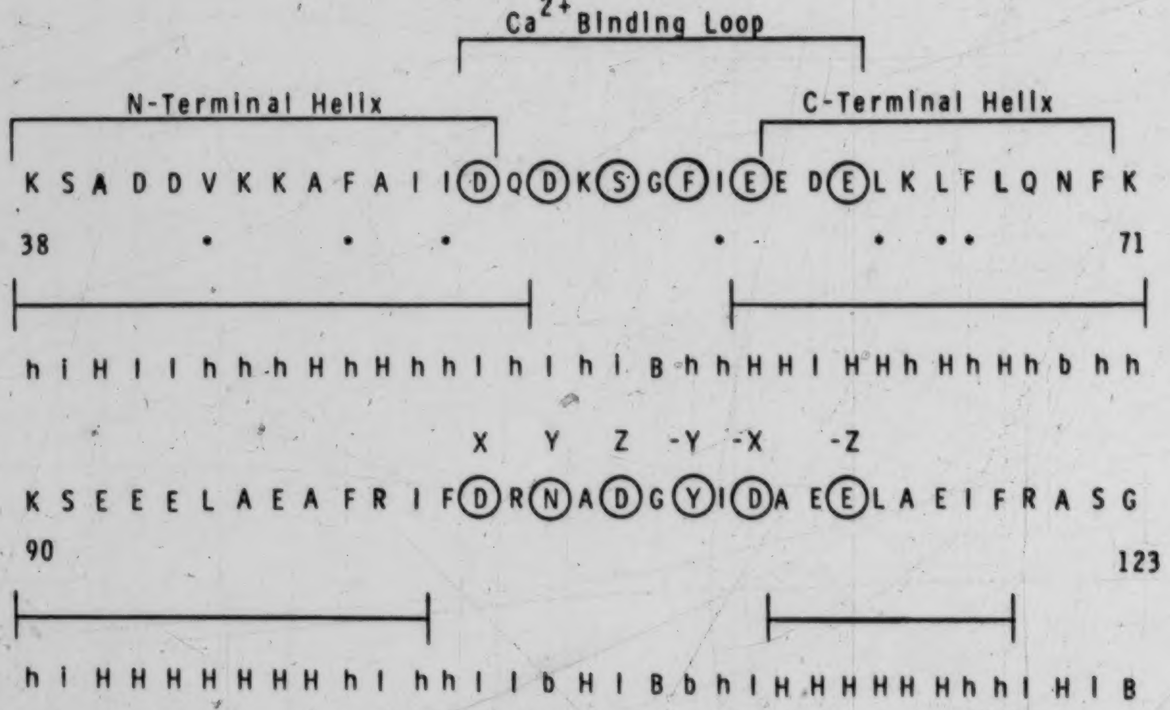
Ca2+ Binding Loop
N-Terminal Helix
C-Terminal Helix
K S A D D V K K A F A I I D Q D K S G F I E E D E L K L F L Q N F K
38
71
h i H I I h h h H h H h h I h I h I B h h H H I H H h H h H h b h h
X Y Z -Y -X -Z
K S E E E L A E A F R I F D R N A D G Y I D A E E L A E I F R A S G
90
123
h i H H H H H H H h I h h I I b H I B b h I H H H H H H h h I H I B

Fig. III.5 Amino acid sequences of carp parvalbumin (MCBP 4.25) site II and of rabbit skeletal troponin C site III. Cysteine 98 of rabbit skeletal troponin C has been replaced by alanine as in the case of our synthetic analogs. The six octahedral calcium coordinating positions are designated X,Y,Z,-Y,-X, and -Z. The calcium binding residues in the corresponding positions are circled. The residues with side chains as part of the hydrophobic core of parvalbumin site II are denoted with an asterisk. The predicted helical regions, according to the Chou and Fasman (1978) parameters, are shown below the parvalbumin and troponin C sequences. H, and h represent helix-forming residues, I, and i are helix-indifferent ones while B, and b are helix-breaking residues.

N-terminal α-helix predicted for the 34-residue analog by the Chou and Fasman method (Fig. III.5, residues 90-101). The disagreement of the amount of α-helix from our studies with the crystal structure of carp MCBP 4.25 may be due to the contribution from other areas of the larger protein to stabilization of the α-helix in the region studied whereas the smaller peptide does not have some of these interactions. The fact that the amount of C-terminal helix of these synthetic peptides in hydrophobic medium agrees with the predicted helix as well as the fact that the majority of the C-terminal helix occurs only in hydrophobic medium and is not Ca^{2+}-sensitive suggests two possibilities. Either the C-terminal helix is not formed in rabbit skeletal TnC site III in the presence or absence of calcium, or the helix is preformed through side chain interactions with the protein hydrophobic core. The latter possibility agrees with the assumptions of Nagy *et al*. (1978) that the C-terminal helix of CB9 is preformed and the N-terminal helix is Ca^{2+}-sensitive.

The conformational changes elicited in the model peptides, especially the 34-residue peptide, suggest some interesting speculations on the conformational changes involved in Ca^{2+}-binding to the four units in rabbit skeletal TnC. Assuming that the C-terminal helix of the Ca^{2+}-binding unit is preformed due to interactions of residues in the helix with the hydrophobic core of the protein and that the calcium sensitivity of the Ca^{2+}-binding unit is due to Ca^{2+}-induced conformational changes in the N-terminal region of the unit (i.e., Ca^{2+}-induced helix formation as demonstrated by CD changes of the peptides in aqueous medium), then the Ca^{2+} induced conformational changes occurring in the helix regions of the four units in rabbit skeletal TnC or calmodulin may occur by the sequential binding of calcium (Reid and Hodges, 1980) as outlined in Fig. III.6.

The apoprotein is assumed to have approximately 57 residues of helical structure (Table III-4) which we assign to the C-terminal helices of all four sites (Fig. III.6) and to partial formation of the N-terminal helices of sites I and II. These preformed helices are stabilized by side chain interactions with the protein hydrophobic core. Addition of the first calcium ion results in Ca^{2+} complexation at site III (Reid and Hodges, 1980) and induction of the N-terminal helix of site III (Fig. III.6). The formation of the N-terminal helix at site III affects the interaction of TnC with TnI since one of the TnI binding sites on TnC is thought to be around residues 89-120 (Weeks and Perry, 1977; Leavis *et al.*, 1978). Binding of the second Ca^{2+} ion to site IV results in formation of the N-terminal helix in site IV and stabilization of the complex through helix interactions with

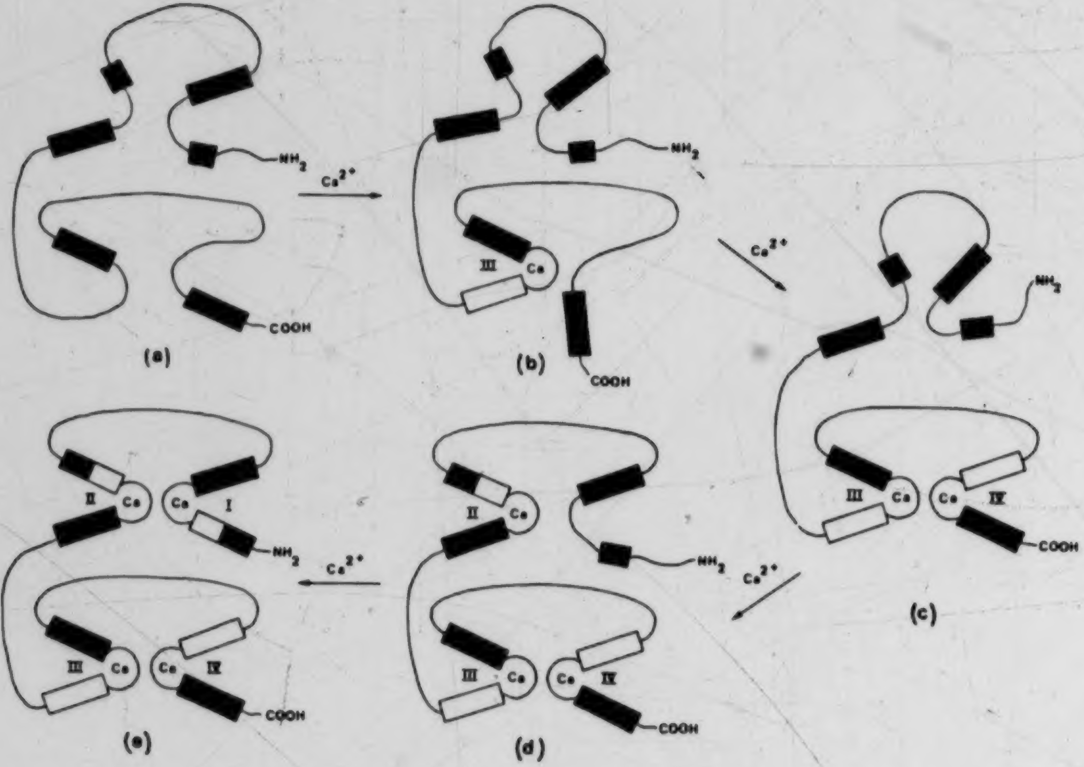

Fig. III.6 A model depicting calcium-induced protein folding in rabbit skeletal troponin C during calcium binding to the four calcium binding units. The closed rectangles denote preformed α-helix in the absence of calcium and the open rectangles denote helical regions induced by calcium binding. The apoprotein (a) binds calcium first to site III (b), followed by site IV (c), then site II (d), and finally site I [Reid and Hodges, 1980].

TABLE III-4

Correspondence between the number of residues in α-helical regions and molar ellipticity values in TnC and its fragments

Fragments[a]	Sites[b]	$[\theta]_{222}$		Calculated residues[c]	
		$-Ca^{2+}$	$+Ca^{2+}$	$-Ca^{2+}$	$+Ca^{2+}$
TnC	I,II,III,IV (159)	-9,600	-14,800	57	87
TR1	I,II (76)	-14,800	-14,800	42	42
TR2	III,IV (71)	-5,900	-12,900	16	34
TH1	I,II,III (120)	-9,000	-12,000	40	53
TH2	IV (39)	-5,800	-9,700	8	14
CB9	III (52)	-5,730	-10,800	11	20

[a] TR1,TR2,TH1,TH2 and TnC correspond to the natural protein and fragments isolated by Leavis *et al.*, 1978. CB9 corresponds to the fragment isolated by Nagy *et al.*, 1978.

[b] Values in parentheses correspond to number of residues in the fragment.

[c] Calculation of helix content is described under experimental procedures (chapter II).

the hydrophobic core (Fig. III.6). We suggest here that the N-terminal regions of sites I and II are also partially preformed prior to Ca^{2+} interaction with the high-affinity sites. This assumption is necessary in light of the evidence for a small conformational change upon Ca^{2+}-binding to the low-affinity Ca^{2+}-selective sites (Potter and Gergely, 1975; Potter *et al.*, 1976; Levine *et al.*, 1977: Nagy and Potter, 1978; Leavis *et al.*, 1978; Sin *et al.*, 1978; Johnson *et al.*, 1978). Based on a comparison of the differences in ellipticity values between Ca^{2+}-saturated TnC and apoTnC and Ca^{2+}-saturated sites III and IV (TR2 and apoTR2) (Table III-4), our calculations suggest that Ca^{2+} addition to the low-affinity sites results in roughly 12 residues of α-helix which could be equally divided between the N-terminal regions of sites I and II. Thus, a third cation binds to site II (Reid and Hodges, 1980), inducing the remainder of N-terminal helix formation (Fig. III.6), that is approximately 6 residues of α-helix, and hence affecting the second site of interaction of TnC with TnI assumed to be in residues 46-77 of TnC (Weeks and Perry, 1977; Leavis *et al.*, 1978). This may indicate the reason for the assumption that the low-affinity Ca^{2+}-selective sites trigger the physiological activity of TnC meaning that both TnI binding sites on TnC must be altered before the physiological activity can be elicited. Finally, site I binds calcium

(Reid and Hodges, 1980) with complete formation of the final N-terminal helix (Fig. III.6).

This sequence of events agrees with the conformational changes which occur in the fragments containing sites III and IV together and separate (TR2, TH2, CB9 in Table III-4) which, in general, show a near doubling of the $[\theta]_{222}$ values upon addition of calcium (Leavis *et al.*, 1978) which could be explained by Ca^{2+}-induced formation of one of the two helices while the other is preformed.

If we assume that there are 11 residues in each of the eight helices, then preformation of the four C-terminal helices and half of each of the N-terminal helices around sites I and II (Fig. III.6) will produce 55 residues of α-helix, close to the estimate of 57 residues suggested by the $[\theta]_{222}$ of apoTnC (Table III-4). Addition of 2 moles of calcium to our model (Fig. III.6) results in formation of a total of 77 residues of helix which is 65% of the total change (Table III-4). This value is similar to the 62% suggested by Johnson *et al.* (1978) but less than the 80% suggested by Nagy and Gergely (1979). This then leaves a 35% of total ellipticity change for Ca^{2+}-binding to the low-affinity sites which is accounted for by twelve residues of helix distributed between the N-terminal helices of sites I and II.

This model is in disagreement with that outlined by Nagy and Gergely (Nagy and Gergely, 1979; Evans *et al.*, 1980; Carew *et al.*, 1980) in which they claim that of the eight helices present in the final Ca^{2+}-saturated protein, five are preformed and insensitive to Ca^{2+} while three remain sensitive to calcium. The five Ca^{2+}-insensitive helices are said to be the four helices flanking sites I and II as well as the helix on the C-terminal side of site III. This leaves the helices around site IV and the helix on the N-terminal side of site III as the Ca^{2+}-sensitive helices. These deductions are based heavily on the fragments TR1 containing sites I and II (Table III-2) which shows no CD change on Ca^{2+} addition (Leavis *et al.*, 1978) and fragment CB9 containing site III which increases $[\theta]_{222}$ by 50% on binding Ca^{2+} (Nagy *et al.*, 1978). However, their model offers no explanation for TH1 which contains sites I, II and III, yet shows more helix change than CB9 alone or TR2 containing sites III and IV which shows sixteen residues of helix structure present (Table III-4) in the absence of calcium, more than can be accounted for by one preformed helix, and this fragment also shows 47% increase in helix on Ca^{2+} addition which would more likely be accounted for by formation of two, not three, helices. Nagy and Gergely's model also fails to account for TR2 containing site IV alone which shows an eight residue helix in the absence of calcium and the addition of six more residues in the presence of calcium (Table III-4). The fragment TR1 containing sites I and II which shows no change upon addition of Ca^{2+} and the fragment TH1 containing sites I, II and III which changes only slightly upon binding calcium are inconsistent with the changes predicted by our model (Table III-4). The explanation we suggest for these discrepancies is that the conformations of the helical regions in site I and II are heavily dependent upon control by the high-affinity sites III and IV. Cleavage of the two low-affinity sites from one or both of the high-affinity sites removes the high-affinity site control of the low-affinity sites and results in hydrophobic interactions between the two low-affinity sites such that these sites behave as our peptides in hydrophobic medium (Fig. III.3) and all helices become preformed and Ca^{2+}-insensitive.

Our model is different from that of Nagy and Gergely in that we maintain that the N-terminal helices of site I and II are partially Ca^{2+}-sensitive and partially preformed in the absence of calcium. The latter conclusion had to be made in light of the large amount of helix in the apopeptide and the former conclusion was drawn from the fact that the $[\theta]_{222}$ in TnC involved in Ca^{2+}-binding to the low-affinity sites is approximately 38% of the total change (Johnson *et al.*, 1978) and thus must involve significant α-helix formation rather than the subtle changes such as tightening of β-turns or additions of one or two peptide units to existing helices suggested by Nagy and Gergely (1979).

Our model for Ca^{2+}-induced conformational changes in TnC outlined in Fig. III.6 is more consistent than previous models and agrees with the two major assertions that:

(1) the majority of conformational change in TnC occurs during addition of calcium to the high-affinity Ca^{2+}/Mg^{2+} sites in TnC (Potter and Gergely, 1975; Potter *et al.*, 1976; Levine *et al.*, 1977; Leavis *et al.*, 1978; Sin *et al.*, 1978), and

(2) the low-affinity Ca^{2+}-selective sites are responsible for the physiological activity of TnC (Potter and Gergely, 1975; Potter *et al.*, 1976).

The major conclusion that we draw from these results on the Ca^{2+}-induced conformational changes in rabbit skeletal TnC is that all *helix-loop-helix* units undergo induction of the N-terminal α-helix upon Ca^{2+}-binding and this conformational change is the event of importance for the functioning of the Ca^{2+}-binding proteins.

C. ANALYSIS OF SIDE CHAIN PERTURBATIONS

The small size of our analogs make them attractive for NMR studies. The proton spectrum is relatively simple to interpret and fluorine or other types of nuclear probes can be synthetically integrated to permit the study of dynamic events occurring upon Ca^{2+} addition.

In this section, we have investigated using a selected number of ^1H NMR resonances, the effect of calcium on the environment of several side chains in all three analogs prepared.

1. Assignment of resonances in the apopeptides

Looking at Fig. III.7, we note that the apopeptide spectra reveal the presence of two sharp doublets which have central resonances around 7.08 and 6.82 ppm. These doublets can be assigned to the meta (2,6) and ortho (3,5) protons of tyrosine 109, respectively. Similar resonance patterns were observed for bovine cardiac apo-TnC Tyr-111 (Hincke *et al.*, 1981b), rabbit skeletal apo-TnC Tyr-109 (Seamon *et al.*, 1977) and apo-CB9 Tyr-109 (Birnbaum and Sykes, 1978). The 21-residue analog possesses a single phenylalanine (Phe-119), the resonance of which is readily assigned to the multiplet region situated around 7.3 ppm, and resembles the free amino acid spectrum. All other analogs show a more complex phenylalanine region because their sequence contains

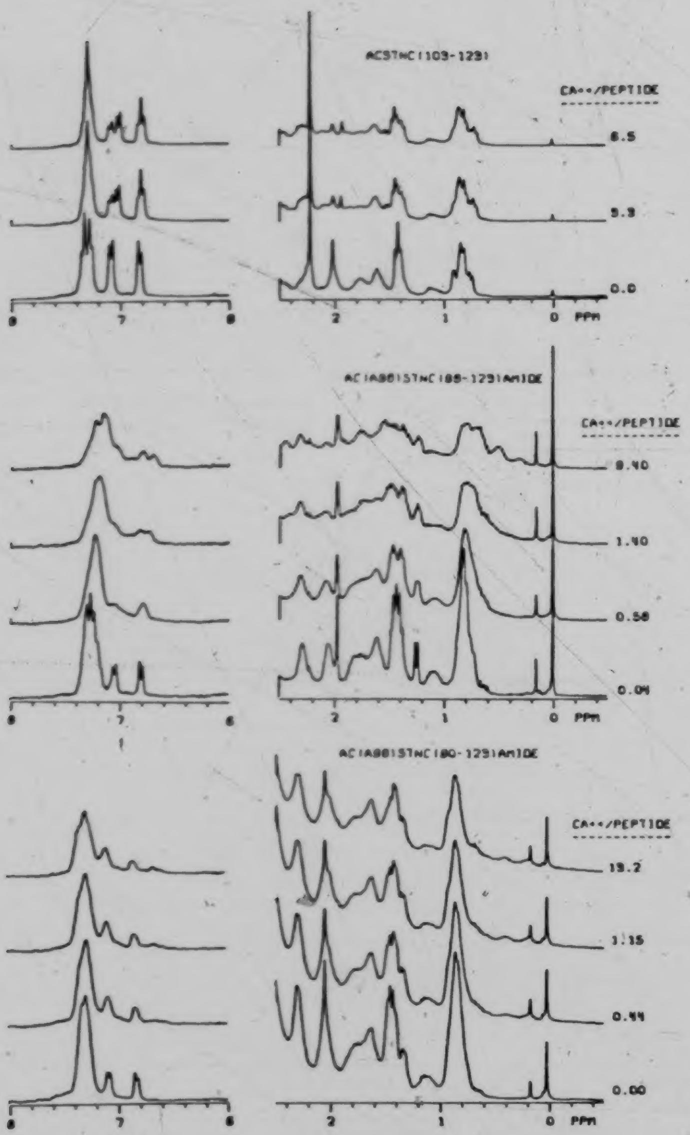

Fig. III.7 ^{1}H NMR spectra of the synthetic peptides at various stages of calcium addition. [Peptide] = 0.5 mM in 10 mM Pipes, 100 mM KCl, 0.5 mM DSS, pH 6.8. Resonances at 0.00 and 0.18 ppm arise from the presence of DSS.

3 phenylalanines (Phe-119, Phe-102 and Phe-99), instead of one. Nevertheless, all the phenylalanine resonances are located in the region extending from 7.2 to 7.4 ppm as similarly observed for the free amino acid itself.

In the aliphatic region, the CH_3 protons of the acetylated N-terminal residue can be seen as a sharp singlet in the 2.00 ppm region. Its resonance position fluctuates only slightly in going from the 21-residue apopeptide to the longer fragments. This fact points out again the unfolded nature of these peptides, since temperature denaturation of carp parvalbumin shifts the acetyl protons of the N-terminal from 2.13 to 2.00 ppm (Cave *et al.*, 1979). The sharp doublet situated at 1.24 ppm in the 26-residue peptide has been tentatively assigned to the methyl protons of alanine 98. This assignment is based on the absence of such a resonance in the other analogs and because Ala-98 represents the acetylated N-terminus of the 26-residue analog. Finally, all the glutamic acid residues present in the 26-residue peptide are located at the beginning of the C-terminal region of this fragment. The γ-CH_2 protons of these amino acids generate a clean signal at 2.30 ppm which will be used to investigate this part of the molecule upon calcium addition.

2. Effect of calcium addition

Figure III.7 shows the effect of calcium addition on each of the analogs. In the aromatic region of the 21-residue peptide, the sharp tyrosine ortho and meta doublets are decreased in intensity upon the addition of calcium and a new set of doublets appears. In addition, the new set of doublets shifts continuously upfield with increasing calcium concentration (for example, the new meta doublet shifts from 7.08 to 7.01 ppm). From the behavior of the tyrosine resonance we can suggest that two populations of the fragment exist in the presence of calcium; one which is not affected by and may not bind calcium and a second which binds calcium with an *off rate* large enough so that the spectra are in the NMR fast-exchange limit.

This pattern is very different for the 26- and 34-residue fragments. First of all there is no fraction of either peptide which is not affected by calcium binding. Secondly, especially for the 34-residue fragment, the off exchange rate for calcium must be much smaller so that the spectra are in the NMR slow exchange rate with the calcium-bound spectrum coexisting with and sequentially replacing the calcium-free spectrum. The *off rate* for calcium for the 26-residue peptide is intermediate in that there is considerable slow-exchange broadening of the calcium-free and calcium-bound peptide resonances when the peptide is fractionally saturated with Ca^{2+}. The meta resonance of the 26-residue free peptide is broad at a calcium to peptide ratio of 0.58. This transition to slower exchange processes may be explained as increased stabilization of the Ca^{2+} ion in the binding site as the N-terminal region ~~of~~ these analogs is lenghtened.

The phenylalanine region of the 21-residue analog indicates that Ca^{2+} does affect the Phe-119 located in the C-terminal region of this peptide. It has been proposed that the C-terminal α-helix of this site in rabbit skeletal troponin C and CB9 is Ca^{2+}-insensitive (Nagy *et al.*, 1979). However circular dichroism would not detect changes in side chain environment. It should be noted here that the resonances of His-125 of CB9 remain unaffected by Ca^{2+} addition (Birnbaum and Sykes, 1978).

The two other analogs show a broadened upfield shifted phenylalanine region in the presence of the calcium. The 34-residue analog has an additional phenylalanine resonance in the calcium-saturated protein positioned at 7.07 ppm. This resonance corresponds to phenylalanine protons as shown by the iodination experiment (Fig. III.8). Such an assignment was also made in CB9. This different resonance pattern suggests that the environment of Phe-102 and Phe-99 is affected by the lengthening of the peptide from 26 to 34 residues. The Ca^{2+} sensitivity of these aromatic residues

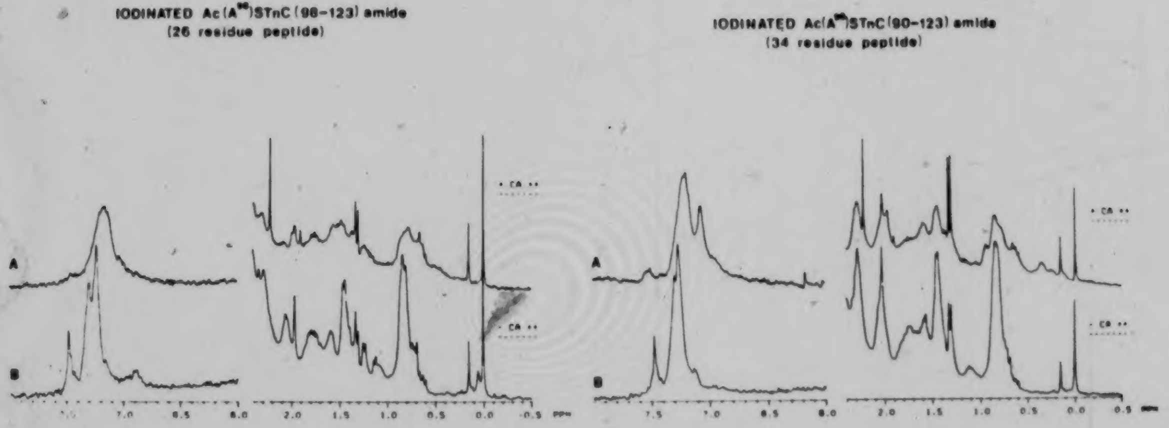

Fig. III.8 ^{1}H NMR spectra of the iodinated peptides. (A) Excess calcium; (B) no calcium. The new tyrosine-109 meta proton singlet is positioned at 7.47 ppm. [Peptide] ≅ 0.5 mM in 10 mM Pipes, 100 mM KCl, 0.5 mM DSS, pH 6.8. The sharp resonances observed at 1.3 and 2.3 ppm are contamination artifacts from the iodination step.

correlates well with their location in the proposed Ca^{2+}-sensitive N-terminal region (Nagy *et al.*, 1979; Reid *et al.*, 1981).

In the 21-residue peptide, Asp-103 is acetylated. The acetyl group methyl proton peak centered at 2.01 ppm in the Ca^{2+}-free fragment is split into two distinct singlets (2.01 and 1.92 ppm) in the presence of calcium. On extension of the N-terminal region only peak broadening is observed with the N-terminal acetyl group.

The sharp doublet centered at 1.24 ppm in the 26-residue peptide was assigned to Ala-98 methyl protons. This doublet broadens considerably as a function of Ca^{2+} addition which suggests that the binding of Ca^{2+} affects the environment of residues as far along as Ala-98 in the N-terminal region.

The 26-and 34-residue fragments also show characteristic shifted CH_3 resonances in the 0.15 to 0.50 ppm region, in the presence of calcium. These resonances are most likely due to the interactions of leucine or isoleucine side chains with aromatic rings. Calcium thus promotes the rearrangement of the peptide to allow the positioning of a phenylalanine or tyrosine ring near one of the leucine or isoleucine residues. The use of Kretsinger's (1973) molecular coordinates for parvalbumin CD and EF loops suggests that only I^{101}-F^{102}, Y^{109}-I^{110} and I^{118}-F^{119} could come in close proximity to allow such possible ring shifted upfield resonances in our analogs.

Glu-113, -114 and -117 are all located at the beginning of the C-terminus of the Ca^{2+}-binding loop. These amino acids can be uniquely detected in the 26-residue analog since their γ-CH_2 protons produce a resonance located at 2.28 ppm. This region in the 34-residue peptide is further complicated by the addition of four glutamic acid residues on extension of the N-terminal. The resonance broadens as the metal ion concentration increases. This agrees with Glu-114 being one of the ligands in the coordination sphere and helix induction of this region upon Ca^{2+}-binding (Reid *et al.*, 1981).

3. Titration of iodinated peptides

In order to study the effect of calcium addition on the meta (2,6) protons of tyrosine 109 and to aid in assigning resonances, we have selectively removed the ortho (3,5) protons from the ring, using the lactoperoxidase iodination method (Morrison and Bayse, 1970).

In Fig. III.8, the spectra of two iodinated peptides are presented. The ortho proton resonances centered around 6.82 ppm have disappeared and the meta proton doublet

(7.07 ppm) has now become a singlet shifted downfield to 7.47 ppm. This resonance in both analogs almost vanishes in the presence of calcium, suggesting they are either broadened or shifted into the main phenylalanine envelope. This observation, coupled with the appearance of a resonance at 7.07 ppm in the Ca^{2+}-saturated spectrum of the modified 34-residue fragment, suggests that this resonance arises from a phenylalanine contribution in the unmodified peptide (Fig. III.7). This peak (7.07 ppm) was assigned to the combined effect of meta tyrosine protons and phenylalanine ring protons in CB9 (Birnbaum and Sykes, 1978). Birnbaum and Sykes (1978) commented that the possible presence of rather significant amount of unfolded CB9 in their Ca^{2+}-saturated spectrum may explain the appearance of residual meta proton resonance at 7.07 ppm.

A comparison of the apo-iodinated peptides to the unmodified peptides shows subtle modifications in the phenylalanine splitting patterns. Since this chemical modification is selective for tyrosine only and the reaction was carefully monitored, it suggests that the environment of our phenylalanines is affected by the substituents on the tyrosine ring. A general upfield shift (0.03 ppm) of the region situated between 7.2 and 7.4 ppm can be observed when comparing the unmodified and iodinated apopeptides.

4. Laser Photo-CIDNP of Ca^{2+}-saturated peptides

The laser photo-CIDNP spectrum provides an assignment of the tyrosine ortho (3,5) protons and an indication of tyrosine exposure in the peptide. This arises because the tyrosine ortho (3,5) protons experience a characteristic enhanced emission in the free amino acid, and the appearance of enhanced emission in the peptide indicates exposure of the tyrosine to the dye. In Fig. III.9, the calcium-saturated spectrum of each of our analogs is shown. The large negative enhancements in the laser photo-CIDNP difference spectra have permitted the immediate assignment of the tyrosine protons in the calcium-saturated spectra.

In the laser CIDNP difference spectra for the free tyrosine amino acid, the meta (2,6) protons show a small enhanced absorption. However in proteins, with slower overall rotational correlation times, this can be reversed by cross relaxation of the meta (2,6) and ortho (3,5) protons carrying the much larger negative enhancement of the ortho (3,5) protons to the meta (2,6) protons. This suggests that the resonance at 6.7 ppm in the calcium-saturated 26-residue peptide is the upfield shifted meta (2,6) protons. The situation is less convincing for the 34-residue fragment.

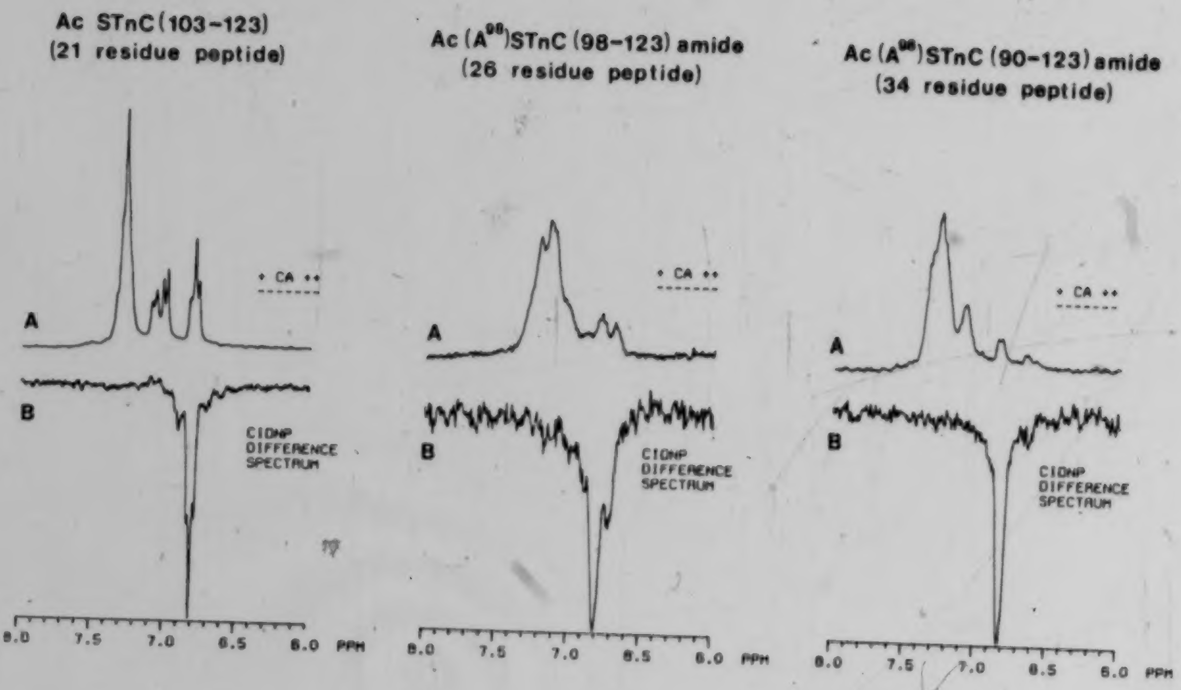

Fig. III.9 ^{1}H NMR laser photo-CIDNP difference spectra of the aromatic region of each analog in the presence of calcium. (A) proton NMR spectra of the aromatic region; (B) CIDNP difference spectra as described in the experimental procedures section. The sharp emission peak corresponds to the resonance position of the ortho protons of tyrosine-109.

The interaction of the flavin dye with the tyrosine ring suggests that tyrosine 109 is exposed in all the analogs, in agreement with the results obtained on skeletal troponin C (McCubbin and Kay, 1975; Seamon *et al.*, 1977) and CB9 (Birnbaum and Sykes, 1978).

5. Kinetic and thermodynamic aspects

^{1}H NMR allows us to investigate some thermodynamic aspects of Ca^{2+}-induced peptide folding. The lengthening of the N-terminal region of the calcium binding site can dramatically increase its Ca^{2+}-binding ability (K_{Ca} from 10^2 M^{-1} to 10^5 M^{-1}). Since the carbonyl group of tyrosine 109 is thought to be involved in the chelation of calcium by analogy with MCBP (Kretsinger and Nockolds, 1973), it is of interest to discuss qualitatively the various exchange rates observed for the ring meta (2,6) protons in each of the synthetic fragments. In going from the 21-residue to the 34-residue analog, the exchange rate appears to decrease so that the NMR spectra go from the fast-exchange limit to the slow-exchange limit. For the 21-residue fragment (part of the population of which remains unfolded), only a lower limit for the *off rate* constant (much greater than 100 sec^{-1}) can be obtained from the spectra using the shift of the calcium-sensitive meta (2,6) protons upon calcium addition. For the 26-residue peptide, we have determined by a computer lineshape analysis of the broadening of the meta proton resonances as a function of added calcium that the *off rate* constant (k*off*) is 135 ± 50 sec^{-1}. This k*off* value agrees well with the 230 - 350 sec^{-1} range obtained for the low-affinity sites of cardiac TnC (Johnson *et al.*, 1978). For the 34-residue peptide only an upper limit on the *off rate* constant (much less than 100 sec^{-1}) can be obtained, from the fact that no exchange contribution to the linebroadening is observed. The value also agrees well with that calculated from the previously measured binding constant (K*ca* of 3.8×10^4 M^{-1}) and the assumption that the *on rate* is diffusion controlled (i.e., 10^7 M^{-1} S^{-1}) (Hammes and Schimmel, 1970).

The Ca^{2+}-*off rate* (k*off*) can be described in terms of compactness of the coordination sphere surrounding the metal. Compactness is dependent on both the type and the proper positioning of the ligands around the cation. The tertiary structure of a protein can affect the positioning of the ligands. For example, one can readily compare the calcium binding affinity of site III of rabbit skeletal troponin C either as an isolated EF hand site (CB9 fragment, ~$10^5 M^{-1}$) or as part of TnC (~$10^7 M^{-1}$). Lanthanide-induced ^1H NMR shifts (Lee *et al.*, 1979) have permitted the estimation of average distances of metal to the various ligand nuclei. Results suggested that such distances were larger in CB9 than in the intact Ca^{2+}-binding protein parvalbumin. The loss of molecular compactness was correlated to the fact that the binding constant for CB9 was three orders of magnitude lower than for MCBP (10^5 M^{-1} vs. 10^8 M^{-1}). We can consider that the extra residues of parvalbumin aided metal binding through at least partial prefolding of the sites. The positioning of the ligands is also apparently dependent on the amount of calcium-inducible α-helix present near the binding loop since the lengthening of the N-terminal region in the synthetic peptides raises the binding constant significantly. Circular dichroism results showed a large increase in the α-helical content for the apopeptides in 50% TFE. In such a hydrophobic environment (50% TFE), all the fragments bound calcium with a similar binding constant of the order of 10^5 M^{-1}. The constancy of the binding constant in this medium points out the need of the C-terminal helical region for Ca^{2+}-binding since the 21-residue analogs only possess the C-terminal region in addition to the calcium loop. Calcium-sensitive environmental changes in the C-terminal region have been revealed from the ^1H NMR spectra of our fragments (Phe-119, Glu-113, -114 and -117). The binding constant of a 12-residue analog of the binding loop (lacking both N- and C-terminal regions) (Reid *et al.*, 1980) remains low (10^3 M^{-1}) in 50% TFE and confirms our view that the C-terminal is probably essential to the affinity of the site for calcium. The importance of the type of ligands forming the binding loop remains to be tested by new synthetic analogs.

These peptides are excellent models to study the thermodynamics of protein folding. Firstly, Ca^{2+} is a benign perturbant as compared to strong denaturants like urea or heat. Secondly, the small size of these peptides will most likely provide a simple two-state model for protein folding (unfolded $\rightleftarrows$ folded) in comparison to the multi-site calcium binding proteins. For example, the present model for skeletal troponin C suggests that for the Ca^{2+}-specific sites (low-affinity sites), the binding constant, K_{Ca}, depends primarily on the enthalpy term, $\Delta H°$, the entropy contribution, $\Delta S°_{reaction}$, being rather small (Potter *et al.*, 1977; Moeschler *et al.*, 1980). If we analyse the source of a large $\Delta H°$ term, the present hypothesis (Filimonov *et al.*, 1978) suggests a change in heat capacity during unfolding or denaturation arising from the exposure of apolar groups to water. This explanation does not apply in the case of our analogs since the exposure of such aromatic residues as Tyr-109 has been demonstrated in the presence and absence of the metal. Similarly, it is doubtful that the formation of helical segments helps to bury apolar groups in such small peptides. In fact, the use of hydrophobic conditions has partly proven that the side chains located in the α-helical region are exposed (Reid *et al.*, 1981).

Any significant contribution to the heat of unfolding would come from the rupture of intramolecular hydrogen bonds. Interactions of water molecules with polar groups otherwise involved in the Ca^{2+} chelation or in intramolecular H bonding would lead to a negative thermal effect (Privalov and Khechinashvili, 1974). This would better explain the alteration of the ΔH° term by addition of α-helical segments on each side of the calcium loop. This enthalpy value for Ca^{2+}-binding to high- or low-affinity sites remains around -30 to -40 kJ per site (Moeschler *et al.*, 1980).

Finally, in view of large calcium-induced conformational changes observed by CD and ^{1}H NMR, we have to consider the possibility of the increasing binding constant value arising from a significant positive entropy of reaction, $\Delta S^\circ_{reaction}$ following the relations

$$-RT \ln K_{Ca} = \Delta H^\circ - T\Delta S^\circ_{reaction} \qquad (1)$$

$$\Delta S^\circ_{reaction} = \Delta S^\circ_{conformation} - \Delta S^\circ_{hydration} \qquad (2)$$

We can probably predict that the entropy involved in peptide conformation, $\Delta S^\circ_{conformation}$, is comparable to the large hydration entropy for calcium, $\Delta S^\circ_{\text{hydration}}$, i.e., -183.9 JK^{-1} mol^{-1} (Filimonov *et al.*, 1978). We base our prediction on the value of the binding constant for the analogs (10^4 - 10^5 M^{-1}) which corresponds to the binding ability of low-affinity binding sites of TnC (Potter *et al.*, 1977; Moeschler *et al.*, 1980). The difference between both entropy terms of comparable magnitude would yield, following relation (2), a small $\Delta S^\circ_{\text{reaction}}$ contribution. This would agree with the expected entropy contribution for a low-affinity site in troponin C (Moeschler *et al.*, 1980).

D. SUMMARY

Three synthetic analogs of site III of rabbit skeletal troponin C (21-, 26- and 34-residues in length) have been prepared by the solid-phase method. The CD spectra of the 21-residue fragment indicated very little secondary structure in aqueous media in the absence of calcium. Addition of Ca^{2+} increased the secondary structure of the peptide but the K_{ca} was very weak, 3.1×10^3 M^{-1}. The same peptide in hydrophobic medium in the absence of calcium had considerable secondary structure and the K_{ca} value increased considerably, 3.5×10^5 M^{-1}. The 26-residue peptide, containing five more residues on the N-terminus of the 21-residue peptide, showed slightly more secondary structure in aqueous medium in the absence of calcium. Addition of

Ca^{2+} to this peptide raised the amount of secondary structure in the metal ion-peptide complex and resulted in a higher K*ca* value, 3.8×10^4 M^{-1}. By assuming that the C-terminal region of the 26-residue peptide metal ion complex adopts a structure similar to that of the 21-residue metal:peptide complex, one is able to assign the increase in structure to the N-terminal side of the Ca^{2+}-binding loop. Hydrophobic medium further increased the secondary structure of this peptide and also increased the K*ca* value to 4.5×10^5 M^{-1}, a value similar to that obtained for the 21-residue peptide. The 34-residue peptide contained a further eight amino acid residues on the N-terminus of the 26-residue peptide. This peptide had considerable secondary structure in aqueous medium which increased in the presence of calcium. The peptide has a reasonable affinity for Ca^{2+} in aqueous medium, K*ca* = 2.6×10^5 M^{-1}. Again, a hydrophobic medium increased both the amount of secondary structure and the Ca^{2+} affinity constant, K*ca* = 9.2×10^5 M^{-1}. A model of Ca^{2+}-induced folding of the three peptides under different conditions is described and results obtained from this model are used to describe Ca^{2+}-binding to the four calcium binding units in rabbit skeletal troponin C.

The dimension of our analogs has enabled us to analyse by proton magnetic resonance, the effect of calcium on selected peptide side chains. The resonance patterns observed for tyrosine 109, phenylalanine 119 and the acetyl group located on the N-terminal residue of each peptide are indicative of the unfolded nature of the fragments in the absence of calcium. Ca^{2+}-induced changes in the environment of residues located in the Ca^{2+}-binding loop (Asp-103, Tyr-109 and Glu-114) as well as in the N- and C-terminal regions of the *helix-loop-helix* calcium binding unit (Phe-99, Phe-102, Phe-119 and Ala-98) were followed by their characteristic proton resonances. Lactoperoxidase iodination and laser photo-CIDNP experiments demonstrated the exposure of Tyr-109 in the presence and absence of calcium in all the analogs and also aided in the assignment of the tyrosine 109 ring protons. An upfield shifted resonance associated with Phe-99 and/or -102 ring protons was observed in the calcium-saturated spectra. The exchange rate for the meta proton resonances of tyrosine 109 indicates a transition to slower rates as the N-terminal of the calcium site is elongated. This finding correlates with the observed increase in the calcium binding constant of the synthetic analogs occurring upon peptide elongation and confirms the importance of the N-terminal helical region in stabilizing the cation in the peptide binding loop. Finally, the observation of changes in phenylalanine 119 resonances located in the C-terminal of our smallest fragment coupled with the increased calcium binding constants observed for the 21- and 26-residue peptides (K*ca* of 10^5 M^{-1}) in 50% trifluoroethanol in aqueous buffer (helix inducing conditions) is consistent with the involvement of the C-terminal region in the Ca^{2+} stabilization process.

CHAPTER IV

LANTHANIDE-INDUCED FOLDING OF A SYNTHETIC CALCIUM BINDING LOOP

A. THE USE OF LANTHANIDES AS CALCIUM ANALOGS

The physico-chemical properties of lanthanide (Ln) ions approximate in some cases, the ones observed for the calcium ion. For example, lanthanide ions form ionic rather than covalent bonds and in this respect they resemble the alkaline earth elements (Moeller *et al.*, 1965). These metals also prefer to form complexes involving oxygen ligands rather than nitrogen ones and this aspect of their chemistry is analogous to calcium rather than magnesium (Nieboer, 1975). In addition, a variety of trivalent lanthanides possess an ionic radius comparable to calcium. However, Shannon (1976) indicated that for any given cation, the observed radius depends significantly on the assigned coordination number. Table IV-1 illustrates this point for some key metal ions. This factor becomes relevant if one considers that the coordination numbers reported for Ln ions range in value from 6 to 10 and that the most common values observed are 8 and 9. In contrast, calcium prefer to form complexes having a coordination number of six, seven or eight (Nieboer, 1975; Einsphar and Bugg, 1977). Nevertheless, lanthanides possess spectroscopic properties

TABLE IV-1

Ionic radius of several alkali, alkali earth and lanthanide cations as a function of coordination number

Cation	CN	Ionic radius[a] (Å)	Cation	CN	Ionic radius[a] (Å)
$^{11}\text{Na}^{+}$	IV	0.99	$^{57}\text{La}^{3+}$	VI	1.03
	V	1.00		VII	1.10
	VI	1.02		VIII	1.16
$^{12}\text{Mg}^{2+}$	IV	0.57		IX	1.22
	V	0.66	$^{63}\text{Eu}^{3+}$	VI	0.95
	VI	0.72		VII	1.01
	VIII	0.89		VIII	1.07
$^{19}\text{K}^{+}$	IV	1.37		IX	1.12
	VI	1.38	$^{64}\text{Gd}^{3+}$	VI	0.94
	VII	1.46		VII	1.00
$^{20}\text{Ca}^{2+}$	VI	1.00		VIII	1.05
	VII	1.06		IX	1.11
	VIII	1.12	$^{65}\text{Tb}^{3+}$	VI	0.92
$^{38}\text{Sr}^{2+}$	VI	1.18		VII	0.98
	VII	1.21		VIII	1.04
	VIII	1.26		IX	1.10
	IX	1.31	$^{70}\text{Yb}^{3+}$	VI	0.88
$^{56}\text{Ba}^{2+}$	VI	1.35		VII	0.93
	VII	1.38		VIII	0.99
	VIII	1.42		IX	1.04
	IX	1.47	$^{71}\text{Lu}^{3+}$	VI	0.86
				VIII	0.98
				IX	1.03

[a] Taken from Shannon, 1976.

not exhibited by calcium and have thus been employed as substitutes for calcium in order to probe various types of calcium binding environments. Reviews by Nieboer (1975), Reuben (1977), Martin and Richardson (1979) and dos Remedios (1981) summarize the biological applications of such metals.

The lanthanides have been used as calcium analogs in structural studies of several EF hand containing proteins. The spectroscopic properties of Tb^{3+} and Eu^{3+}, for instance, have been advantageously used to measure distances between the calcium binding sites of carp parvalbumin (Rhee *et al.*, 1981) and of troponin C (Wang *et al.*, 1982a); or to determine the sequential order of metal binding to calmodulin (Kilhoffer *et al.*, 1980a,b; Wang *et al.*, 1982b) and troponin C (Leavis *et al.*, 1980). In the case of carp parvalbumin, the paramagnetic properties of the lanthanide Yb^{3+} induces considerable shifting and broadening of the ^1H NMR resonances from protons in proximity to this metal. These ytterbium-induced spectral perturbations can then be analysed in terms of the structure of the metal binding site (Lee and Sykes, 1979, 1980a,b, 1981, 1982).

We have been involved in the "molecular dissection" of a model EF hand domain using synthetic analogs of site III of rabbit skeletal troponin C (chapter III). It was previously shown that the removal of one or both helical regions reduces the calcium binding constant of the resulting site to about 10^2M^{-1}. This was demonstrated by the poor calcium binding affinity exibited by a 12- and a 21-residue synthetic fragment of this site (AcSTnC(103-114), K_{Ca} = 2 x 10^2M^{-1}; AcSTnC(103-123), K_{Ca} = 3.1 x 10^2M^{-1})(chapter III). However, lanthanides are known to bind tighter to calcium binding proteins. In the case of rabbit skeletal troponin C (Wang *et al.*, 1981), terbium(III) binding constants of 5.2 x 10^8M^{-1} and 9.7 x 10^6M^{-1} and europium(III) binding constants of 4.7 x 10^9M^{-1} and 5.3 x 10^7M^{-1} have been calculated for the calcium high (2 x 10^7M^{-1}) and low (5 x 10^5M^{-1}) affinity sites (Potter and Gergely, 1975). These facts have enabled us to reduce the size of our synthetic EF site to only the metal binding region. We therefore synthesized a 13-residue fragment representing the calcium binding region of site III of rabbit skeletal troponin C (residues 103-115) and made use of high-field ^1H NMR methods to analyse the binding events during a metal titration of this simpler system.

The diamagnetic lanthanides La^{3+} ($4f^0$) and Lu^{3+} ($4f^{14}$) were used in a first set of ^1H NMR experiments. They were selected over other lanthanides because, as in the case of calcium, their observable effect on the ^1H NMR spectrum of AcSTnC(103-115)amide is free of paramagnetically induced shifting and broadening of resonances. The spectrum perturbations are solely the result of a restricted geometry adopted by the peptide upon metal binding. Another advantage in using these two lanthanides is their difference in ionic radius (Lu^{3+}, 0.86 Å; La^{3+}, 1.03 Å; Ca^{2+}, 1.00 Å; Shannon, 1976). The results obtained from these lanthanide titrations of the peptide should indicate the importance of both the metal charge and radius on the metal binding affinity of the site and yield information concerning the conformation adopted by the synthetic peptide in their presence.

B. VARIATIONS IN LANTHANIDE AFFINITY AND INDUCED PEPTIDE CONFORMATION

1. Assignment of apoAcSTnC(103-115)amide resonances

The peptide AcSTnC(103-115)amide sequence is presented in Fig. IV.1. One should note the presence of two alanines, three aspartic acids and two glutamic acids in the sequence as this factor will influence the complexity of the observed ^1H NMR spectrum.

The apopeptide spectrum is shown in Fig. IV.2. The initial assignment of resonances was aided by the published list of proton NMR resonance positions recorded for synthetic peptides containing each amino acid (Bundi and Wurthrich, 1979) and by a spectral record of all the free amino acids at 270 MHz. The integration and decoupling of

Rabbit Skeletal Troponin C Site 3 - Synthetic fragment of the Ca++ binding region

```
          103     105     107     109   111        114
Acetyl- Asp-Arg-Asn-Ala-Asp-Gly-Tyr-Ile-Asp-Ala-Glu-Glu-Leu-NH2
         X       Y       Z      -Y     -X          -Z
```

Fig. IV.1 Primary sequence of the synthetic fragment AcSTnC(103-115) amide. The letters X,Y,Z,-Y,-X, and -Z represent the calcium-coordinating ligands of the peptide.

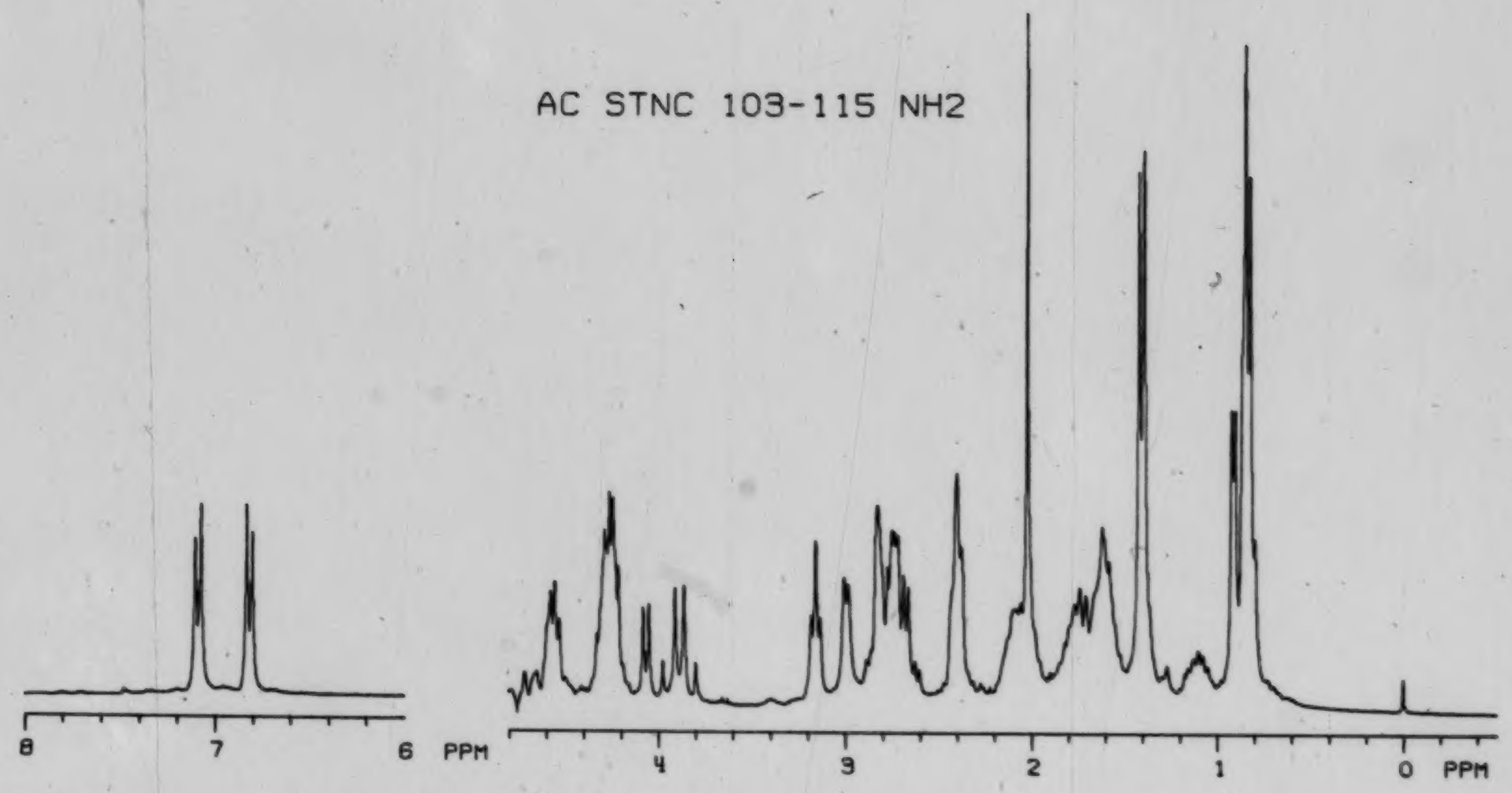

Fig. IV.2 ^{1}H NMR spectrum of apo-AcSTnC(103-115) amide. [Peptide] = 8.3 mM in deuterated imidazole, 100 mM KCl, and 0.2 mM DSS, pH 7.0.

all the spectral lines permitted the assignment of all spectral regions. However, some regions of the proton spectrum remain complex because of the sequence composition. Table IV-2 lists all the assignments made. Note that each amino acid in the peptide sequence can be partly characterized by one or several resonances (Table IV-2). In the absence of metal, the peptide possesses little structure as the resonances of Tyr-109 (β-CH_2, 3.0 ppm; ring [2,6], 7.1 ppm; ring [3,5], 6.8 ppm), N-acetyl-Asp-103 (2.0 ppm) and Ala-106, -112 (β-CH_3 , 1.4 ppm) resemble, in terms of lines position and pattern, the resonances observed in model compounds. The absence of secondary structure is further exemplified by the overlapping methyl doublets (1.4 ppm) of alanine 106 and 112.

An important assignment is that of the quartet pattern centered at 3.90 ppm to the Gly-108 α-carbon protons. In the spectrum of the free amino acid, the α-carbon protons of glycine are magnetically equivalent and yield a singlet. For the peptide however, these protons are not equivalent as indicated by the AB pattern in the spectrum. This is in agreement with the spectrum observed for the internal glycine of the synthetic tetrapeptide H-Gly-Gly-Tyr-Ala-OH (Bundi and Wurthrich, 1979). These α-protons also behaved as an AB spin system but were located around 4 ppm ($|\delta_A - \delta_B| = 0.016$ ppm). Bundi and Wurthrich commented that

TABLE IV-2

Assignment of proton magnetic resonances of Apo-AcSTnC(103-115)amide

Resonance position (ppm)	Resonance pattern observed	Proton assignment
0.76-0.87	uneven doublet	ε- and δ-CH$_3$,Leu-115 δ-CH$_3$,Ile-110
0.88-0.94	doublet	γ-CH$_3$,Ile-110
1.00-1.20	complex multiplet	γ-CH$_2$,Ile-110
1.36-1.44	doublet	β-CH$_3$,Ala-106,-112
1.55-1.65	broad asymmetric peak	γ-CH$_2$,Arg-104 β-CH,Ile-110 β-CH$_2$,Leu-115
1.67-1.85	complex multiplet	β-CH$_2$,Arg-104 γ-CH,Leu-115
2.00	singlet	N-terminal acetyl group,Asp-103
1.95-2.20	broad peak	β-CH$_2$,Glu-113,-114
2.35-2.45	asymmetric peak	γ-CH$_2$,Glu-113,-114
2.55-2.90	broad asymmetric multiplet	β-CH$_2$,Asp-103,-107 and -111 β-CH$_2$,Asn-105
2.95-3.05	doublet	β-CH$_2$,Tyr-109
3.10-3.22	triplet	δ-CH$_2$,Arg-104
3.80-4.00	quartet	α-CH$_2$,Gly-108
4.03-4.10	doublet	α-CH,Ile-110
4.15-4.38	broad multiplet	α-CH,Glu-113,-114 α-CH,Ala-106,-112 α-CH,Arg-104
6.82-6.85	doublet	ring,aromatic 3,5 Tyr-109
7.08-7.11	doublet	ring,aromatic 2,6 Tyr-109

non-random spacial arrangements of the amino acid side chains arise from intramolecular short range interactions independent of the peptide length. In our peptide, the $|\delta_A - \delta_B|$ value is much larger (0.109 ppm) and might be attributed to a further selective orientation of these protons near the ring of tyrosine 109. In the metal-free form, this peptide sequence possesses little secondary structure as observed from C.D. analysis in the presence and absence of 8 M urea (Reid *et al.*, 1981). A similar conclusion can be drawn from the appearance of a single resonance at 1.4 ppm for the two alanine methyl groups.

2. Lanthanide titrations

a. Lanthanum and lutetium titrations

The addition of lanthanum to the peptide solution resulted in a shifting of most of the peptide resonance lines (Fig. IV.3). The methyl group of N-acetyl-Asp-103 (2.0 ppm) and some of the methyl groups of Ile-110 and Leu-115 (0.8 ppm region) appear the least affected by the presence of the metal. This is expected for free rotating methyl groups located along long aliphatic side chains or at the extremities of the peptide. However, large shifts are observed in the aspartic acid and asparagine β-CH_2 region (2.5-2.9 ppm), residues which are involved in the metal

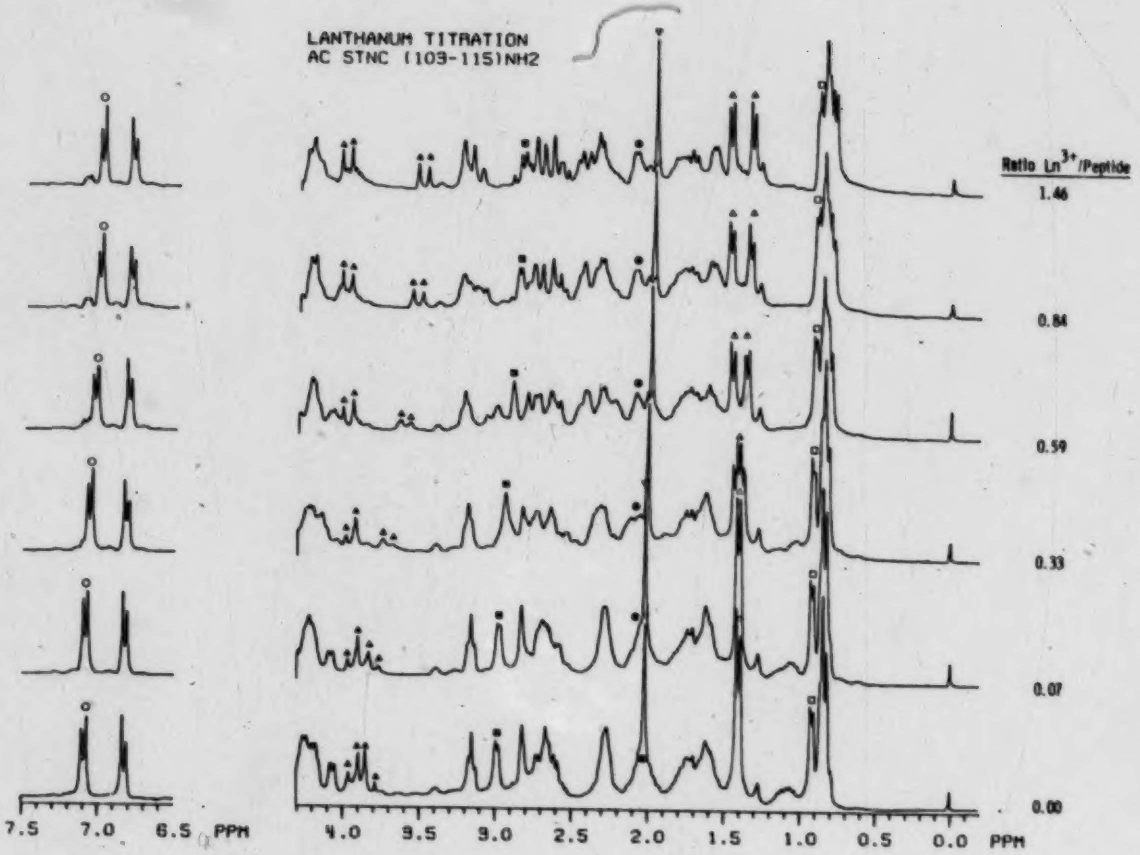

Fig. IV.3 Lanthanum titration of AcSTnC(103-115) amide. [Peptide] = 0.8 mM in 100 mM KCl and 0.1 mM DSS, pH 6.0. Symbols highlight changes in the ^{1}H NMR spectrum. The titration was carried out beyond a metal to peptide ratio of 4.

ligation. Similar events occur in the β-CH_2 (2.0 ppm) and γ-CH_2 (2.28 ppm) resonance regions of Glu-113 and Glu-114 (-Z).

A remarkable shift of the α-protons resonances of Gly-108 (3.90 ppm) is observed . This result suggests that one of the protons is magnetically shielded upon peptide folding. The doublet centered at 3.82 ppm is shifted to 3.50 ppm in the La^{3+}-saturated spectrum. Another interesting metal-induced shift is that of the methyl resonances of Ala-106 and Ala-112 into different environments. The initial doublet at 1.39 ppm gives rise to two doublets centered at 1.47 ppm and 1.33 ppm respectively.

In Fig. IV.4, the lutetium titration of AcSTnC-(103-115)amide reveals less extensive shifting of resonances. For example, the Gly-108 α-carbon protons quartet at 3.9 ppm only shifts apart by 0.146 ppm ($[\delta_A - \delta_B]_{init.}$ = 0.109 ppm; $[\delta_A - \delta_B]_{final}$ = 0.255 ppm) as compared to 0.395 ppm ($[\delta_A - \delta_B]_{init.}$ = 0.109 ppm; $[\delta_A - \delta_B]_{final}$ = 0.504 ppm) for the La^{3+} titration. A similar observation can be made for the alanine methyl protons (1.4 ppm) where both doublets remain poorly resolved in the presence of lutetium. The β-CH_2 envelope of Asp-103 (+X), -107 (+Z), -111 (-X) and Asn-105 (+Y) located in the 2.5 to 2.8 ppm region remains sensitive to the addition of

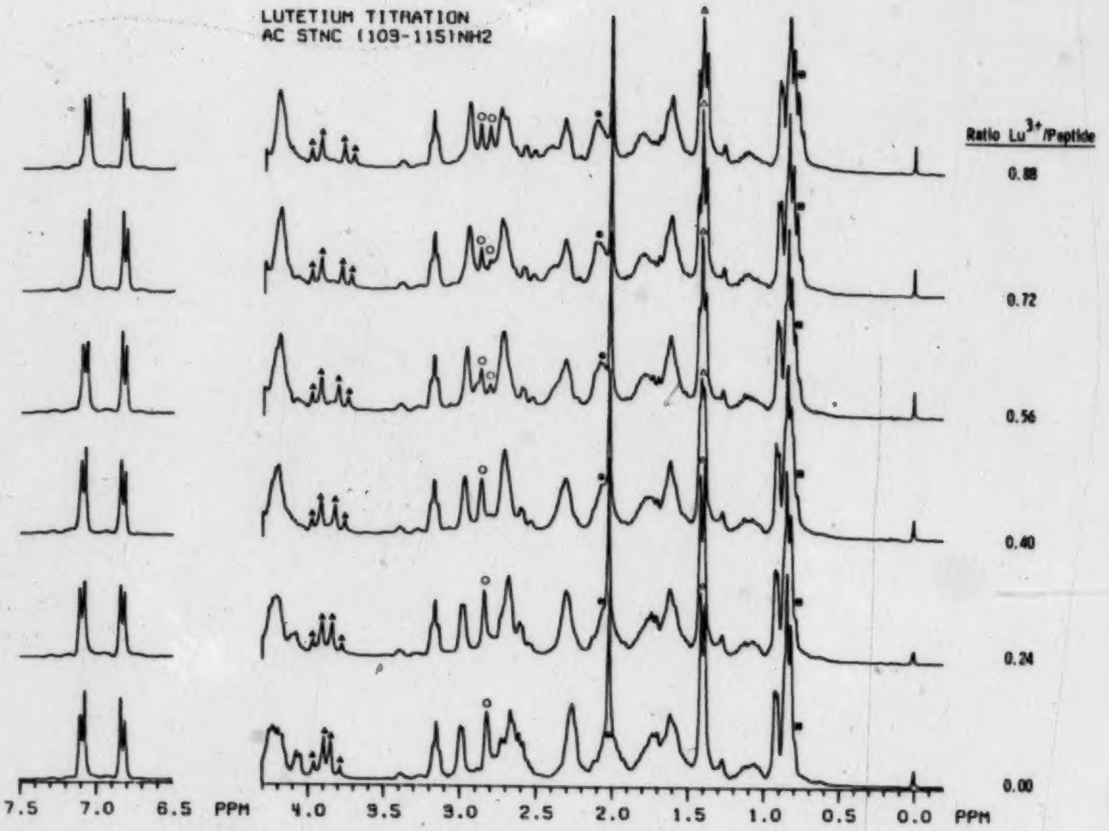

Fig. IV.4 Lutetium titration of AcSTnC(103-115) amide. [Peptide] = 0.8 mM in 100 mM KCl and 0.1 mM DSS, pH 6.0. Symbols highlight changes in the ^{1}H NMR spectrum. The titration was carried out beyond a metal to peptide ratio of 4.

the metal as does the β-CH_2 (2.0 ppm) and γ-CH_2 (2.28 ppm) regions of glutamic acid 113 and 114 (-Z).

The results from both lanthanide titrations indicate clearly that both metals do not fold the peptide into the same conformation. It should be noted at this point that La^{3+} (ionic radius , 1.03 Å) has a larger ionic radius than Lu^{3+} (ionic radius, 0.86 Å) or calcium (ionic radius, 1.00 Å).

b. Lanthanide binding constants

As described in chapter II, the quantity *Y* was evaluated for several resonances during each addition of a metal solution . The *Y* values were determined from the spectral lines of N-acetyl-Asp-103, the methyl groups of Ala-106 and Ala-112, the α-CH_2 protons of Gly-108, the β-CH_2 group and aromatic (2,6) ring protons of Tyr-109. Figure IV.5 shows plots obtained for a typical lanthanum (frame A) and lutetium (frame B) titration of the peptide as a function of metal to peptide ratio. In the case of both metals, the maximum shift observed for all resonances monitored appears to be reached near a metal to peptide ratio of one to one suggesting a 1:1 stoichiometry for the metal to peptide complex. The calculated La^{3+} binding constant was equal to $1.1 \times 10^5 M^{-1}$ (average of 3 titrations). The peptide showed a lesser ability to bind lutetium ($K(Lu^{3+})$ of $1.3 \times 10^4 M^{-1}$;

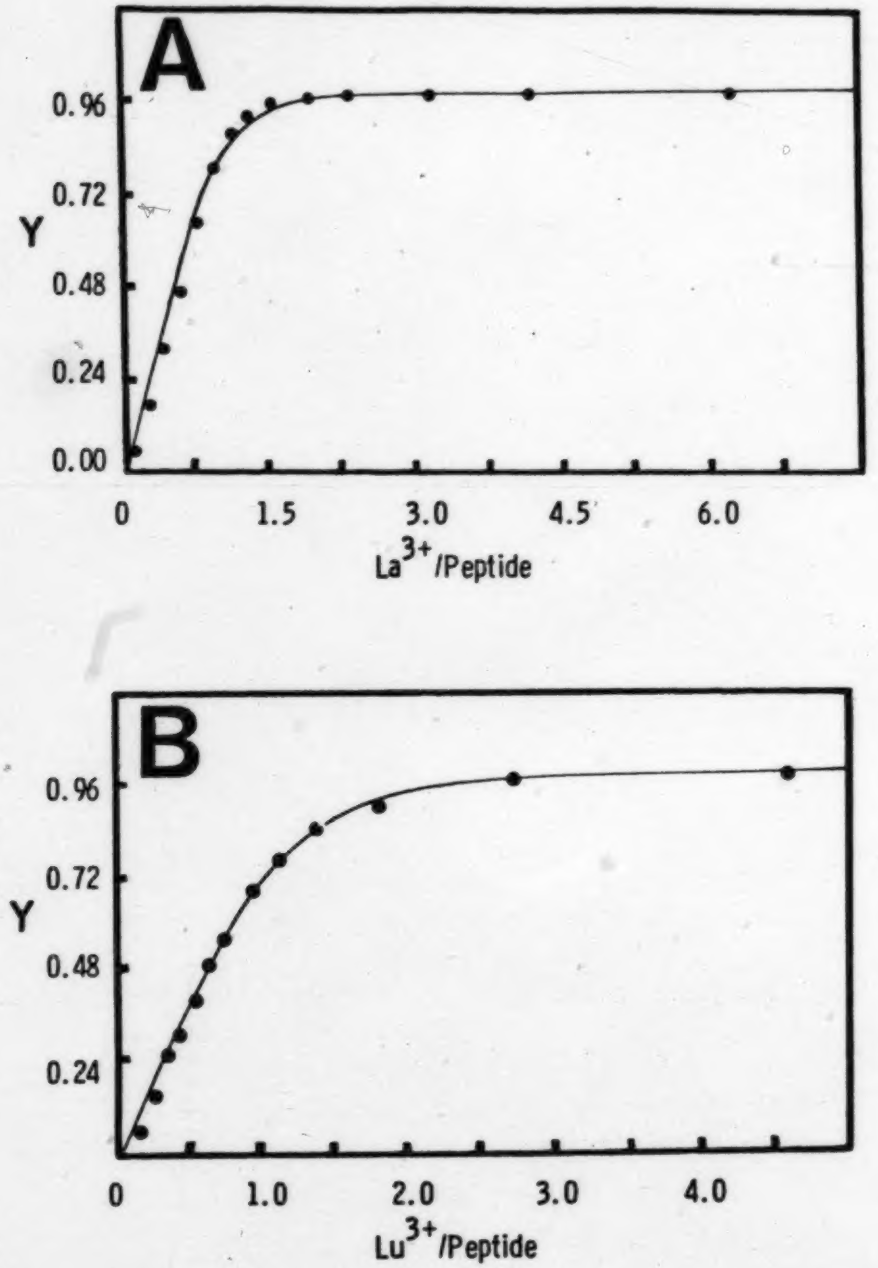

Fig. IV.5 Lanthanide titration plots of AcSTnC(103-115) amide. (A) lanthanum titration; (B) lutetium titration. The observed chemical-shift ratio (Y) was plotted as a function of metal added to the peptide solution. The quantity Y is described under experimental procedures.

average of 2 titrations). We rationalize a lowering of the metal binding constant on the fact that the peptide geometry around the metal is less compact. This can be visualized by the fact that in the case of lutetium, the peptide ligands interact with a metal which is 20% smaller than lanthanum. This situation will bring the 4 negatively charged side chains (Asp-103, -107, -111 and Glu-114) closer together and thus cause ligand repulsion. If the peptide was to assume the same conformation as in the presence of lanthanum, then the bonds between ligands and metal would be 0.17 Å longer, a factor that could well reduce the stability of the metal:peptide complex. Furthermore, the qualitative behavior of the line widths of the AB pattern of the glycine α-protons centered at 3.90 ppm is an indication of the *off rate* (k*off*) for the bound metal ion. These resonances initially broaden and then sharpen during the lanthanum titration as compared to a simple shifting pattern observed in the case of lutetium addition (Figures IV.4 and IV.5). This suggests that the *off rate* for the bound La^{3+} is lower than for Lu^{3+} which correlates with the larger binding constant. The binding order observed also agrees with the lanthanide affinities measured on native troponin C (Wang *et al.*, 1981) where Eu(III) (ionic radius, 0.95 Å) binds tighter than Tb(III) (ionic radius, 0.92 Å) to both the high- and low-affinity sites.

3. Peptide folding pattern

A look at isolated resonances of the peptide yields information about the actual folding of the peptide. Position 6 of the calcium binding loop (Fig. IV.1) for example, is highly conserved throughout the sequence alignment of calcium binding proteins (Barker *et al.*, 1978; Reid and Hodges, 1980). Glycine normally occupies this position. Notable exceptions are a serine substitution observed for the alkali light chain of rabbit skeletal muscle myosin , a known non calcium binding EF hand. Proline or lysine substitutions at this position in intestine calcium binding proteins (Hofmann *et al.*, 1979; Fullmer and Wasserman; 1981) and in brain S-100 a,b (Isobe and Okuyama, 1981) are followed by an inserted residue and lead to a distorted metal binding region (Szebenyi *et al.*, 1981) that retains its calcium binding ability . Our ^{1}H NMR results suggest that Gly-108 adopts a rigid environment even in the apopeptide form. This conclusion was drawn from the observation that its α-carbon protons appear as an AB quartet centered at 3.90 ppm. The addition of either lanthanum or lutetium promotes the shielding of one of the α-carbon protons as observed from the upfield shift of two resonances (3.85 and 3.78 ppm) of the quartet (Figures IV.3 and IV.4). The shielding effect is larger in the presence of

La^{3+} than in the case of Lu^{3+} addition (upfield shift: La^{3+}, 0.315 ppm; Lu^{3+}, 0.095 ppm). This upfield shift can be rationalized by looking at a stereoprojection of this synthetic fragment presented in Fig. IV.6. This projection was constructed using the peptide backbone coordinates of carp parvalbumin (Kretsinger and Nockolds, 1973) to which our peptide side chain sequence was substituted. It points out that the glycine α-carbon protons are in close proximity to the aromatic side chain of Tyr-109 and may be shielded through a ring current effect. Another possibility is the proximity of one of the protons to the carbonyl group of Tyr-109 involved in the coordination sphere. The carbonyl group generates a shielding cone perpendicular to its C-O double bond plane. The lack of evolutionary divergence at this position of the loop is probably linked to the presence of the α-carbon near various ligands involved in metal chelation. These ligands require some flexibility in order to properly fold around the metal. One can appreciate this fact, by considering a substitution to a bulkier side chain. The presence of such a side chain could well hinder the binding of Asp-103 side chain or Tyr-109 carbonyl group to the metal (Fig. IV.6). Also, the protein backbone chain undergoes a large change in direction in this part of the EF loop (Kretsinger, 1980).

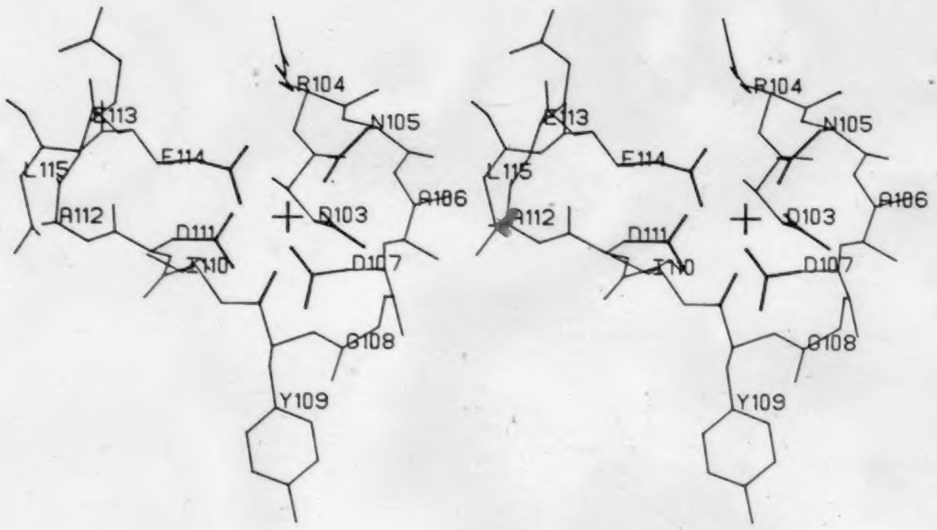
R104
N105
E113
E114
L115
R112
A106
D103
D111
I110
D107
G108
Y109
R104
N105
E113
E114
L115
R112
A106
D103
D111
I110
D107
G108
Y109

Fig. IV.6 Stereoprojection of rabbit skeletal troponin C region 103-115. This representation was constructed by using the crystal coordinates of carp parvalbumin for the metal binding loop of the CD hand (residues 51-63) [Kretsinger and Nockolds, 1973]. The original set of coordinates from the peptide backbone was retained, but the rabbit skeletal troponin C side chains of residues 103-115 were substituted for the parvalbumin side chains. The orientation of the side chains along their respective Cα-Cβ bond was maintained. This drawing can more easily be viewed in stereo with a stereoscope from Hubbard Scientific Co., Northbrook, IL.

Another site of interest is the -Y position occupied by Tyr-109. This site represents the least conserved position of the calcium binding loop in terms of amino acid substitutions (chapter VI). However the carbonyl group at this position represents the -Y ligand and the side chain, because of its location in the loop, is thought to play a role in the metal dehydration process (Reid and Hodges, 1980). In view of its hydrophobic side chain, Tyr-109 appears to be a residue of choice in helping to dehydrate the metal inner-sphere complex. The ^{1}H NMR spectrum of the peptide aromatic region pointed out the upfield movement of the ring 2,6 protons resonances during addition of lanthanides and in particular lanthanum. A crossover of the ring protons resonances had been observed in earlier studies on both synthetic (Gariépy *et al.*, 1982; chapter III) and natural fragments of this site (Birnbaum and Sykes, 1978). In all cases, the 2,6 proton lines appear upfield shifted while the 3,5 proton resonances were not significantly altered by the presence of calcium. These observations have led to the idea that geometric constraints were placed on the ring, in the metal bound conformation. It was further thought that the shielding effect on the tyrosine 2,6 ring protons was a reflection of the change of environment of the side chain. Our present lanthanide results point out that the metal bound environment of the tyrosine side chain remains closely associated with the loop (upfield shift of the 2,6 ring proton resonances). Furthermore, the addition of the relaxation probe gadolinium, to the metal bound or metal free peptide produces a rapid broadening of the meta protons doublet as compared to the ortho protons doublet and does indicate that these protons are closer to the metal than the ortho protons (next section). One possible position for the ring can be obtained by a simple rotation of the side chain along its $C\alpha$-$C\beta$ bond toward the carbonyl group of Asp-107 or Gly-108. These latter groups will provide a shielding mechanism for the meta protons which remain closer to the metal than the ortho ones.

The reason for wanting to investigate the tyrosine environment in our fragment comes from the observation that it is also exposed to the solvent in calcium-saturated troponin C. For example, the tyrosine rings of troponin C have been labelled by lactoperoxidase iodination (Seamon *et al.*, 1977) and by tetranitromethane (McCubbin and Kay, 1975) in the presence or absence of calcium. Similarly , ^{1}H NMR CIDNP experiments demonstrated clearly that although the exposure of the rings to the excited flavin dye is reduced in the presence of calcium, the effect is quite apparent (Hincke *et al.*, 1981b). If one considers the dimensions of the dye and its hydrophobic nature, one can conclude that the tyrosine ring remains exposed to the solvent, in the metal-saturated protein. The troponin C model proposed by Kretsinger and Barry (1975) illustrates this point. The tyrosine ring exposure is thus similar to the one observed for our peptide . Looking at Fig. IV.6, one realizes that if the tyrosine side chain gets partly immobilized in between the peptide backbone of Gly-108 and Asp-107, it might well explain the shielded environment of one of the α-carbon protons of Gly-108.

C. DETERMINATION OF METAL-PROTON DISTANCES IN A GADOLINIUM:PEPTIDE COMPLEX

1. Distance measurements

The uncertainty surrounding the actual geometry of the lanthanide:peptide complex has triggered a second set of ^1H NMR experiments where the relaxation probe gadolinium was used to determine metal-proton distances involved in this complex. These studies were carried out with a view to reconstruct the conformation adopted by this synthetic fragment in the presence of gadolinium using the available set of distance restrictions.

a. Gadolinium titration

The gadolinium titration was performed on a lanthanum-saturated peptide solution (La^{3+} to peptide ratio of 1.6 to 1) since in the presence of excess lanthanum, the peptide adopts a bound conformation where an improved resolution of key resonances is observed (i.e. β-CH$_3$ of alanine 106 and 112; β-CH$_2$ of Glu-113 and -114) (Fig. IV.7). Other technical reasons for the use of the peptide in its lanthanide-saturated form were discussed earlier (chapter II, gadolinium titration).

The experimental strategy used to obtain information concerning metal to proton distances was to replace the lanthanum ion by gadolinium with the peptide always in the metal bound geometry. Gadolinium possesses isotropic relaxation enhancement properties due to its 4f^7 electronic configuration. A gadolinium titration of the lanthanum bound peptide is presented in Fig. IV.8 and illustrates the broadening effect induced by gadolinium on the proton resonances of AcSTnC(103-115)amide.

The changes in resonance line width due to the presence of this paramagnetic metal can be related to the metal-proton distance involved following the Solomon-Bloembergen equations (appendix). Since the β-CH$_2$ protons of Asp-103, -107 and -111, of Asn-105 and of Glu-114 (2.2 to 2.9 ppm region) are parts of side chains involved in metal chelation (Fig. IV.7, sequence), these particular protons should lie closer to the metal than the methyl groups of

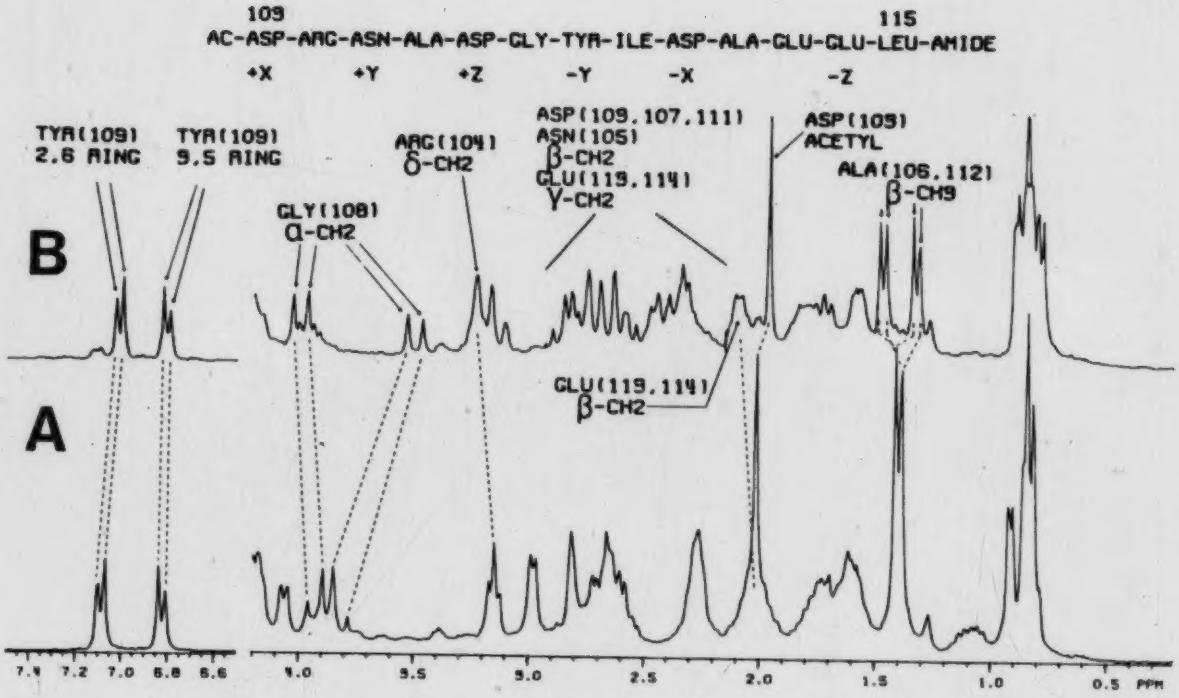

Fig. IV.7 Assignment of AcSTnC(103-115) amide ^1H NMR resonances. (A) ^1H NMR spectrum of the apopeptide; (B) ^1H NMR spectrum of the peptide in the presence of 1.27 mM $LaCl_3$. The primary sequence of the peptide is listed above spectrum B. [Peptide] = 0.77 mM in 100 mM KCl, 0.1 mM DSS, pH 6.0.

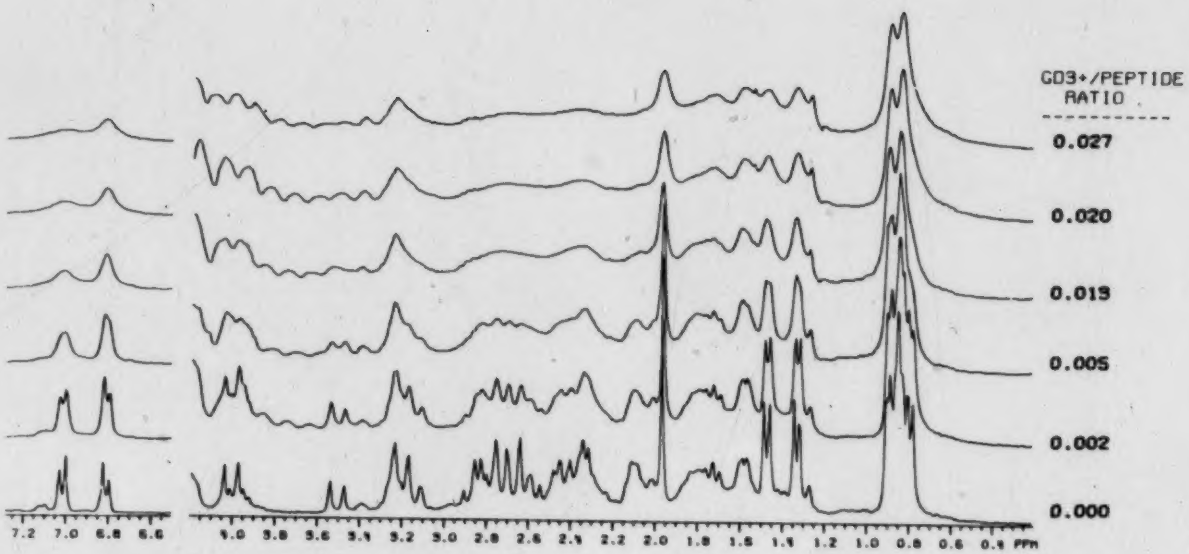

Fig. IV.8 Gadolinium titration of AcSTnC(103-115) amide in the presence of excess lanthanum. [Peptide] = 0.77 mM in 100 mM KCl, 0.1 mM DSS, 1.27 mM $LaCl_3$, pH 6.0. The Gd^{3+}/peptide ratio represents the ratio of gadolinium bound to the peptide as described in the experimental procedures section.

Ala-106 and -112 (doublets centered at 1.30 and 1.45 ppm), or the acetyl group of Asp-103 (singlet at 2.00 ppm), or the tyrosine ring protons (doublets situated at 6.80 and 7.00 ppm). This assumption is verified readily by the observation of the greater broadening of the resonances associated with the coordinating side chains as compared to other proton resonances seen in Fig. IV.8.

b. Determination of relaxation times

The spin-lattice relaxation times (T_1) associated with individual resonance patterns shown in Fig. IV.7 were determined at each addition of gadolinium to the NMR tube. The measured $1/T_1$ values were then plotted as a function of the percent of the peptide bound to gadolinium, and a $T_{1}m$ value at a 1 to 1 ratio of Gd^{3+} to peptide was extrapolated from a least squares fit of the data. Similarly, $1/T_2$ values calculated from line width measurements for the well defined resonances were plotted as a function of the percent of peptide bound to Gd^{3+} and yielded a linear relation from which a value of $T_{2}m$ at a 1 to 1 ratio of gadolinium to peptide could be extrapolated. Table IV-3 lists relaxation times calculated for the resonances assigned in Fig. IV.7.

Note that in the determination of $T_{2}m$ values the spectral line broadening contribution of 1 Hz was substracted from all line width estimates, as described in

TABLE IV-3

Relaxation times[a] and calculated proton-metal distances[b]

Proton species	T_{1m} (msec)	T_{2m} (msec)	T_{1m}/T_{2m}	r (Å)
Asp-103				
Acetyl-CH_3	1.0	0.43	2.32	8.2 ± 0.4
Ala-106,-112				
β-CH_3, 1.30 ppm	0.83	0.50	1.66	8.4 ± 0.3
β-CH_3, 1.45 ppm	0.60	0.44	1.36	8.3 ± 0.2
Tyr-109				
3,5 ring protons	0.56	0.38	1.47	8.0 ± 0.2
2,6 ring protons	0.23	0.19	1.21	7.2 ± 0.4
Gly-108				
α-CH, 3.5 ppm	0.80	0.15	5.33	6.9 ± 1.0
α-CH, 4.0 ppm	1.2	----	----	(9)
Arg-104				
δ-CH_2, 3.2 ppm	1.6	----	----	(9)

[a] Determined by linear least squares fitting of $1/T_1$ and $1/T_2$ values as a function of % peptide bound to gadolinium.

[b] Represent metal-proton distances calculated from the relaxation times observed. Values in parentheses are estimates based on T_{1m} values obtained.

chapter II. However, this factor and any other contributions affecting the initial line width should not influence the extrapolated T_2m value since it is the slope characterising the linear relation between $1/T_2$ observed and the % peptide bound to Gd^{3+} that dictates the final T_2m value calculated. Also, the increase in line width for a given resonance due to Gd^{3+} bound to the peptide will represent a direct T_2m measurement only in the case where the peptide exchange rate between its metal free and bound state is fast on the NMR time scale (i.e. fast exchange). We have assumed a fast exchange process between the bound and free states of the peptide in light of the following facts:

i) differential line broadening is observed for various resonances so that exchange cannot be in the slow exchange limit except for the closest nuclei.

ii) the T_1m/T_2m ratio remains constant for a variety of resonances (Table IV-3), except for the Gly-108 α-CH_2 protons. However, if the value of the exchange lifetime were becoming significant for the closer Gly protons, the value of T_1m/T_2m should be reduced and not increased. The deviation in the value T_1m/T_2m for Gly-108 α-CH_2 proton (3.5 ppm) reflects experimental errors associated with the T_1m and T_2m values.

iii) the largest frequency shift observed during the peptide lanthanum titration was of 0.32 ppm (Gly-108 α-CH;

preceeding section). This implies that the lifetime of the metal bound state is small compare to the reciprocal maximum observed frequency difference (< 2 *m*s).

The major source of uncertainty in the determination of T_{1m} and T_{2m} values is associated with the measurement of slopes from 1/T versus %Gd^{3+} bound plots (appendix). For example, a slope calculated from a regression analysis of 3 or 4 points as in the case for the T_1 extrapolation is less reliable than from an analysis involving 8 to 10 data points as in the case of a T_2 measurement.

c. Calculation of metal-proton distances

An average T_{1m}/T_{2m} value of 1.6 ± 0.4 was determined from the summation of individual values listed in Table IV-3. The value of 5.33 obtained for the Gly-108 3.5 ppm resonance was dropped from the computation of this average T_{1m}/T_{2m} term on the basis of its statistical significance (Dean and Dixon, 1951). A correlation time τ_c value of 0.48 ± 0.06 *n*s was then computed and is in good agreement with a value of 0.6 *n*s ($[MW \times 10^{-12}]/2.4$ s for a MW~1,500; Cantor and Schimmel, 1980) predicted for our peptide. Note that the correlation time τ_c is related to: τ_m, the lifetime of a nucleus in the bound state; τ_s, the electron spin relaxation time; and τ_r, the rotational correlation time of the

Gd^{3+}:peptide complex, by the equation

$$\frac{1}{\tau_c} = \frac{1}{\tau_m} + \frac{1}{\tau_s} + \frac{1}{\tau_r}$$

Since $\tau_s >> \tau_r$ in the case of Gd^{3+} and Eu^{2+} (Nieboer, 1975) and τ_m is large in comparison to τ_r ($\sim 10^4 - 10^6$ times), the correlation time value reflects the shortest term of the equation i.e. τ_r.

Metal-proton distances were calculated using T_{2m} values. When such a value was not available, the distance was estimated using the corresponding T_{1m} value. The calculated distances are listed in Table IV-3.

2. Key assumptions

One key assumption in the use of lanthanides as calcium substitutes is that their binding to these EF domains is analogous to calcium. This assumption may not be necessarily true since lanthanides prefer to form complexes having a coordination number of 8 or 9 rather than six, seven and eight as in the case of calcium (Nieboer, 1975; dos Remedios, 1981). Variations in the geometry adopted by our synthetic peptide were observed by ^1H NMR in the case of lanthanum and lutetium additions. Also, Leavis *et al.* (1980) pointed out that the intrinsic fluorescence of tyrosine 109 in site III of rabbit skeletal troponin C is enhanced upon calcium and magnesium binding but remains unaffected in the case of terbium, lanthanum, neodynium or holium binding. These results were rationalized in terms of subtle differences in the tertiary structure of TnC induced by these ions. However, the ability of calmodulin to bind to troponin I or calcineurin and to stimulate phosphodiesterase activity is retained when terbium is used as a calcium analog (Wallace *et al*., 1982). A similar behavior of lanthanides on the biological activity of rabbit skeletal troponin C remains a difficult question to answer in view of the multiprotein complex involved in the actin-activated ATPase assay (Oikawa *et al*., 1980). One can thus conclude that variations in the protein geometry near the metal binding site do occur and are dependent on the properties of the cation present but the overall structure of the protein remains comparable to the calcium bound form.

The gadolinium titration of β-CH_2 and γ-CH_2 resonances of Glu-113 and -114 suggests on the basis of the large broadening of these resonances that these side chains are close to the metal and may well be both part of the coordination sphere. This would imply an additional oxygen ligand supplied by the peptide (Glu-113 side chain). This possibility is particularly appealing if one considers that this position in calcium binding proteins is often occupied by a negatively charged amino acid (Reid and Hodges, 1980;

chapter VI).

Note that the association constant of Gd^{3+} to the peptide was assumed comparable to the one calculated for La^{3+} ($K(La^{3+}) = 1.1 \times 10^5 M^{-1}$). Added proof for this premise comes from fluorescence measurements on a 12-residue synthetic fragment of site II of rabbit skeletal troponin C where the Tb^{3+} association constant was estimated to be $2\text{-}3 \times 10^5 M^{-1}$ (Kanellis *et al.*, 1983).

The assumption that the peptide adopts a similar conformation in the presence of Gd^{3+} and La^{3+} is not critical in the measurement of proton-metal distances since these distances are determined in relation to the gadolinium ion only. However, one should appreciate the fact that the peptide folding pattern around other lanthanides might differ, as demonstrated earlier.

Finally, one should discuss the sources and extent of non-specific binding since at the end of the gadolinium titration, the concentration of free lanthanum was about 0.5 mM while the concentration of unbound gadolinium was less than 7 μM. Free carboxyl groups represent the major class of ligands that would bind La^{3+} or Gd^{3+} from this pool of unbound lanthanides. The presence of an amide group at the C-terminal of the peptide eliminates one source of carboxyl group. However, the side chain of Glu-113, is not a calcium binding ligand based on the crystal structure of carp parvalbumin (Kretsinger and Nockolds, 1973) and represents a possible source of free ligand. The concentration of this ligand at the end of the gadolinium titration was 0.74 mM. Using the binding constants of La^{3+} and Gd^{3+} to acetate ion ($K(La^{3+})$, $1.05 \times 10^2 M^{-1}$; $K(Lu^{3+})$, $1.46 \times 10^2 M^{-1}$; Kolat and Powell, 1962), where the acetate ion represents a model ligand for the side chain of glutamic acid 113, one can calculate that less than 5% of the available carboxyl ligand would exist in a lanthanum bound state and less than 0.01% in a gadolinium bound state. These results consequently demonstrate that non-specific binding does not represent a significant factor in the gadolinium broadening experiments in terms of a contribution to the T_1m and T_2m estimates.

3. Distance restrictions

In order to reconstruct the geometry of the peptide AcSTnC(103-115)amide in solution, one should establish all available distance restrictions imposed on the site. These restrictions fall into 3 categories:

1) The set of distances calculated from the relaxation time measurements represents a first level of folding restrictions.

2) The rapid broadening of the β-CH_2 resonances of

aspartic acids, asparagine, glutamic acids and tyrosine residues as well as the γ-CH_2 resonances of glutamic acids suggests that their distances to the metal are less than 7 Å. This value represents an upper limit on these distances. We can also assume that none of these side chain protons are within 2.5 Å of the metal, since this value corresponds to a typical Gd^{3+}-O bondlength.

3) The oxygen atoms coordinating the lanthanide Gd^{3+} can be assumed to lie at a distance of 2.5 ± 0.3 Å from the metal as indicated from the crystal structure of a variety of lanthanide complexes (Alberston, 1968; Grenthe, 1969, 1971, 1972).

These distance constraints can now be used as boundary conditions in a distance-geometry algorithm devised recently by Kuntz and his co-workers (Havel *et al.*, 1979; Kuntz *et al.*, 1979). A series of allowed configurations for the gadolinium:peptide complex is generated from this array of distance restrictions. Convergence of the generated structures is expected to occur provided one has sufficient distance constraints. The analysis of a preliminary set of structures has indicated that this type of algorithm may prove sufficient to restrict the range of allowed conformations to a few highly homologous ones (Gariépy, Sykes, Hodges, and Kuntz; unpublished results).

D. SUMMARY

In this chapter, we have demonstrated the utility of the diamagnetic lanthanides lutetium and lanthanum as metal binding probes for a synthetic 13-residue fragment representing the calcium binding site III of rabbit skeletal troponin C (residues 103 to 115). The peptide conformation induced by these metals was monitored by proton magnetic resonance at 270 MHz. The peptide affinity for these rare earths is 50 to 400 times higher than for calcium ($K(Lu^{3+})$, $1.3 \times 10^{4} M^{-1}$; $K(La^{3+})$, $1.1 \times 10^{5} M^{-1}$; $K(Ca^{2+})$, $3 \times 10^{2} M^{-1}$) which is related to the change in cation charge from +2 to +3. The peptide conformation induced by the presence of La^{3+} generates a different ^1H NMR spectrum than the one observed for the lutetium-saturated peptide. Thus, it appears that these metals do not fold the peptide into exactly the same conformation. The resonance shifts observed during the Lu^{3+} titration are much smaller than in the case of La^{3+} addition. The fact that lutetium binds less tightly than lanthanum to the peptide may be linked directly or indirectly to the difference in ionic radius between these metals (Lu^{3+}, 0.86 Å; La^{3+}, 1.03 Å). This may in turn indicate that the peptide primary sequence encodes for some aspects of metal ion specificity. The ^1H NMR results also demonstrate that Gly-108 adopts a restricted geometry in the absence of metal such that its two α-carbon protons are in different environments which are further affected by the addition of either metal. These observations support the concept that geometric constraints arising from the particular peptide folding pattern near this residue correlate with the highly conserved nature of this site of the EF hand. This position remains occupied by glycine in most EF hand domains with the exception of known distorted calcium binding sites present in intestine calcium binding proteins and S-100 (Szebenyi *et al.*, 1981).

The binding of Gd^{3+} to this peptide was investigated by proton magnetic resonance. The relaxation enhancement property of this lanthanide was used as an analytical tool in order to determine a series of proton-metal distances for this Gd^{3+}:peptide complex. Measurements of relaxation times (T_1, T_2) were performed at various stages during the gadolinium titration of a lanthanum-saturated peptide solution. The relaxation times values derived for a 1:1 complex of Gd^{3+} to peptide, were used to estimate the proton-gadolinium distances involved. These distance measurements were then treated as boundary conditions in a distance-geometry algorithm. This approach will yield a series of possible conformations adopted by the gadolinium:peptide complex in solution.

CHAPTER V

PHENOTHIAZINE BINDING SITE IN THE N-TERMINAL REGION OF SITE III OF RABBIT SKELETAL TROPONIN C

A. CALCIUM-INDUCED EXPOSURE OF HYDROPHOBIC REGIONS ON TROPONIN C AND CALMODULIN

In chapter III, we have demonstrated the importance of the C- and N-terminal helical domains on the ability of site III of rabbit skeletal troponin C to bind calcium tightly. These results have also indicated that the reciprocal action of calcium binding to the loop region is to induce the formation of α-helical regions. A closer investigation of the residues involved in these helical regions provides some insight toward the mechanism of action of CaM and TnC. As stated in chapter VI, the sequence alignment of EF domains from various types of calcium binding proteins reveals that the C- and N-terminal regions are related by a partial sequence homology indicating that EF domains possess some elements of internal symmetry. Kretsinger (1977, 1980) indicated the presence of regularly placed hydrophobic residues on both sides of the calcium binding loop. Each terminal region possesses two pairs of hydrophobes located 4 residues apart. If these regions adopt an α-helical arrangement then the spacial orientation of these side chains will generate a hydrophobic plane on each side of the calcium binding loop (assuming that 1 turn of α-helix requires 3.6 amino acids). Since the N-terminal region of site III of rabbit skeletal troponin C is known to undergo a coil to helix transition upon Ca^{2+} addition (Nagy *et al.*, 1978; Nagy and Gergely, 1979; Reid *et al.*, 1981) one can conclude that the creation of a hydrophobic surface in the N-terminal region is a calcium-dependent event. The use of hydrophobic compounds such as fluorescent probes (Johnson *et al.*, 1978; LaPorte *et al.*, 1980; Malencik and Anderson, 1982), antipsychotic drugs (Levin and Weiss, 1977, 1978, 1979, 1980; Prozialeck and Weiss, 1982; Johnson, 1983) and certain muscle relaxing agents and anesthetics (Hidaka *et al.*, 1978; Kobayashi *et al.*, 1979; Hidaka *et al.*, 1979; Nishikawa *et al.*, 1980; Tanaka *et al.*, 1980, 1981a,b) have provided ample evidence that such hydrophobic domains become exposed on TnC and CaM in the presence of calcium. Furthermore, the activity of various enzymes modulated by calmodulin is depressed by the presence of antipsychotic drugs (Levin and Weiss, 1977, 1980; Kuznicki *et al.*, 1981), W-7 derivatives (Hidaka *et al.*, 1977, 1978a,b, 1979; Kobayashi *et al.*, 1979; Nishikawa *et al.*, 1980) and neuropeptides (Sellinger-Barnette and Weiss, 1982). Although the interaction of CaM with these hydrophobic compounds appears to be a non-stereospecific one (Norman *et al.*, 1979;

LaPorte *et al.*, 1980; Landry *et al.*, 1981; Roufogalis, 1981), the selectivity demonstrated by these molecules in blocking calmodulin regulated events has popularized their use and has led Prozialeck and Weiss (1982) and our group to propose a working model for the structure and action of phenothiazines on calmodulin and troponin C. The structure and pK*a* values of four representative phenothiazines are presented in Fig. V.1. The following key points can be stated in relation to their antagonistic action:

1) The inhibitory action of these agents on the CaM stimulated phosphodiesterase activity is related to the presence of hydrophobic and positively charged domains on all these compounds and

2) The distance separating both domains correlates with the extent of the observed inhibitory effect.

Benjamin Weiss group studied the mechanism of action of antipsychotic drugs on calmodulin using analogs of these drugs and comparing their inhibitory strength toward a CaM stimulated phosphodiesterase assay. Our approach was to localize a phenothiazine binding site on troponin C and to analyse some of the structural features relevant to the drug:peptide complex.

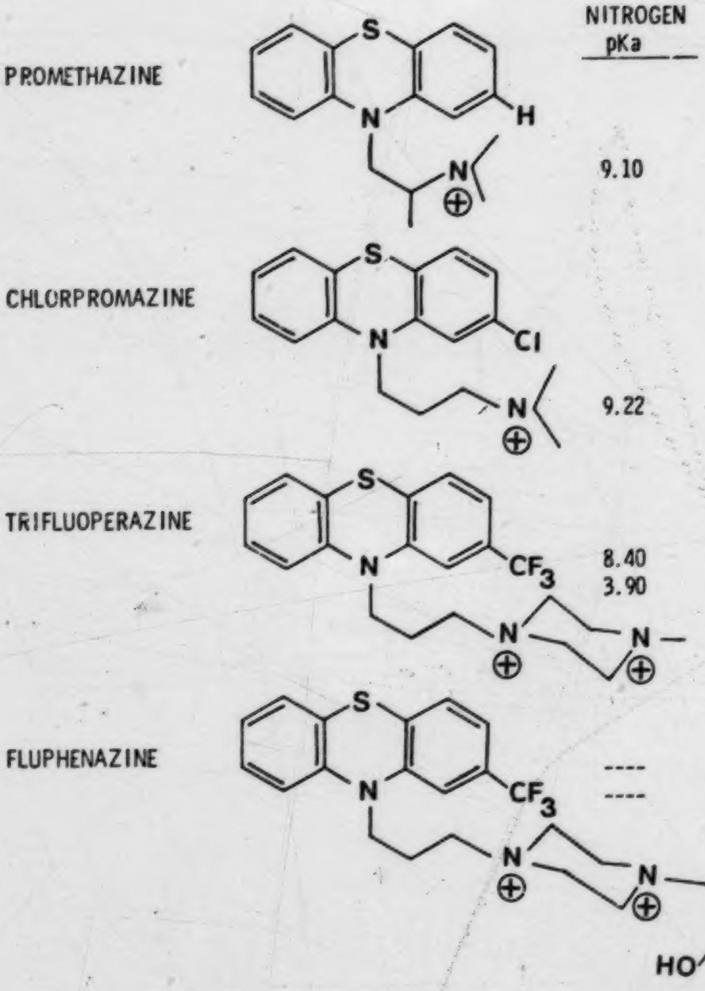
NITROGEN
pKa
PROMETHAZINE
S
N
H
N
⊕
9.10
CHLORPROMAZINE
S
N
Cl
N
⊕
9.22
TRIFLUOPERAZINE
S
N
CF3
8.40
3.90
N
⊕
N
⊕
FLUPHENAZINE
S
N
CF3

N
⊕
N
⊕
HO

Fig. V.1 Structure and nitrogen pK_a's of some representative phenothiazines [Adapted from Chatten and Harris, 1962].

B. LOCALIZATION OF A PHENOTHIAZINE BINDING SITE ON TROPONIN C

It was shown by Levin and Weiss (1977) that the activation of bovine brain phosphodiesterase by calmodulin could be selectively inhibited by phenothiazine antipsychotics. The specificity of these drugs for calmodulin was partly demonstrated by the failure of other calcium binding proteins to bind trifluoperazine. Besides calmodulin, only troponin C displayed a significant calcium-dependent binding of trifluoperazine (Levin and Weiss, 1978). Recently however, the brain-specific calcium binding protein S-100 has been shown to interact in a calcium-dependent manner with either a W-7-coupled or a phenothiazine-linked Sepharose matrix (Endo *et al.*, 1981; Marskak *et al.*, 1981). Two high-affinity calcium-dependent trifluoperazine binding sites (K_d =1 μM) exist on calmodulin. At concentrations of TFP above 10 μM, troponin C binding of this drug was comparable to calmodulin (K_d =5 μM) (Levin and Weiss, 1978). The number of calcium-dependent TFP binding sites on troponin C has not been established.

We suspected that one of the phenothiazine binding site on calmodulin was near its third calcium binding site since the use of tryptic fragments of calmodulin had revealed that this site was essential for the interaction of CaM with several target proteins (Kuznicki *et al.*, 1981; Drabikowski *et al.*, 1982) (Fig. V.2). Similarly , trifluoperazine (TFP) has been shown to interact with the TR2C fragment of CaM (residues 78-148, sites III and IV) as demonstrated by its inhibition of the TR2C-stimulated phosphorylase kinase activity (Kuznicki *et al.*, 1981). It was discovered that a cyanogen bromide fragment (residues 77-124, site III) resulting from the incomplete digestion of bovine brain CaM remains bound to a fluphenazine affinity column in the presence of calcium (Head *et al.*, 1982) (Fig. V.3). Fragments containing regions of bovine brain CaM (78-148 & 1-106) as well as the cyanogen bromide fragment CB9 of rabbit skeletal troponin C (residue 84 to 135) were shown to interact with rabbit skeletal TnI and release the inhibition of actomyosin ATPase by troponin I (Weeks and Perry, 1978; Grabarek *et al.*, 1981; Kuznicki *et al.*, 1981). It was further proven that a homologous 11- to 12-residue long region of troponin C (89-100) and of CaM (78-90) is an important region in the binding of TnI to these calcium binding proteins (Grabarek *et al.*, 1981; Kuznicki *et al.*, 1981).

Thus the peptide region of troponin C comprising the sequence 90-100 appeared to be a trifluoperazine binding region. Our first step was to make use of a cyanogen bromide fragment of troponin C containing both the proposed region

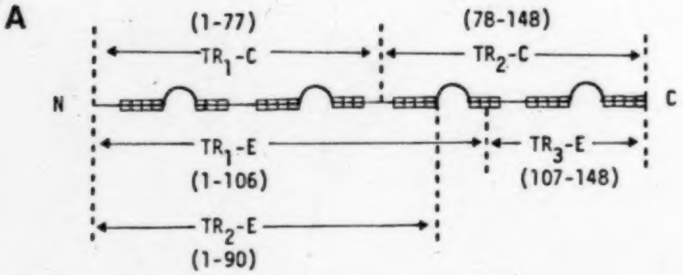

B

Target protein	Tryptic fragment	Relative effectiveness of modulation
Myosin light chain kinase	1-106	0.005
Phosphorylase kinase	78-148 1-106	0.01 0.0005
Cyclic nucleotide phosphodiesterase	78-148 1-106	0.0012 0.005
		Binding
Troponin I	78-148 1-90 1-106	Strong Weak Weak
Myelin basic protein	78-148 1-90 1-106	Strong Weak Weak
Histone H2B	All fragments studied	Strong

Fig. V.2 (A) Tryptic fragments of bovine brain calmodulin. TR-C fragments are obtained by limited tryptic digestion in the presence of calcium while TR-E fragments in the presence of EDTA. The 4 calcium binding domains are represented by the hatched areas [Adapted from Kuznicki *et al.*, 1981].
(B) Interaction of tryptic fragments with target proteins. The relative effectiveness of modulation of these fragments is in relation to calmodulin. The effective ness of modulation is measured by the amount of calmodulin or its fragments needed for half maximal activation of an enzyme [Adapted from Drabikowski *et al.*, 1982].

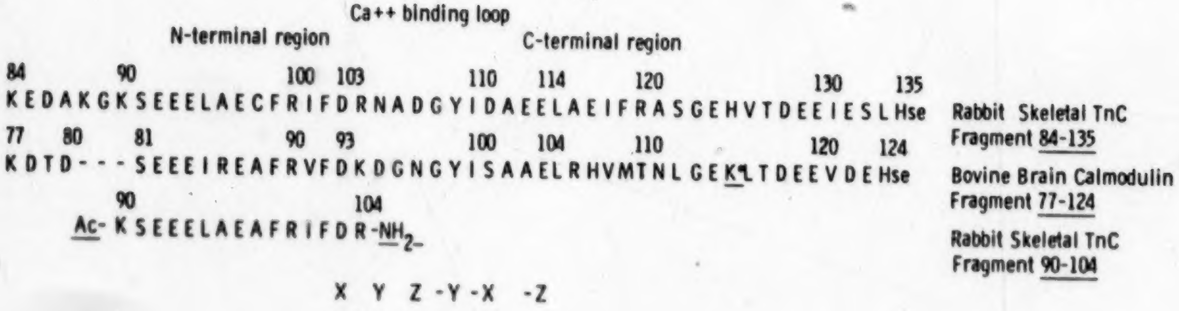
Ca++ binding loop
N-terminal region
C-terminal region
84 90 100 103 110 114 120 130 135
K E D A K G K S E E E L A E C F R I F D R N A D G Y I D A E E L A E I F R A S G E H V T D E E I E S L Hse
Rabbit Skeletal TnC Fragment 84-135
77 80 81 90 93 100 104 110 120 124
K D T D - - - S E E E I R E A F R V F D K D G N G Y I S A A E L R H V M T N L G E K* L T D E E V D E Hse
Bovine Brain Calmodulin Fragment 77-124
90 104
Ac- K S E E E L A E A F R I F D R -NH2-
Rabbit Skeletal TnC Fragment 90-104
X Y Z -Y -X -Z

Fig. V.3 Primary sequence alignment of peptides shown to bind phenothiazines. Fragment 84-135 of rabbit skeletal troponin C is abbreviated CB9. Fragment 77-124 of bovine brain calmodulin was recently shown to bind to a fluphenazine affinity column in the presence of calcium [Head *et al.*, 1982]. Fragment 90-104 represents our synthetic fragment comprising the proposed TFP binding site. The letters X,Y,Z,-Y,-X, and -Z represent the calcium coordinating ligands of the peptides. The symbol K* stands for trimethyllysine. The deletion between residues 80 and 81 in the calmodulin fragment sequence represents the alignment optimization described by Barker *et al.*, 1978.

of TFP binding and also a high-affinity calcium binding site. This peptide abbreviated CB9 contains residues 84 to 135 (Fig. V.3). Our experimental strategy was to monitor perturbations in the peptide secondary structure using circular dichroism while proton magnetic resonance could be used to investigate which amino acid side chains were involved in the drug:peptide complex.

1. Trifluoperazine behavior in solution

The two nitrogen atoms of the piperazine moiety of trifluoperazine have respective pK*a*'s of 3.9 and 8.4 (Chatten and Harris, 1962; Fig. V.1). This implies that at the experimental and physiological pH range used (6.0-7.4), the molecule possesses a positive charge on one of the piperazine nitrogens. Going to low pH's will protonate both nitrogens and will affect some of the aliphatic ^{1}H NMR resonances (results not shown). Going to high pH's (higher than 7.5) will promote TFP precipitation due to the hydrophobic nature of trifluoperazine in its unprotonated form. This fact can be correlated with the observed sharp decrease in drug binding to CaM at pH's above 7.5 (Levin and Weiss, 1977).

Increasing the drug concentration at constant pH, produces large shifts in the ^{1}H NMR spectrum of trifluoperazine (Fig. V.4). Changes in the observed chemical shifts of the drug resonances probably arise from the aggregation or stacking of the phenothiazine aromatic rings. Most of the protons of the drug appear shielded from or by the aromatic network in this "aggregated" geometry. One should note that recent ^{1}H NMR and ^{113}Cd NMR investigations dealing with the influence of trifluoperazine on the overall structure of calmodulin and the location of drug binding regions (Forsén *et al.*, 1980; Klevit *et al.*, 1981; Krebs and Carafoli, 1982) have all been performed at a drug concentration range in which the drug itself undergoes aggregation (greater than 1 mM TFP). One should thus be cautious in assessing the drug behavior above the 1 mM range and in interpreting the resulting spectra in terms of interactions between trifluoperazine and protein.

Increasing the concentration of anionic buffers like phosphate (Fig. V.4b) may promote the drug interaction with itself by bridging together the positive charges of two piperazine groups for example. This may explain the readily observed resonance of the piperazine ring methyl protons (2.7 ppm), which appears in a fast-exchange mode (sharp peak) in the presence of phosphate at a relatively low TFP concentration (0.25 mM). In contrast, we observe only a broad peak at 2.7 ppm, in the absence of phosphate for a 0.5 mM TFP solution. A related behavior of the drug in PIPES

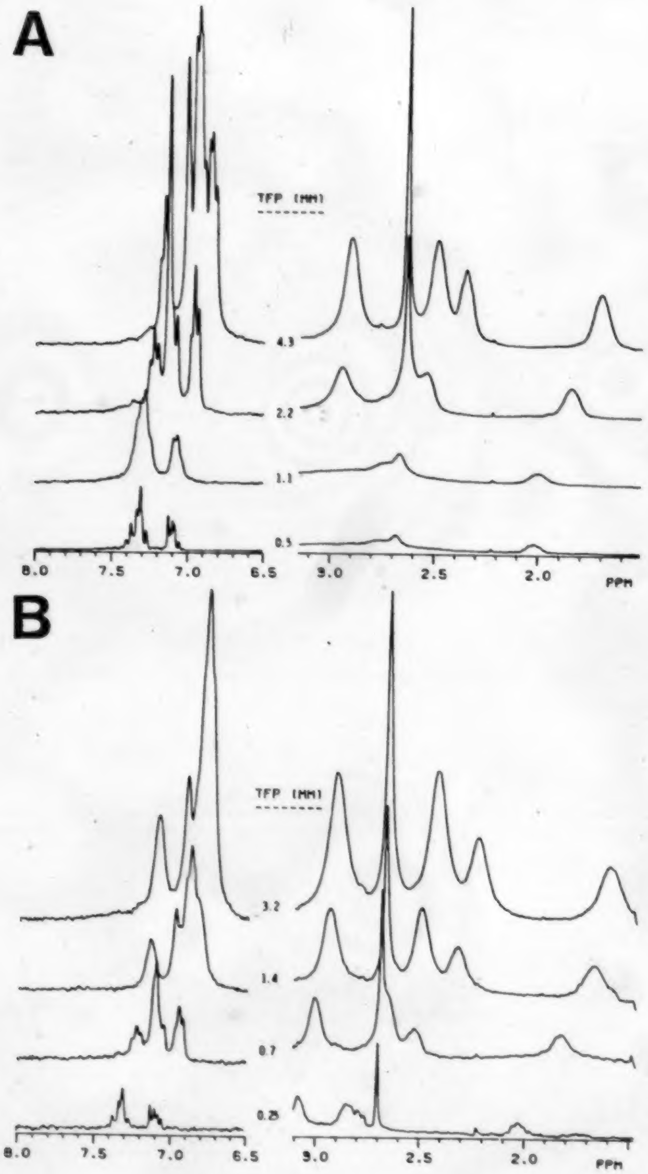

Fig. V.4 Effect of TFP and divalent anion concentration on the proton NMR spectrum of TFP.
(A) No divalent anion present but increasing TFP concentration. The spectra were recorded in 50 mM KCl, pH 6.0.
(B) Phosphate present and increasing TFP concentration. The spectra were recorded in 300 mM KH_2PO_4, 50 mM KCl, pH 6.0.

was noted. We suspect that other sulphonic acid type buffers like MES and MOPS may also produce such artifacts. We have thus performed all our experiments at TFP concentrations not exceeding 1 mM. A control spectrum of the drug alone was recorded for each addition of the drug during TFP titrations of the peptides in buffers such that the ^{1}H NMR spectra remain unaffected by the changing concentration of trifluoperazine.

2. Effect of Ca^{2+} and TFP on the secondary structure of CB9 and troponin C

The effects of trifluoperazine on the secondary structure of CB9 can be monitored by circular dichroism. In the absence of calcium, CB9 already possesses some secondary structure (-5,700 degrees of ellipticity at 222 nm; Fig. V.5, spectrum A). This was in accordance with the value of -5,730 observed by Nagy *et al.*, (1978). Figure V.5 indicates that the addition of drug to a TFP/peptide ratio of 1.6/1, induces a further increase in helical content (spectrum B). We did not go beyond a phenothiazine concentration of 1 mM because of a significant noise factor introduced in the CD spectrum by TFP. In the presence of calcium, the maximum ellipticity content of CB9 is induced so that addition of TFP yielded no observable effect on the CD spectrum (spectrum C).

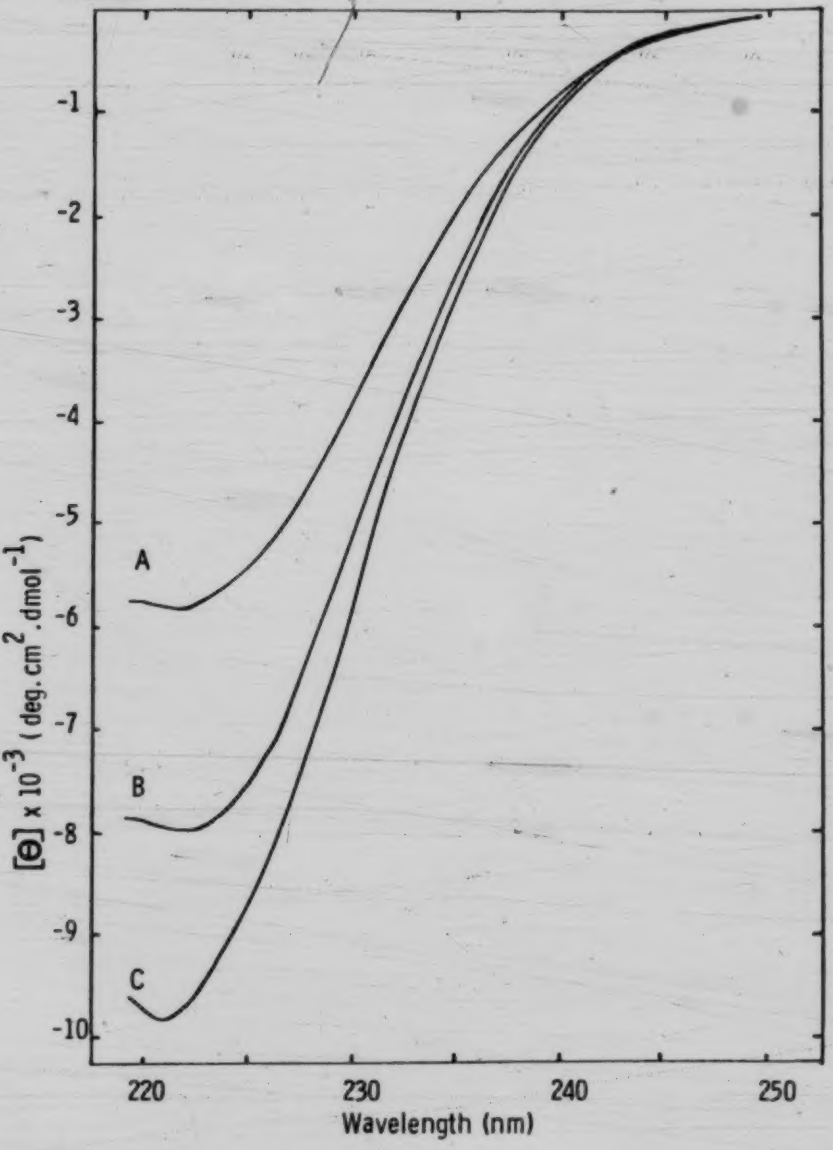

Fig. V.5 Effect of calcium and TFP on the circular dichroism spectrum of CB9. Spectrum A, CB9 spectrum in the absence of calcium and TFP. Spectrum B, CB9 spectrum in the absence of calcium but presence of TFP, TFP/CB9 ratio of 1.6. Spectrum C, CB9 spectrum in the presence of excess calcium with or without TFP. TFP/Calcium/CB9 ratios of 1.6/8/1 and 0/8/1.

Calcium titration in the presence or absence of trifluoperazine yielded identical calcium binding constants of 1.3×10^5 M^{-1}, in agreement with K*ca* values of 2.6×10^5 M^{-1} for a synthetic 34-residue fragment of this region (Reid *et al.*, 1981) and 5×10^5 M^{-1} for an earlier study of CB9 (Nagy *et al.*, 1978).

Determination of the drug binding constant in the absence of calcium was possible with CB9 from the ellipticity change observed at 222 nm. The binding constant calculated was equal to 1.2×10^5 M^{-1} (K*d* = 8 μM) which is comparable to the observed dissociation constant of 5 μM obtained from equilibrium dialysis experiments on calcium-saturated rabbit skeletal troponin C (Levin and Weiss, 1978). Thus it appears that the flexibility of this fragment allows for the induced folding of the site by TFP and unlike the native protein, does not necessitate the binding of calcium to induce the proper TFP binding site geometry.

The trifluoperazine titration of rabbit skeletal troponin C was monitored by circular dichroism. The results showed no increase in ellipticity at 222 nm upon TFP addition in the presence or absence of calcium.

3. Investigation of peptide side chains involved in the TFP:peptide complex using proton magnetic resonance

a. Addition of calcium to CB9 in the presence and absence of trifluoperazine

In the absence of TFP and calcium, the CB9 ^{1}H NMR spectrum obtained corresponds to apo-CB9 (Birnbaum and Sykes, 1978) and closely resembles the spectrum of synthetic fragments of this site (Gariépy *et al.*, 1982; Fig. V.6a). As calcium was added, most of the spectral features expected were observed including the shift of Tyr-109 ring protons resonances to 6.64 and 6.51 ppm and the appearance of upfield shifted resonances in the 0.2 to 0.8 ppm region. Shifts in this region are thought to arise from methyl groups of leucine or isoleucine side chains placed in proximity to aromatic side chains (Birnbaum and Sykes, 1978; Gariépy *et al.*, 1982). Also the methyl group of one or more of the 6 alanines present in CB9, are affected by the presence of calcium as the resonance envelope situated around 1.4 ppm is altered considerably.

In the presence of TFP (Fig. V.6b), the addition of calcium generates the same Ca^{2+}-induced resonances observed in the absence of drug (the Tyr-109 resonances at 6.64 and 6.51 ppm (Fig. V.6a) as well as the alanine methyl resonances at 1.4 ppm). In general, the presence of the drug does not appear to alter the binding of calcium to the coordinating region of CB9 and is thus evidence that the

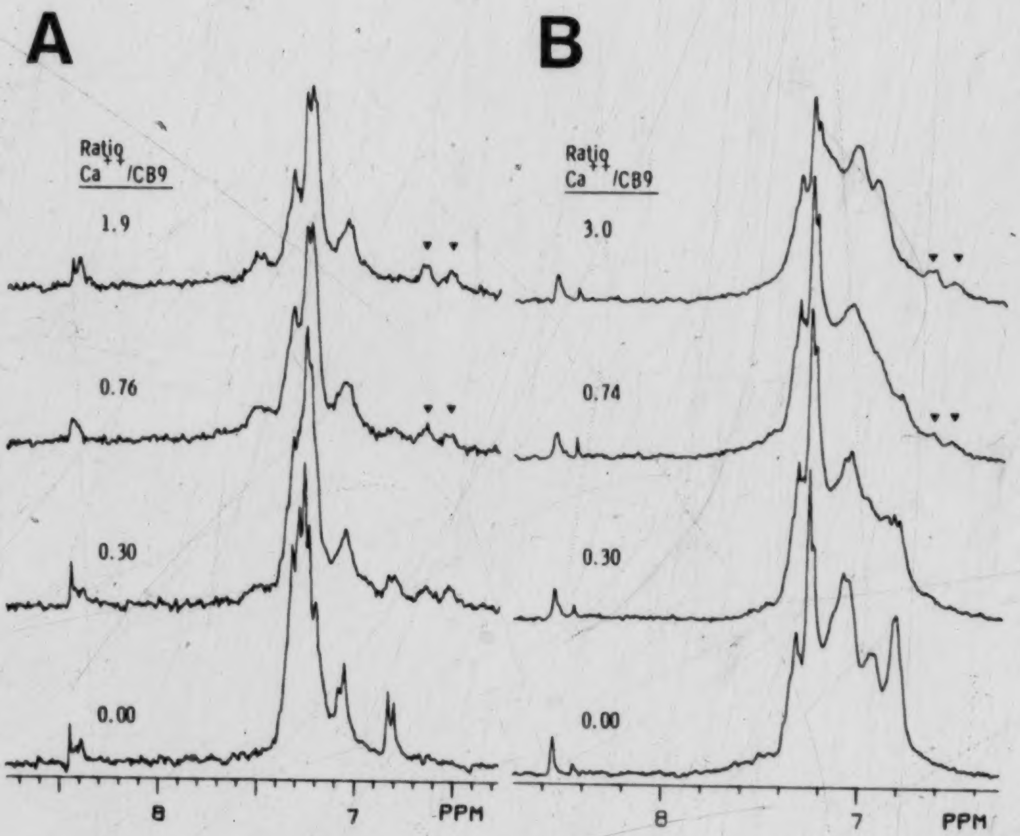

Fig. V.6 Calcium titration of CB9 in the presence and absence of TFP. (A) Calcium titration of the aromatic region of CB9 in the absence of TFP. [CB9] = 0.33 mM. (B) Calcium titration of the aromatic region of CB9 in the presence of TFP (0.37 mM). [CB9] = 0.34 mM. Symbols highlight changes in the proton magnetic resonance spectrum.

drug binding site is probably not located in the calcium coordinating region. This is in agreement with the circular dichroism results where equivalent binding constants of $1.3 \times 10^5 M^{-1}$ were calculated from the ellipticity measurements at 222 nm in the presence or absence of trifluoperazine.

b. Addition of trifluoperazine to CB9 in the presence and absence of calcium

Figure V.7a illustrates the effect of TFP on CB9. In the absence of calcium, the addition of TFP affects both the phenylalanines and the drug aromatic region (7.0 to 7.4 ppm region), when compared to the initial spectrum of CB9 (no drug) and the TFP control spectrum. A large broadened multiplet appears at 6.9 ppm. Similarly, the leucine/isoleucine methyl region centered at 0.9 ppm and the alanine methyl region at around 1.4 ppm are significantly influenced by the presence of this phenothiazine.

Trifluoperazine titration of this cyanogen bromide fragment in the presence of calcium is shown in Fig. V.7b. Some features arising from the presence of calcium are retained (Tyr-109 ring protons resonances for example), while changes occur in the phenylalanine envelope (around 7.25 ppm) with new aromatic resonances appearing as a

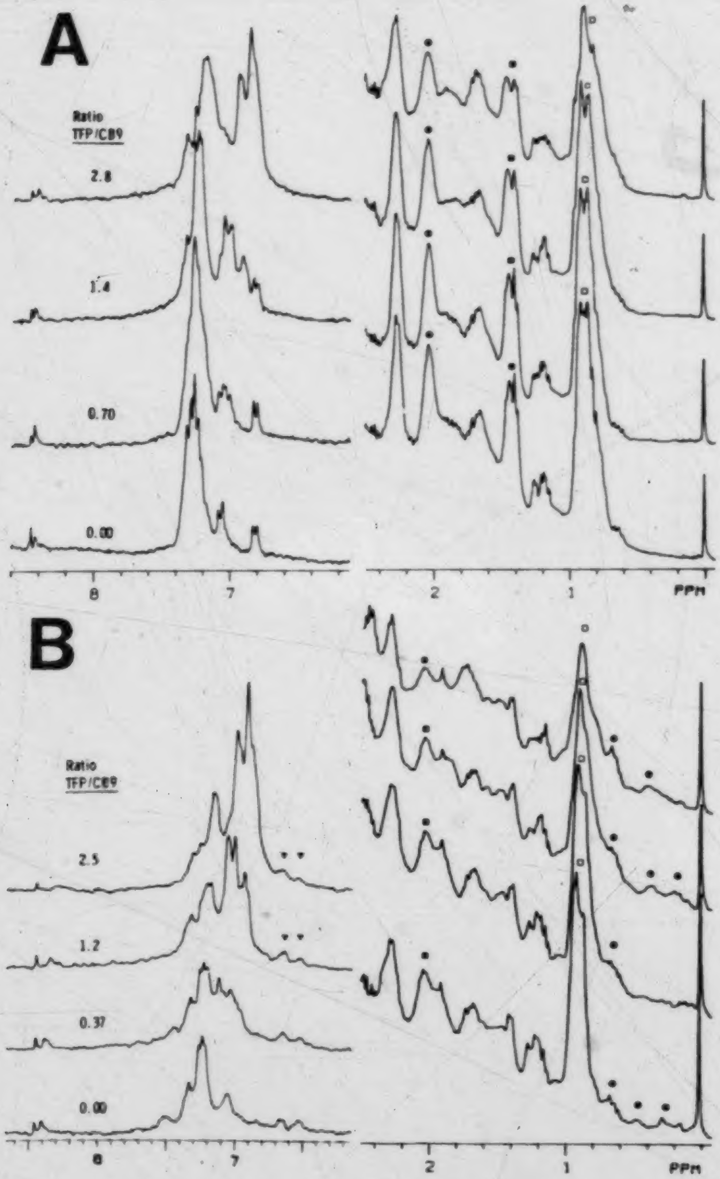

Fig. V.7 TFP titration of CB9 in the presence and absence of calcium.
(A) TFP titration of CB9 in the absence of calcium. [CB9] = 0.27 mM.
(B) TFP titration of CB9 in the presence of calcium (2.6 mM). [CB9] = 0.33 mM.
Control spectra of the drug were identical to the ones shown in Fig. V.8. At the concentrations of TFP used, no shifting of resonances in the control spectra was observed. Symbols highlight changes in the proton NMR spectrum.

broadened multiplet centered at 6.9 ppm. Changes are also observed in the aliphatic upfield shifted resonances (0.2 to 0.8 ppm) and the methyl region of leucine and isoleucine (0.9 ppm area). These resonances are not observed in the drug control spectrum. Thus it appears that a region of CB9 involving phenylalanines, alanines and leucines and/or isoleucines side chains is in spacial proximity to the drug. The fact that calcium was not a necessary requirement for drug binding was confirmed by circular dichroism results which showed an increase in ellipticity at 222 nm upon addition of TFP to apo-CB9 (Fig. V.5). The calculated drug binding constant was $1.2 \times 10^5 M^{-1}$ in the absence of calcium. Since upon calcium addition, no more ellipticity at 222 nm could be induced, it was impossible to determine by this approach, the phenothiazine binding constant to CB9 in the presence of calcium. Levin and Weiss (1978) estimated the dissociation constant of the drug to troponin C to be 5 μM in the presence of calcium which closely corresponds to the CB9 dissociation constant in the absence of calcium ($1/K_d = 8\ \mu M$) determined in this study.

Though the binding of phenothiazines to both CaM and TnC has been shown to be Ca^{2+}-dependent (Levin and Weiss, 1978), the finding that TFP binds to apo-CB9 is not surprising. There is no evidence that these drugs do not bind to isolated single Ca^{2+}-binding sites represented by

CB9 (residues 84 to 135 of TnC) and by the region 77 to 124 of calmodulin, in the absence of calcium. This binding of the drug to CB9 in the absence of calcium can be explained by the fact that the N-terminal region of CB9 is probably flexible and exposed in the fragment and readily induced to the correct conformation by the drug . Our CD and ^{1}H NMR results support this conclusion.

c. Interaction of trifluoperazine with a synthetic analog of site III of rabbit skeletal troponin C

It appears that the side chains of phenylalanines and methyl groups of leucine and/or isoleucine are in spacial proximity to the drug. We strongly suspected that the region 90 to 104 was the site of trifluoperazine binding. This fragment was synthesized and used to test this hypothesis. We did not expect a strong TFP binding to the peptide since the fragment lacks the actual calcium binding site and appears to possess little secondary structure as monitored by circular dichroism. Drug addition did not yield any significant CD change probably due to a weaker TFP binding constant to such a fragment. Some CD constraints also made this approach inadequate to study the TFP/peptide interaction. For example, the upper limit of 1 mM TFP and the necessity to have a high concentration of a small peptide to observe a few residues of helix being formed, does not permit us to go far enough in the titration. However the proton NMR results pointed out again large shifts in the phenylalanine resonances around 7.5 ppm and the aliphatic alanine (1.4 ppm), leucine and isoleucine methyl resonances (1.0 ppm region) were affected by the presence of the phenothiazine (Fig. V.8a). These altered resonances correspond to those observed in CB9 and suggest that the amino acid sequence 95 to 102 of CB9 interacts with TFP. Nagy *et al.*, (1978) commented that the N-terminal helical region of CB9 containing residues 94 to 103, is induced by Ca^{2+} and stabilized by hydrophobic patches formed by residues 95, 98, 99, 101 and 102. This statement was recently confirmed by our work on synthetic peptides of that site (Reid *et al.*, 1981; Gariépy *et al.*, 1982).

d. Proposed model of a phenothiazine binding site on rabbit skeletal troponin C

In view of the present results, we suggest that the drug acts as a steric blocker of a hydrophobic interphase, in proximity to, or part of the binding site to phosphodiesterase in CaM and to TnI in both TnC and CaM. This hydrophobic site is probably a small helical region involving a stretch of 7 or 8 amino acids rich in aliphatic and aromatic side chains resembling the sequence 95 to 102 of rabbit skeletal troponin C. A key feature of this segment

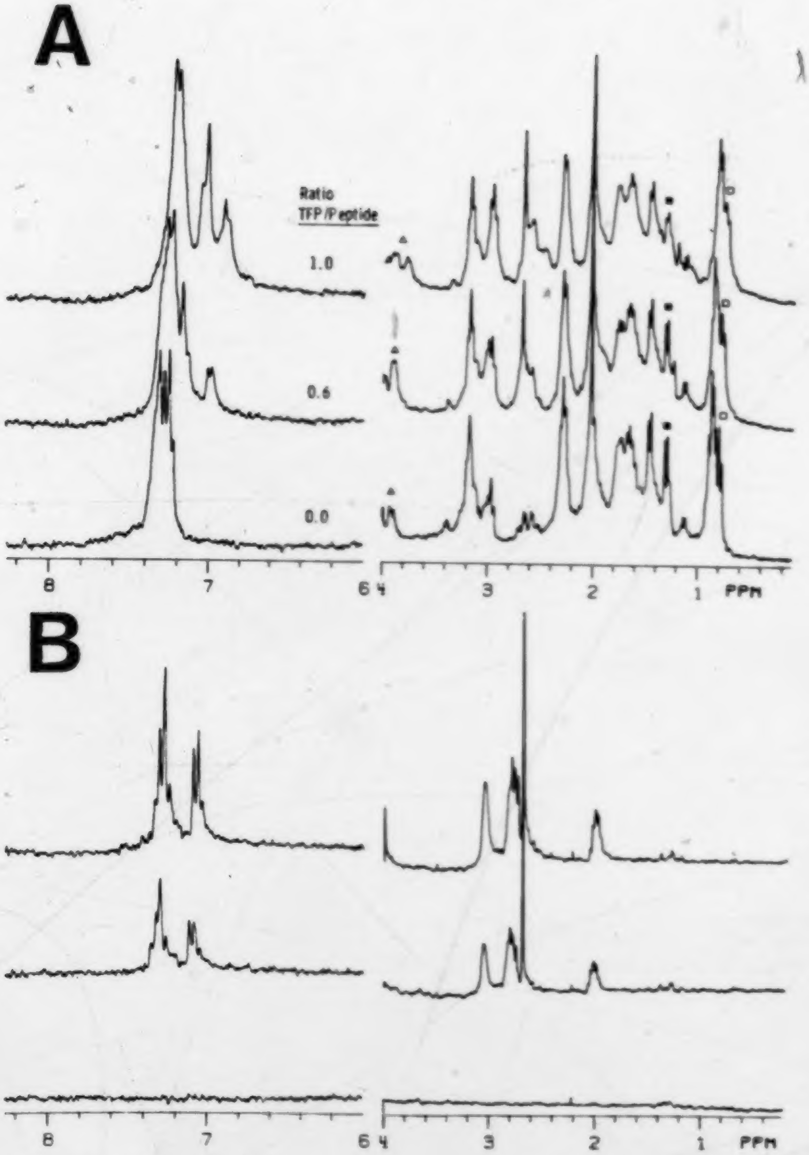

Fig. V.8 TFP titration of the synthetic fragment AcA^{98}STnC (90-104) amide. [peptide] = 1.0 mM.
(A) Proton NMR spectrum of the fragment at various additions of the drug.
(B) Control spectrum of TFP at additions of drug corresponding to the TFP/peptide titration.
Symbols highlight changes in the proton NMR spectrum.

is the presence of two phenylalanine rings separated by one turn of helix, which orients both aromatic side chains on the same side of the helix.

Another interesting feature that may favor the binding of trifluoperazine is the presence of a positive charge at physiological pH on the piperazine part of the molecule (Fig. V.1). Evidence from circular dichroism results on a synthetic peptide representing the region 90 to 123 of rabbit skeletal troponin C has indicated a correlation between the distance separating the aromatic and positively charged domains of phenothiazines and their ability to increase the α-helical content of this analog upon drug binding. Promethazine and chlorpromazine for example, possess short positively charged aliphatic chains and only weakly induce the formation of α-helix while trifluoperazine and fluphenazine have both a long piperazine moiety and yield a large increase in ellipticity at 222 nm upon binding to the peptide (chapter V, section C). Also, the addition of TFP to CB9 in the presence or absence of calcium promotes the broadening of the β-CH_2 and γ-CH_2 resonances of glutamic acid side chains (2.1 and 2.3 ppm regions; Figures V.7a and V.7b), a result that suggests a reduction in mobility of some of these side chains of CB9. In the case of trifluoperazine , the positive charge of the drug is situated 6 to 10 Å away from its aromatic region depending on which of the piperazine nitrogens is carrying the positive charge. The presence of this flexible "piperazine arm" of TFP may thus be crucial in the blocking of negatively charged side chains of troponin C and calmodulin thought to be involved in an interaction with TnI (Grabarek *et al.*, 1981) (residues such as Glu-92, -93, -94 and -97). It may well explain the differential ability of trifluoperazine to inactivate the CaM-regulated phosphodiesterase activity over the less potent phenothiazine chlorpromazine (Levin and Weiss, 1979).

A stereoprojection of the proposed TFP binding site is presented in Fig. V.9. This projection was constructed using the peptide backbone coordinates of carp parvalbumin segment 38 to 52 (Kretsinger and Nockolds, 1973). The representation points out the proximity of the two phenylalanine rings. Rotation along the phenylalanines Cα-Cβ bond can bring the aromatic side chains even closer. These rings may thus lie along the same plane and permit the stacking of the TFP rings or, the drug aromatic system may intercalate between the phenylalanine side chains. As for the piperazine positive charge, it remains close to most of the glutamic acid side chains if one considers the flexibility of both the negatively charged side chains and the "piperazine arm".

The interaction of trifluoperazine and other phenothiazines with calmodulin and TnC can be correlated with the

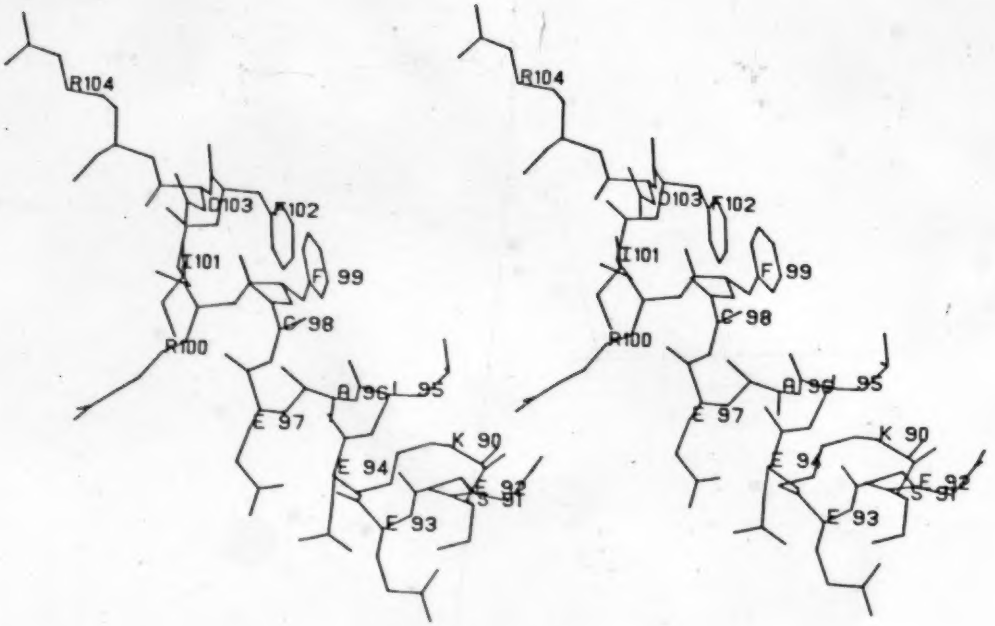
R104
D103
F102
I101
F 99
G 98
R100
A 96
L 95
E 97
K 90
E 94
E 92
S 91
E 93
R104
D103
F102
I101
F 99
G 98
R100
A 96
L 95
E 97
K 90
E 94
E 92
S 91
E 93

Fig. V.9 Stereoprojection of rabbit skeletal troponin C, region 90-104. This representation was constructed using the crystal coordinates of carp parvalbumin for the N-terminal region of the CD hand (residues 38 to 52) [Kretsinger and Nockolds, 1973]. The original set of coordinates for the peptide backbone was retained but the rabbit skeletal troponin C side chains of residues 90 to 104 were substituted to the parvalbumin ones. The orientation of the side chains along their respective Cα-Cβ bond was maintained. This drawing can more easily be viewed in stereo with a stereoscope obtained from Hubbard Scientific Co., Northbrook, IL.

fact that these drugs offer structural features present in peptides and proteins shown to interact with CaM and TnC. The primary sequence alignment of several opioid peptides and of CaM-binding proteins, has indicated the presence of 8-residue long sequences containing both a hydrophobic and a positively charged domain (Malencik and Anderson, 1982; Sellinger-Barnette and Weiss, 1982).

e. Possible location of other TFP binding sites on troponin C and calmodulin

Levin and Weiss (1977) mentioned the fact that two TFP high-affinity sites exist on CaM in the presence of Ca^{2+}. Phosphorylase kinase activation assays on calmodulin fragments (Kuznicki *et al.*, 1981) pinpointed that TFP-binding sites exist on a fragment containing the calcium binding sites I & II and on another fragment containing sites III & IV, the first fragment however having a stronger affinity for TFP. A search through the primary sequence of CaM and TnC was performed in order to find possible helical sites having two phenylalanines separated by 1 turn of helix. Figure V.10 shows 4 possible regions. The N-terminal regions of site I and III of both proteins are homologous for this short helical sequence while the beginning of the C-terminal of site II and IV are also quite similar and offer 2 other possibilities. Some evidence suggests that the

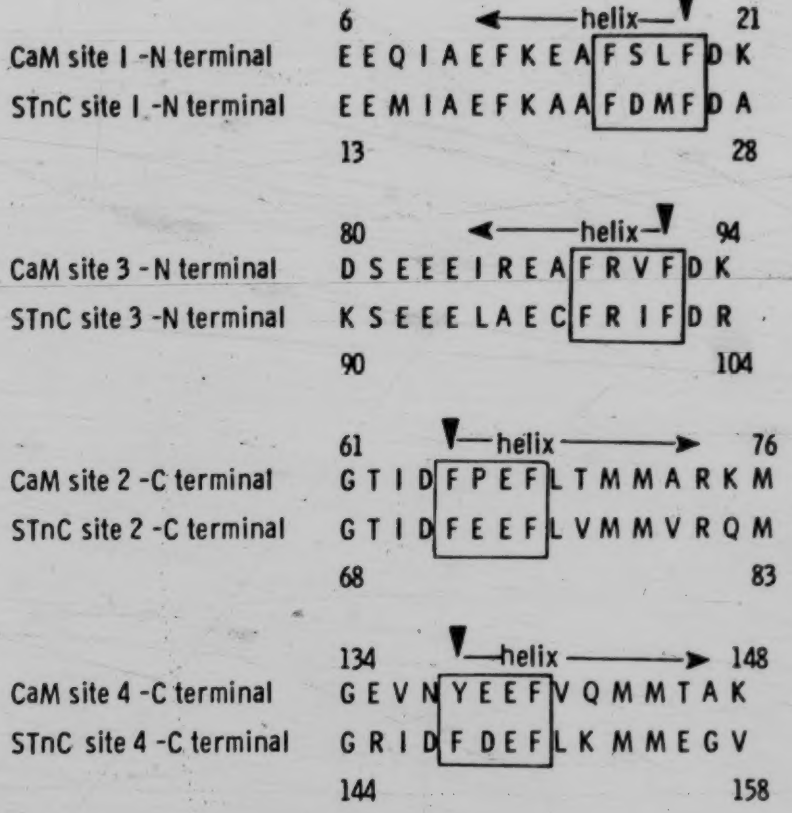
6
helix
21
CaM site I -N terminal
E E Q I A E F K E A F S L F D K
STnC site I -N terminal
E E M I A E F K A A F D M F D A
13
28
80
helix
94
CaM site 3 -N terminal
D S E E E I R E A F R V F D K
STnC site 3 -N terminal
K S E E E L A E C F R I F D R
90
104
61
helix
76
CaM site 2 -C terminal
G T I D F P E F L T M M A R K M
STnC site 2 -C terminal
G T I D F E E F L V M M V R Q M
68
83
134
helix
148
CaM site 4 -C terminal
G E V N Y E E F V Q M M T A K
STnC site 4 -C terminal
G R I D F D E F L K M M E G V
144
158

Fig. V.10 Homologous sequence regions of rabbit skeletal troponin C and bovine brain calmodulin containing short helical regions involving two aromatic side chains separated by one turn of helix. Framed sequences represent possible sites of hydrophobic interaction with the aromatic moiety of trifluoperazine. Arrows indicate the beginning and direction of helical regions.

N-terminal region of site I might be the other TFP high-affinity site. Rabbit skeletal troponin C has ten methionines, but upon addition of 4 moles of calcium, methionine 25 is preferentially labelled by the hydrophobic fluorescent tag, dansylaziridine (Johnson *et al.*, 1978). This methionine is part of the hydrophobic segment of site I (Fig. V.10). This result suggests that this segment is selectively exposed in the presence of calcium. The C-terminal of site IV is a less probable choice since, the CaM tyrosine 138 ring proton resonances are not affected by the drug presence (Klevit *et al.*, 1981; Krebs and Carafoli, 1982). It is thus doubtful that the drug reaches this part of the molecule (Fig. V.10). The oxidation of CaM methionines by chlorosuccinimide, in the presence of calcium suggested that methionines 71, 72, 76 and possibly 109 were exposed in the Ca^{2+}-saturated state (Walsh *et al.*, 1978). This modified calmodulin showed a reduced ability to activate a CaM-dependent phosphodiesterase. Klevit *et al.* (1981) and Krebs & Carafoli (1982) have also observed by ^1H NMR the shifting of methionines resonances of CaM in the presence of TFP to suggest that one of the drug binding sites was located near these methionines and thus our proposed site II region. However caution should be observed in making such an assignment since Walsh *et al.* (1978) mentioned that the modified CaM secondary structure had been altered significantly by the chemical treatment and the loss of regulatory activity may not be solely due to the oxidation of these particular amino acids. Krebs and Carafoli (1982) have also pointed out the possibility that the phenothiazine might bind to our proposed site III region.

C. INTERACTION OF NEUROLEPTIC DRUGS WITH A SYNTHETIC CALCIUM BINDING ANALOG OF RABBIT SKELETAL TROPONIN C

1. Controversy surrounding the interaction of antipsychotic drugs with calmodulin

Following the discovery of a calcium binding protein (calmodulin) which could be shown to activate both cAMP-dependent phosphodiesterase (Cheung, 1970; Kakiuchi and Yamazaki, 1970) and adenylate cyclase (Cheung *et al.*, 1975; Brostrom *et al.*, 1975,1977,1978; Lynch, 1976) in a calcium-dependent manner, Levin and Weiss (1976) demonstrated that antipsychotic drugs inhibited the activation of cAMP phosphodiesterase. Later, these same authors demonstrated that the phenothiazine antipsychotic trifluoperazine binds to calmodulin and troponin C in the presence of calcium (Levin and Weiss, 1977, 1978), and that several types of antipsychotic drugs such as the butyrophenones, diphenylbutylpiperidines, phenothiazines and thioxanthenes interact with calmodulin to a greater extent than did other psychoactive drugs like the benzodiazepines, the tricyclic antidepressants, barbiturates, and adrenergic agonists and antagonists (Levin and Weiss, 1979). Since neuroleptically inactive phenothiazine derivatives such as promethazine and inactive phenothiazine metabolites such as the phenothiazine sulfoxides did not bind to calmodulin in a significant amount, Levin and Weiss concluded that the binding of antipsychotics to calmodulin may be the mechanism by which these drugs exert their pharmacological activity. However, three pieces of evidence suggest that the calmodulin binding hypothesis of antipsychotic drug action is questionable. Firstly, haloperidol, a butyrophenone, is a very active antipsychotic drug but only demonstrates a weak binding to calmodulin (Levin and Weiss, 1979). Secondly, the (+) stereoisomer of butaclamol is the only effective tranquilizer when compared to the (-) isomer (Seeman, 1977) whereas the (+) isomer was only 5-fold more active in binding to calmodulin (Levin and Weiss, 1979). Thirdly, the geometric isomers of the thioxanthenes have similar binding to calmodulin (Norman *et al.*, 1979) but differ vastly in their antipsychotic activity (Moller-Nielsen *et al.*, 1973).

The nature of the drug interaction with calmodulin at the molecular level remains a major question. Some authors (Norman *et al.*, 1979; Raess and Vincenzi, 1980; Vincenzi and Ashelman, 1980; Roufogalis, 1980) feel that the antipsychotic interaction with calmodulin is more in parallel with the hydrophobicity of the drugs and that the binding is a nonspecific hydrophobic interaction (Norman *et al.*, 1979; LaPorte *et al.*, 1980; Landry *et al.*, 1981; Roufogalis, 1981). However other groups have demonstrated that the hydrophobicity of drugs is not the only factor involved in making them potent calmodulin inhibitors (Weiss *et al.*, 1982; Prozialeck and Weiss, 1982).

We wanted to analyse using our model phenothiazine binding site if different classes of neuroleptic drugs interacted similarly with the site. We have synthesized analogs of site III of rabbit skeletal troponin C and particularly a 34-residue peptide (AcA''STnC(90-123)amide; chapters II and III) containing both the proposed trifluoperazine binding site and a high-affinity calcium binding region (Reid *et al.*, 1980,1981). The calcium binding ability of this 34-residue fragment equalled that of CB9 and has proven to be a simpler model to examine the effect of a variety of neuroleptic drugs on the CD-detectable conformation and the Ca^{2+}-binding properties of this calcium binding unit.

2. Circular dichroism results

A 34-amino acid residue peptide analog of calcium binding site III of troponin C and, by sequence homology, site III of calmodulin (Fig. V.11) has been tested for its interaction with representatives of four different classes of neuroleptic drugs. The butyrophenones, represented by benperidol and haloperidol could not induce any CD-detectable structural change in the peptide up to a concentration ratio of 2.3/1, drug/peptide (Fig. V.12). Earlier investigations (Levin and Weiss, 1979; Prozialeck and Weiss, 1982) has indicated that haloperidol did not bind to calmodulin as strongly as the phenothiazines. Thus the hydrophobic character of these drugs does not represent the sole criteria for a drug:peptide interaction in our case.

Both of the thioxanthenes, *cis-* and *trans*-thiothixene, induced a small amount of structure in the peptide and this class was the only class tested that prevented the peptide from responding normally to the addition of calcium, i.e. with an increase in CD-detectable structural change (Fig. V.12). The possibility exists that the inflexibility of the side chains linked to the tricyclic ring structure by a double bond may have some effect on the ability of the drug-peptide complex to bind calcium.

A third class tested, the dihydroinolones, a nonclassical group of neuroleptics represented by molindone (Kebabian and Calne, 1979), also failed to induce structural change in the peptide and did not affect the subsequent

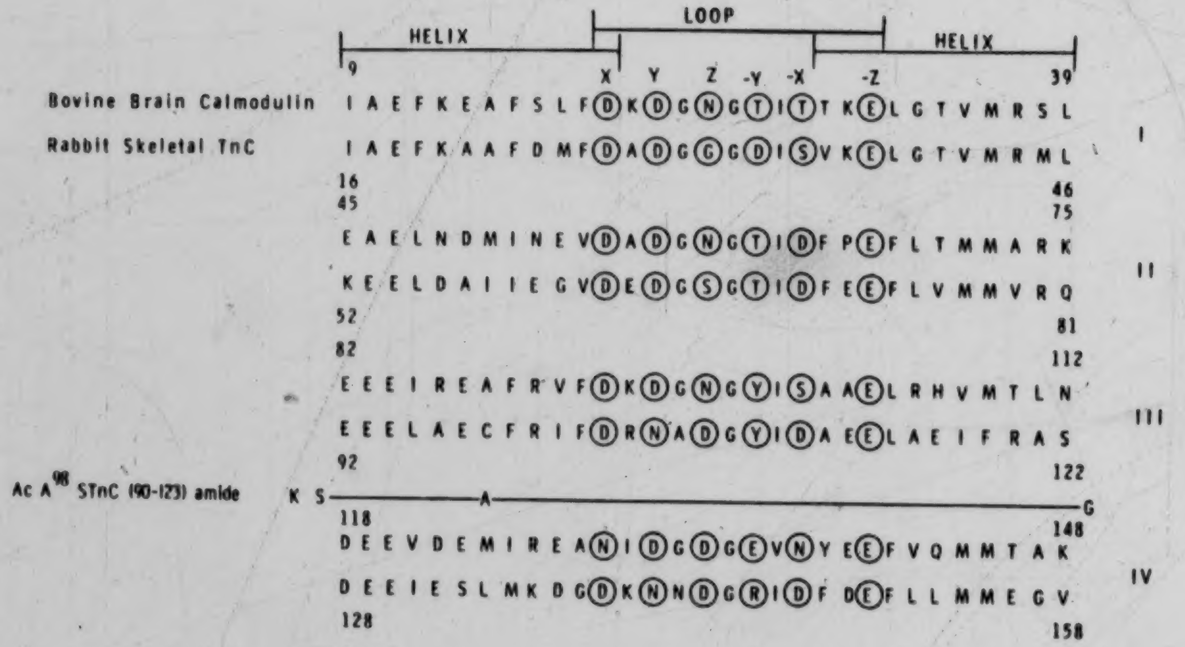
HELIX
LOOP
HELIX
9
X Y Z -Y -X -Z
39
Bovine Brain Calmodulin
I A E F K E A F S L F D K D G N G T I T T K E L G T V M R S L
Rabbit Skeletal TnC
I A E F K A A F D M F D A D G G G D I S V K E L G T V M R M L
I
16
46
45
75
E A E L N D M I N E V D A D G N G T I D F P E F L T M M A R K
K E E L D A I I E G V D E D G S G T I D F E E F L V M M V R Q
II
52
81
82
112
E E E I R E A F R V F D K D G N G Y I S A A E L R H V M T L N
E E E L A E C F R I F D R N A D G Y I D A E E L A E I F R A S
III
92
122
Ac A98 STnC (90-123) amide
K S
A
G
118
148
D E E V D E M I R E A N I D G D G E V N Y E E F V Q M M T A K
D E E I E S L M K D G D K N N D G R I D F D E F L L M M E G V
IV
128
158

Fig. V.11 Amino acid sequence of bovine brain calmodulin, rabbit skeletal troponin C and the 34-residue peptide. The calcium binding sites are numbered I-IV. Bovine brain calmodulin is the upper sequence while rabbit skeletal troponin C is the lower sequence. The 34-residue peptide, AcA^{98}STnC(90-123) amide, is indicated directly below rabbit skeletal troponin C site III and has an identical sequence to this site with the exceptions indicated. The sequences comprising the *helix-loop-helix* regions are indicated by bars at the top of the figure. The six octahedral calcium coordinating positions are designated X,Y,Z,-Y,-X, and -Z. The amino acid residues in the corresponding calcium coordinating positions are circled.

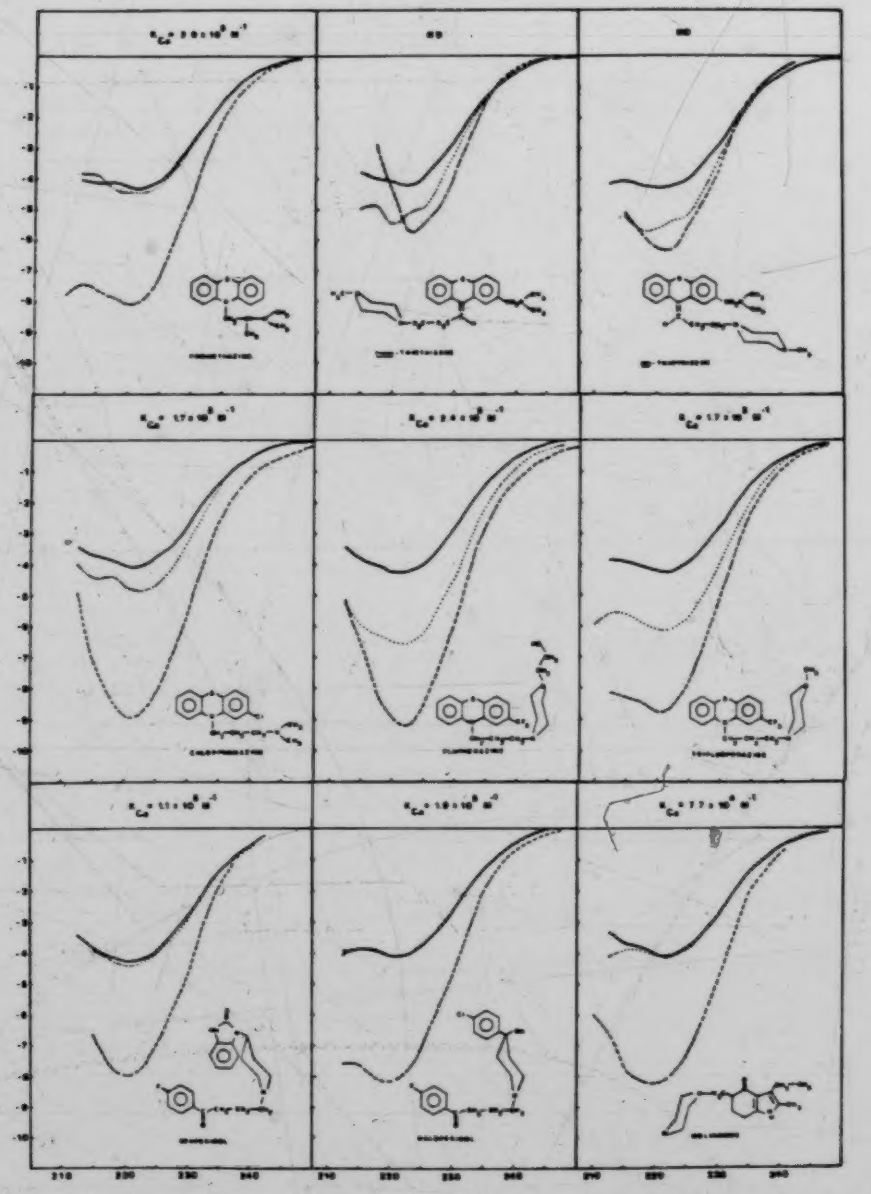

Fig. V.12 Effect of various classes of drugs on the circular dichroism spectrum of a synthetic peptide. Drug- and calcium-induced CD spectra of the 34-residue peptide; native peptide (—), peptide + drug (···), peptide + drug + calcium (---). The peptide concentration was 0.43 mM. The chemical structures of the drugs are indicated beneath the corresponding spectrum. The K_{Ca} values of the peptide (in 1 mM drug) are indicated at the top of the corresponding spectrum. The K_{Ca} value of the peptide in the absence of drug is equal to 2.6×10^5 M^{-1} [chapter III]. The CD spectrum for peptide + calcium is identical to the one observed for peptide + calcium + TFP. ND, not determined.

structural change induced by addition of calcium (Fig. V.12). Finally, the phenothiazines represented by promethazine, chlorpromazine, trifluoperazine and fluphenazine induced structural change in the peptide in a manner correponding to their *in vitro* ability to inhibit phosphodiesterase activation by calmodulin (Levin and Weiss, 1979; Prozialeck and Weiss, 1982) but had no effect on the Ca^{2+}-induced structural change (Fig. V.12). Note that the calcium binding constant of this model peptide is equal to $2.6 \times 10^{5} M^{-1}$ in the absence of drug (Reid *et al.*, 1981; chapter III). Except for the case of the thioxanthene isomers, the binding or presence of these drugs did not alter the calcium binding property of the synthetic analog. This observation is in agreement with proton magnetic resonance and circular dichroism results obtained for the binding of trifluoperazine to a cyanogen bromide fragment representing site III of rabbit skeletal troponin C (chapter V, section B).

In light of the interaction of calmodulin with a variety of peptides, proteins (Grand and Perry, 1980; Itano *et al.*, 1980; Malencik and Anderson, 1982; Sellinger-Barnette and Weiss, 1982) and structurally related antipsychotics (Levin and Weiss, 1979; Prozialeck and Weiss, 1982), it was concluded that all these structures share in common a hydrophobic and a positively charged domain (Weiss *et al*., 1982; Prozialeck and Weiss, 1982). The analysis of the trifluoperazine binding site of site III of rabbit skeletal troponin C reveals that complementary hydrophobic and negatively charged centers exist and are optimally positioned when calcium induces the formation of an α-helical arrangement in the N-terminal region of the peptide.

Differences in ellipticity induced by phenothiazines on the model peptide can be rationalized in terms of the distance separating the positively charged domain and the aromatic moiety of the drug, as postulated recently (Prozialeck and Weiss, 1982; chapter V, Fig. V.9). For instance, the positive charge on trifluoperazine can be associated with either of the nitrogens of the piperazine ring thus placing the charge at a distance of 4 to 7 bondlengths from the aromatic center. The same holds true for fluphenazine, but in the case of chlorpromazine and promethazine, 4 and 3 bondlengths respectively separate the two centers.

In conclusion, this section has pointed out the selectivity of a 34-residue synthetic peptide representing site III of rabbit skeletal troponin C for a particular class of neuroleptics and indicated its potential use as a phenothiazine selective binding region.

D. SUMMARY

Trifluoperazine (TFP) was shown to interact with the cyanogen bromide fragment CB9 (residues 84-135) of rabbit skeletal troponin C and with a synthetic peptide representing the N-terminal region of CB9. The phenothiazine did not affect the calcium binding property of CB9 as observed by proton magnetic resonance and circular dichroism spectroscopy. The calculated calcium binding constants for CB9 in the presence and absence of trifluoperazine, were identical ($K_{ca} = 1.3 \times 10^{5} M^{-1}$). Localization of the trifluoperazine binding site was achieved by analysing the ^1H NMR spectrum of CB9 and of a synthetic fragment corresponding to residues 90-104 of CB9. Drug-induced shifting and broadening of the ring protons of phenylalanine residues and the methyl resonances of alanine, leucine and isoleucine residues, suggest that the segment 95 to 102 is in close proximity to the phenothiazine aromatic region. The neighboring negative side chains in the peptide sequence also suggest that the single positive charge present on the piperazine nitrogens of trifluoperazine may interact with them and sterically block a region of interaction of calmodulin (CaM) and troponin C (TnC) with modulated proteins such as phosphodiesterase. Primary sequence analysis of CaM and troponin C reveals that a homologous hydrophobic region to site III is also found in the N-terminal region of site I of both calcium binding proteins. Binding of TFP to CB9 occurs in both the presence and absence of calcium since the hydrophobic region in these small fragments is completely accessible to TFP whether calcium is present or not. The dissociation constant of the drug to apo-CB9 (8 μM) was obtained by ellipticity measurements at 222 nm and was comparable to the 5 μM value obtained by Levin and Weiss (1978) for calcium-saturated rabbit skeletal troponin C.

A synthetic peptide representing site III of rabbit skeletal troponin C (90-123) and by homology, site III of calmodulin (80-113), was tested for its ability to interact with representatives of four different classes of neuroleptic drugs. The effects of nine drugs examined on the CD spectra of the model peptide, could generally be divided into three groups. The first group consisting of representatives of the butyrophenone neuroleptic, haloperidol and benperidol, as well as the dihydroinolone, molindone and the phenothiazine antihistamine, promethazine, had no effect on the CD spectrum or calcium sensitivity of the apopeptide. The second group, composed of the structurally rigid thioxanthenes represented by *cis*- and *trans*-thiothixene, induced CD-detectable structural change in the apopeptide but prevented Ca^{2+}-induced structural change. The third group, consisting of the phenothiazines, chlorpromazine, trifluoperazine and fluphenazine, induced structural change in the peptide in a manner corresponding to their *in vitro* ability to inhibit phosphodiesterase activation by calmodulin but had no effect on the Ca^{2+}-induced structural change. It thus appears that the trifluoperazine binding site located in the N-terminal region of site III of rabbit skeletal troponin C demonstrates some structural selectivity for a particular class of neuroleptic drugs. Finally, this peptide may prove useful as a phenothiazine selective binding region.

CHAPTER VI

COMMENTS ON THE STRUCTURE AND FUNCTION OF EF HANDS AND EXPERIMENTAL APPROACHES TO ACHIEVE A BETTER UNDERSTANDING OF THEIR DESIGN.

A. PRIMARY SEQUENCE ANALYSIS AND FOLDING BEHAVIOR OF EF HANDS IN RELATION TO THE MECHANISM OF ACTION OF TROPONIN C AND CALMODULIN.

The EF hand represents the major building block of key modulator proteins such as troponin C and calmodulin. When calcium binds to the EF hands of these proteins, it induces changes in the secondary and tertiary structure of TnC and CaM. These changes in turn, result in the formation and exposure of hydrophobic surfaces that are in close proximity or represent binding regions to target proteins such as troponin I and phosphodiesterase.

The functional role of an EF hand is dependent on its primary sequence which encodes for elements of secondary structure. For example, the secondary structure analysis of various EF hand containing proteins has indicated that helical regions are present on both sides of the calcium binding loop, that the C-terminal α-helical region is initiated in the loop region and that a β-turn region separates both helical segments (Argos, 1977). The β-turn probability is particularly high for the first four residues (+X,+Y region) of the loop (Vogt *et al.*, 1979). These results agree with the folding pattern of EF hands as observed in the crystal structures of carp parvalbumin (Kretsinger and Nockolds, 1973; Fig. I.14) and bovine ICBP (Szebenyi *et al.*, 1981; Fig. I.15). One should thus examine the possible features of EF hands that could describe the mechanism of action of these calcium binding proteins.

1. Generation of an average EF hand sequence

The primary sequence of 30 different EF sites, exemplifying the six families of EF hand containing proteins, were aligned in order to trace common features to all EF sites (Fig. VI.1). Note that all sequences listed represent EF hand sites *that bind calcium* including 4 sequences containing double amino acid insertion sites (Isobe and Okuyama, 1978, 1981; Hofmann *et al.*, 1979; Fullmer and Wasserman, 1981; Shelling *et al.*, 1983; Mani *et al.*, 1983). A general sequence pattern emerges from our analysis when one tabulates the type and frequency of amino acid at each position of the EF hand (Table VI-1). Note that the amino acids were grouped by order of polarity (Grantham, 1974; Go and Miyazawa, 1980). We did not include in our tabulation, the inserted residues present in the S-100 and

++N-Helix++++	++++Loop+++++	++C-Helix+++		
	X Y Z-Y -X -Z			
IAEFKAAFDMF*	DADGGGD*ISVKE	LGTVMRML	I	RSTnC
KEELDAIIEEV*	DEDGSGT*IDFEE	FLVMMVRQ	II	RSTnC
EEELAECFRIF*	DRNADGY*IDAEE	LAEIFRAS	III	RSTnC
DEEIESLMKDG*	DKNNDGR*IDFDE	FLKMMEGV	IV	RSTnC
PEELQEMIDEV*	DEDGSGT*VDFDE	FLVMMVRC	II	BCTnC
EEELSDLFRMF*	DKNADGY*IDLEE	LKIMLQAT	III	BCTnC
EDDIEELMKDG*	DKNNDGR*IDYDE	FLEFMKGV	IV	BCTnC
IAEFKEAFSLF*	DKDGDGT*ITTKE	LGTVMRSL	I	BBCalm
EAELQDMINEV*	DADGNGT*IDFPE	FLTMMARK	II	BBCalm
EEEIREAFRVF*	DKDGNGY*ISAAE	LRHVMTNL	III	BBCalm
DEEVDEMIREA*	NIDGDGQ*VNYEE	FVQMMTAK	IV	BBCalm
IAEFKEAFSLF*	DKDGDGT*ITTKE	LGTVMRSL	I	TCalm
EAELQDMINEV*	DADGDGT*IDFPE	FLSLMARK	II	TCalm
EEELIEAFKVF*	DRDGDGL*ITAAE	LRHVMTNL	III	TCalm
DEEVDEMIREA*	DIDGDGH*INYEE	FVRMMAK	IV	TCalm
ADAVDKVMKEL*	DEDGDGE*VDFQE	YVVLVAAL	II	S-100a
QEVVDKVMETL*	DSDGDGE*CDFQE	FMAFVAMI	II	S-100b
ADDVKKAFAII*	DQDKSGF*IEEDE	LKLFLQNF	II	Cparv
DGETKTFLKAG*	DSDGDGK*IGVDE	FTALVKA	III	Cparv
TEDVKKVFHIL*	DKDKSGF*IEEEE	LGFILKGF	II	Rparv
VKETKTLMAAG*	DKDGDGK*IGADE	FSTLVSES	III	Rparv
PRTLDDLFQEL*	DKNGDGE*VSFEE	FQVLVKKI	II	PICBP
PSTLDELFEEL*	DKNGDGE*VSFEE	FQVLVKKI	II	BICBP
IQEFKEAFTVI*	DQNRNGI*IDKED	LRDTFAAM	I	DTNB
IQEFKEAFNMI*	DQNRDGF*IDKED	LHDMLASM	I	CGRLC
IQEMKEAFSMI*	DVDRDGF*VSKDD	IKAISEQL	I	SRLC

Double insertion sites

METLINVFHAHS	GKEGDKYKLSKKE	LKELLQTE	I	S-100a
VVALIDVFHQYS	GREGDKHKLKKSE	LKELINNE	I	S-100b
PAELKSIFEKYA	AKEGDPNQLSKEE	LKQLIQAE	I	PICBP
PEELKGIFEKYA	AKEGDPNQLSKEE	LKLLLQTE	I	BICBP

Fig. VI.1 Primary sequence of thirty EF hands that bind calcium. Abbreviations: RSTnC, rabbit skeletal troponin C [Collins *et al.* , 1977]; BCTnC, bovine cardiac troponin C [van Eerd and Takahashi, 1975]; BBCalm, bovine brain calmodulin [Watterson *et al.* , 1980]; TCalm, tetrahymena calmodulin [Yazawa *et al.* , 1981]; S-100a and S-100b, α and β subunits of bovine brain S-100 proteins [Isobe and Okuyama, 1978, 1981]; Cparv, carp parvalbumin [Coffee and Bradshaw, 1973]; Rparv, rabbit parvalbumin [Enfield *et al.*, 1975]; PICBP, porcine intestinal calcium binding protein [Hofmann *et al.* , 1979]; BICBP, bovine intestinal calcium binding protein [Fullmer and Wasserman, 1981]; DTNB, rabbit skeletal DTNB light chain [Collins, 1976]; CGRLC, chicken gizzard regulatory light chain [Jakes *et al.* , 1976]; SRLC, scallop regulatory light chain [Jakes *et al.* , 1976]; *, insertion site. The italicized portion of the sequence denotes the calcium binding loop region where X,Y,Z,-Y,-X, and -Z represent the calcium coordinating positions of the loop. The roman numerals indicate which of the native protein EF hand sites are listed.

TABLE VI-1

Tabulation of amino acid frequencies at each position of the EF hand

N-terminal region

Residue position

	1	2	3	4	5	6	7	8	9	10	11
Met	1	0	0	1	0	0	5	5	0	4	0
Cys	0	0	0	0	0	0	1	0	0	0	0
Ile	6	0	0	3	3	0	3	6	0	3	4
Leu	0	0	0	13	0	0	6	1	0	2	5
Val	2	1	1	6	0	0	5	0	0	3	4
Phe	0	0	0	5	0	0	1	18	0	0	7
Tyr	0	0	0	0	0	0	0	0	0	0	3
Trp	0	0	0	0	0	0	0	0	0	0	0
Ala	2	6	2	0	1	2	9	0	2	3	2
Gly	0	1	0	0	0	1	0	0	0	0	4
Pro	5	0	0	0	0	0	0	0	0	0	0
Ser	0	1	0	0	1	2	0	0	3	0	0
Thr	1	0	3	2	0	3	0	0	1	1	0
Asn	0	0	0	0	0	1	0	0	3	0	0
Gln	1	3	0	0	3	0	0	0	1	1	0
Asp	4	3	3	0	7	5	0	0	2	2	0
Glu	7	13	21	0	2	13	0	0	5	9	0
His	0	0	0	0	0	0	0	0	3	0	1
Arg	0	1	0	0	1	0	0	0	5	0	0
Lys	1	1	0	0	12	4	0	0	5	2	0

Calcium binding region

Residue position

	+X	2	+Y	4	+Z	6	-Y	8	-X	10	11	-Z
Met	0	0	0	0	0	0	0	0	0	0	0	0
Cys	0	0	0	0	0	0	0	1	0	0	0	0
Ile	0	2	0	0	0	0	1	19	0	0	0	0
Leu	0	0	0	0	0	0	1	4	0	1	0	0
Val	0	1	0	0	0	0	0	6	0	2	0	0
Phe	0	0	0	0	0	0	4	0	0	9	0	0
Tyr	0	0	0	0	0	0	4	0	0	3	0	0
Trp	0	0	0	0	0	0	0	0	0	0	0	0
Ala	2	3	0	2	0	0	0	0	0	4	3	0
Gly	2	0	0	21	1	26	0	0	2	0	1	0
Pro	0	0	0	0	0	2	0	0	0	0	2	0
Ser	0	2	0	0	4	0	0	0	8	0	1	0
Thr	0	0	0	0	0	0	6	0	3	2	0	0
Asn	1	0	8	2	4	0	2	0	2	0	0	0
Gln	0	3	0	0	0	0	1	0	0	0	2	0
Asp	25	0	18	0	21	0	1	0	12	0	7	3
Glu	0	3	4	0	0	0	4	0	2	2	11	27
His	0	0	0	0	0	0	2	0	0	0	0	0
Arg	0	3	0	3	0	0	2	0	0	0	0	0
Lys	0	13	0	2	0	2	2	0	1	7	4	0

C-terminal region

Residue position

	1	2	-Z	4	5	6	7	8	9	10	11
Met	0	0	0	0	1	0	8	13	0	2	2
Cys	0	0	0	0	0	0	0	0	0	0	1
Ile	0	0	0	1	0	1	3	2	0	0	3
Leu	1	0	0	15	6	2	10	6	0	0	7
Val	2	0	0	0	3	5	5	6	2	0	2
Phe	9	0	0	13	0	1	3	2	0	0	2
Tyr	3	0	0	1	0	0	0	0	0	0	0
Trp	0	0	0	0	0	0	0	0	0	0	0
Ala	4	2	0	0	1	3	0	0	7	7	0
Gly	0	1	0	0	4	0	0	0	0	3	0
Pro	0	2	0	0	0	0	0	0	0	0	0
Ser	0	1	0	0	1	1	0	1	1	3	2
Thr	2	0	0	0	1	5	1	0	3	2	1
Asn	0	0	0	0	0	0	0	0	1	4	0
Gln	0	2	0	0	2	2	0	0	5	1	1
Asp	0	7	3	0	0	2	0	0	0	0	0
Glu	2	11	27	0	0	4	0	0	2	1	4
His	0	0	0	0	1	2	0	0	0	0	0
Arg	0	0	0	0	3	1	0	0	4	4	0
Lys	7	4	0	0	7	1	0	0	5	3	3

ICBP sequences. The *average* amino acid sequence deduced from this sequence analysis is listed in Fig. VI.2a.

2. Composition of the calcium binding loop

The primary sequence of a calcium binding loop (twelve residues) reflects more than just a series of ligands and side chains designed to maximize the binding of calcium ions. The segment *Asp,P,Asx,Gly,Asx,Gly* where P is a positive side chain, represents the most conserved sequence of the EF hand site and is predicted to be a strong β-turn forming region (Chou and Fasman, 1978; Cid *et al.*, 1983). The side chains of aspartic acid and/or asparagine residues represent calcium coordinating ligands at positions +X, +Y, and +Z (Fig. VI.2a). In view of the fact that glutamic acid residues rarely occur in β-turn structures (Chou and Fasman, 1974b, 1978) and are only present in this region of the EF hand in the case of distorted EF sites (site I of S-100a,b and ICBP's), one can conclude that other structural requirements besides the type of calcium ligand must be met in order to generate a functional EF hand. This β-turn region is shown in Fig. VI.2b as part of a model EF hand.

The *average* sequence pattern in this part of the EF hand also points out the presence of conserved glycine residues which probably play an important role in the

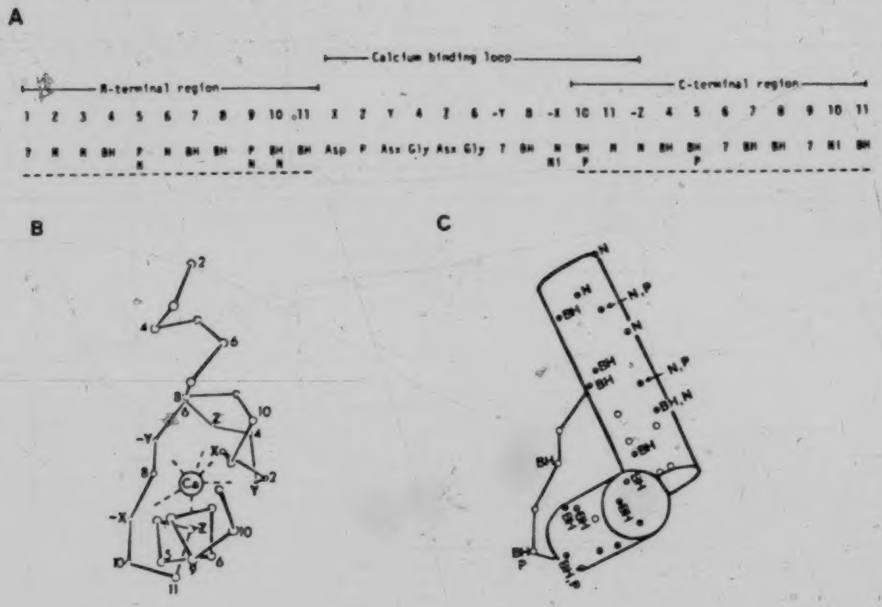
A
Calcium binding loop
N-terminal region
C-terminal region
1 2 3 4 5 6 7 8 9 10 11 X 2 Y 4 Z 6 -Y 8 -X 10 11 -Z 4 5 6 7 8 9 10 11
? N N BH P N BH BH P BH BH Asp P Asx Gly Asx Gly ? BH N BH N N BH BH ? BH BH ? NI BH
N N N NI P P
B
2
4
6
8
10
Z
-Y
X
Y
Ca
-X
-Z
11
C
N
N,P
BH
BH,N
P

Fig. VI.2 Primary sequence and folding pattern of EF hands. (A) Average sequence of an EF hand. The dotted lines denote regions of pseudo sequence homology. The coordinating residues in the sequence occupy positions X,Y,Z,-Y,-X, and -Z. (B) Representation of a model EF hand along its α-carbon backbone [Adapted from Kretsinger, 1977]. (C) Location of hydrophobic and charged domains in the helical regions of EF hands. Abbreviations: BH, bulky hydrophobic residue; N, negatively charged residue; P, positively charged residue; Ni, non ionic residue; ?, weakly conserved residue; Asp, aspartic acid; Asx, aspartic acid or asparagine; Gly, glycine; ○ represents a calcium binding loop residue while ● is a residue located in the helical regions.

construction of the β-turn segment (position 4) and represent an essential residue (position 6) that allows the peptide backbone to undergo a large change in direction in this part of the EF loop (Kretsinger, 1980) and permits the proper folding of ligands around the metal (chapter IV). Noticeable exceptions again include the distorted site I of S-100a,b and ICBP's, and the defunct sites II and III of rabbit skeletal muscle alkali light chains (Frank and Weeds, 1974; Barker *et al.*, 1978).

Position 8 and to a lesser extent, position 10 of the EF loop region are conserved hydrophobic sites that offer a natural extension to the hydrophobic region of the C-terminal α-helical region (Fig. VI.2c). Their presence in association with the C- and N-terminal hydrophobic surfaces may aid toward the dehydration of the calcium ion inner-sphere complex and suggest a global involvement of the EF site in a metal dehydration process. This explanation appears more plausible than the dehydration mechanism proposed by Reid and Hodges (1980) which only involves the residues at positions 7 (least conserved site of the loop) and 10 of the EF loop.

The omnipresence of a glutamic acid at position -Z (Table VI-1) may well be linked to its frequent occurrence in α-helices (Pα, 1.53; strong α-former; Chou and Fasman,

1978) as compared to aspartic acid (Pα, 0.98; α-helix indifferent). In addition, the side chain length at this position (-Z) may represent a critical factor in the ability of calcium to induce part of the C-terminal helix.

3. Composition of the C- and N-terminal regions

Another striking feature from this analysis is the internal sequence homology between the N- and C-terminal α-helical regions (Fig. VI.2a; dotted line regions). Kretsinger (1977, 1979) pointed out the presence of regularly spaced hydrophobes in the helical regions of EF hands. The internal sequence homology is best emphasized in the case of site III of rabbit skeletal troponin C where the homologous segments EELAECFR and EELAEIFR are present on opposite sides of the calcium binding loop (Fig. VI.1). From the *average* sequence, we notice that these pseudo-homologous regions are composed of an ordered array of charged and hydrophobic residues. Considering the α-helical nature of these two regions, one realizes that the spacing of the hydrophobes will place these side chains on the same side of the helix, creating hydrophobic surfaces on both sides of the calcium binding loop. A similar observation can be made for charged residues in the N-terminal region of the EF hand. Figure 2C depicts the position of hydrophobic and charged surfaces on a model EF hand domain. Kanehisa and

Tsong (1980) pointed out the frequent occurrence of this feature in globular proteins. They conducted a study on the secondary structure of 47 globular proteins which indicated that helices are generally found nearer to the surface of proteins and tend to have hydrophobic and hydrophilic surfaces on opposite sides of their helices as a result of an alternating sequence of hydrophobic and charged residues.

Our group has demonstrated using synthetic peptide analogs of site III of rabbit skeletal troponin C that the formation of a calcium:peptide complex is concomitant with the induction of helices in parts of these regions and that the presence of α-helices prior to calcium binding (presence of trifluoroethanol) enhances the affinity of the site for calcium (chapter III). The removal of these helical regions however leads to a large decrease in the ability of the resulting EF hand site to interact with calcium.

In summary, the primary sequence of a protein represents a *degenerate* code, in relation to its ability to code for elements of secondary structure. This statement implies that a moderately substituted sequence as in the case of EF hands, can still retain its basic structural properties and folding pattern. In addition, although all EF hands possess potential hydrophobic and charged domains, their formation and exposure remains a function of calcium concentration and of the tertiary structure of the protein.

4. Importance of the EF hand structure in the function of calcium binding proteins

It has recently become clear, that the mechanism of action of calmodulin correlates with the calcium-induced exposure of hydrophobic patches on its surface (LaPorte *et al.*, 1980; Tanaka and Hidaka, 1980, 1981; Johnson, 1983). The presence in solution of various aromatic ligands such as antipsychotic drugs (Levin and Weiss, 1977, 1978, 1979; Procialeck and Weiss, 1982) and W compounds (Hidaka *et al.*, 1978) effectively inhibits the interaction of this modulator protein with target enzymes. The localization of a phenothiazine binding site in the N-terminal region of site III of rabbit skeletal troponin C (chapter V) and probably bovine brain calmodulin (Head *et al.*, 1982) indicates that target proteins may recognize a helical arrangement of hydrophobic and negatively charged side chains (chapter V). It was demonstrated using a W-7-coupled Sepharose column or a phenothiazine-Sepharose conjugate, that hydrophobic regions on rabbit skeletal troponin C and bovine brain S-100 proteins are also exposed in the presence of calcium (Endo *et al.*, 1981; Marshak *et al.*, 1981). It should be noted that carp parvalbumin and chicken ICBP failed to interact with the phenothiazine-bound matrix, in the presence of calcium

(Marshak *et al.*, 1981).

Finally, spectroscopic studies on rabbit skeletal troponin C and its fragments (Leavis *et al.*, 1978; Nagy *et al.*, 1978; Nagy and Gergely, 1979; Levine *et al.*, 1977; Evans *et al.*, 1978; Johnson *et al.*, 1978; Carew *et al.*, 1980) have indicated that the binding of calcium to the calcium specific sites of troponin C (regulatory sites) results in changes in the tertiary structure of the protein and the exposure of hydrophobic site(s) but, has little effect on the secondary structure of the protein. These regulatory sites probably possess some partly formed helices (Leavis *et al.*, 1978; Nagy and Gergely, 1979; Reid *et al.*, 1981) having their hydrophobic surfaces buried and it is the binding of calcium to these Ca^{2+}-binding sites that locally exposes the hydrophobic and charged domains. Similar conclusions can be drawn for calmodulin (Klee, 1977; LaPorte *et al.*, 1980; Tanaka and Hidaka, 1980, 1981; Drabikowski *et al.*, 1982; Johnson, 1983). The extent of exposure of these hydrophobic sites varies, as exemplified by the reduced exposure of the hydrophobic domain(s) of *Tetrahymena* calmodulin in comparison to bovine brain calmodulin (Inagaki *et al.*, 1983). One should note that none of the 11 substitutions observed (Yazawa *et al.*, 1981) when comparing the sequence of these two calmodulins results in the loss of hydrophobic residues. However, these two calmodulins are equally able to activate enzymes such as adenylate cyclase, NAD and myosin light chain kinases, but differ in their ability to modulate phosphodiesterase and guanylate cyclase (Kudo *et al.*, 1982). A similar conclusion can be made when one compares the ability of troponin C to substitute for calmodulin in activating phosphodiesterase (Potter *et al.*, 1977). Thus, the action of calcium on these EF hand containing proteins is not limited to the induction of α-helical regions and the formation of hydrophobic and charged surfaces but lies also in its ability to properly expose these sites.

5. Conclusions on the mode of action of EF hand containing proteins

In conclusion, we propose that

a) The primary sequence of EF hands codes for elements of secondary structure such as C- and N-terminal helical regions flanking a β-turn segment. The calcium binding loop spans over the β-turn and the beginning of the C-terminal helix and is composed of an arrangement of properly positioned calcium binding ligands. The calcium binding affinity of an EF hand however remains largely a function of the tertiary structure it adopts as part of a protein.

b) EF hands possess homologous hydrophobic domains flanking both sides of their calcium binding loop. In the presence of calcium, parts of the C- and N-terminal regions of an isolated EF hand adopt an α-helical arrangement thus optimizing the geometry of their hydrophobic and charged domains.

c) In the case of EF hand containing proteins, these N- and C-terminal α-helical regions may be preformed in the absence of calcium. These regions are differentially exposed in the presence of calcium so that proteins such as parvalbumin and ICBP do not expose these sites upon calcium binding while troponin C and S-100 protein only partly expose these domains in comparison to calmodulin.

e) The degree of exposure of these hydrophobic and charged domains may explain the selective affinity of *Tetrahymena* calmodulin for guanylate cyclase, bovine brain calmodulin for brain phosphodiesterase, and troponin C for troponin I.

6. Origins of the ancestral EF hand gene ?

The examination of double insertion sequences (Fig. VI.1) reveals that these insertions are positioned at the beginning and at the end of the β-turn region. This suggests that a DNA segment coding for this region would have been 20 to 30 nucleotides. In addition, the sequence homology between the C- and N-terminal regions indicates that both regions could have been coded for by the same DNA fragment (~ 30 nucleotides). Based on these two premises, one can speculate that the ancestral EF hand gene probably arose from the duplication of a ~30-nucleotide fragment coding for an α-helical domain (Fig. VI.3a). The insertion of a ~30-base segment coding for the β-turn region of the EF hand, may then have followed this initial duplication step. Alternatively, the initial fragment may have coded for a ~60-base long *loop-helix* domain (Fig. VI.3b). Following an initial duplication step, the resulting nucleotide sequence evolved through a partial sequence deletion to the ancestral EF hand gene sequence. Although one intuitively imagines the ancestral EF hand gene has coding for an *helix-loop-helix* domain, the ~120-base long intermediate (Fig. VI.3b) of scheme B, may represent the real ancestral gene. The 5' end of this intermediate sequence would provide a rationale for the coding of *spacer* regions between EF hand domains. Argos (1977) noticed the strong β-turn character of these *spacer* sequences. The crystal structures of carp parvalbumin (Kretsinger and Nockolds, 1973) and bovine ICBP (Szebenyi *et al.*, 1981) clearly indicate the presence of a turn region between their respective EF hands.

B. FUTURE DIRECTION OF THE PROJECT

1. Technical problems

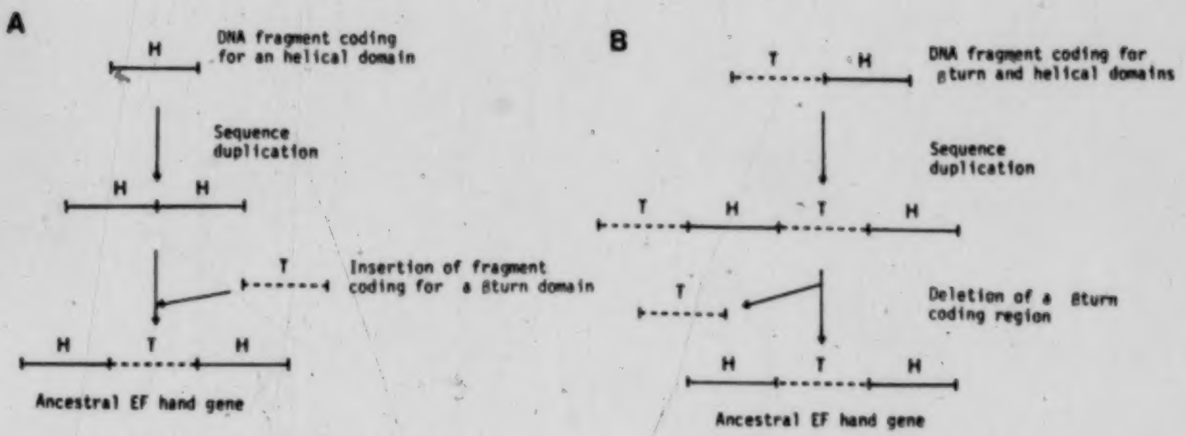
A
H
DNA fragment coding for an helical domain
Sequence duplication
H
H
T
Insertion of fragment coding for a βturn domain
H
T
H
Ancestral EF hand gene
B
T
H
DNA fragment coding for βturn and helical domains
Sequence duplication
T
H
T
H
T
Deletion of a βturn coding region
H
T
H
Ancestral EF hand gene

Fig. VI.3 Possible pathways leading to the biosynthesis of an ancestral EF hand gene (∿90-base long). (A) Scheme involving the initial duplication of a 30-nucleotide long DNA fragment coding for a helical domain followed by the insertion of a 30-base long fragment coding for a β-turn domain. (B) Scheme where a 60-base long sequence coding for a *loop-helix* domain is duplicated (intermediate sequence). A β-turn coding segment is then deleted from the sequence.

The major obstacles in studying the structure and function of EF hands have been technical ones. For example, the uncertainties surrounding binding constant values measured by CD, fluorescence and NMR techniques are often large in the case of low affinity calcium binding sites (10^3 to $10^5 M^{-1}$). Thus, any conclusions relative to the effect of amino acid substitutions on the observed metal binding constant of a site, will remain speculative unless the analogs investigated vary significantly in their ability to bind calcium (10 fold difference for example). Attempts to lenghten the peptide to 30-35 amino acids, will improve dramatically the calcium binding affinity of a site (chapter III) but represent a difficult synthetic task, especially if several peptide analogs are to be synthesized.

In view of the strong binding of lanthanides to a 13-residue long analog of a calcium binding loop (chapter IV), the use of lanthanides as calcium analogs may prove to be an excellent approach for the study of ligand requirements at the level of the EF loop. However, we have observed variations in the folding pattern of our model peptide around different lanthanides such as lutetium and lanthanum (chapter IV). One should thus pursue the elucidation of the structure of the lanthanide:peptide complex in solution before pursuing the synthesis of other analogs. The study of individual loop regions could lead to artifactual results due to the absence of α-helical regions. Finally, the titration of our peptides with lanthanides such as terbium and ytterbium, leads to an excessive broadening of the proton resonances (unpublished results). This factor limits the usefulness of several lanthanides, when used in conjunction with nuclear magnetic resonance techniques.

2. Key questions to answer

Attempts to solve the solution structure of our short lanthanide:peptide complex should be pursued. However, the analysis presented in the first part of this chapter indicates that one should try to answer questions relating to the overall secondary structure of the EF site. This implies the synthesis of longer analogs (30 to 35 residues). Although there exits an endless array of sequence permutations, our strategy should be to make analogs having altered helical domains or an altered β-turn region.

QUESTIONS

a. **Does the binding of calcium induce the formation of an helical segment in the C-terminal region of the EF hand ?**

and

b. **What is the importance of the C-terminal region, in relation to the calcium binding affinity of the site ?**

Since the starting point of the C-terminal α-helical region is at position 10 of the calcium binding loop, one needs to synthesize EF hand analogs lacking part of the C-terminal helix (beyond the -Z coordinate) to verify these issues. Another approach would be to synthesize a peptide containing helix breaking residues such as glycine, proline, tyrosine or asparagine. Note that a single residue substitution may not be sufficient to break a folding pattern as observed in the case of a proline substitution in site II of calmodulin (Fig. VI.1). Finally, such substitution(s) should be made beyond the -Z coordinate to avoid artifacts from perturbing the calcium binding loop region.

c. Does the presence of hydrophobic and charged surfaces on the helical regions represent parts of recognition sites for target proteins or for other parts of the protein or, are these regions involved in the calcium binding process or both ?

Analogs where hydrophobes and charged residues are substituted by a small strong α-helix forming amino acid such as alanine, should be informative since the helical nature of these regions would be maintained, but not the hydrophobic or charged domains.

d. What is the importance of the β-turn region ?

Figure VI.1 lists EF hand sequences where two additional residues have been inserted in the highly conserved β-turn region of their calcium binding loop. Although these sites retain their ability to bind calcium, the geometry of the β-turn generated is different from the one observed in the carp parvalbumin model (Szebenyi *et al.*, 1981; Fig. I.15). An analog of site I of bovine intestinal calcium binding protein may represent an interesting model peptide to study this aspect of the EF hand since this site is known to bind calcium strongly ($10^6 M^{-1}$). Alternatively, one may work with analogs of site III of rabbit skeletal troponin C and attempt to substitute one or more weak β-turn formers in this region without removing or adding any ionic ligands. Individual and simultaneous substitutions at position 2 (Arg to Leu) and +Y (Asn to Gln) of the loop region, should prove sufficient to disrupt the turn region. The conserved glycine residue at position 6 appears to be critical for the turn to helix transition, although its presence may also be a function of its proximity to the N-terminal helix. Its substitution by alanine (good helix former) or leucine (bulky side chain; good helix former) may provide some information about its importance in the folding behavior of the EF hand.

e. How to study protein:peptide interactions involving the helical domains of EF hands ?

Attempts to answer questions relating to the interaction of the helical regions of EF hand sites with target proteins have faced several technical problems often linked to the relative weakness of the interaction involved. One should briefly revise the strategy used in the study of such interactions.

Firstly, the sequence of site III of rabbit skeletal troponin C was our initial choice as a model site. However, sites I and III of bovine brain calmodulin offer a similar sequence and probably possess a binding domain to a wider variety of peptides and proteins (including TnI) as indicated recently by Malencik and Anderson (1982). Synthesis of calmodulin analogs may prove necessary if one wishes to pursue such interaction studies.

Secondly, the weakness of these interactions makes techniques such as gel filtration and urea PAGE, inadequate. One should use radioactively labelled peptides (I^{125}-iodination of a tyrosine residue for example) and techniques such as PAGE in non-denaturing conditions or affinity chromatography using a target protein linked to a sepharose matrix. Alternatively, the labelled peptide may be left to interact in the presence of calcium, with the matrix of a fluphenazine-bound Sepharose column (Head *et al.*, 1982). Following this step, a target protein would be loaded on the column and would then compete with the phenothiazine matrix for the drug binding site on the labelled peptide. Note that natural fragments of calmodulin could be used for this work.

Attempts should also be made to prepare a calmodulin affinity column. Then chemical and enzymatic fragments of troponin I, myelin basic protein, histone H2B or the β subunit of phosphorylase kinase should be tested for their ability to interact with calmodulin in the presence of calcium, since all these proteins share a partial sequence homology (Malencik and Anderson, 1982).

The essential goal of this work would be to locate the site of interaction of these target proteins on calmodulin and troponin C and to prove that the terminal helical regions of these EF hands are directly involved in the mechanism of action of EF hand containing proteins. Analogs of calmodulin EF hands lacking hydrophobic and negatively charged domains should confirm this hypothesis.

BIBLIOGRAPHY

Ahrland, S., Chatt, J., and Davies, N.R. (1958) *Quart. Rev. Chem. Soc.* 12, 265-276.

Alberston. J. (1968) *Acta Chem. Scand.* 22, 1563-1578.

Amos, L.A., Huxley, H.E., Holmes, K.C., Goody, R.S., and Taylor, K.A. (1982) *Nature* 299, 467-469.

Anderson, G.W., Zimmerman, J.E. and Callahan, F.M. (1964) *J. Am. Chem. Soc.* 86, 1839-1842.

Argos, P. (1977) *Biochemistry* 16, 665-672.

Bagshaw, C.R., and Kendrick-Jones, J. (1979) *J. Mol. Biol.* 130, 317-336.

Baimbridge, K.G., Selke, P.A., Ferguson, N., and Parkes, C.O. (1980) in *Calcium-Binding Proteins: Structure and Function* (Siegel, F.L., Carafoli, E., Kretsinger,R.H., MacLennan, D.H., and Wasserman, R.H., editors), pp. 401-404, Elvesier North-Holland, Inc., New York.

Baimbridge, K.G., Miller, J.J., and Parkes, C.O. (1982) *Brain Research* 239, 519-525.

Barker, W.C., Ketcham, L.K., and Dayhoff, M.O. (1980) in *Calcium-Binding Proteins: Structure and Function* (Siegel, F.L., Carafoli, E., Kretsinger, R.H., MacLennan, D.H., and Wasserman, R.H., editors), pp. 73-75, Elvesier North-Holland, Inc., New York.

Barker, W.C., Ketcham, L.K., and Dayhoff, M.O. (1978) in *Atlas of Protein Sequence and Structure*, Vol. 5, Suppl. 3, p. 273 (Dayhoff, M., ed.), The National Biomedical Research Foundation, Silver Spring, Maryland.

Baron, G., Demaille, J., and Dutruge, E. (1975) *FEBS Lett.* 100, 156-160.

Baudier, J., Briving, C., Deinum, J., Haglid, K., Sorskog, L., and Wallin, M. (1982) *FEBS Lett.* 147, 165-167.

Benzonana, G., Capony, J.-P., and Pechère, J.-F. (1972) *Biochim. Biophys. Acta* 278, 110-116.

Berchtold, M.W., Heizmann, C.W., and Wilson, K.J. (1982a) *Eur. J. Biochem.* 127, 381-389.

Berchtold, M.W., Wilson, K.J., Heizmann, C.W. (1982b) *Biochemistry* 21, 6552-6558.

Bernheim, R.A., Brown, T.H., Gutowsky, H.S., and Woessner, D.E. (1959) *J. Chem. Phys.* 30, 950-956.

Birnbaum, E.R., and Sykes, B.D. (1978) *Biochemistry* 17, 4965-4971.

Blaedel, W.J., and Knight, H.T. (1954) *Anal. Chem.* 26, 743-746.

Bloembergen, N. (1957) *J. Chem. Phys.* 27, 572-573 and 595-596.

Blumenthal, D.K., and Stull, J.T. (1980) *Biochemistry* 19, 5608-5614.

Bock, E. (1978) *J. Neurochem.* 30, 7-14.

Bode, W., and Schwager, P. (1975) *FEBS Lett.* 56, 139-143.

Brostrom, C.O., Huang, Y-C., Breckenridge, B.M., and Wolff, D.J. (1975) *Proc. Nat. Acad. Sci. U.S.A.* 72, 64-68.

Brostrom, C.O., Brostrom, M.A., and Wolff, D.J. (1977) *J. Biol. Chem.* 252, 5677-5685.

Brostrom, M.A., Brostrom, C.O., Breckenridge, B.M., and Wolff, D.J. (1978) *Adv. Cyclic Nucleotide Res.* 9, 85-99.

Bundi, A., and Wurthrich, K. (1979) *Biopolymers* 18, 285-297.

Burtnick, L.D., McCubbin, W.D., and Kay, C.M. (1975) *Can. J. Biochem.* 53, 15-20.

Burtnick, L.D., and Kay, C.M. (1977) *FEBS Lett.* 75, 105-110.

Busing, W.R., and Levy, H.A. (1957) *J. Chem. Phys.* 26, 563-568.

Calissano, P., Moore, B.W., and Friesen, A. (1969) *Biochemistry* 8, 4318-4326.

Calissano, P., Alemà, S., and Fasella, P. (1974) *Biochemistry* 13, 4553-4560.

Cantor, C.R., and Schimmel, P.R. (1980) *Biophysical Chemistry* (Bartlett, A.C., Vapnek, P.C., and McCombs, L.W., editors) Part II, p. 461, W.H. Freeman and Company, San Francisco.

Capony, J.-P., Pina, C., and Pechère, J.-F. (1976) *Eur. J. Biochem.* 70, 123-135.

Carafoli, E. (1980) in *Calcium-Binding Proteins: Structure and Function* (Siegel, F.L., Carafoli, E., Kretsinger, R.H., MacLennan, D.H., and Wasserman, R.H., editors), pp. 121-130, Elvesier North-Holland Inc., New York.

Carew, E.B., Leavis, P.C., Stanley, H.E. and Gergely, J. (1980) *Biophys. J.* 30, 351-358.

Cave, A., Pages, M., and Morin, P. (1979) *Biochimie* **61**, 607-613.

Celio, M.R., and Heizmann, C.W. (1981) *Nature* **293**, 300-302.

Chacko, S., Conti, M.A., and Adelstein, R.S. (1977) *Proc. Nat. Acad. Sci. U.S.A.* **74**, 129-133.

Chang, C.T., Wu, C.-S.C. and Yang, J.T. (1978) *Anal. Biochem.* **91**, 13-31.

Chantler, P.D., and Szent-Gyorgyi, A.G. (1978) *Biochemistry* 17, 5440-5448.

Chantler, P.D., and Szent-Gyorgyi, A.G. (1980) *J. Mol. Biol.* 138, 473-492.

Charbonneau, H., and Cormier, M.J. (1979) *Biochem. Biophys. Res. Commun.* **90**, 1039-1047.

Chatten, L.G., and Harris, L.E. (1962) *Anal. Chem.* **34**, 1495-1501.

Chen, Y.-H., Yang, J.T. and Chau, K.H. (1974) *Biochemistry* 13, 3350-3359.

Cheung, W.Y. (1970) *Biochem. Biophys. Res. Commun.* **38**, 533-538.

Cheung, W.Y., Bradham, L.S., Lynch, T.J., Lin, Y.M., and Tallant, E.A. (1975) *Biochem. Biophys. Res. Commun.* **66**, 1055-1062.

Cheung, W.Y. (1980) *Science* **207**, 19-27.

Chong, P.C.S., and Hodges, R.S. (1981) *J. Biol. Chem.* **56**, 5064-5070.

Chou, P.Y., and Fasman, G.D. (1974a) *Biochemistry* **13**, 211-222.

Chou, P.Y., and Fasman, G.D. (1974b) *Biochemistry* **13**, 222-245.

Chou, P.Y., and Fasman, G.D. (1978) *Ann. Rev. Biochem.* **47**, 251-276.

Cid, H., Bunster, M., Arriagada, E., Campos, M. (1982) *FEBS Lett.* **150**, 247-254.

Clarke, E.G.C. (1969) in *Isolation and Identification of Drugs* (Todd, R.G., Ed.) The Pharmaceutical Press, London, England.

Clement-Cormier, Y.C., Kebabian, J.W., Petzold, G.L., and Greengard, P. (1974) *Proc. Nat. Acad. Sci. U.S.A.* **71**, 1113-1117.

Coffee, C.J., and Bradshaw, R.A. (1973) *J. Biol. Chem.* **248**, 3305-3312.

Cohen, P., Burchell, A., Roulkes, J.G., Cohen, P.T.W., Vanaman, T.C., and Nairn, A.C. (1978) *FEBS Lett.* **92**, 287-293.

Collins, J.H., Potter, J.D., Horn, M.J., Wilshire, G., and Jackman, N. (1973) *FEBS Lett.* **36**, 268-272.

Collins, J.H. (1976) *Nature* **259**, 699-700.

Collins, J.H., Greaser, M.L., Potter, J.D., and Horn, M.J. (1977) *J. Biol. Chem.* **252**, 6356-6362.

Cook, W.J., Dedman, J.R., Means, A.R., and Bugg, C.E. (1980) *J. Biol. Chem.* **255**, 8152-8153.

Cook, W.J., Bugg, C.E., Dedman, J.R., and Means A.R. (1980) *Ann. N.Y. Acad. Sci.* **356**, 365-366.

Cotton, F.A., Bier, C.J., Day, V.W., Hazen, E.E., and Larson, S. (1971) *Cold Spring Harbor Symp. Quant. Biol.* **36**, 243-255.

Cotton, F.A., and Wilkinson, G. (1976) *Basic Inorganic Chemistry*, John Wiley & Sons, Inc., New York.

Cox, J.A., Winge, D.R., and Stein, E.A. (1979) *Biochimie* 61, 601-605.

Creese, I., Burt, D.R., and Snyder, S.H. (1976) *Science* 192, 481-483.

Crompton, M., Capano, M., and Carafoli, E. (1976) *Eur. J. Biochem.* 69, 453-462.

Crompton, M., Moser, R., and Carafoli, E. (1978) *Eur. J. Biochem.* 102, 615-623.

Crouch, T.H., and Klee, C.B. (1980) *Biochemistry* 19, 3692-3698.

Dabrowska, R., and Hartshorne, D.J. (1978) *Biochem. Biophys. Res. Commun.* 85, 1352-1359.

Dabrowska, R., Sherry, J.M., Aromatorio, D.K., and Hartshorne, D.J. (1978) *Biochemistry* 17, 253-258.

Dayhoff, M. (1976) in *Atlas of Protein Sequence and Structure*, Vol. 5, Suppl. 2, (Dayhoff, M., editor), pp. 7-8, The National Biomedical Research Foundation, Silver Spring, Maryland.

Dean, R.B., and Dixon, W.J. (1951) *Anal. Chem.* 23, 636-638.

Dedman, J.R., Potter, J.D., and Means, A.R. (1977) *J. Biol. Chem.* 252, 2437-2440.

Dedman, J.R., Potter, J.D., Jackson, R.L., Johnson, J.D., and Means, A.R. (1977) *J. Biol. Chem.* 252, 8415-8422.

Dedman, J.R., Jackson, R.L., Schreiber, W.E. and Means, A.R. (1978) *J. Biol. Chem.* 253, 343-346.

Demaille, J., Dutruge, E., Baron, G., Pechè, J.-P., and Fischer, E.H. (1975) *Biochem. Biophys. Res. Commun.* 67, 1034-1040.

Derancourt, J., Haiech, J., and Pechère, J.-F. (1978) *Biochim. Biophys. Acta* 532, 373-375.

Deuticke, H.J. (1934) *Hoppe-Seyler's Z. Phys. Chem.* 224, 216-228.

Dijkstra, B.W., Drenth, J., Kalk, K.H., and Vandermaelen , P.J. (1978) *J. Mol. Biol.* 124, 53-60.

Dijkstra, B.W., Drenth, J., and Kalk, K.H. (1981) *Nature*

289, 604-606.

Donato, R., and Michetti, F. (1974) *Experientia* 30, 511-512.

Donovan, J.W. (1969) in *Physical Principles and Techniques of Protein Chemistry* (Leach, S.J., ed) pp. 101-170, Academic Press, New York.

Dorrington, K.J., Hui, A., Hofmann, T., Hitchman, A.J.W., and Harrison, J.E. (1974) *J. Biol. Chem.* 249, 199-204.

Dorrington, K.J., Kells, K.I.C., Hitchman, A.J.W., Harrison, J.E., and Hofmann, T. (1978) *Can. J. Biochem.* 56, 492-499.

dos Remedios, C.G. (1981) *Cell Calcium* 2, 29-51.

Drabikowski, W., Brzeska, H., Kuznicki, J., and Grabarek, Z. (1980) *Ann. N.Y. Acad. Sci.* 356, 374-375.

Drabikowski, W., Dobrowolski, Z., and Brzeska, H. (1982a) *Biophys. J.* 37, 384a.

Drabikowski, W., Brzeska, H., and Venyaminov, S.Y. (1982b) *J. Biol. Chem.* 257, 11584-11590.

Dreizen, P., Gershman, L.C., Trotta, P.P., and Stracher, A.J. (1967) *J. Gen. Physiol.* 50 (part 2), 85-118.

Drescher, D., and DeLuca, H.F. (1971) *Biochemistry* 10, 2302-2307.

Dwek, R.A., Richards, R.E., Morallee, K.G., Nieboer, E., Williams, R.J.P., and Xavier, A.V. (1971) *Eur. J. Biochem.* 21, 204-209.

Ebashi, S., Kodama, A., and Ebashi, F. (1968) *J. Biochem. (Tokyo)* 64, 465-477.

Ebashi, S., and Endo, M. (1968) *Prog. Biophys. Mol. Biol. 18*, 123-183.

Ebashi, S., Nonomura, Y., Nakamura, S., Nakasone, H., and Kohama, K. (1982) *Fed. Proc.* 41, 2863-2867.

Eigen, M. (1963) *Pure Appl. Chem* 6, 97-115.

Eigen, M., and Wilkins, R.G. (1965) in *Mechanism of Inorganic Reaction, Advances in Chemistry Series* 49, 55.

Einspahr, H., and Bugg, C.E. (1977) in *Calcium-Binding Proteins and Calcium Function* (Wasserman, R.H., Corradino, R.A., Carafoli, E., Kretsinger, R.H., MacLennan, D.H., and Siegel, F.L., editors), pp. 13-20, Elvesier North-Holland, Inc., New York.

Endo, T., Tanaka, T., Isobe, T., Kasai, H., Okuyama, T. and Hidaka, H. (1981) *J. Biol. Chem.* **256**, 12485-12489.

Enfield, D.L., Ericsson, L.H., Blum, H.E., Fischer, E.H., and Neurath, H. (1975) *Proc. Nat. Acad. Sci. U.S.A.* 72, 1309-1313.

Erickson, B.W. and Merrifield, R.B. (1976) in *The Proteins* (Neurath, H., and Hill, R.L., eds) Vol. 2, pp. 255-527, Academic Press, New York.

Evans, J.S., Levine, B.A., Leavis, P.C., Gergely, J., Grabarek, Z., and Drabikowski, W. (1980) *Biochim. Biophys. Acta* **623**, 10-20.

Feder, J., Garrett, L.R., and Wildi, B.S. (1971) *Biochemistry* **10**, 4552-4556.

Filimonov, V.V., Pfeil, W., Tsalkova, T.N., and Privalov, P.L. (1978) *Biophys. Chem.* **8**, 117-122.

Forsén, S., Thulin, E., Drakenberg, T., Krebs, J., and Seamon, K. (1980) *FEBS Lett.* **117**, 189-194.

Frank, G., and Weeds, A.G. (1974) *Eur. J. Biochem.* **44**, 317-324.

Frearson, N., Focant, B.W.W., and Perry, S.V. (1976) *FEBS Lett.* **63**, 27-32.

Frederiksen, D.W., and Holtzer, A. (1968) *Biochemistry* 7, 3935-3950.

Fullmer, C.S., and Wasserman, R.H. (1973) *Biochim. Biophys. Acta* **317**, 172-186.

Fullmer, C.S., and Wasserman, R.H. (1981) *J. Biol. Chem.* **256**, 5669-5674.

Gaffin, S.L., and Oplatka, A. (1974) *J. Biochem. (Tokyo)* **75**, 277-281.

Gillis, J.M. (1980) in *Calcium-Binding Proteins: Structure and Function* (Siegel, F.L., Carafoli, E., Kretsinger, R.H., MacLennan, D.H., and Wasserman, R.H., editors), pp. 309-311, Elvesier North-Holland, Inc., New York.

Gariépy, J., Sykes, B.D., Reid, R.E., and Hodges, R.S. (1982) *Biochemistry* 21, 1506-1512.

Gisin, B.F. and Merrifield, R.B. (1972) *J. Am. Chem. Soc.* **94**, 3102-3106.

Gisin, B.F. (1973) *Helv. Chim. Acta* **56**, 1476-1482.

Gisin, B.F., Kobayashi, S. and Hall, J.E. (1977) *Proc. Nat. Acad. Sci. U.S.A.* **74**, 115-119.

Gnegy, M.E., Uzunov, P., and Costa, E. (1976) *Proc. Nat. Acad. Sci. U.S.A.* 73, 3887-3890.

Go, M., and Miyazawa, S. (1980) *Int. J. Pep. Prot. Res.* 15, 211-224.

Goldstein, A., Tachibana, S., Lowney, L.I., Hunkapiller, M., and Hood, L. (1979) *Proc. Nat. Acad. Sci. U.S.A.* 76, 6666-6670.

Goodman, M., Pechère, J.-F., Haiech, J., and Demaille, J.G. (1979) *J. Mol. Evol.* 13, 331-352.

Goodman, M. (1980) in *Calcium-Binding Proteins: Structure and Function* (Siegel, F.L., Carafoli, E., Kretsinger, R.H., MacLennan, D.H., and Wasserman, R.H., editors), pp. 349-354, Elvesier North-Holland, Inc., New York.

Gopalakrishna, R., and Anderson, W.B. (1982) *Biochem. Biophys. Res. Commun.* **104**, 830-836.

Gopinpath, R.M., and Vincenzi, F.F. (1977) *Biochem. Biophys. Res. Commun.* 77, 1203-1209.

Grabarek, Z., Drabikowski, W., Leavis, P.C., Rosenfeld, S.S. and Gergely, J. (1981) *J. Biol. Chem.* **256**, 13121-13127.

Grand, R.J.A., and Perry, S.V. (1980) *Biochem. J.* **189**, 227-240.

Grand, R.J.A., Shenolikar, S., and Cohen, P. (1980) *Eur. J. Biochem.* 113, 359-367.

Grand, R.J.A., Levine, B.A., and Perry, S.V. (1982) *Biochem. J.* **203**, 61-68.

Grantham, R. (1974) *Science* **185**, 862-864.

Greaser, M.L., and Gergely, J. (1971) *J. Biol. Chem.* **246**, 4226-4233.

Green, A.L. (1966) *J. Pharm. Pharmac.* **19**, 10-16.

Green, N.M., Allen, G.M., Hebdon, and Thorley-Lawson, D.A. (1977) in *Calcium-Binding Proteins and Calcium Function*, (Wasserman, R.H., Corradino, R.A., Carafoli, E., Kretsinger, R.H., MacLennan, D.H., and Siegel, F.L., editors) pp. 164-172, Elvesier North-Holland, Inc., New York.

Grenthe, I. (1969) *Acta Chem. Scand.* **23**, 1752-1764.

Grenthe, I. (1971) *Acta Chem. Scand.* **25**, 3347-3359.

Grenthe, I. (1972) *Acta Chem. Scand.* **26**, 1479-1489.

Guyton, A.C. (1971) *Textbook of Medical Physiology* W.B. Saunders Company, Philadelphia.

Haglid, K.G., and Stavrov, D. (1973) *J. Neurochem.* **20**, 1523-1532.

Haiech, J., Derancourt, J., Pechère, J.-F., and Demaille, J.G. (1979) *Biochemistry* **18**, 2752-2758.

Hammes, G.G., and Schimmel (1970) in *The Enzymes*, Vol. 2, p. 67 (Boyer, P.D., ed.), Academic Press, New York.

Hamoir, G., and Konosu, S. (1965) *J. Biochem.* **96**, 85-97.

Hamoir, G. (1968) *Acta Zool. Pathol. Antv.* **46**, 69-76.

Harmeyer, J., and DeLuca, H.F. (1969) *Arch. Biochem. Biophys.* **133**, 247-254.

Haselgrove, J.C. (1972) *Cold Spring Harbor Symp. Quant. Biol.* **37**, 341-352.

Hasselbach, W., and Makinose, M. (1963) *Biochem. Z.* **339**, 94-111.

Hathaway, D.R., and Adelstein, R.S. (1979) *Proc. Nat. Acad. Sci. U.S.A.* **76**, 1653-1657.

Hauschka, P.V., and Gallop, P.M. (1977) in *Calcium-Binding Proteins and Calcium Function* (Wasserman. R.H., Corradino, R.A., Carafoli, E., Kretsinger, R.H., MacLennan, D.H., Siegel, F.L., editors), pp. 338-347, Elvesier North-Holland, Inc., New York.

Hauschka, P.V., and Carr, S.A. (1982) *Biochemistry* 21, 2538-2547.

Havel, T.F., Crippen, G.M., and Kuntz, I.D. (1979) *Biopolymers* 18, 73-81.

Head, J.F., Masure, R.H., and Kaminer, B. (1982) *FEBS Lett.* 137 , 71-74.

Heilmann, J., Barollier, J. and Watzke, E. (1957) *Hoppe-Seyler's Z. Phys. Chem.* 309, 219-220.

Hidaka, H., Yamaki, T., Asano, M., and Totsuka, T. (1978a) *Blood Vessels* 15, 55-64.

Hidaka, H., Asano, M., Iwadare, S., Matsumoto, I., Totsuka, T., and Aoki, N. (1978b) *J. Pharm. Exp. Therap.* 207, 8-15.

Hidaka, H., Yamaki, T., Totsuka, T., and Asano, M. (1979a) *Mol. Pharm.* 15, 49-59.

Hidaka, H., Naka, M., and Yamaki, T. (1979b) *Biochem. Biophys. Res. Commun.* 90, 694-699.

Hincke, M.T., McCubbin, W.D., and Kay, C.M. (1978) *Can. J. Biochem.* 56, 384-395.

Hincke, M.T., Sykes, B.D., and Kay, C.M. (1981a) *Biochemistry* 20, 3286-3294.

Hincke, M.T., Sykes, B.D., and Kay, C.M. (1981b) *Biochemistry* 20, 4185-4193.

Hitchman, A.J.W., and Harrison, J.E. (1972) *Can. J. Biochem.* 50, 758-765.

Hodges, R.S. and Merrifield, R.B. (1975) *Anal. Biochem.* 65, 241-272.

Hoel, P.G. (1971) *Elementary Statistics*, pp. 201-207, John Wiley & Sons, Inc., New York.

Hofmann, T., Kawakami, M., Hitchman, A.J., Harrison, J.E., and Dorrington, K.J. (1979) *Can. J. Biochem.* 57, 737-748.

Holroyde, M.J., Robertson, S.P., Johnson, J.D., Solaro, R.J., and Potter, J.D. (1980) *J. Biol. Chem.* 255, 11688-11693.

Horl, W.H., Jennissen, H.P., and Heilmeyer, L.M.G. (1978) *Biochemistry* 17, 759-765.

Huheey, J.E. (1972) *Inorganic Chemistry: Principal of Structure and Reactivity*, Harper & Row, Publishers, New York.

Huxley, H.E. (1972) *Cold Spring Harbor Symp. Quant. Biol.* 37, 361-376.

Hyden, H., Lange, P.W., and Larson, S. (1980) *J. Neurol. Sci*. 45, 303-316.

Iida, Y. (1982) *Bull. Chem. Soc. Jpn* 55, 2683-2684.

Inagaki, M., Naka, M., Nozawa, Y., and Hidaka, H. (1983) *FEBS Lett*. 151, 67-70.

Isobe, T., Nakajima, T., and Okuyama, T. (1977) *Biochim. Biophys. Acta* 494, 222-232.

Isobe, T., and Okuyama, T. (1978) *Eur. J. Biochem.* 89, 379-388.

Isobe, T., Ishioka, N., and Okuyama, T. (1981) *Eur. J. Biochem*. 115, 469-474.

Isobe, T., and Okuyama, T. (1981) *Eur. J. Biochem.* 116, 79-86.

Itano, T., Itano, R., and Penniston, J.T. (1980) *Biochem. J.* 189, 455-459.

Jackson, R.L., Dedman, J.R., Schreiber, W.E., Bhatnagar, P.K., Knapp, R.D., and Means, A.R. (1977) *Biochem. Biophys. Res. Commun*. 77, 723-729.

Jakes, R., Northrop, F., and Kendrick-Jones, J. (1976) *FEBS Lett*. 70, 229-234.

Jamieson, G.A.Jr., and Vanaman, T.C. (1979) *Biochem. Biophys. Res. Commun*. 90, 1048-1056.

Jarret, H.W., and Penniston, J.T. (1977) *Biochem. Biophys. Res. Commun*. 77, 1210-1216.

Johnson, J.D., Collins, J.H., Robertson, S.P., and Potter, J.D. (1978a) *Circulation* 58, II-71 (272).

Johnson, J.D., Collins, J.H., and Potter, J.D. (1978b) *J. Biol. Chem*. 253, 6451-6458.

Johnson, J.D. (1983) *Biophys. J.* **41**, 306a.

Jones, R., Dwek, R.A., and Forsén, S. (1974) *Eur. J. Biochem.* **47**, 271-283.

Kakiuchi, S., and Yamazaki, R. (1970) *Biochem. Biophys. Res. Commun.* **41**, 1104-1110.

Kallfelz, F.A., Taylor, A.N., and Wasserman, R.H. (1967) *Proc. Soc. Exp. Biol. Med.* **125**, 54-58.

Kanamori, M., Endo, T., Shirakawa, S., Sakurai, M., and Hidaka, H. (1982) *Biochem. Biophys. Res. Commun.* **108**, 1447-1453.

Kanehisa, M.I., and Tsong, T.Y. (1980) *Biopolymers* **19**, 1617-1628.

Kanellis, P., Yang, J., Cheung, H., and Lenkinski, R.E. (1983) *Arch. Biochem. Biophys.* **220**, 530-540.

Kaptein, R. (1978) in *Nuclear Magnetic Resonance Spectroscopy in Molecular Biology* p. 211, (Pullman, B., ed.), D. Reidel Publishing Co., Dorsbrecht, The Netherlands.

Katz, S., and Remtulla, M.A. (1978) *Biochem. Biophys. Res. Commun.* **83**, 1373-1379.

Kebabian, J.W., and Calne, D.B. (1979) *Nature* **277**, 93-96.

Kendrick-Jones, J., Lehman, W., and Szent-Gyorgyi, A.G. (1970) *J. Mol. Biol.* **54**, 313-326.

Kendrick-Jones, J., Szentkiralyi, E.M., and Szent-Gyorgyi, A.G. (1976) *J. Mol. Biol.* **104**, 747-775.

Kendrick-Jones, J., and Jakes, R. (1977) in *International Symposium on Myocardial Failure* (Riecker, G., Weber, A., Goodwin, H., editors), pp. 28-48, Springer-Verlag, Berlin.

Kilhoffer, M.C., Demaille, J.G., and Gerard, D. (1980) *FEBS Lett.* **116**, 269-272.

Kilhoffer, M.C., Gerard, D., and Demaille, J.G. (1980) *FEBS Lett.* **120**, 99-103.

Klee, C.B. (1977) *Biochemistry* **16**, 1017-1024.

Klee, C.B., Crouch, T.H., and Richman, P.G. (1980) *Ann. Rev.*

Biochem. **49**, 489-515.

Klevit, R.E., Levine, B.A., and Williams, R.J.P. (1981) *FEBS Lett.* 123, 25-29.

Kobayashi, R., Tawata, M., and Hidaka, H. (1979) *Biochem. Biophys. Res. Commun.* 88, 1037-1045.

Kolat, R.S., and Powell, J.E. (1962) *Inorg. Chem.* 1, 293-296.

Kominz, D.R., Carroll, W.R., Smith, E.N., and Mitchell, E.R. (1959) *Arch. Biochem. Biophys.* 79, 191-199.

Konig, W. and Geiger, R. (1970) *Chem. Ber.* 103, 788-798.

Krebs, J., and Carafoli, E. (1982) *Eur. J. Biochem.* **124**, 619-627.

Kretsinger, R.H. and Nockolds, C.E. (1973) *J. Biol. Chem.* **248**, 3313-3326.

Kretsinger, R.H. and Barry, C.D. (1975) *Biochim. Biophys. Acta* **405**, 40-52.

Kretsinger, R.H. (1976) *Ann. Rev. Biochem.* **45**, 239-266.

Kretsinger, R.H. (1977) in *Calcium-Binding Proteins and Calcium Function* (Wasserman, R.H., Corradino , R.A., Carafoli, E., Kretsinger, R.H., MacLennan, D.H., and Siegel, F.L., editors), pp. 63-72, Elvesier North-Holland Inc., New York.

Kretsinger, R.H. (1979) *Adv Cycl Nucl Res* 11, 1-26.

Kretsinger, R.H. (1980a) *Ann. N.Y. Acad. Sci.* 356, 14-19.

Kretsinger, R.H. (1980b) *CRC Crit. Rev. Biochem.* 8, 119-174.

Kretsinger, R.H., Rudnick, S.E., Sneden, D.A., and Schatz, V.B. (1980) *J. Biol. Chem.* 255, 8154-8156.

Kudo, S., Muto, Y., Nagao, S., Naka, M., Hidaka, H., Sano, M., and Nozawa, Y. (1982) *FEBS Lett.* 149, 271-276.

Kuntz, I.D., Crippen, G.M., and Kollman, P.A. (1979) *Biopolymers* 18, 939-957.

Kuznicki, J., Grabarek, Z., Brzeska, H., Drabikowski, W., and Cohen, P. (1981) *FEBS Lett.* 130, 141-145.

Labourdette, G., and Mandel, P. (1978) *Biochem. Biophys. Res. Commun.* **85**, 1307-1313.

Landry, Y., Amellal, M., and Ruckstuhl, M. (1981) *Biochem. Pharmac.* **30**, 2031-2032.

LaPorte, D.C., Wierman, B.M., and Storm, D.R. (1980) *Biochemistry* **19**, 3814-3819.

Leavis, P.C., and Kraft, E.L. (1978) *Arch. Biochem. Biophys.* **186**, 411-415.

Leavis, P.C., Rosenfeld, S.S., Gergely, J., Grabarek, Z., and Drabikowski, W. (1978), *J. Biol. Chem.* **253**, 5452-5459.

Leavis, P.C., Nagy, B., Lehrer, S.S., Bialkowska, H., and Gergely, J. (1980) *Arch. Biochem. Biophys.* **200**, 17-21.

Leavis, P.C., Evans, J.S., and Levine, B.A. (1982) *J. Inorg. Biochem.* **16**, 257-277.

Lee, L., Sykes, B.D., and Birnbaum, E.R. (1979) *FEBS Lett.* **98**, 169-172.

Lee, L., and Sykes, B.D. (1980a) *Biochemistry* **19**, 3208-3214.

Lee, L., and Sykes, B.D. (1980b) *Biophys. J.* **32**, 193-210.

Lee, L., and Sykes, B.D. (1981) *Biochemistry* **20**, 1156-1162.

Lee, L., and Sykes, B.D. (1982) in *Biochemical Structure Determination by NMR* (Bothner-By, A.A., Glickson, J.D., and Sykes, B.D., editors) pp.169-188, Marcel-Dekker, New York.

Lehn, J.-M. (1973) *Structure and Bonding* **16**, 1-69.

Lenkinski, R.E., Yang, J., Cheung, H.C., Stephens, R.L., and Kanellis, P. (1983) *Biochim. Biophys. Acta* (in press).

Levin, R.M., and Weiss, B. (1976) *Mol. Pharmacol.* **12**, 581-589.

Levin, R.M., and Weiss, B. (1977) *Mol. Pharmacol.* **13**, 690-697.

Levin, R.M., and Weiss, B. (1978) *Biochim. Biophys. Acta* **540**, 197-204.

Levin, R.M., and Weiss, B. (1979) *J. Pharmacol. and Exptl.*

Therapeutics 208, 454-459.

Levin, R.M., and Weiss, B. (1980) *Neuropharmacology* 19, 169-174.

Levine, B.A., Mercola, D., Coffman, D., and Thornton, J.H. (1977) *J. Mol. Biol.* 115, 743-760.

Levine, B.A., Thornton, J.M., Fernandes, R., Kelly, C.M., and Mercola, D. (1978) *Biochim. Biophys. Acta* 535, 11-24.

Lewis, P.N., Momany, F.A., and Scheraga, H.A. (1971) *Proc. Nat. Acad. Sci. U.S.A.* 68,2293-2297.

Lin, Y.M., Yung, P.L., and Cheung, W.Y. (1974) *J. Biol. Chem.* 249, 4943-4954.

Lui, Y.P. and Cheung, W.Y. (1976) *J. Biol. Chem.* 251, 4193-4198.

Lynch, T.J., Tallant, E.A., and Cheung, W.Y. (1976) *Biochem. Biophys. Res. Commun.* 68, 616-625.

MacManus, J.P. (1981) *FEBS Lett.* 126, 245-249.

MacLennan, D.H., and Wong, P.T.S. (1971) *Proc. Nat. Acad. Sci. U.S.A.* 68, 1231-1235.

MacLennan, D.H., and Holland, P.C. (1975) *Ann. Rev. Biophys. Bioeng.* 4, 377-404.

Malencik, D.A., and Anderson, S.R. (1982) *Biochemistry* 21, 3480-3486.

Mani, R.S., Boyes, B.E., and Kay, C.M. (1982) *Biochemistry* 21, 2607-2612.

Mani, R.S., Shelling, J.G., Sykes, B.D., and Kay, C.M. (1983) *Biochemistry* (in press).

Marcum, M., Dedman, J.R., Brinkley, B.R., and Means, R.A. (1978) *Proc. Nat. Acad. Sci. U.S.A.* 75, 3771-3775.

Marinetti, T.D., Snyder, G.H., and Sykes, B.D. (1976) *Biochemistry* 15, 4600-4608.

Marshak, D.R., Watterson, D.M., and Van Eldik, L.J. (1981) *Proc. Nat. Acad. Sci. U.S.A.* 78, 6793-6797.

Martell, A.E., and Smith, R.M. (1974) *Critical Stability*

Constants, vol. 1: amino acids, Plenum Press, New York.

Martin, R.B., and Richardson, F.S. (1979) *Quart. Rev. Biophys.* 12, 181-209.

Matthews, B.W., Weaver, L.H., and Kester, W.R. (1974) *J. Biol. Chem.* 249, 8030-8044.

McCubbin, W.D., and Kay, C.M. (1975) *FEBS Lett.* 55, 183-187.

McCubbin, W.D., and Kay, C.M. (1980) *Acc. Chem. Res.* 13, 185-192.

Means, A.R., Tash, J.S., and Chafouleas, J.G. (1982) *Physiol. Reviews* 62, 1-39.

Miani, N., Michetti, F., DeRenzis, G., and Caniglia, A. (1973) *Experientia* 29, 1499-1501.

Mikawa, T., Nonomura, Y., Hirata, M., Ebashi, S., and Kakiuchi, S. (1978) *J. Biochem. (Tokyo)* 84, 1633-1636.

Moeller, T., Martin, D.F., Thompson, L.C., Ferrus, R., Feistel, G.R., and Randall, W.J. (1965) *Chem. Reviews* 65, 1-50.

Moeschler, H.J., Schaer, J.J., and Cox, J.A. (1980) *Eur. J. Biochem.* 111, 73-78.

Moller-Nielsen, I., Pederson, V., Nymak, M., Franc, K.F., Boek, U., Fjallan, B., and Christiansen, A.V. (1973) *Acta. Pharmacol. Toxicol.* 33, 353-362.

Moore, B.W. (1965) *Biochem. Biophys. Res. Commun.* 19, 739-744.

Moore, P.B., Huxley, H.E., and DeRosier, D.J. (1970) *J. Mol. Biol.* 50, 279-295.

Morgan, M., Perry, S.V., and Ottaway, J. (1976) *Biochem. J.* 157, 687-697.

Morimoto, K., and Harrington, W.F. (1974) *J. Mol. Biol.* 88, 693-709.

Morrissey, R.L., Zolock, D.T., Bikle, D.D., Empson, R.N.Jr., and Bucci, T.J. (1978a) *Biochim. Biophys. Acta* 538, 23-33.

Morrissey, R.L., Empson, R.N.Jr., Zolock, D.T., Bikle, D.D., and Bucci, T.J. (1978b) *Biochim. Biophys. Acta* 538, 34-41.

Morrison, M., and Bayse, G.S. (1970) *Biochemistry* 9, 2995-3000.

Mrakovcic, A., Oda, S., and Reisler, E. (1979) *Biochemistry* 18, 5960-5965.

Murray, A.C. and Kay, C.M. (1972) *Biochemistry* 11, 2622-2627.

Nagy, B., Potter, J.D., and Gergely, J. (1978) *J. Biol. Chem.* 253, 5971-5974.

Nagy, B., and Gergely, J. (1979) *J. Biol. Chem.* 254, 12732-12737.

Nieboer, E. (1975) *Structure and Bonding* 22, 1-47.

Nishikawa, M., Tanaka, T., and Hidaka, H. (1980) *Nature* 287, 863-865.

Nockolds, C.E., Kretsinger, R.H., Coffee., C.J., and Bradshaw, R.A. (1972) *Proc. Nat. Acad. Sci. U.S.A.* 69, 581-584.

Norman, J.A., Drummond, A.H., and Moser, P. (1979) *Mol. Pharm.* 16, 1089-1094.

Ochiai, Ei-Ichiro (1977) *Bioinorganic Chemistry: An Introduction* , Allyn and Bacon, Inc., Boston.

Oikawa, K., McCubbin, W.D., and Kay, C.M. (1980) *FEBS Lett.* 118, 137-140.

Parry, D.A.D., and Squire, J.M. (1973) *J. Mol. Biol.* 75, 33-55.

Pato, M.D., and Adelstein, R.S. (1980) *J. Biol. Chem.* 255, 6535-6538.

Pearson, R.G. (1963) *J. Am. Chem. Soc.* 85, 3533-3539.

Pearson, R.G. (1968) *J. Chem. Educ.* 45, 581-587.

Pechère, J.-F., and Focant, B. (1965) *Biochem. J.* 96, 113-118.

Pechère, J.-F., and Capony, J.-P. (1969) *Comp. Biochem. Physiol.* 28, 1089-1102.

Pechère, J.-F., Capony, J.-P., and Ryden, L. (1971) *Eur. J. Biochem.* 23, 421-428.

Pechère, J.-F. (1977) in *Calcium-Binding Proteins and Calcium Function*, (Wasserman, R.H., Corradino, R.A., Carafoli, E., Kretsinger, R.H., MacLennan, D.H., Siegel, F.L., editors), pp. 213-221, Elvesier North-Holland, Inc., New York.

Pechère, J.-F., Derancourt, J., and Haiech, J. (1977) *FEBS Lett.* 75, 111-114.

Perrie, W.T., and Perry, S.V. (1970) *Biochem. J.* 135, 151-164.

Perrie, W.T., Smillie, L.B., and Perry, S.V. (1973) *Biochem. J.* 135, 151-164.

Perrin, D.D., and Sayce, I.C. (1967) *Talanta* 14, 833-842.

Pershadsingh, H.A., McDaniel, M.L., Landt, M., Bry, C.G. , Lacy, P.E., and McDonald, J.M. (1980) *Nature* 288, 492-495.

Pietta, P.G. and Marshall, G.R. (1970) *J. Chem. Soc. (London)*, section D, 650-651.

Potter, J.D., and Gergely, J. (1974) *Biochemistry* 13, 2697-2703.

Potter, J.D. (1975) *Fed. Proc.* 34, 671.

Potter, J.D., and Gergely, J. (1975) *J. Biol. Chem.* 250, 4628-4633.

Potter, J.D., Seidel, J.C., Leavis, P.C., Lehrer, S.S. and Gergely, J. (1976) *J. Biol. Chem.* 251, 7551-7556.

Potter, J.D., Fu-Juan, H., and Pownall, H.J. (1977a) *J. Biol. Chem.* 252, 2452-2454.

Potter, J.D., Johnson, J.D., Dedman, J.R., Schreiber, W.E., Mandel, F., Jackson, R.L., and Means, A.R. (1977b) in *Calcium-Binding Proteins and Calcium Function* (Wasserman, R.H., Corradino, R.A., Carafoli, E., Kretsinger, R.H., MacLennan, D.H., and Siegel, F.L., editors), pp. 239-249, Elvesier North-Holland, Inc., New York.

Privalov, P.L., and Khechinashvili, N.N. (1974) *J. Mol. Biol.* 86, 665-684.

Prozialeck, W.C., and Weiss, B. (1982) *J. Pharm. Exp. Therap.* **222**, 509-516.

Raess, B.U., and Vincenzi, F.F. (1980) *Mol. Pharmacol.* **18**, 253-258.

Reid, R.E. and Hodges, R.S. (1980) *J. Theor. Biol.* **84**, 401-444.

Reid, R.E., Clare, D.M. and Hodges, R.S. (1980) *J. Biol. Chem.* **255**, 3642-3646.

Reid, R.E., Gariépy, J., Saund, A.K., and Hodges, R.S. (1981) *J. Biol. Chem.* **256**, 2742-2751.

Reuben, J. (1971) *Biochemistry* **10**, 2834-2838.

Reuben, J. (1977) in *Calcium-Binding Proteins and Calcium Function* (Wasserman, R.H., Corradino, R.A., Carafoli, E., Kretsinger, R.H., MacLennan, D.H., and Siegel, F.L., editors), pp. 21-28, Elvesier North-Holland Inc., N.Y.

Reynolds, C.H., and Claxton, P.T.J. (1982) *Biochem. Pharm.* **31**, 419-421.

Rhee, M.-J., Sudnick, D.R., Arkle, V.K., and Horrocks, W. DeW. Jr. (1981) *Biochemistry* **20**, 3328-3334.

Ringer, S. (1882) *J. Physiol. (London)* **3**, 380-393.

Rottenberg, H., and Scarpa, A. (1974) *Biochemistry* **13**, 4811-4817.

Roufogalis, B.D. (1981) *Biochem. Biophys. Res. Commun.* **98**, 607-613.

Rusca, G., Calissano, P., Alemà, S. (1972) *Brain Research* **49**, 223-227.

Scharff, O. (1981) *Cell Calcium* **2**, 1-27.

Schatzmann, H.J., and Vincenzi, F.F. (1969) *J. Physiol. (London)* **201**, 369-395.

Schatzmann, H.J., and Roelofsen, B. (1977) in *Biochemistry of Membrane Transport*, pp. 389-400, Springer-Verlag, Berlin.

Seamon, K.B., Hartshore, D.J., and Bothner-By, A.A. (1977) *Biochemistry* **16**, 4039-4046.

Seamon, K.B. (1979) *Biochem. Biophys. Res. Commun.* **86**, 1256-1265.

Seamon, K.B. (1980) *Biochemistry* **19**, 207-215.

Seeman, P. (1977) *Biochem. Pharmacol.* **26**, 1741-1748.

Sellinger-Barnette, M., and Weiss, B. (1982) *Mol. Pharm.* **21**, 86-91.

Seymour, J., and O'Brien, E.J. (1980) *Nature* **283**, 680-682.

Shannon, R.D. (1976) *Acta Cryst.* **A32**, 751-767.

Shelling, J.G., Sykes, B.D., O'Neil, J.D.J., and Hofmann, T. (1983) *Biochemistry* (in press).

Sigel, H., and McCormick, D.B. (1970) *Acc. Chem. Res.* **3**, 201-208.

Sillin, L.B. and Martell, A.E. (1964) *Stability Constants of Metal Ion Complexes*, 2nd Ed, Special Publication No. 17, The Chemical Society, Burlington House, London.

Sin, I.L., Fernandes, R. and Mercola, D. (1978) *Biochem. Biophys. Res. Commun.* **82**, 1132-1139.

Sinha, S.P. (1976) *Structure and Bonding* **25**, 69-149.

Sinha, S.P. (1976) *Structure and Bonding* **30**, 1-64.

Skinki, T., Takahashi, N., Kawate, N., and Suda, T. (1982) *Endocrinology* **111**, 1546-1531.

Sobieszek, A. (1977) *Eur. J. Biochem.* **73**, 477-483.

Solomon, I. (1955) *Phys. Rev.* **99**, 559-565.

Spencer, R., Charman, M., Wilson, P.W., and Lawson, D.E.M. (1976) *Nature* **263**, 161-163.

Spencer, R., Charman, M., Wilson, P.W., and Lawson, D.E.M. (1978) *Biochem. J.* **170**, 93-101.

Stefansson, I., Wollmann, R.L., and Moore, B.W. (1980) *Nature* **295**, 63-64.

St-Pierre, S.A. and Hodges, R.S. (1977) *Can. J. Biochem.* **55**, 636-643.

Szebenyi, D.M.E., Obendorf, S.K., and Moffat, K. (1981)

Nature **294**, 327-332.

Szent-Gyorgyi, A.G., Szentkiralyi, E.M., and Kendrick-Jones, J. (1973) *J. Mol. Biol.* **74**, 179-203.

Szent-Gyorgyi, A.G. (1975) *Biophys. J.* **15**, 707-723.

Szent-Gyorgyi, A.G. (1980) in *Muscle Contraction; Its Regulatory Mechanisms*, (Ebashi *et al.*, eds), pp. 375-389, Springer-Verlag, Berlin.

Takagi, T., Nemoto, T., Konishi, K., Yazawa, M., and Yagi, K. (1980) *Biochem. Biophys. Res. Commun.* **96**, 377-381.

Takahashi, K., Yamaguchi, H., Ishizeki, J., Nakajima, T., and Nakazoto, Y. (1981) *Virchows Arch. [Cell Pathol.]* 37, 125-135.

Tanaka, T., and Hidaka, H. (1980) *J. Biol. Chem.* **255**, 11078-11080.

Tanaka, T., and Hidaka, H. (1981a) *Biochem. Biophys. Res. Commun.* 101, 447-453.

Tanaka, T., and Hidaka, H. (1981b) *Biochem. International* 2, 71-75.

Taube, H., and Posey, F.A. (1953) *J. Am. Chem. Soc.* 75, 1463-1467.

Taylor, A.N., and Wasserman, R.H. (1965) *Nature* **205**, 248-250.

Taylor, A.N. (1981) *J. Histochem. Cytochem.* **29**, 65-73.

Taylor, A.K., and Amos, L.A. (1981) *J. Mol. Biol.* **147**, 297-324.

Teo, T.S., and Wang, J.H. (1973) *J. Biol. Chem.* **248**, 5950-5955.

Thomasset, M., Cuisinier-Gleizers, P., and Mathieu, H. (1979) *FEBS Lett.* 107, 91-94.

Tufty, R.M., and Kretsinger, R.H. (1975) *Science* 187, 167-169.

van Eerd, J.-P., and Takahashi, K. (1975) *Biochem. Biophys. Res. Commun.* **64**, 122-127.

Verheij, M., Volwerk, J.J., Jansen, E.H.J.M., Puyk, W.C., Dijkstra, B.W., Drenth, J., and deHaas, G.H. (1980) *Biochemistry* 19, 743-750.

Vincendon, G., Zanetta, J.P., and Gombos, G. (1970) *Adv. Exp. Med. Biol.* 32, 9-19.

Vincenzi, F.F. (1979) *Proc. West. Pharmacol. Soc.* 22, 289-294.

Vincenzi, F.F., and Ashelman, B.T. (1980) in *Calcium-Binding Proteins: Structure and Function* (Seigel, F.L., Carafoli, E., Kretsinger, R.H., MacLennan, D.H., and Wasserman, R.H., editors) pp. 173-179, Elsevier North-Holland, Inc., New York.

Vincenzi, F.F. (1981) *Trends Pharm. Sci.* 2, VII-IX.

Vogt, H.-P., Strassburger, W., Wollmer, A., Fleischhauer, J., Bullard, B., and Mercola, D. (1979) *J. Theor. Biol.* 76, 297-310.

Voordouw, G., and Roche, R.S. (1975) *Biochemistry* 14, 4667-4673.

Waddington, T.C. (1959) *Adv. Inorg. Chem. Radiochem.* 1, 157-221.

Wallace, R.W., Ann Tallant, E., Dockter, M.E., Cheung, W.Y. (1982) *J. Biol. Chem.* 257, 1845-1854.

Walsh, M., Stevens, F.C., Oikawa, K., and Kay, C.M. (1978) *Biochemistry* 17, 3924-3930.

Walsh, M., Stevens, F.C., Oikawa, K., and Kay, C.M. (1979) *Can. J. Biochem.* 57, 267-278.

Wang, C-L.A., Leavis, P.C., Horrocks, W.De.W.Jr., and Gergely, J. (1981) *Biochemistry* 20, 2439-2444.

Wang, C-L.A., Tao, T., and Gergely, J. (1982a) *J. Biol. Chem.* 257, 8372-8375.

Wang, C-L.A., Aquaron, R.R., Leavis, P.C., and Gergely, J. (1982b) *Eur. J. Biochem.* 124, 7-12.

Wang, J.H., and Waisman, D.M. (1979) *Current Topics in Cellular Regulation* 15, 47-107.

Wasserman, R.H. (1980) in *Calcium-Binding Proteins: Structure and Function* (Seigel, F.L., Carafoli, E., Kretsinger, R.H., MacLennan, D.H., and Wasserman, R.H., editors), pp. 357-361, Elvesier North-Holland, Inc., New York.

Watterson, D.M., Harrelson, W.G., Keller, P.M., Sharief, F., and Vanaman, T.C. (1976) *J. Biol. Chem.* 251, 4501-4513.

Watterson, D.M., Sharief, F. and Vanaman, T.C. (1980) *J. Biol. Chem.* 255, 962-975.

Weber, A., Herz, R., and Reiss, I. (1966) *Biochem. Z.* 345, 329-369.

Weeds, A.G. (1969) *Nature* 223, 1362-1364.

Weeds, A.G., and Lowey, S. (1971) *J. Mol. Biol.* 61, 701-725.

Weeds, A.G., and McLachlan, A.D. (1974) *Nature* 252, 646-649.

Weeks, R.A. and Perry, S.V. (1977) *Biochem. Soc. Trans.* 5, 1391-1392.

Weeks, R.A., and Perry, S.V. (1978) *Biochem. J.* 173, 449-457.

Weiss, B., and Levin, R.M. (1978) *Adv. Cyclic Nucl. Res.* 9, 285-303.

Weiss, B., Prozialeck, W.C., and Wallace, T.L. (1982) *Biochem. Pharm.* 31, 2217-2226.

Werber, M.M., and Oplatka, A. (1974) *Biochem. Biophys. Res. Commun.* 57, 823-830.

Williams, R.J.P. (1970) *Quaterly Reviews* 24 , 331-365.

Williams, R.J.P. (1977) in *Calcium-Binding Proteins and Calcium Function* (Wasserman, R.H., Corradino, R.A., Carafoli, E., Kretsinger, R.H., MacLennan, D.H., and Siegel, F.L., editors) pp. 3-12, Elvesier North-Holland, Inc., New York.

Williams, R.J.P. (1980) in *Calcium-Binding Proteins: Structure and Function* (Siegel, F.L., Carafoli, E., Kretsinger, R.H., MacLennan, D.H., and Wasserman, R.H., editors) pp. 3-10, Elvesier North-Holland, Inc., New York.

Winkler, R. (1972) *Structure and Bonding* 10, 1-24.

Wolff, D.J., Poirier, P.G., Brostrom, C.O., and Brostrom , M.A. (1977) *J. Biol. Chem.* 252, 4108-4117.

Wong, P.Y.-K., and Cheung, W.Y. (1979) *Biochem. Biophys. Res. Commun.* 90, 473-480.

Yazawa, M., Yagi, K., Toda, H., Kondo, K., Narita, K., Yamazaki, R., Sobue, K., Kakiuchi, S., Nagao, S., and Nozawa, Y. (1981) *Biochem. Biophys. Res. Commun.* 99, 1051-1057.

APPENDIX

When a diamagnetic lanthanide such as lanthanum or lutetium is bound to a peptide, it may alter the relaxation times T_1 and T_2 of nuclei in the peptide. If the paramagnetic lanthanide gadolinium is used in the place of La^{3+} or Lu^{3+}, there will be an additional large contribution to the relaxation rates from the unpaired 4f electrons on the metal ion. It is this difference in relaxation rates between La^{3+} and Gd^{3+} for nuclei in the metal peptide complex that we wish to extract and analyse in terms of the geometry of the complex.

The Solomon-Bloembergen equations (Solomon, 1955; Bloembergen, 1957) relate the observed increase in relaxation rates of a nucleus in the metal:peptide complex caused by the unpaired electrons on gadolinium to the distance between the nucleus and the metal.

$$\frac{1}{T_{1,m}} = \frac{2\gamma^2\beta^2g^2J(J+1)}{15\,r^6}\left\{\frac{3\,\tau_c}{(1+\omega_I^2\tau_c^2)}+\frac{7\,\tau_c}{(1+\omega_S^2\tau_c^2)}\right\} + \frac{2J(J+1)}{3}(A/h)^2\left\{\frac{\tau_e}{(1+\omega_S^2\tau_e^2)}\right\} \qquad (1)$$

$$\frac{1}{T_{2m}} = \frac{\gamma^2\beta^2 g^2 J(J+1)}{15\, r^6}\left[4\tau_c + \frac{3\tau_c}{(1+\omega_I^2\tau_c^2)} + \frac{13\tau_c}{(1+\omega_S^2\tau_c^2)}\right] + \frac{J(J+1)}{3}(A/\hbar)^2\left[\tau_e + \frac{\tau_e}{(1+\omega_S^2\tau_e^2)}\right] \quad (2)$$

where the symbols in these equations are defined as follows: ω_I and ω_S are the nuclear and electronic Larmor precession frequencies; g, the Landé g-factor; $A/\hbar$, the scalar electron-nuclear hyperfine interaction constant; J , the total angular momentum for the Gd^{3+} ion (7/2); β, the Bohr magneton; γ , the nuclear magnetogyric ratio; r, the metal to nucleus distance; τ_c and τ_e , the correlation times for the dipolar interaction and the contact interaction, respectively.

Two simplifications reduce the apparent complexity of these two expressions:

1) The term ω_S is greater than ω_I since the electronic magnetic moment is 654 times larger than that of the proton.

2) The scalar terms in both expressions are assumed insignificant as demonstrated by temperature variation studies (Bernheim *et al*., 1959; Dwek *et al*., 1971; Reuben *et al*., 1971).

The quantity $[\gamma^2\beta^2 g^2 J(J+1)]/15$ has a value of $2.583 \times 10^{17} s^{-2}$Å^6 (Marinetti *et al.*, 1976), so that the two expressions can now be rewritten in terms of only two unknowns, τ_c and r

$$\frac{1}{T_1m} = \frac{5.166 \times 10^{17}}{r^6} \left\{ \frac{3\,\tau_c}{(1 + \omega_I^2\tau_c^2)} \right\} \qquad (3)$$

$$\frac{1}{T_2m} = \frac{2.583 \times 10^{17}}{r^6} \left\{ 4\,\tau_c + \frac{3\,\tau_c}{(1 + \omega_I^2\tau_c^2)} \right\} \qquad (4)$$

and the ratio of the relaxation times is given by the expression

$$\frac{T_1m}{T_2m} = \frac{7}{6} + \frac{4\,\omega_I^2\tau_c^2}{6} \qquad (5)$$

Given that the quantities T_1m and T_2m can be obtained for a selected number of proton resonances from gadolinium relaxation experiments, one can determine the correlation time τ_c of the dipolar interaction from equation (5). This later value can then be used to solve equations (3) or (4) for the metal to proton distance involved for each nucleus studied.

The quantities $1/T_1m$ and $1/T_2m$ are obtained in this case under the assumption that the metal binding to the peptide is in the NMR fast-exchange limit. In this limit, the relaxation rate $1/T_2$, for example, for peptide nuclei in the La^{3+}:peptide solution is given by

$$\frac{1}{T_2}(\mathrm{La}^{3+}) = \frac{[\mathrm{P}]}{\mathrm{P}_0 T_{2\mathrm{p}}} + \frac{[\mathrm{PM}]}{\mathrm{P}_0 T_{2\mathrm{pm}}} \qquad (6)$$

where $T_{2\mathrm{p}}$ and $T_{2\mathrm{pm}}$ are the spin-spin relaxation times for the free peptide and the diamagnetic metal ion peptide complex, respectively.

In the presence of a very small amount of gadolinium such that the fractional saturation of the peptide is unchanged, and with the additional assumptions that the binding constants for La^{3+} and Gd^{3+} are equal, that the complexes are isostructural, and that exchange is fast enough that the NMR spectrum is still in the fast-exchange limit for Gd^{3+}, the relaxation rate $1/T_2$ becomes,

$$\frac{1}{T_2}(\mathrm{La}^{3+}+\mathrm{Gd}^{3+}) = \frac{[\mathrm{P}]}{\mathrm{P}_0 T_{2\mathrm{p}}} + \frac{[\mathrm{PM}]}{\mathrm{P}_0 T_{2\mathrm{pm}}} + \frac{[\mathrm{PM}]\quad [\mathrm{Gd}]_0}{\mathrm{P}_0 T_{2\mathrm{pm}}([\mathrm{Gd}]_0+[\mathrm{La}]_0)} \qquad (7)$$

$1/T_2m$ is then obtained from the slope of a plot of $1/T_2$ (La^{3+}+Gd^{3+}) vs % peptide bound to Gd^{3+} and similarly for $1/T_1$m.

Propagation of error

The uncertainty surrounding the T_2m estimates is the result of the indeterminate error associated with the slope measurements from $1/T_2$ vs %Gd^{3+} bound plots. A 90-percent confidence interval was thus calculated for each T_2m value determined, taking in account the standard deviation associated with each linear regression and the number of data points used to construct each plot (Hoel, 1971). A similar approach for the measurement of the uncertainty associated with T_1m values was difficult because of the small number of data points involved in these plots (reduced degree of freedom in the Student's *t* distribution) and the large standard deviation associated with the regression analysis of $1/T_1$ vs %Gd^{3+} bound as compared to the plots involving T_2 values.

The standard deviation obtained from averaging the observed T_1m/T_2m values was used to estimate the error surrounding the averaged correlation time value. The uncertainty associated with distance measurements was then calculated from the errors surrounding the T_2m and estimates. The distances calculated from T_1m values represent gross estimates having an uncertainty of more than 1 Å.